Doctoral theses at NTNU, 2024:103

Alicia Vallejo Olivares

Aluminium Recycling Pre-treatments: Compaction and Thermal De-coating

Doctoral thesis

NTNU
Norwegian University of Science and Technology
Thesis for the Degree of
Philosophiae Doctor
Faculty of Natural Sciences
Department of Materials Science and Engineering

NTNU
Norwegian University of
Science and Technology

Alicia Vallejo Olivares

Aluminium Recycling Pre-treatments: Compaction and Thermal De-coating

Thesis for the Degree of Philosophiae Doctor

Trondheim, March 2024

Norwegian University of Science and Technology
Faculty of Natural Sciences
Department of Materials Science and Engineering

NTNU
Norwegian University of
Science and Technology

NTNU
Norwegian University of Science and Technology

Thesis for the Degree of Philosophiae Doctor

Faculty of Natural Sciences
Department of Materials Science and Engineering

ISBN 978-82-326-7800-6 (printed ver.)
ISBN 978-82-326-7799-3 (electronic ver.)
ISSN 1503-8181 (printed ver.)
ISSN 2703-8084 (online ver.)

Doctoral theses at NTNU, 2024:103

Printed by NTNU Grafisk senter

Preface

This thesis is submitted in partial fulfilment of the degree of Doctor of Philosophy (PhD) at the Norwegian University of Science and Technology, detailing the findings and scientific contributions made during this doctoral work. The doctoral work has been performed at the Department of Materials Science and Engineering, Faculty of Natural Sciences, Norwegian University of Science and Technology, Trondheim, Norway, between December 2019 and December 2023, under the guidance of Professor Gabriella Tranell as the supervisor of this work, with Sr. Research Scientist Anne Kvithyld, Professor Hans J. Roven, and Adjunct Professor Trond Furu as co-supervisors.

This work was performed at NTNU within *Alpakka* (NFR project nr. 296276), co-sponsored by the Norwegian Research Council and industry partners. The research activities in collaboration with the Institute of Metallurgy (IME) at RWTH Aachen were funded by *Extreme-Alloys and Coatings* (NFR project nr. 310048). The LCA study was carried out in collaboration with the Industrial Ecology Programme at NTNU as part of the EU H2020 *SisAl pilot* project (grant agreement nr. 869268).

Alicia Vallejo Olivares
Trondheim, December 2023

Abstract

Due to their light weight and versatility, aluminium alloys are found everywhere around us, from food packaging to aerospace applications. Aluminium recycling saves substantial amounts of energy, resources, and waste compared to the primary production route. In addition, the processes for collecting and recycling aluminium are some of the most effective in the market, so aluminium is becoming a popular choice as a sustainable material by producers and consumers. Aluminium packaging products have particularly short lifetimes and are made of valuable wrought alloys with high purity requirements. As the demand for these products is expected to keep growing while the industrial emissions and environmental impacts need to be cut, it is imperative to increase their circularity and keep optimising recycling processes so that the metal lost in each cycle loop is minimal.

This thesis examines how conditioning aluminium materials by shredding, briquetting, and thermal de-coating pre-treatments affects the main mechanisms behind the metal losses during recycling: oxidation and metal entrainment by salt-slag or dross residues. Several types of aluminium foils, sheets, and incinerator bottom ash (IBA), with diverse contents of oxides and organics, were recycled via laboratory experiments to understand the relationship between their properties (size/thickness, coated or bare) and their recyclability. Subsets of the foils and sheet materials were shredded into chips, pre-treated by different routes, and finally re-melted by one of two methods: using molten salts or an aluminium heel. Emphasis was placed on understanding the interaction between compaction and thermal de-coating. This was investigated by thermally treating and subsequently re-melting materials in various compaction states: loose chips and briquettes of multiple densities, compacted by applying uniaxial pressure, moderate-pressure-torsion (MPT), or MPT at elevated temperature (450 °C). The efficiency of the thermal de-coating was evaluated by measuring the weight losses and the off-gas emissions. A final study assessed the environmental impacts of recycling a tonne of aluminium-containing side/waste streams (dross, IBA, shavings) in a rotary

furnace with salt-flux, a standard industrial route to recycle partially oxidised and contaminated scrap. The LCA analysis discussed the main environmental impacts of the process, with detail on those linked to the usage of salts and the consequent generation of salt-slag residues, by comparing two end-of-life alternatives: valorisation or landfill.

Compacting thin, clean aluminium proved an effective way to reduce their susceptibility to oxidation and promote the coalescence of the aluminium droplets when re-melting in salt flux. This was especially beneficial for the thinnest materials with large amounts of exposed surface area, such as aluminium household foil. The metal yields of IBA also showed a direct dependence on their specific surface area. Since the thickness of the oxide layer was comparable across sizes (68 μm in average), smaller particles have a lower specific metallic content, hence lower yields, which ranged from 76 to 93 % for sizes between 2-30 mm.

The observations from recycling coated and bare aluminium sheets in salt-flux highlighted that organic contamination, e.g. from coatings, increases the re-melting losses by hindering the coalescence of the metallic droplets when re-melting in molten salts. This can be tackled by applying a thermal de-coating pre-treatment, which promotes the degree of coalescence up to similar levels to those obtained when re-melting bare materials. The re-melting experiments in molten heel showed that the char residues from the incomplete combustion of organics is the main factor impacting the metal losses due to dross formation. Furthermore, the high densification of the briquettes by the MPT method limited the de-coating efficiency, thus increasing the re-melting losses for both re-melting processes.

The LCA study outlined the environmental benefits of recycling aluminium, all of which increase if the salt-slag residue is treated for recovery instead of landfilling it. The most critical parameters for improved sustainability were the metal recovery, process emissions, energy consumption and recovery of byproducts from the salt-slag. A sensitivity analysis illustrated how the metal yield could affect the global warming contributions: from -3.5 to -17 tonnes CO_2-eq for treating Al-containing streams of metal yields of 20 wt% or 95 %, respectively.

Acknowledgements

My most precious learnings from the past four years are the fruits of sharing the way with an engaged and dedicated team of scientists, professionals, and students. First and foremost, I am grateful to my supervisor, Prof. Gabriella Tranell. You have been a truly inspiring and supportive mentor. I deeply appreciate the way you encouraged me to pursue challenges and ideas and let me learn from my failures. I have also been fortunate to work under the supervision of Dr Anne Kvithyld. Thank you for sharing your expertise and enthusiasm in the field of aluminium recycling and for facilitating the collaborations between partners within the Alpakka project. I would also like to acknowledge Ad. Prof. Trond Furu for opening the doors of industry, which was decisive for my next career stage. Finally, I would also like to remember the kindness and optimism of Prof. Hans J. Roven when guiding my initial steps in research and the trust he and Prof. Geir Martin Haarberg placed in me when teaching in their course "Materials and Sustainable Development".

I jumped into the world of process metallurgy without much theoretical background or experience. Luckily, at the very start, I counted on the invaluable help of Dr Mertol Gökelma. This thesis would neither have been the same without the contributions of Harald Philipsson and Solveig Høgåsen. The workforce and dedication you put into your projects were admirable, and I enjoyed sharing the burdens and excitements of research with you. Furthermore, I am grateful for the work that Tom Gertjegerdes (with Prof. Bernd Friedrich) and Elisa Pastor Vallés (with Prof. Johan Pettersen) have brought to our collaborations, enriching considerably the scientific outcomes of the thesis. Thank you as well to Rafael De Vecchis and the rest of Prof. Gleeson's welcoming group at Pittsburgh University, and to Veronica Milani and Prof. Timelli from Padova University for the engaging discussions and cooperation. My gratitude goes as well to scientists Morten Raanes, Cathrine Solem, Kristian Skorpen, Heiko Gærtner, Are Bergin, Per Erik Vullum, and Prof. Ragnhild Aune, for your time and contributions to my research

endeavours. Finally, I would like to acknowledge the engineers Pål Skaret and Berit Kramer for running the labs at IMA with such dedication and positivity.
A strong hug to all the colleagues/friends who have accompanied me during these four years. Thanks to you, I was always happy when coming into the office (and lunch table), and I really enjoyed the time we spent together at conferences/research trips.

I dedicate this PhD thesis to my first and most objective teachers: my grandparents. Looking at myself through your eyes nurtured my courage in life. To my parents, for inspiring me with their values while letting me build my own. Even when you do not recycle aluminium correctly, I still love you. My deepest thanks to Elena and Haakon, for their understanding and love.

Table of Contents

List of Tables

List of Figures

List of abbreviations

Abbreviation	Definition
CFCs	Chlorofluorocarbons
CFFs	Ceramic Foam Filters
CO_2 eq	Carbon dioxide equivalent
CT	Computed Tomography
DRS	Deposit Return Scheme
EDS	X-ray spectroscopy
EPMA	Electron Probe Micro Analyser
F.U.	Functional Unit
FEG	Field Emission Gun
FTIR	Fourier-transform infrared spectroscopy
GHG	Green-house Gases
Hot MPT	Moderate Pressure Torsion at elevated temperature
IBA	Incinerator Bottom Ash
ICP-MS	Inductively coupled plasma mass spectrometry
LCA	Life Cycle Assessment
LCI	Life Cycle Inventory
LIBS	Laser Induced Breakdown Spectroscopy
MRF	Municipal Recycling Facilities
MPT	Moderate Pressure Torsion
MSWI	Municipal Solid Waste Incinerators
NMCs	Non-Metallic-Compounds
OES	Optical Emission Spectrometry
PAHs	Polyaromatic Hydrocarbons
PFCs	Perfluorinated Compounds
PoDFA	Porous Disc Filtration Analysis
SEM	Scanning Electron Microscope
STD	Standard Deviation
UBCs	Used Beverage Cans
VOCs	Volatile Organic Compounds
XRD	X-ray powder diffraction
XRF	X-ray fluorescence

Chapter 1. Introduction

1.1 Background

Over a third of the aluminium produced globally in 2021 came from recycling. Approximately 60 % of the scrap used for making these secondary ingots was classified as *old scrap* (post-consumer), the rest being *new scrap* (internal, from production). Recycling this record amount of post-consumer scrap (22 kT), instead of producing primary aluminium, saved 300 million tonnes of greenhouse gas emissions [1].

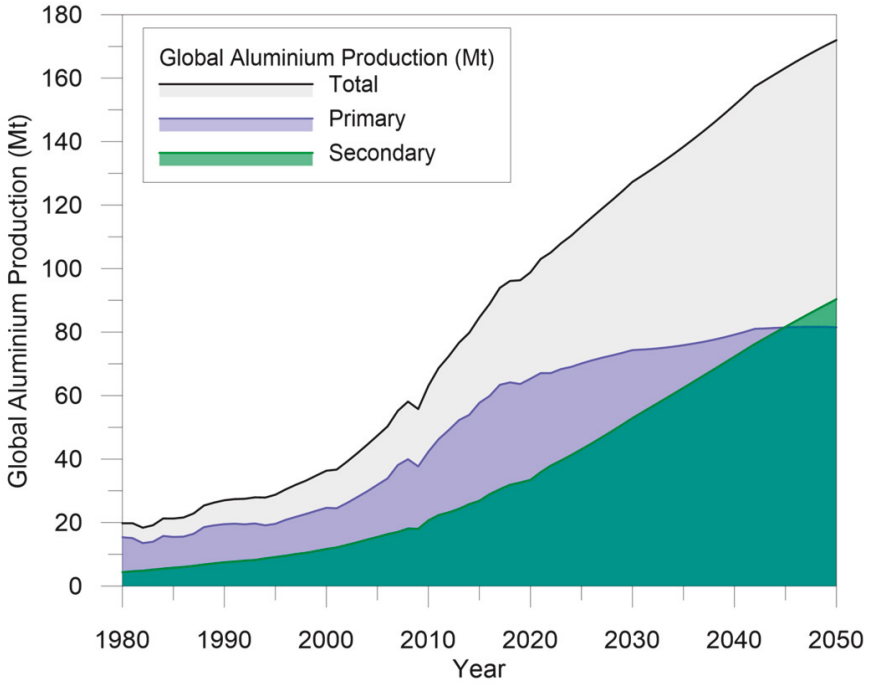

Figure 1. Global aluminium produced (and projected) from primary and secondary sources. Reproduced from Milani and Timelli, Solid Salt Fluxes for Molten Aluminum Processing – A review. Metals 2023 MDPI. doi.10.3390/met13050832 [2] based on data from [1] under CC BY license.

Aluminium packaging products have an excellent potential for circularity due to their increasing demand and short lifetimes, hence bringing significant economic and environmental benefits of recycling compared to primary production. Accordingly, a recent regulation proposal by the European Commission set a target to recycle at least 60 % of the annual weight of the aluminium packaging entering the market by the end of 2030 [3].

1.2 Motivation and Thesis Outline

The main part of the research presented in this thesis is part of the "Alpakka" project: a Norwegian Research Council-funded collaboration between Hydro, Metallco, Infinitum, Norsk Metallgjenvinning, Kavli, Speira, NTNU and SINTEF, that aims to increase the aluminium packaging circularity in Norway by value-chain cooperation between collectors, food producers/packaging designers, and aluminium producers and recyclers.

The focus of this thesis was to study the mechanisms behind the material (yield) and quality losses in aluminium packaging recycling, and how these parameters are affected by the scrap preparation routes. The literature suggests that re-melting losses in aluminium packaging scrap are promoted mainly by its high surface to volume ratio and the presence of contaminants, as illustrated below.

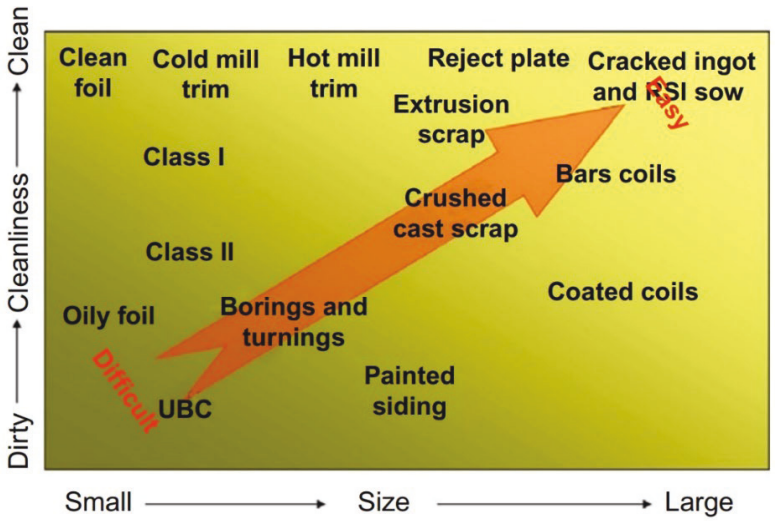

Figure 2. Relative comparison of various scrap types for ease of processing. [4]

The initial research hypothesis was that a compaction step before melting could increase the recyclability due to a reduction of the surface exposed, which would prevent oxidation. This effect might vary depending on the re-melting technique, i.e., recycling under salt flux or via scrap addition to a molten metal heel. However, compacting scrap which is coated or contaminated by organics may limit the thermal de-coating process and increase the re-melting losses. The project therefore examined the recyclability of aluminium food packaging materials with varying thickness, coatings, and surface to area ratio, as well as the compaction and thermal de-coating pre-treatments, their interaction and their impact into the quantity, and the quality of the material recovered.

The influence of briquetting coated materials on the thermal de-coating efficiency was investigated by analysing the off-gases emitted during the de-coating of aluminium in various compaction states: loose chips, briquettes compacted uniaxially, or highly densified briquettes compacted by the moderate-pressure-torsion (MPT) method. This study was part of a collaboration with the Institute of Process Metallurgy and Metal Recycling (IME) at RWTH Aachen, funded by the project Extreme-Alloys and Coatings for Space and other Extreme Applications (NFR project nr. 310048), including a research stay of 1 month.

Another line of research focused on understanding the oxidation losses of aluminium products when they undergo incineration in waste-to-energy plants, and the consequent recyclability of the aluminium-containing-fractions recovered from the Incineration Bottom Ash (IBA). In 2018, approximately 19 million tonnes of bottom ash were generated at European waste-to-energy plants, from which 1.3-3.3 % is estimated to be aluminium [5]. The IBA particles vary in size, and hence surface area, which affects their recyclability.

It is widely accepted that recycling aluminium brings forth significant environmental and economic benefits when compared to its primary production route. Re-melting in rotary furnaces with salt-fluxes allows recovering the metal from hard-to-recycle scrap flows, i.e., partly oxidised, or contaminated, such as post-consumer scrap, dross, and bottom ash. However, the use of salt-fluxes generates large amounts of salt-slag hazardous wastes, which can challenge the sustainability of the recycling process. To assess this, a life-cycle assessment (LCA) was conducted in collaboration with

NTNU's Industrial Ecology Program, partly funded by the EU H2020 project SisAl pilot, for recycling a mix of hard-to-recycle aluminium scrap in a rotary furnace, comparing the environmental impacts when treating the salt-slag residues for recovery or disposing it at the landfill.

Deepening the scientific understanding of the mechanisms involved in aluminium recycling, will help in optimising the recycling routes ultimately improving the circularity of aluminium packaging products.

The figure below shows the thesis structure and activities with the objectives and scientific outcomes.

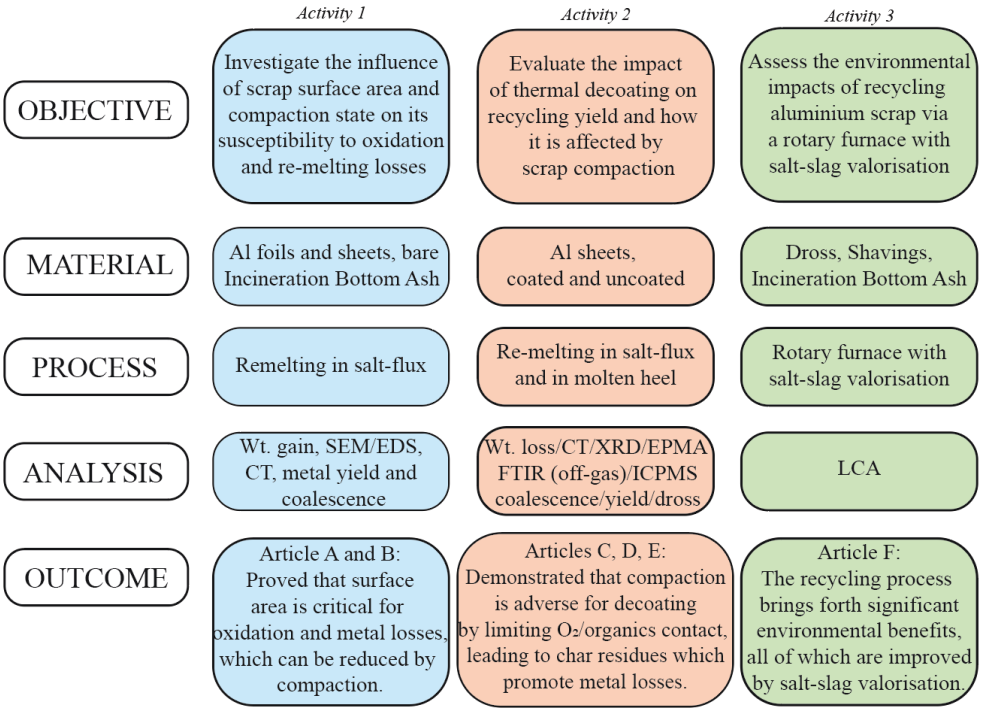

Figure 3. Outline of the thesis activities.

The work resulted in six scientific publications, which are included at the end of this document as supplements and were partly disseminated through presentations at five conferences.

1.3 List of Publications

Article A

Compaction of Aluminium Foil and Its Effect on Oxidation and Recycling Yield. In: Perander, L. (eds) Light Metals 2021. The Minerals, Metals & Materials Series. Springer, Cham. https://doi.org/10.1007/978-3-030-65396-5_133

Statement of contribution:

Vallejo-Olivares	Designed plan and experimental setup, conducted part of re-melting experiments, analysed X-ray tomography images, formulated manuscript, modified graphs.
Philipson	Discussed experimental setup, conducted experimental work (shredding, characterisation, compaction into briquettes, re-melting, surface roughness measurements), analysed and plotted data, proofread paper.
Gökelma	Discussed the concept and contributed with feedback and proofreading.
Roven	Co-supervisor. Discussed the concept and contributed with feedback and proofreading.
Furu	Co-supervisor. Discussed the concept and contributed with feedback and proofreading.
Kvithyld	Co-supervisor. Discussed the concept and contributed with feedback and proofreading.
Tranell	Supervisor. Discussed the concept and contributed with scientific feedback and proofreading.

Article B

Characteristic properties and recyclability of the aluminium fraction of MSWI bottom ash. Waste Management, Volume 130, Pages 65-73. https://doi.org/10.1016/j.wasman.2021.05.012

Statement of contribution:

Gökelma	Designed plan and exp. setup, analysed and plotted data, formulated manuscript.

Vallejo-Olivares	Conducted experimental work (re-melting and SEM/EDS characterisation, prepared and sent samples to ICPMS analysis), analysed data, performed statistical analysis and model, formulated and revised manuscript.
Tranell	Supervisor of the project. Discussed the concept and contributed with scientific feedback and proofreading article.

Article C

Effect of Compaction and Thermal De-coating Pre-treatments on the Recyclability of Coated and Uncoated Aluminium. In: Eskin, D. (eds) Light Metals 2022. The Minerals, Metals & Materials Series. Springer, Cham. https://doi.org/10.1007/978-3-030-92529-1_134

Statement of contribution:

Vallejo-Olivares	Designed plan and setup of experimental work, analysed X-ray tomography images, formulated manuscript, modified graphs.
Høgåsen	Conducted experimental work (shredding, compaction into briquettes, re-meltings, SEM characterisation), analysed and plotted data, proofread paper.
Kvithyld	Co-supervisor. Discussed the concept and contributed with scientific feedback and proofreading article.
Tranell	Supervisor. Discussed the concept and contributed with scientific feedback and proofreading article.

Article D

Thermal De-coating Pre-treatment for Loose or Compacted Aluminium Scrap and Consequences for Salt-Flux Recycling. J. Sustain. Metall. 8, 1485–1497 (2022). https://doi.org/10.1007/s40831-022-00612-x

Statement of contribution:

Vallejo-Olivares	Designed plan and setup of experimental work, analysed and plotted data, prepared samples for ICPMS analysis, formulated manuscript.
Høgåsen	Designed experimental plan for de-coating experiments, conducted experimental work (shredding, compaction into briquettes, re-

	meltings, sample preparation, optical microscopy, XRD analysis), analysed and plotted data, proofread article.
Kvithyld	Co-supervisor. Discussed the concept and contributed with scientific feedback and proofreading article.
Tranell	Supervisor. Discussed the concept and contributed with scientific feedback and proofreading article.

Article E

Effects of compaction and thermal pre-treatments on generation of dross and off-gases in aluminium recycling. J. Sustain. Metall. (2023) https://doi.org/10.1007/s40831-023-00773-3

Statement of contribution:

Vallejo-Olivares	Designed experimental plan and setup, conducted experimental work (dross analysis and re-melting, molten heel re-melting) analysed and plotted re-melting and characterisation data, formulated manuscript.
Gertjegerdes	Designed experimental plan and setup, conducted experimental work (FTIR off-gas analysis, molten heel re-melting), analysed and plotted FTIR data, formulated and revised manuscript.
Høgåsen	Conducted experimental work (shredding, compaction into briquettes, briquette characterisation, molten heel re-melting), analysed data, proofread article.
Friedrich	Supervisor. Discussed the concept and contributed with scientific feedback and proofreading article.
Tranell	Supervisor. Discussed the concept and contributed with scientific feedback and proofreading article.

Article F

LCA of recycling aluminium incineration bottom ash, dross and shavings in a rotary furnace and environmental benefits of salt-slag valorisation. Waste Management. Under review.

Vallejo-Olivares	Designed plan and scenarios, analysed data, carried out LCA, analysed data, carried out sensitivity evaluation, formulated manuscript.
Pastor-Vallés	Designed plan and scenarios, supervised LCA, analysed data, created graphics, formulated manuscript.
Pettersen	Supervisor. Discussed the concept and contributed with scientific feedback and proofreading article.
Tranell	Supervisor. Discussed the concept and contributed with scientific feedback and proofreading article.

Other Publications

Milani, V., Vallejo-Olivares, A., Tranell, G., Timelli, G. (2023). Influence of Cryolite Content on the Thermal Properties and Coalescence Efficiency of NaCl–KCl Salt Flux. In: Broek, S. (eds) Light Metals 2023. TMS 2023. The Minerals, Metals & Materials Series. Springer, Cham. https://doi.org/10.1007/978-3-031-22532-1_123

Scientific Outreach

From waste to value, blogpost NTNU TekNat, July 2020.

https://www.ntnu.no/blogger/teknat/2020/07/02/from-vaste-to-value/

Pushing the limits of aluminium recycling, Interview by Pint of Science Norway, Sept 2021

https://www.pintofscience.no/post/interview-alicia

Chapter 2. Theory and Literature Survey

2.1 The Life Cycle of Aluminium Packaging Products

Aluminium is the third most abundant element present in the Earth's crust. Due to its versatile properties, it can be used for a wide range of applications: e.g., as structural material in the transportation or construction sectors, or as packaging for food, drinks, pharmaceutic or cosmetic products. Figure 4 illustrates the life cycle of aluminium packaging products, divided into five stages: production, manufacturing, use, recovery, and recycling. To achieve circularity, each of these stages must be optimized, and coordinated with the others, to prevent any material losses as aluminium metal goes through the cycle.

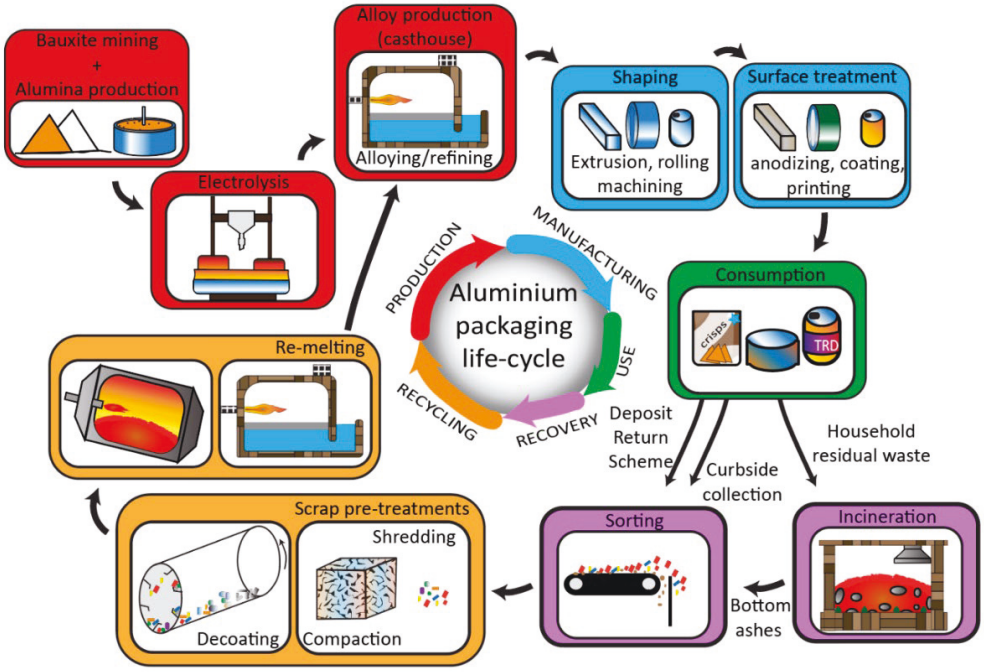

Figure 4. Life cycle of aluminium packaging products.

2.2 Primary Production

The cycle of aluminium products starts by mining the raw material: bauxite ore. In 2022, a total of 380 thousand million tonnes was mined globally, where the main producers are located in tropical and sub-tropical areas in Australia, China, Guinea, Brazil, Indonesia and India, in descending order [6]. Bauxite is then refined into aluminium oxide (alumina, Al_2O_3) through a hydrometallurgical process – the Bayer process. It begins by finely milling the bauxite together with limestone and subsequently reacting the raw material mix with a sodium hydroxide (NaOH) solution under pressure at 150-200°C. The aluminium oxide in the bauxite present as hydroxide will dissolve in the solution, forming a sodium aluminate solution, while other oxides largely stay in a tailing, commonly denoted "red mud" or bauxite residue, which is filtered off. Subsequently, alumina hydrate is used as seed to precipitate aluminium hydroxide ($Al(OH)_3$) from the sodium aluminate solution, which is then filtered, washed, and calcined into metallurgical grade alumina [4]. The bauxite residues pose great environmental challenges [7], and continuous efforts are hence placed on reducing their generation and/or valorisation into industrial products, for example in concrete [8]. In 2022, 139 million tonnes of alumina were produced globally, mainly in China, followed by Australia and Brazil [6].

The next step is to extract the aluminium from the aluminium oxide by the Hall-Héroult electrochemical process. This involves dissolving the alumina into an electrolyte consisting of cryolite (Na_3AlF_6), calcium fluoride (CaF_2) and aluminium fluoride (AlF_3). The overall reduction reaction, producing aluminium at the cathode and CO_2 at the carbon-based anode, may be written:

Hall-Héroult main reaction: $$2Al_2O_3 + 3C = 4Al(l) + 3CO_2(g) \qquad \text{(Eq. 1)}$$

The standard Gibbs free energy of the reaction at the process typical temperatures of 960 °C is 345.1 kJ/mol, and therefore large amounts of energy (provided as electricity) are required to drive the reaction to the right [9]. The electrolysis is the most energy intensive step in the aluminium cycle, with approximately 14 MWh of energy consumed per tonne aluminium produced [1]. Once the aluminium metal is produced, either by the primary or secondary route (recycling), it is transferred to a holding

furnace, where alloying and refining elements are added to meet the specifications of the alloy under demand. The product is generally solidified into simi-finished products (ingots, slabs, billets…) which are delivered to the product manufacturer for further processing, although sometimes the metal is transported in the molten state as a strategy to save energy [10]. Aluminium alloys are classified as cast or wrought alloys, according to whether they are shaped through casting or forming processes. Casting consists of pouring or injecting the molten metal into moulds with one or several cavities of the desired shape, using technologies such as pressure die casting, sand casting, permanent mould, or investment casting. Forming processes shape the metal in the solid state by applying thermal and mechanical energy, for example through extrusion, rolling, forming or hot stamping. In addition, the semi-finished products undergo machining, thermal (e.g., homogenisation [4]) or surface treatments (e.g., anodising, printing/coating) to improve the product's mechanical, durability (e.g., corrosion resistance), safety (e.g., contact with food) and aesthetical properties. The aluminium residues generated by these processes (dross/skimmings, shavings/machining chips, discarded parts, scalpings) constitute what is known as internal scrap.

2.3 Scrap Collection and Sorting

The recovery/recycling of aluminium from post-consumer products starts by collecting the aluminium scrap and, if needed, sorting it from other materials in the waste stream. The waste management routes and the recovery/recycling rates of aluminium products widely vary between regions. The recovery rate of a given packaging category (e.g., aluminium, steel, glass, plastic…) is defined as *the weight of the packaging products recovered relative to the total amount disposed*. This definition of recovery linked to recent Eurostat data [11] includes energy recovery (e.g. waste to-energy incineration plants) and other types of recovery in addition to recycling. Recent statistics from Europe show that the recovery rates of packaging in general in 2021 were in average 79.9 %, ranging between 38.5 % in Malta and 99.1 % in Belgium. The highest recovery rates for aluminium packaging in 2020, above 95 %, were reported in Norway, Germany, Estonia, Liechtenstein and Denmark, and the lowest (below 20 %) in Malta, Czechia, Portugal and Romania. The recycling rate is

defined as *the total amount (wt.) of products which are delivered to an effective recycling process divided by the total amount disposed.* The European recycling rates of aluminium packaging in the year 2020 were the highest in Norway (78.1 %), Belgium (73.1 %), Germany (62.1 %), Italy (56.9 %) and Spain (54.7 %) [11].

2.3.1 Collection

The schemes in place to collect aluminium packaging products from households in Europe are:

- The deposit-return-scheme (DRS) for used beverage cans (UBCs). An additional fee (0.2-0.3 € in 2023) is charged at purchase for those beverage products included in the scheme. The customers can deliver the empty UBCs to the collection points at food stores, incentivised by recovering the money as cash, a voucher for the next grocery shopping, or a charity donation lottery. DRS schemes have proved successful in increasing collection rates [12] and reducing littering, and the European Commission proposes implementing them across Europe to reach the 2030 recycling goals [3].
- Curb-side recycling: aluminium packaging is collected from households mixed with other recyclable packaging products, e.g., made of glass, plastic, or cardboard, depending on the region. The different material streams are sorted at Municipal Recycling Facilities (MRF) and sent for recycling.
- Residual waste collection. Despite the high collection rates of packaging through the DRS and curb-side recycling, a significant fraction of the household aluminium waste still ends up in the "residual waste" streams, treated via incineration or landfilled. This is especially the case for non-packaging products, such as kitchenware, and for those packaging products containing aluminium that are not deemed recyclable by current technologies. These are for example multi-layered products, also known as flexible packaging, such as crisps bags, coffee capsules or aseptic juice boxes, where a very thin layer of aluminium is glued to plastic and/or paper. During incineration, part of the metallic aluminium in the waste is lost as it oxidises or reacts with other compounds. The residual metal can however be recovered from the incineration bottom ashes (IBA) if sorted and processed adequately.

Warrings [13] represented the material flows of Al packaging & non-packaging household waste in Austria in 2013, at the level of the product groups rigid, semi-rigid and flexible, as illustrated in Figure 5.

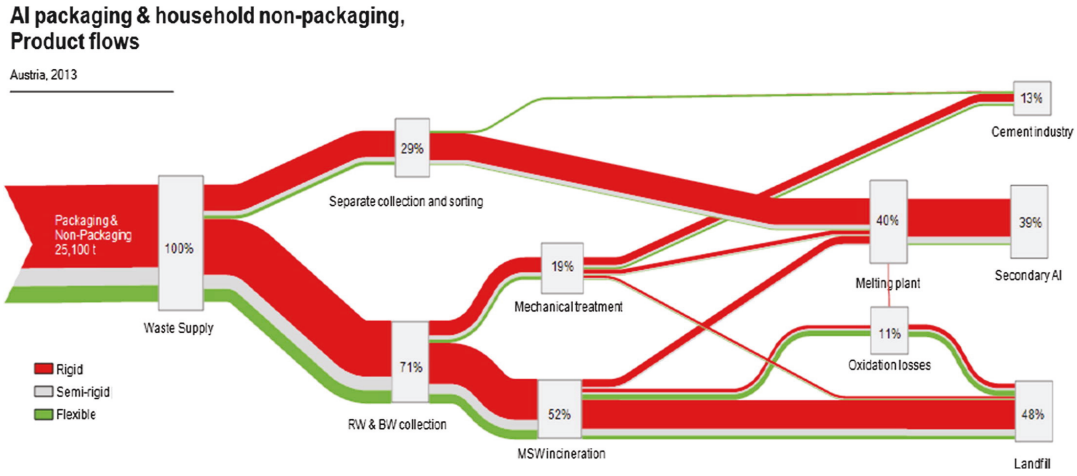

Figure 5. Material flows of Al packaging & household non-packaging in Austria at the level of the product groups rigid, semi-rigid and flexible [13]. Reproduced with permission © 2018 Elsevier Ltd. All rights reserved.

In this example, 29 % was collected by separate collection (DRS or curb-side recycling) plus sorting, and 71 % was disposed of together with the residual waste. A small fraction of the residual waste was sorted and sent to the melting plant or cement industry, and 52 % of the scrap was incinerated. The scheme shows that 13 % of the scrap weight, including flexible packaging, was utilised as a source of oxide filler in the cement industry, 39 % was recycled into secondary aluminium, and 48 % was disposed at landfill, from which 11 % had been transformed into oxides during the different waste management steps.

Skramstad's [14] study of the aluminium packaging flows in Norway in 2019 shows that the largest scrap category sent for recycling were UBCs collected by DRS (8834 tonnes, 89.5 % of those put into market). The rest of recycled aluminium packaging (61 tonnes), including foreign UBCs not included in the DRS, and other aluminium food/drink packaging, was collected for recycling via the glass and metal packaging curb-side recycling scheme. Still, some UBCs and metal packaging were disposed as household waste, and although a small part of it was sorted before incineration at the MRF and sent for recycling, a substantial amount of aluminium (including some non-

packaging) was incinerated in waste-to-energy plants, generating 5693 tonnes of metallic-non-ferrous fraction of IBA. According to a recent annual report from Infinitum [15] (managing the DRS scheme in Norway), in 2022 91.5 % out of the 13.9 thousand tonnes UBCs put into the Norwegian market were collected for recycling through DRS, and their recovery rate (including waste to energy) reached 100 %.

2.3.2 Incineration

Incinerating household waste is a way to reduce landfilling while generating thermal energy that can be used for electricity or heating. In the EU, Norway and Switzerland, approximately 90 Mt of municipal solid waste and industrial waste of similar composition are incinerated per year [16]. This results in an annual production of Incineration Bottom Ash (IBA) of 17.6 million tons, which is sorted out for utilisation/recycling into different fractions: minerals (50-70 wt%), glass and ceramics (10-30 wt%), ferrous metals (5-15 wt%) and non-ferrous metals (1-5 wt%) [17]. During incineration, the waste is conveyed through an incineration zone, burning its organic content and generating temperatures as high as 1100 °C [18]. As a result of the exposure to these high temperatures and oxidising atmospheres, part of the aluminium is oxidised. According to Warrings [13] around 11 % of the aluminium mass is oxidized during incineration, while Bunge [18] estimated that a third of the mass of used beverage cans (UBCs) is oxidized if they undergo this process. The content of recoverable aluminium in the non-magnetic metallic fraction of the IBA may depend, in addition to the incineration operation conditions, on the characteristics of the scrap. The oxidation losses of aluminium packaging products during incineration were investigated by Hu [19] and Biganzoli [20], highlighting the negative influence of Mg content in the alloy and the low thickness of the packaging products. Gökelma [21] studied aluminium IBA of sizes 5-25 mm recovered from Norwegian waste-to-energy plants. Their oxide content was estimated between 8-15 % based on measurements of the oxide layer, and their recycling metal yield ranged between 84-92 %.

2.3.3 Sorting

The leading technologies employed to sort aluminium (alloys) from other materials are based on their density and electrical or magnetic properties. The magnetic separator is used to sort aluminium from ferrous materials and nickel-based alloys,

according to their magnetic susceptibility, into magnetic or non-magnetic fractions. The eddy-current-separator sorts materials based on electrical conductivity, shape and density, determining their response to a magnetic field and, thus, their degree and deflection path [22]. This is an effective method to separate the plastic bottles from the UBCs collected in e.g Norway's deposit-return scheme, the glass from metal packaging from the Norwegian curb-side scheme, and aluminium from other metals of higher density, such as copper or steel. Since aluminium's mass and density are higher than paper, foams, and plastic, these can also be sorted out by air or dense media separators (e.g. sink-float) [23].

New technologies, for example LIBS (Laser-Induced Breakdown Spectroscopy) or, to some extent, X-ray or γ-ray sorting technologies, make it possible to sort the aluminium into several groups depending on its composition (alloy). It is also possible to manually sort into cast or wrought alloys after their visual appearance [24] or into different alloy families using image analysis technologies that detect the scrap's colour [25] after a chemical treatment.

2.4 Aluminium Recycling Processes

Depending on the scrap characteristics and the re-melting process, the scrap may be prepared by shearing or shredding, cleaning, de-coating or compaction. The metal is subsequently re-melted at temperatures between 700-800 °C. Its composition may be adjusted based on quality requirements by adding alloying elements, diluting with primary aluminium, mixing with other types of scrap, or refining to remove contaminants. Finally, the metal is solidified and shaped into new products by casting, rolling, machining, etc., similarly to the primary production route.

2.4.1 Scrap Pre-treatments

The pre-treatments, or conditioning or preparation routes, are applied to aluminium scrap before re-melting in order to facilitate the scrap handling (transport/charging operations), increase process control and safety by reducing the presence of moisture or organics, and to optimise the process performance (metal yield and quality). For example, shredding or shearing, compacting into bales or briquettes, de-lacquering or de-coating.

Shredding

Shredding or shearing liberates the aluminium from other materials that may be assembled or attached. Shredding also reduces the scrap size, facilitating subsequent sorting and compaction treatments. It also promotes the cleaning or de-coating treatments by exposing the inner surfaces of the packaging so that eventual liquids or organic residues trapped inside the scrap containers can be removed. The shredding machines can be classified into shears, impact shredders, and rotary shredders [22]. The most widely used for aluminium scrap are the swing-hammer shredders [26] since they guarantee the liberation of assembled parts while maintaining a specific size distribution [27]. The main challenge of recycling aluminium shreddings is that they are more prone to being lost during transport or plant operations. Their low density and high specific surface area make them more susceptible to floating and oxidising during re-melting. Fine scrap may be compacted into briquettes to address these challenges, as discussed in the following section.

Compaction

Post-consumer scrap is often compacted into bales or briquettes to ease transport and storage. If the scrap at a later step needs to go through sorting or de-coating, the bales are generally loosened up. They may remain loose or undergo compaction before re-melting, depending on the process and scrap characteristics.

Compacting thin, clean aluminium before re-melting reduces the risk of oxidation losses since compaction decreases the surface area exposed to the oxidising atmosphere. The susceptibility to oxidation increases for scrap with thinner gauges and higher Mg contents, as shown by Rossel [28]. When recycling machining chips or shavings from primary scrap, these are often compacted into briquettes before being charged into the furnace since they float, oxidise, and favour hydrogen pick-up if charged while loose. In addition, their compaction helps to squeeze out potential organic contaminants as lubricants/machining oils, thereby preventing combustion reactions during re-melting. Puga [29] and Klingauf [30] showed the benefits of compacting machining swarf before re-melting it in crucibles with a molten aluminium heel and by an industrial tilted rotary furnace with salts, respectively.

When it comes to post-consumer packaging scrap containing coatings or food residues, compacting the scrap into bales or briquettes of high densities may challenge the removal of the organics by a thermal de-coating process, described in the following section. Therefore, compaction into logs of lower densities, which are easier to shred, is widespread [22]. This agrees with the conclusions reached by Steglich [31, 32] after thermally de-coating and re-melting UBC bales of different densities. However, in those studies, the bales of different densities also had different levels of organic contamination. This could affect some results since more organics may require, for instance, longer de-coating times.

Thermal De-coating

Post-consumer scrap is often contaminated by paint, ink, oil, paper, plastics, or other organics such as food residues. The thermal de-coating pre-treatment aims to remove the volatile and organic compounds. That is beneficial in many ways: it pre-heats the scrap, prevents re-melting losses caused by the reaction of the aluminium with the contaminants, and additionally it improves process control and safety by avoiding the generation of toxic, explosive or combustible gases during re-melting [33] [34]. However, the de-coating process must also be controlled to minimise the emissions of harmful by-products, such as volatile organic compounds (VOCs), dioxins/furans or nitrous oxides [35], and be cost and energy-efficient. This can be pursued, for instance, by gas treatment or recirculation, since the decomposition reactions are exothermic [22]. The three main industrial de-coating units are rotary kiln, belt de-coater (also known as packed-bed reactor) and fluidised bed de-coater.

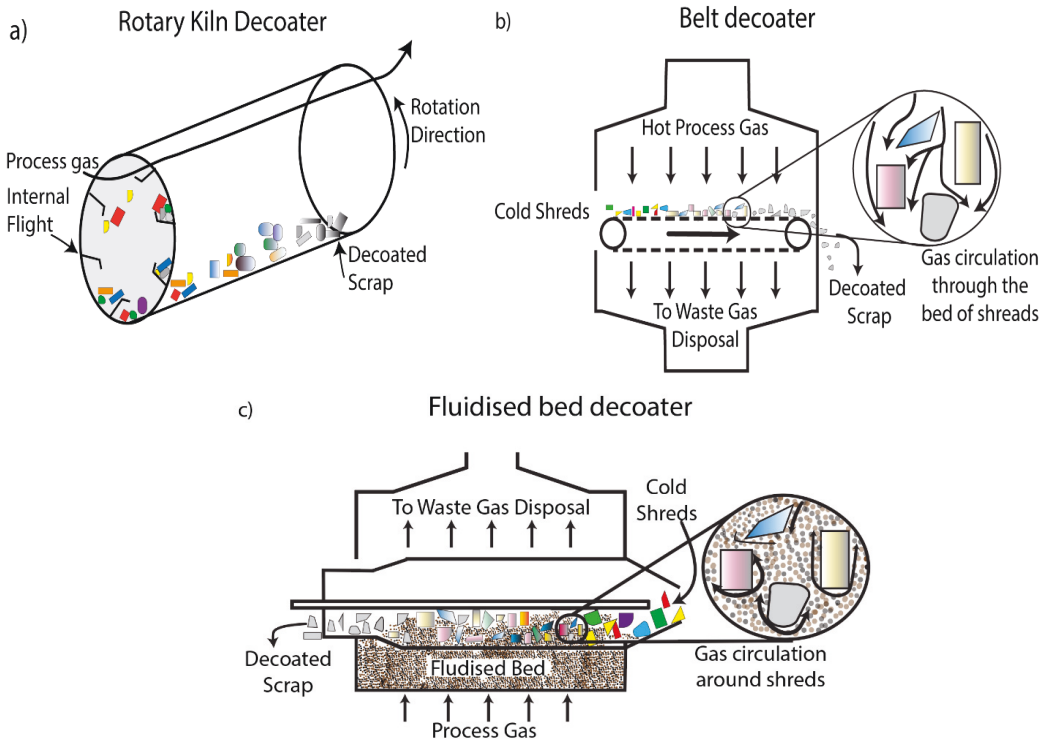

Figure 6. Schematic of de-coating units: rotary kiln, belt and fluidised bed.

When de-coating in a rotary kiln, the scrap goes through an inclined rotating drum while heated by a fired torch or hot air. The drum usually has internal flights which lift and stir the scrap. When de-coating via a belt de-coater, the scrap is transported by a conveyor belt through which passes oxygen-containing hot air. Finally, de-coating in a fluidised bed involves heating the scrap on top of a porous conveyor belt with a bed of inert solid particles while an oxygen-containing gas is injected through the bed [36] [37].

Extensive research shows the benefits of removing moisture and organic contamination from the scrap before re-melting. McAvoy showed that a thermal pre-treatment could prevent the re-melting losses otherwise caused by the presence of lacquer and that re-melting with salts was also beneficial [33]. Capuzzi [38] showed that thermally de-coating aluminium small discs promote the coalescence of metal droplets when re-melting under salts. This benefits the recycling yield in re-melting processes using salts, such as rotary furnaces, by lowering the risk of entrainment of

the metal droplets into the salt slag instead of merging with the rest of the melt. Gökelma [39] shared similar results on the beneficial effects of de-coating coffee capsules before salt re-melting. When scrap is re-melted in furnaces without salts, de-coating scrap can reduce the metal losses by reducing the amount of dross generated. This was observed by Steglich [31, 32] for the recycling of UBCs. These results are coherent with the findings of Dittrich [40] on the interaction between molten aluminium and pyrolysis gases, which showed that CO_2 and CO gases tend to oxidise aluminium and consequently increase the formation of dross significantly. Furthermore, Kvithyld [41] studied the quality of secondary aluminium melts by comparing the bi-film index, which measures the quantity of non-metallic inclusions. Their results indicate that even small amounts of coatings lead to a higher bi-film index and, thus, melts of lower quality.

A typical thermal de-coating can be divided into two phases. When the material is exposed to a sufficiently high temperature (above 250 °C), the organic molecules rapidly decompose (cracking). This releases volatile components such as short-chain hydrocarbons. The decomposition leaves a carbon-rich residue, which is gasified in the second stage, provided there is oxygen in the gas atmosphere [42] [31] [32]. If no oxygen is available, the combustion phase is substituted by a pyrolysis phase, which leaves a layer of carbonaceous residue attached to the metal. The thermal decomposition (thermolysis) reactions in the presence of oxygen for two of the most common polymers used for packaging products, Epoxy and Polyester, are the following:

$$\text{Epoxy: } C_{21}H_{24}O_5 + 21O_2 = 14CO_2 + 7CO + 12H_2O \qquad \text{(Eq. 2)}$$

$$\text{Polyester: } C_8H_6O_4 + 6O_2 = 5CO_2 + 3CO + 3H_2O \qquad \text{(Eq. 3)}$$

The de-coating phases described are illustrated in Figure 7.

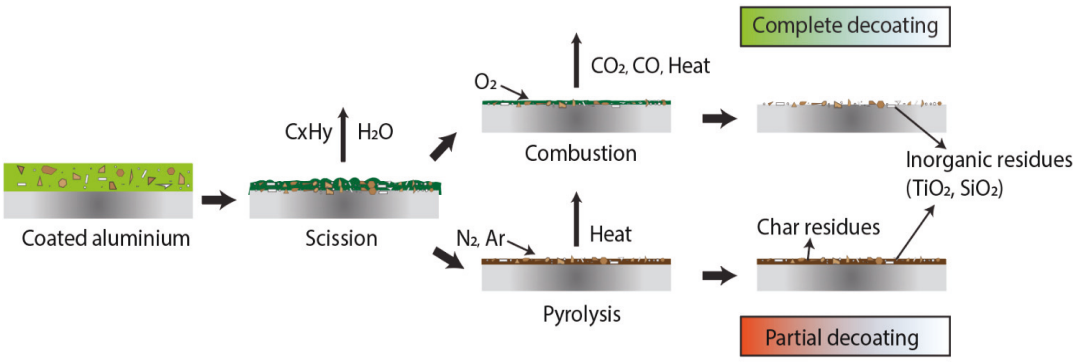

Figure 7. De-coating reaction stages for atmospheres with and without oxygen.

The conditions to which scrap is exposed during thermal de-coating (temperature, residence time, oxygen content in the gas and gas/scrap contact) must be carefully controlled to ensure that organic residues are fully removed whilst the metal is not oxidised [37]. In Capuzzi's study [43], pre-treatments at 400 °C were insufficient to fully de-coat the discs and improve the coalescence. In comparison, treatments at 500 °C and 600 °C successfully increased the coalescences to similar levels to those obtained for the uncoated materials. Stiglich [31] showed that de-coating in an Ar atmosphere (pyrolysis reactions), or in oxygen containing atmospheres at lower temperatures (450 °C), left char residues on the surface. The char residues promoted dross generation, resulting in more quantities of dross than those samples which were directly re-melted without a thermal pre-treatment. In contrast, the amount of dross was lower for the samples treated in oxygen-containing atmospheres of (air or Ar + 4 % O_2) and temperatures above 550 °C. The mechanisms behind dross formation due to the presence of coating residues are illustrated in Figure 8.

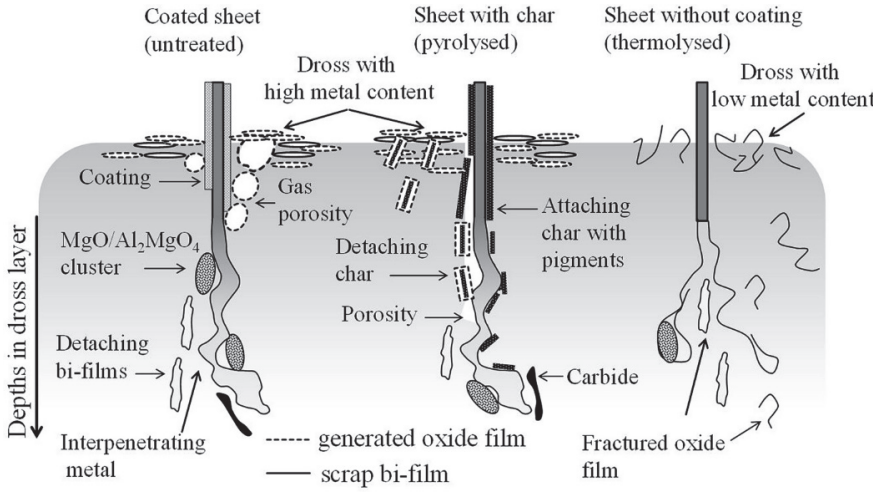

Figure 8. Dross formation mechanisms with and without thermal pre-treatment for UBCs [31]. Reproduced with permission © The Minerals, Metals & Materials Society.

According to the mechanisms proposed by the scheme, re-melting coated sheets untreated or after a pyrolysis treatment increases the amount of dross generated. The metallic content of the dross is also higher in those cases, since the char and organic residues in the surface form carbides and oxide bi-films, which adhere to the metal and entrain it.

While the organic contamination is removable by a thermal treatment, the coatings in packaging also contain a significant fraction of inorganic compounds, such as TiO_2, ZnO, or Fe_2O_3, which remain loosely adhered to the scrap after the thermal treatment. Some of these residues could be removed by mechanical abrasion, as it occurs during the rotary-kiln or fluidized-bed de-coating routes [42]. The inorganic residues in the scrap may concentrate on the dross or salt slag during re-melting, increasing metal losses, or be partly reduced by the aluminium and dissolved in the melt [22]. Another option to remove non-metallic contaminants from scrap is to apply chemical de-coating instead of thermal de-coating, as studied by Fujisawa [44]. This allows the removal of inorganic components, such as the mentioned TiO_2 pigments, but has disadvantages, such as using acid solvents and generating residues.

2.4.2 Re-melting

An optimal re-melting process should be time, energy and cost-efficient and maximise the metal recovery. The choice of the type of furnace depends mainly on the

characteristics of the scrap and the source and price of energy. The two main furnaces used for aluminium recycling are known as reverberatory and rotary furnaces.

Reverberatory Furnaces

Reverberatory furnaces have a curved roof lined with refractories, and as the term reverberatory indicates, during this re-melting process, the metal is heated directly by the combustion of fuels and indirectly by the heat reverberated from the refractory walls.

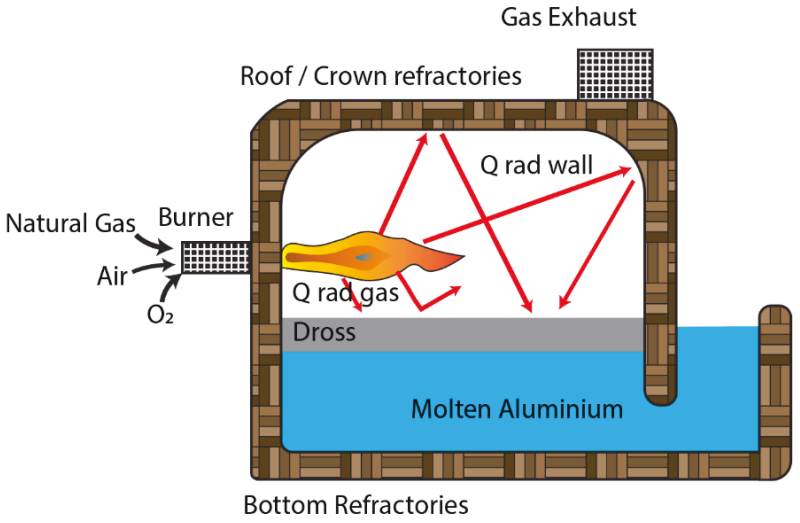

Figure 9. Schematic representation of a reverberatory furnace.

The furnace may have one single chamber or multiple, with diverse designs and charging methods. In *wet-hearth* furnaces, the charge is directly placed in the hearth of the furnace, while the *dry-hearth* furnaces feature a sloping hearth on which scrap is pre-heated before pouring down into the hearth. There are also *multiple chamber furnaces*, including the *side well, vortex* and *twin-chamber* described in [22]. Some of these designs include an integrated de-coating compartment, e.g., *twin-chamber* and *side well* furnaces, where the scrap is pre-treated. Using a vortex to sink the scrap offers some advantages for thin, clean and dry scrap, such as increasing the melting speed and preventing the oxidation of the small metal pieces that would otherwise float on top of the melt. However, for scrap coated or contaminated with organics, submerging the carbonaceous materials can lead to gases forming aluminium oxides or carbides, increasing metal losses and lowering the melt quality. Compared with rotary furnaces, reverberatory furnaces provide high volume processing rates and low

operating and maintenance costs. However, they also have lower energy efficiencies, significant space requirements and high metal oxidation rates [27].

Rotary Furnaces

Rotary furnaces allow recycling scrap with a higher oxide content, for example, incineration bottom ash or aluminium dross, and scrap with moderate organics content, such as UBCs.

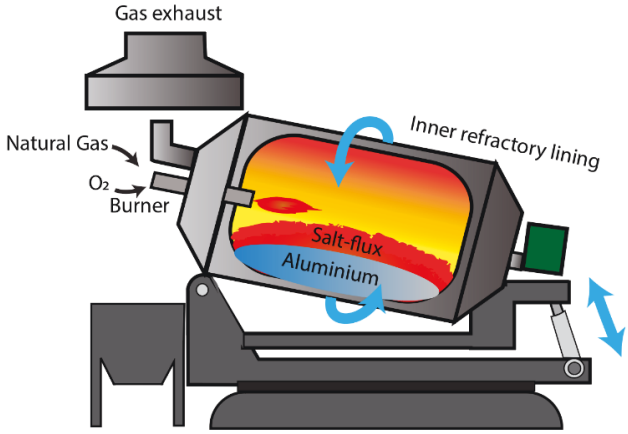

Figure 10. Schematic representation of a tilting rotary furnace.

The rotational movement of the furnace stirs and mixes the scrap with the salt fluxes. This enhances the metal-flux reactions, the liberation of metal from its oxides and the coverage of metal by molten salts, thus protecting it from oxidation. The primary fuel is natural gas, and often, furnaces can tilt backwards during charging and firing and forward to discharge the molten metal and salt slag. The remelting cycles are generally faster and more energy efficient than ordinary reverberatory furnaces, at the expense of higher installation costs and maintenance [45]. A drawback of this method is that it requires high quantities of salt flux to maximise the metal recovery, generating salt-slag residues. The salt-slag residues are considered hazardous waste and were traditionally landfilled. However, technologies are currently in place that recover the salts, non-metallic-compounds, aluminium concentrates and other byproducts from the salt slags, which can be reused in the re-melting process or commercialised, e.g., for use in the construction or chemical industries [46-48].

2.4.3 Refining

After re-melting, the molten aluminium is transferred to a holding furnace to adjust its temperature and composition by adding alloying elements or refining [22]. Before casting, the melt may undergo several refining techniques to remove impurities and prevent adverse effects on the properties of the final products. A typical refining cycle is illustrated below:

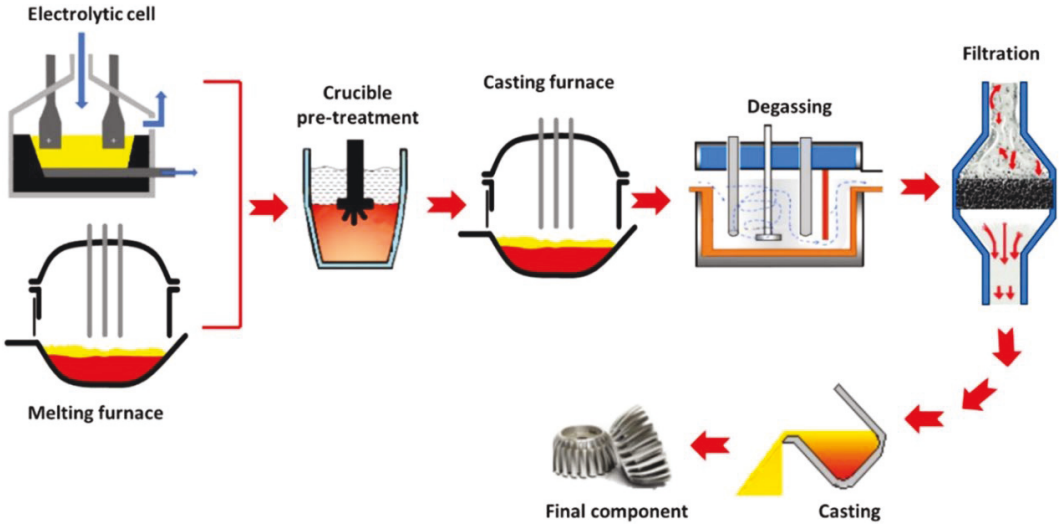

Figure 11. Main processing steps of aluminium melt refinement, including pre-treatment crucible, casting furnace, degasser, and filtration. Reproduced under the Creative Commons Attribution 4.0 licence from Wu et al. Melt refining and purification processes in Al alloys: a comprehensive study. Materials Research Express doi:10.1088/2053-1591/ac5b03 [49].

The main refining processes are degassing, fluxing, settling, and filtering. The choice of refining route depends on the type and concentration of impurities and the specifications of the secondary alloy produced.

Typical Impurities in Molten Aluminium

The main impurities targeted when refining molten aluminium are classified into hydrogen, dissolved elements (mainly alkali metals), and non-metallic inclusions. Table 1 below lists their concentrations in both primary and secondary aluminium.

Table 1. Common Impurities in Primary and Secondary Melts [50].

Group	Characteristic	Primary	Secondary
Hydrogen	Hydrogen	0.1-0.3 ppm	0.2-0.6 ppm
Alkali metals	Na	30-150 ppm	<10 ppm
	Ca	2-5 ppm	5-40 ppm
	Li	0-20 ppm	<1 ppm
Inclusions (PoDFA scale)		>1 mm^2/kg Al_4C_3	0.5<mm^2/kg<5.0 Al_20_3, MgO, $MgAl_2O_4$, TiB_2

Hydrogen

The solubility of hydrogen sharply decreases upon solidification, from an equilibrium content at 1 bar of 0.64 ppm in pure aluminium at the melting temperature of 660°C to 0.03 in the solid state [51]. If hydrogen is not refined before casting, the porosity of the final product drastically increases, caused by hydrogen gas escaping the solidifying metal. Hydrogen can be picked up by the melt from the combustion off-gases or moisture in the atmosphere or from moisture present in the scrap. It reacts with the melt and forms dissolved H and oxides as follows:

$$2\,Al(l) + 3H_2O \rightarrow Al_2O_3(s) + 6\underline{H} \qquad \text{(Eq. 4)}$$

Since the metal is converted into oxide inclusions, hydrogen adsorption is also a cause of metallic losses and increased dross generation. Hydrogen adsorption during re-melting is favoured by operations such as charging, skimming or stirring, which disrupt the oxide layer floating on top of the melt, which otherwise would prevent the contact between the atmosphere/moisture and the molten metal [22].

Dissolved Elements

This category includes, in theory, all elements that are dissolved in liquid aluminium. However, in practice, not all of them are considered impurities. For example, iron (Fe), copper (Cu), manganese (Mn), magnesium (Mg), silicon (Si), zinc (Zn) or titanium (Ti) are accepted in the melt as alloying elements in the range of concentrations specified for each alloy, since they improve the mechanical, corrosion or formability properties of aluminium products. Since products made of different alloys are mixed and melted together upon recycling, the alloying elements may surpass the

concentrations of the target alloy and then become undesired elements. Refining many of these alloying elements is yet to be economically viable, so their accumulation in secondary melts must be controlled, as discussed in the upcoming section on quality challenges of recycling. The dissolved elements usually refined are known as reactive metals (Na, Li, and Ca). They are introduced into the melt by reactions with salts from the electrolysis bath or due to scrap contamination. An example of the latter is the automotive pieces contaminated by Ca from the salts used to de-ice roads.

Non-metallic Inclusions

Non-metallic inclusions are particles or films which are non-miscible in the molten aluminium. They are usually non-metallic and intermetallic solid particles, although they can also be present in liquid or gaseous states [51]. Depending on their origin, they are classified as *exogenous* or *indigenous*. Exogenous inclusions come from external sources, such as coating oxides or dirt attached to the scrap or refractory parts. Indigenous (or *in-situ)* inclusions arise from chemical reactions in the melt, such as the reaction of Al or Mg with dissolved elements into oxide films, carbides, or borides. Other sources of inclusions can be the formation of nitrides or chlorides due to the use of nitrogen for de-gassing or the addition of salt fluxes. If inclusions are not refined from molten aluminium, they may cause problems during further processing (casting, rolling, machining) or be a source of product defects and, in the worst case, mechanical failure. Some common examples of defects caused by inclusions are pinholes in rolled thin foils and the fracture of wires during drawing [51]. The formation and entrainment of oxide films is another common phenomenon, where the oxide layers fold into bi-films due to the disruption or turbulences in the melt surface and then sink into the melt. The films are hard to detect because, although they can have a large area, they are usually only a few nanometres thick [52]. Indigenous inclusions are generally smaller; hence although their impact is lower, their removal is more challenging [22, 53].

Refining by Degassing

Degassing effectively removes the dissolved H from aluminium, thereby preventing porosity, diminished tensile properties and blistering during rolling and annealing [51]. The process consists of injecting gases (inert, chlorine or a mixture) to generate

bubbles inside the melt, typically by means of lances or porous plugs. Since the partial pressure of H inside the bubbles is very low, hydrogen atoms tend to diffuse into them as they rise through the melt, and once the bubbles surface, the gas is released. Some other elements with higher vapour pressure than aluminium can also be removed selectively by vacuum treatment or by bubbling inert gases through the melt. Table 2 shows the thermodynamic limits of vacuum refining at 1000 K.

Table 2. Minimum concentration in Al melts achievable by vacuum refining at 1000K [51].

Dissolved Element	Composition, ppm
Na	3.7×10^{-7}
Cd	7×10^{-6}
Zn	3.3×10^{-4}
Mg	1.3×10^{-2}
Li	3.4×10^{-2}
Pb	0.11
Bi	0.41
Ca	39
In	110
Sb	310

The table shows that Na, Cd and Zn can be refined to the lowest concentrations. Removal rates can be increased by lowering the gas p_{H_2} by inducing vacuum or by bubbling gas into the melt, raising the temperature, stirring, or increasing the gas-melt surface area by introducing more and smaller gas bubbles [51] [50].

Refining by Fluxing

Refining reactive metals can be achieved by chemical and de-wetting reactions caused by adding *fluxes* into the melt. Traditionally, the fluxing agent was chlorine gas introduced in the melt by lances or porous plugs [50]. Currently, it is more common to employ chloride-based salt mixes, sometimes with small additions of fluorides. These pose lower environmental and health risks, for instance, related to the formation of $AlCl_3$ (g), HCl (g), and leaks of unreacted Cl_2 (g) [22], than chlorine gas while achieving similar purity targets. Since the concentration of Al is much higher than any of the other elements, the first chemical reaction taking place when adding fluxes into

the melt is the formation of aluminium chlorides or fluorides. Subsequently, these react with the impurity metals (Ca, Li, Na, Mg, or Be), forming their chlorides/fluorides. Examples of these refining reactions are described below for the removal of dissolved Ca and Mg.

$$2\ AlF_3 + 3\ \underline{Ca} \rightarrow 2\ Al + 3\ CaF_2\ (slag) \qquad \text{(Eq. 5)}$$

$$2\ AlCl_3 + 3\underline{Mg} \rightarrow 2Al + 3\ MgCl_2\ (slag) \qquad \text{(Eq. 6)}$$

Utigard [54] evaluated the Gibbs free energy of formation of several non-metallic compounds at the temperatures of re-melting aluminium. The results showed that the fluorides were the most stable thermodynamically, followed by the chlorides, oxides, and sulphides. Hiraki [55] investigated the impurity removal limits of refining by fluxing with chloride salts. According to the results, the main alloying elements in aluminium (Cu, Si, Fe and Mn) are not affected by reactions with chlorine gas in the melt. Only Ca, Li, Mg, Sr, Dy, Ho, La, Ce, Gd are in theory, removable by reaction with a chloride salt-flux.

Other Functions of Fluxes

In addition to refining, the salt fluxes protect the melt from oxidation and promote the coalescence of the aluminium droplets by stripping away the oxide layer they are surrounded by. A drawback of fluxing, besides additional costs and residues generated, is that they can also be a source of metallic losses if metallic droplets are entrapped into the salt slag. To prevent this, it is desired that the fluxes have low viscosity, lower density than liquid aluminium (2.3 g/cm^3) and separate cleanly from the metal. Additionally, it is preferred that they melt at lower temperatures and are cheap, recyclable, non-toxic, non-hygroscopic, and non-aggressive against the refractories [22]. The salt fluxes that best meet these requirements are mixtures of NaCl and KCl. Using equimolar proportions is beneficial for the process performance due to the lower melting temperature of the mixture, as shown in the phase diagram below.

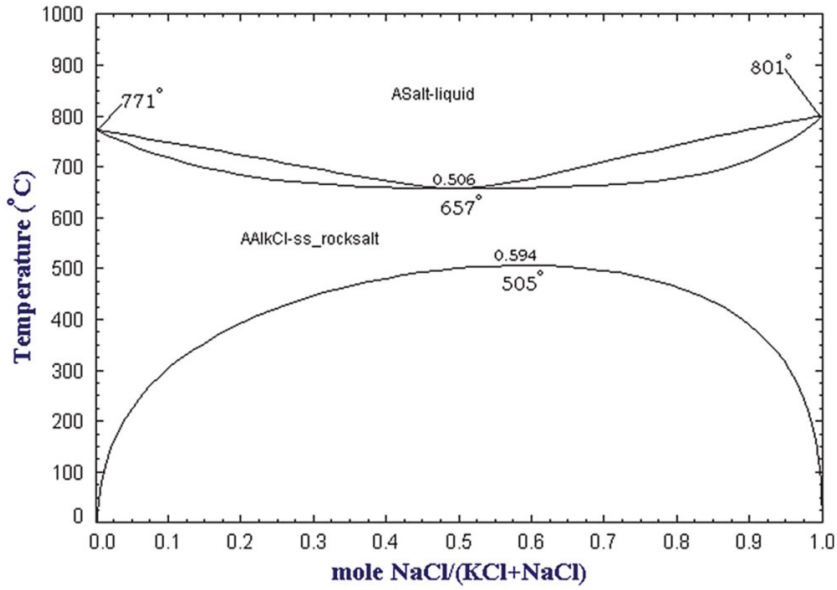

Figure 12. The NaCl-KCl binary phase diagram at atmospheric pressure, as calculated from the FactSage™ FTsalt database [2]. Reproduced from Milani and Timelli, Solid Salt Fluxes for Molten Aluminum Processing – A review. Metals 2023 MDPI. doi.10.3390/met13050832. Creative Common CC BY license.

However, due to the lower cost of NaCl, mixtures with higher ratios of NaCl are also common. While these fluxes are effective at limiting oxidation and separating oxides, it has been demonstrated that small additions of fluorides promote oxide removal and increase the coalescence efficiency significantly. Examples of fluorides are cryolite (Na_3AlF_6), NaF, KF, K_3AlF_6, $KAlF_4$, CaF_2 and AlF_3.

There is extensive research published on the mechanisms behind oxide stripping and metal coalescence, which was recently summarised in a review article by Milani [2]. There is general agreement on the positive effect of small additions of fluoride compounds [54, 56, 57], which is explained by two main mechanisms or their combination:

- The generation of cracks on the oxide layer due to partial dissolution and stresses generated by chemical attacks or thermal stresses [57-59].
- The detachment of the oxide layer due to adjustments in the interfacial tensions and wettability between metal, oxide, and flux. The fluorides promote the adsorption of tension-active elements (Na, K), decreasing the metal surface tension [57, 60, 61].

Refining by Sedimentation, Floatation, and Filtration

Some inclusions may be intrinsic in the re-melted scrap, while others are intermediate products formed deliberately to refine dissolved elements. This is the case of refining by fluxing, discussed in the previous section, where elements with a high affinity for the impurities are added. Regardless of their origin, the inclusions need to be removed, and this is usually achieved by three main refining mechanisms: sedimentation, floatation, and filtration.

Sedimentation consists of the natural settling of inclusions to the bottom of the furnace. The rate at which particles are settled in a fluid generally increases with lower fluid densities and kinematic viscosities, larger inclusions, and more significant differences in densities between the inclusion and the fluid. The removal of inclusions by sedimentation is more challenging in aluminium than in other metals because the density of liquid aluminium (2400 kg/m^3) is very similar to that of many of the inclusions (Al_2O_3, $NaAlF_6$ (cryolite), TiB_2). The oxide layers are also challenging to remove by sedimentation, since they can fold into bi-films with entrained aluminium [51].

Floatation consists of removing inclusions by their attachment to gas bubbles. In this case, the inclusion removal rate increases with larger particle sizes, higher gas flow rates, higher furnaces, and smaller bubble sizes, providing more relative surface area. The rate also depends on the collision efficiency, which is the square of the ratio of the inclusion diameter to the bubble diameter [22]. The inclusions are carried up to the surface due to the surface tension, and the bubbles also refine the aluminium from hydrogen or dissolved elements (e.g Na), as covered in the previous section on de-gassing and fluxing.

Filtration is another effective method to remove inclusions suspended in the melt, primarily solid inclusions and oxide bi-films. There are two main types of industrial filtration for aluminium recycling: cake filtration and deep bed filtration, which rely on physical separation mechanisms, either by mechanically blocking the particles or by their adhesion to the filter surfaces. These mechanisms were illustrated by Bergin in a recent doctoral thesis focused on the performance of ceramic foam filters (CFFs) and are shown in Figure 13 [62].

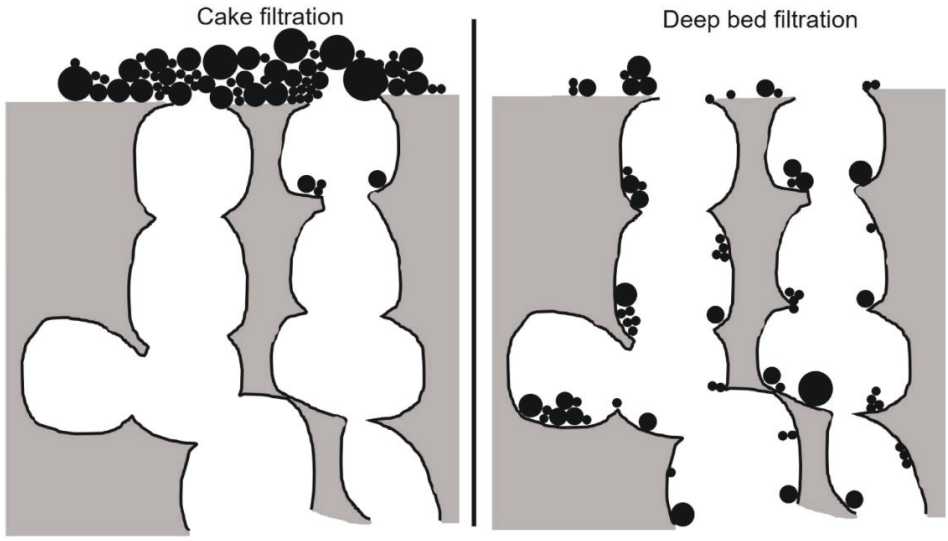

Figure 13. Illustration of the mechanisms of cake filtration, where inclusions are captured at the entrance of the filter (left) and deep bed filtration, where the filter captures inclusions through the whole filter thickness (right). Reproduced from Bergin, PhD Thesis Ceramic Foam Filters (CFFs) for Aluminium Melt Filtration -Stability, Compression, and Performance [62] with permission.

A cake filter relies on having pores smaller than the inclusions so that they are stopped at the surface of the filter. They are rarely used due to the high pressure needed to force metal through the filter. In deep-bed filtration, the solid inclusions are much smaller than the filter pores and channels, so they get attached to the inner walls of the filter rather than the surface. Therefore, this method relies on the previous removal of larger particles by other techniques, such as floatation. The efficiency of the filtration increases for larger size of the inclusions, larger filter surface area, increased tortuosity, filter depth and lower flow velocity [51].

Other Refining Methods

- Three-layer electrolysis. A possibility to refine the alloying elements (Fe, Si, Cu) not removable by fluxing is using the three-layer electrolytic method, a technique which allows refining aluminium into high purity Al (>99.99 %). This process is based on a three-layer electrolytic cell, where the impure aluminium becomes purified as it is transported through the layer of molten salts [61]. However, this process is energy intensive, consuming around 17-18 kWh/kg Al, so its practical applications are limited to producing Al of extremely high purities [63].

- Fe-intermetallic precipitation. Researchers in the Al recycling industry have focused their efforts for decades on developing methods which refine the iron from Al [64] since it is one of the most common impurities and has a maximum tolerance of around 1 % in many applications. A well-established technique is precipitation, where Mn or Cr are added to molten Al to form Fe-rich intermetallic particles, which can then be removed by sedimentation [65, 66], electromagnetic separation [67, 68] or filtration [69].
- Fractional crystallisation removes unwanted elements from the melt based on the segregation of impurities upon controlled melt solidification. The two main approaches are suspension crystallisation, where crystals grow freely in the melt, and layer-based methods, where crystals grow in a layer formed on a cool surface. Suspension crystallisation offers the advantage of larger solid/liquid interface areas but at the expense of a more challenging separation of the crystals later [70]. Both techniques are based on slow solidification, where the unwanted impurities cannot be accommodated in the growing solid crystals and tend to segregate at the liquid/solid interfaces. This leads to a concentration gradient through the solidified material, which depends on the reaction kinetics, diffusion, stirring, crystal sizes, and growth speed [71]. The fraction of the material with a high content of impurities is then discarded, and the process is repeated until it reaches the purity target. Some investigations propose fractional crystallisation as a technique to refine secondary aluminium melts [72], and several recent doctoral thesis focused on this topic: Vendetti [73] evaluated some experimental parameters affecting the fractional crystallisation process for aluminium. Lerma [36] developed a model to assess the theoretical refining performance of fractional crystallisation for recycling aluminium aircraft scrap, and Curtolo [74] modelled and designed a immersed rotational crystalliser able to purify for the first time germanium from aluminium.

2.5 Recycling Challenges

2.5.1 Metal Losses

Oxidation

All aluminium products are covered by a thin layer of aluminium oxide, which forms spontaneously following the reaction:

$$4Al + 3O_2 = 2Al_2O_3 \qquad \text{(Eq. 7)}$$

At room temperature, the nanometre-thick-oxide layer is stable, protecting the metal below from further oxidation. At higher temperatures, the rate of oxidation increases, and with it the thickness of the oxide layer. When the aluminium is molten, the oxide layer, less dense than the metal, floats on top of the melt and protects it from further oxidation. However, this oxide layer is repeatedly disrupted due to operations such as stirring or charging scrap or alloying elements, exposing more metal to the oxidising atmosphere. Before casting, the top layer of the melt is skimmed to separate the floating non-metallics from the metal, generating dross residue: a mix of oxides, other non-metallic compounds, and entrapped aluminium. Traditionally, dross was disposed of at landfills, but today, it is considered a valuable resource due to its metallic content (typically 15-80 %), which can be recovered by re-melting in rotary furnaces with salt fluxes. Still, a review from 2020 [75] reported that nearly half of the aluminium dross generated globally was still disposed of at the landfill.

Oxidation is the leading cause of metal losses during aluminium recycling, and minimising it is of great interest from economic and environmental perspectives. Strategies to prevent oxidation include:

- Reducing the surface area of metal exposed to the atmosphere (e.g., by scrap compaction or furnace design)
- Using drossing fluxes (molten salts) or using inert or reactive cover gases
- Control of furnace temperature
- Minimizing exposure time to high temperatures or oxidising the atmosphere of the metal products and metal-containing residues, e.g., by dross or salt-slag cooling

Metal Entrainment in Dross and Salt-slag Residues

The metal recovery is the *mass fraction of metal recovered after re-melting compared to the initial amount of metal in the scrap*.

$$\%\, Metal\ recovery = \frac{Mass\ of\ metal\ \text{recovered after re–melting}}{Mass\ of\ metal\ in\ the\ scrap} \quad \text{(Eq. 8)}$$

However, the exact metallic content of the scrap is often unknown. Hence, the metal yield is the most common measure to discuss the recyclability of scrap or the performance of the recycling processes. The metal yield is *the mass fraction of metal recovered after re-melting with respect to the initial mass of the scrap recycled*:

$$\%\, Metal\ yield = \frac{Mass\ of\ recovered\ metal\ after\ re–melting}{Mass\ of\ the\ scrap} \quad \text{(Eq. 9)}$$

Table 3 below lists several types of aluminium scrap and their metal yield specifications.

Table 3. Metal yield specifications for types of scrap according to the standards [76-79].

Scrap	Metal* Yield (wt%)	Other specifications
UBCs	≥ 88	The scrap must contain ≤ 2 wt%. Moisture and ≤ 5 wt%. volatiles.
Used packaging	≥ 28	Steel packaging shall be tolerated up to 5 wt%. The scrap shall be free of plastics or paper, even if metallised. No manufacturing scrap from pharmaceutical blisters is permitted. The scrap shall not contain more than 60 % weight volatile substances unless previously agreed.
Packaging (de-coated)	≥ 80^{+}	The scrap shall not contain free iron, the de-coating shall not heavily oxidise it, and it shall not contain fines less than 1 mm in size and be free from non-metallic foreign materials.

* Minimum metal yield related to the mass in the as-delivered conditions.
$^{+}$Different de-coating processes can lead to different values for metal yields. Typical % of volatile substances removable with a thermal process can vary between 25 % and 60 % mass fraction.

A critical source of metallic losses, lowering the metal yields, is the reaction of the molten metal with oxygen, nitrogen, carbides or other elements, forming dross, a mix of non-metallic-compounds (NMCs) and entrapped metal that float on top of the melt due to their lower density. The dross is separated from the melt before casting by

skimming, which also removes the top layer of molten metal. Some research studies measure the mass percentage of the dross formed with respect to the scrap charged [29, 31, 32].

$$\%\, Dross = \frac{Mass\ of\ dross}{Mass\ of scrap\ charged} \qquad \text{(Eq. 10)}$$

In addition, in some studies [32], the metal content of the dross is calculated by another re-melting treatment in salt, and the recovered metal is included in the Metal Yield calculated.

$$\%\, Total\ metal\ yield = \frac{Mass\ ingots + (Mass\ dross * \%dross\ metal\ content)}{Mass\ of metal\ re{-}melted\ (scrap{+}heel)} \qquad \text{(Eq. 11)}$$

In the case of re-melting processes using salts such as rotary furnaces, the primary source of metallic losses are the metal pieces which are not poured out of the furnace together with the rest of the melt but stay trapped within the salt slag residues. A common way to study this phenomenon in laboratory-scale experiments is to calculate the coalescence or coalescence efficiency, as in [43, 80, 81]. Higher degrees of coalescence in the recovered scrap indicate a lower risk of metal entrapped in the salt slag. The coalescence can be calculated through crucible experiments as the combined weight percentage of the recovered pieces over a defined weight or size, or as the percentage of mass recovered which was merged into the larger piece.

Thus, it is vital to carefully read the definitions used before comparing literature results. Moreover, the amounts of metal lost to dross or salt slag residues depend on multiple factors, as the furnace characteristics, the alloying elements, the amount and composition of the fluxes added and the operating conditions. When linking the industrial processes to scientific research studies, the indicators discussed (Metal Yield, Coalescence, Dross…) should not be directly compared if operating conditions are not the same. Instead, the objective should be to compare trends. For example, various studies report an increase of metal losses to salt slag with increased organic content in the scrap [32, 39, 82]. Such trends can also be expected in the industrial processes, revealing strategies for their optimisation, as discussed by Capuzzi in [83]. The table below summarises the literature investigating the influence of scrap properties and pre-treatments on re-melting

Table 4. Literature on the effect of scrap properties and pre-treatments on re-melting losses.

MAIN AUTHOR	YEAR	SCRAP TYPE AND PRE-TREATMENTS	RE-MELTING METHOD	SELECTED RESULTS
ROSSEL, H. [28]	1990	Heavy scrap, crop material, shear scrap, thin sheets. Varied thickness (0,15/ 2/20/200 mm) and Mn/Mg contents. Samples 200 kg.	Fired hearth-furnace (industrial scale). Varied temperatures (700/750/800/900 °C).	Melt loss increased for higher Mg contents, higher temperatures, and thinner scrap.
MCAVOY, B. [33]	1990	Painted, thermally de-coated and bare shreds with varied Mg contents (AA5182/AA3105/AA3003).	Crucible (lab-scale), with and without salt-flux.	Melt loss increases with Mg content and the presence of paint. De-coating reduced melt-losses for low Mg contents. Salt-flux reduced melt losses of high (4.5 %) Mg content.
XIAO, Y. [80]	2002	Al turnings of different sizes, some contaminated by oil or plastics.	Crucible (lab-scale) with salt-flux at 800 °C, N_2 atmosphere.	Higher metal yields and coalescences for larger scrap sizes and lower contamination.
XIAO, Y. [82]	2005	Cast ingots/profiles/rolling mill cuttings/ printing plates/fridge shreds/bottle caps/car plates/granules/turnings/margarine foils. Samples 20-40 g.	Crucible with salt-flux (lab-scale), 2 hours holding time at 800 °C.	More non-metallic contaminants, smaller sizes and higher specific surface areas lead to lower metal recovery and coalescence. Organics led to more carbides in salt-slag.
VERRAN, G.O. [84]	2007	Briquettes of UBCs. Samples 1.3 kg.	Crucible (lab-scale) in an induction furnace, various temperatures,	Re-melting yield increased by flux additions, higher temperature and flux/metal stirring. Decrease in Mg content after re-melting.

MAIN AUTHOR	YEAR	SCRAP TYPE AND PRE-TREATMENTS	RE-MELTING METHOD	SELECTED RESULTS
			various salt-flux additions, flux/metal stirring or not.	
AMINI MASHADI, H. [85]	2009	Turning scrap of AA336 alloy, loose and pressed into briquettes.	Crucible (lab-scale) at 750 °C. Melting scrap alone, scrap + heel and scrap + salts.	Melting in salt-flux reduce metal losses, compaction effect was negligible. Re-melting without salts: higher compactions reduced metal loss.
PUGA, H. [29]	2009	Machining chips of AlSi12Cu1 alloy decanted and centrifuged to lower moisture content and pressed into briquettes of various densities.	Crucible (lab-scale) in resistance and induction furnace, degassing by various methods at varied temperatures (800, 850, 900 and 950 °C) and atmospheres. Scrap fed into a molten heel by automatic feeder, avoiding exposure to furnace atmosphere.	Induction furnace, inert atm. And temp. ≥ 850 °C reduced dross amount and promoted metal recovery. Ultrasonic degassing preferred to gas purging.

MAIN AUTHOR	YEAR	SCRAP TYPE AND PRE-TREATMENTS	RE-MELTING METHOD	SELECTED RESULTS
PUGA, H. [9]	2013	Same as previous [29]	Same as previous.	Intermediate briquette (2.09 g/cm^3) density and inert atmospheres gave higher metal recovery and lower dross formation.
HU, Y. [19]	2011	Combusted packaging waste of various thicknesses: UBCs, foil container, foil	Metal content analysed from hydrogen measured from sodium hydroxide solution.	Thinner packaging (thin foils) tends to form smaller IBA (<2mm) and have lower metal recovery rates than thicker packaging (foil containers UBCs)
BIGANZOLLI, L. [20]	2013	Packaging (UBCs/trays/paper-laminated foil/foil mixed with poly-laminates) recovered after incineration.	Melting in crucible with salt-flux (lab-scale) and soda metal content analysis as in [19] in various stages	From highest to lower recovery: UBCs, trays, paper laminated foil and a mix of poly laminated foil.
DITTRICH, R. [40]	2013	Pyrolysis gases (CO_2/CO/C_xH_y) injected to melt (1 kg) to simulate the effect of submerging scrap with organics.	Crucible (lab-scale) in induction furnace at 750 °C.	CO_2 and CO increase the dross generation.
THORAVAL, M. [81]	2015	Chips of 3104 alloy, oxidised	Lab-scale rotary furnace at 750 °C. Variations in flux composition and time.	Oxide content in slag lowers coalescence, and 2 % cryolite additions were optimal for ≤20 % oxides.

MAIN AUTHOR	YEAR	SCRAP TYPE AND PRE-TREATMENTS	RE-MELTING METHOD	SELECTED RESULTS
CAPUZZI, S. [43]	2017	Coated and uncoated discs of AA3000 alloy. Subsets thermally treated at 400/500/600 °C or untreated.	Crucible (lab-scale) with salt-flux in electric furnace at 790 °C.	The coating hinders Al coalescence. This is prevented by thermal de-coating at 500 or 600 °C.
STEGLICH, J. [31]	2017	UBCs pre-treated in a steel cylinder at different atmospheres.	Crucible (lab-scale) in induction coil furnace with Ar gas shield.	Thermally treating at a lower temp rate reduced the metal lost to dross, but the treatment at high temp. oxidised the bales and led to equal amounts of dross than untreated UBCs.
STEGLICH, J. [32]	2020	UBCs of various densities and organic content. Subsets untreated or de-coated at 450/550 °C under atmospheres Ar, Ar+ 4 % O_2 and air.	Crucible (lab-scale) in an induction coil furnace with the molten heel at 750 °C.	De-coating reduced dross formed if stoichiometric thermolysis is applied at 550-570 °C for 30 minutes. De-coatings for Ar, 450 °C and compact bales increase dross.
GÖKELMA, M. [39]	2020	Coffee capsules: used with coffee residues non-used with or without coffee powder. A subset thermally de-coated at 500 °C.	Crucible (lab-scale) at 800 °C, with salt flux and manual stirring.	De-coating improves scrap metal yield and coalescence. Coffee and water residues reduce yield drastically.
CHAMAKOS, N. [87]	2023	UBCs de-coated in industrial multichamber furnace, lab-scale, and simulations. Bale temp. of 400/580 °C.	No re-melting.	Delacquering degree dependence on temperature, time, oxygen flow and compaction. Bale thermal treatment temp. at surface 500 C, at centre˜100 °C.

2.5.2 Secondary Metal Quality

Even if aluminium recycling is increasing globally, its quality, or more specifically, the high content of impurity and alloying elements in recycled aluminium, is one of the reasons why it still does not substitute primary aluminium in many applications. This comes as a direct consequence of the scrap composition and the limitations of the current industrial refining processes. Regarding the scrap composition, the unwanted elements may originate from the mix of alloys, or from contamination, e.g. from coatings or residues.

The refining processes for aluminium were previously described. Due to aluminium's high reactivity compared to the impurity elements, refining many of them at an industrial scale is not economically viable. Thus, two alternative strategies are followed to deal with mixed contaminated scrap and recycled aluminium of increasing impurity concentrations: dilution and cascading, illustrated in Figure 14.

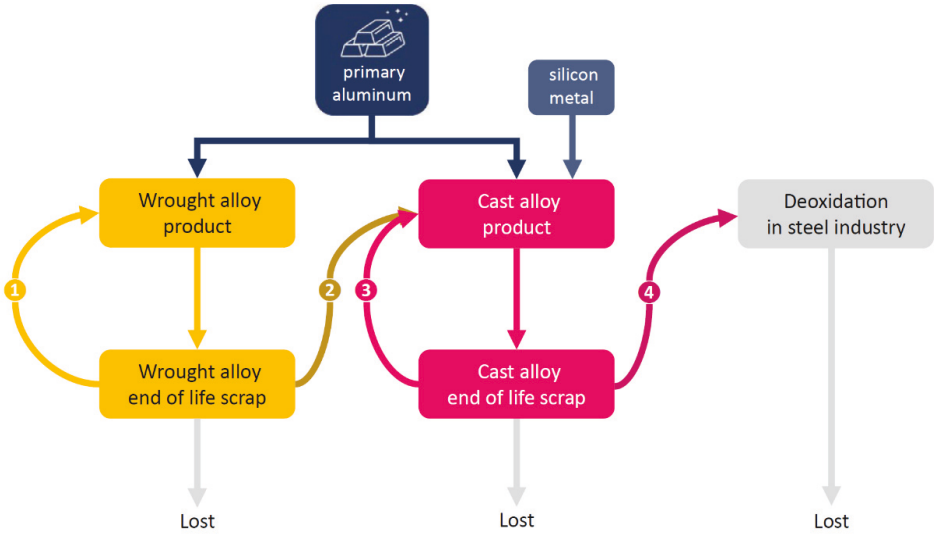

Figure 14. Progression of alloys in recycling. ① Recycling to wrought alloy; ② wrought alloy recycled into cast alloy; ③ recycling to cast alloy; ④ final use as deoxidant. This image is reprinted from [88] Handbook of Recycling: State-of-the-art for Practitioners, Analysts, and Scientists, Chapter 20, Doutre and Kvithyld, Aluminium, pag 322, Copyright Elsevier (2023), modified from Tabereaux and Peterson (2014) [4] with permission © 2014 Elsevier Ltd.

- Dilution: Mix with aluminium of higher purity, e.g., primary.
- Cascading/downgrading: Use the secondary metal for alloys with a higher allowance for impurities or alloying elements. A typical example

is recycling wrought alloys such as aluminium packaging to produce cast alloys of significantly higher concentrations of some elements, such as silicon, for automobile engine components.

Table 5 below shows the composition requirements of different categories of post-consumer packaging scrap. The packaging scrap is often made of wrought alloys, which have higher purity (e.g., lower Si content) than the cast alloys used in automobile components.

Table 5. Composition (wt%) requirements of scrap according to standard EN 13920:2003 [76-79].

Scrap	**Si** max	**Fe** max	**Cu** max	**Mg** max	**Ni** max	**Zn** max	**Ti** max	**Pb** max	**Sn** max	**others each** max	**others total** max	**Al*** min.
UBCs	0.30	0.50	0.20	1.30	0.01	0.05	0.05	0.01	0.05	0.05	0.15	remainder
Used packaging	1.00	1.00	0.40	0.20	0.80	0.20	-	0.20 (Pb+Sn)		0.10	-	remainder
De-coated packaging	1.00	1.00	2.50	0.40	0.20	0.80	0.20	0.20 (Pb+Sn)		0.10	-	remainder

*The aluminium content is the difference between 100 % and the total of all the elements present with values no less than 0,010 % rounded to the second decimal (before the calculation is made).

Van den Eynde estimated in [89] the global flows of aluminium by the year 2030 for each alloy series.

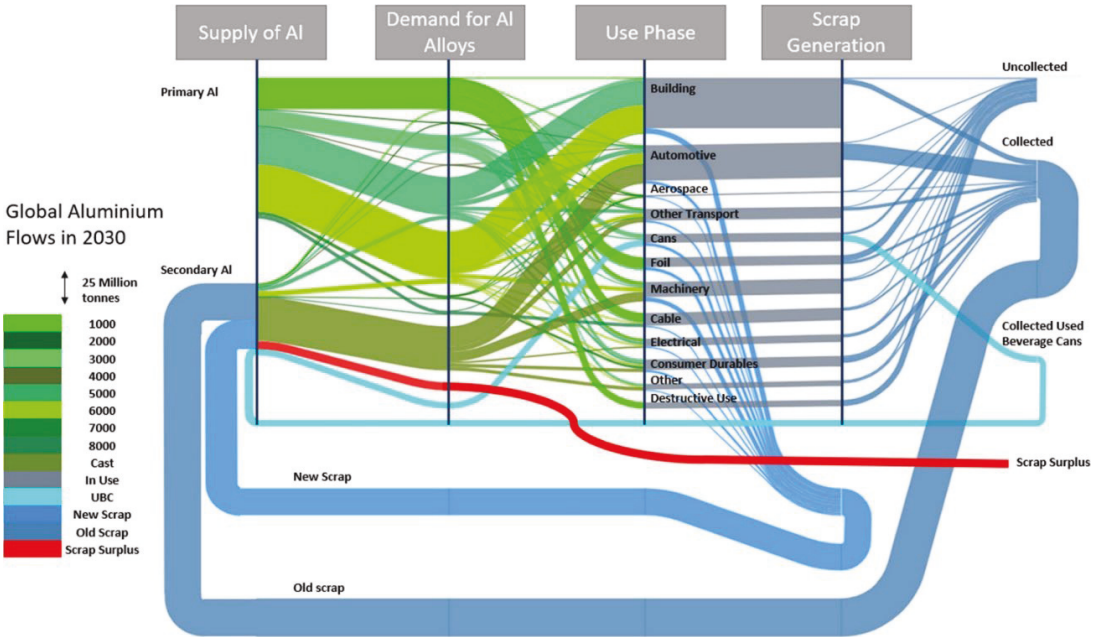

Figure 15. Sankey diagram representing the global aluminium flows in 2030, shades of green represent the alloy series (1000–8000 + cast). Reprinted from [89] "Forecasting global aluminium flows to demonstrate the need for improved sorting and recycling methods, Van den Eynde et al, Waste Management 137, pp. 231-240, 2022", with permission © 2014 Elsevier Ltd.

Downgrading is shown in Figure 15 by the fact that most secondary aluminium produced is cast alloys for the automotive industry, while applications using wrought/purer alloys, as cables or foils are mainly sourced by primary aluminium. Even though downgrading and dilution are effective ways of bringing recycled materials back into use, in the long-term, they can lead to a situation where the demand for primary aluminium keeps increasing even if recycling increases since it is needed to dilute scrap of gradually lower quality. The concern over the accumulation of impurities in recycled aluminium has been raised in several studies, such as Løvik [90], suggesting this may be an issue even with closed-loop recycling systems. Sevigné-Itoiz [91] warns in its sustainability assessment about a surplus of aluminium scrap in Europe in the coming years, which will become a lost opportunity unless more efficient management routes are implemented. The potential surplus of Al scrap is also illustrated in the Sankey diagram of Figure 15, where Van der Eynde estimates it to reach 5.4 million tonnes/year by 2030 [89], and highlights the need of implementing improved sorting and recycling strategies. The criticality of optimising

aluminium collection and sorting techniques is also emphasised by Castro [92], who evaluated which metals can be mixed in recycling processes, considering the subsequent refining possibilities for each material combination. According to their decision tree, separating aluminium wrought alloys from cast alloys and avoiding the contamination of wrought alloy recycling streams by steel, copper, zinc, and lead is critical. In the case of recycling aluminium cast alloys, it was claimed essential to avoid contamination by lead, zinc, and Pt-alloys, as well as by steel and cast iron. In contrast, separating wrought aluminium, copper, and magnesium alloys was not critical but recommended. Understanding the consequences of mixing alloys and introducing impurities in secondary Al melts is essential to achieve more sustainable aluminium production. This knowledge should be considered when selecting alloys for products, designing new alloy specifications, and evaluating waste management and recycling routes to increase the circularity of aluminium products. The environmental benefits of substituting primary aluminium production by recycling are discussed in the following section.

2.6 Environmental Impacts of Al Recycling

Recycling aluminium is more sustainable than primary production mainly because it avoids the substantial use of energy and resources required for mining and processing the raw materials in primary production. Specifically, the Hall-Héroult process, where aluminium metal is extracted from alumina, is the most energy-intensive step with approximately 14 MWh of energy consumed per tonne of aluminium produced [93]. According to a recent review, producing 1 tonne of primary Al releases between 14 and 17 metric tonnes of CO_2 equivalent from the bauxite mine to casting the metal. From these, the dominating part of the emissions are indirect, released in electricity production for electrolysis, and will therefore directly depend on the source of electricity [94]. In comparison, the process of extracting aluminium from scrap by re-melting in a rotary furnace with salts is much more energy efficient; 0.55-0.70 MWh (2–2.5 GJ) per tonne of aluminium produced, and the total specific energy required for producing 1 tonne of secondary aluminium in Europe ranges between 0.55-2.50 MWh (2-9 GJ), depending on the quality of the scrap and the processes involved [46]. Another benefit of the secondary production route is that it does not generate bauxite

residue, commonly known as “red mud”, a hazardous waste [95] which can pose significant environmental risks [7].

The process of re-melting via a rotary furnace allows an efficient recovery of the aluminium from contaminated or oxidised scrap/side streams, as explained in the previous chapters. However, this process leads to the generation of significant quantities (ca. 500 kg/tonne of Al produced) of another residue: salt slag – a mixture of non-metallic compounds (NMCs), salts, and aluminium metal. The salt-slag residue from secondary aluminium production is classified as hazardous waste and its disposal in landfills is forbidden in Europe. The Environmental Protection Agency of USA published a detailed report about the reactivity and characteristics of salt slag, as well as the risks of its disposal at landfill [96]. The current alternative approach to handle this residue is to treat it for partial or total recovery. The total recovery route consists mainly of crushing the salts to separate the trapped aluminium droplets and then use water/water vapour and moderate temperatures to dissolve and then recrystallize the salts, separating them from insoluble non-metallic-compounds (NMCs) as oxides [97]. This process allows recovering on one side salts and Al concentrates which can be fed back into the rotary furnace process, and on the other side ammonium sulphate and NMCs which can be used by the chemical, agricultural or construction industries [46-48]. A recent study [98], also described the production of zeolites, promising for applications such as removal of metal ions from aqueous affluents, from the valorisation of salt slag through a similar process.

There is a debate in the aluminium industry regarding which is the most environmentally sound route for aluminium recycling. The process of re-melting in a tilting rotary furnace with salts has high energy efficiency and performance, but at the expense of potential environmental burdens linked to the usage of salt-fluxes and generation of slag residues which need to be further processed increasing the total demand for energy and resources [46]. Therefore, to better understand this, the study included in Chapter 6 of this thesis analyses the environmental impacts of recycling hard-to-recycle streams (dross, IBA, shavings) in a rotary furnace with subsequent salt-slag treatment.

When assessing the environmental impacts of multifunctional processes, such as recycling systems, the recommended approach as defined by the ISO is system

expansion (substitution) [99]. By expanding the system, the impacts of the alternative production are discounted from the total impact. Therefore, the environmental life cycle assessment (LCA) studies of aluminium recycling generally assume that recycling substitutes primary production, mitigating the need for its associated energy use and emissions (e.g., CO_2, PAHs, and PFCs) and resulting in net impact savings [100, 101]. Since in this studies the avoided burdens due to substitution dominate the overall results, due to the large environmental impacts associated with primary production, considering the underlying assumptions is particularly important for the correct interpretation of the LCA results [102]. This is evident in the environmental assessment of waste management options by Manfredi [103] and the regional variances reported for aluminium primary production emissions presented by McMillan [104]: between 7.07 and 21.9 kg CO_2-eq/kg metal in 2005. Accordingly, Damgaard [100] reported that the reduction of impacts to global warming accomplished by recycling aluminium highly depend on the type and amount of energy used for primary production and its sourcing, leading to variations between 5.0 to 19.3 tonne CO_2 per tonne of Al-containing scrap processed. Liu's review of sustainability studies in the aluminium industry [105] also highlights energy use as a source of uncertainty. In the literature covered by the review, the reported emissions associated with producing a tonne of primary aluminium varied as much as from 5.92 to 41.10 tonnes CO_2 equivalent. Some of the data is represented in the figure below indicating the location and year of the primary production data. Other mentioned challenges include the use of industry-wide inventory data, different system boundaries and diverse assumptions for the allocation of recycling (e.g., recyclability, product lifetime).

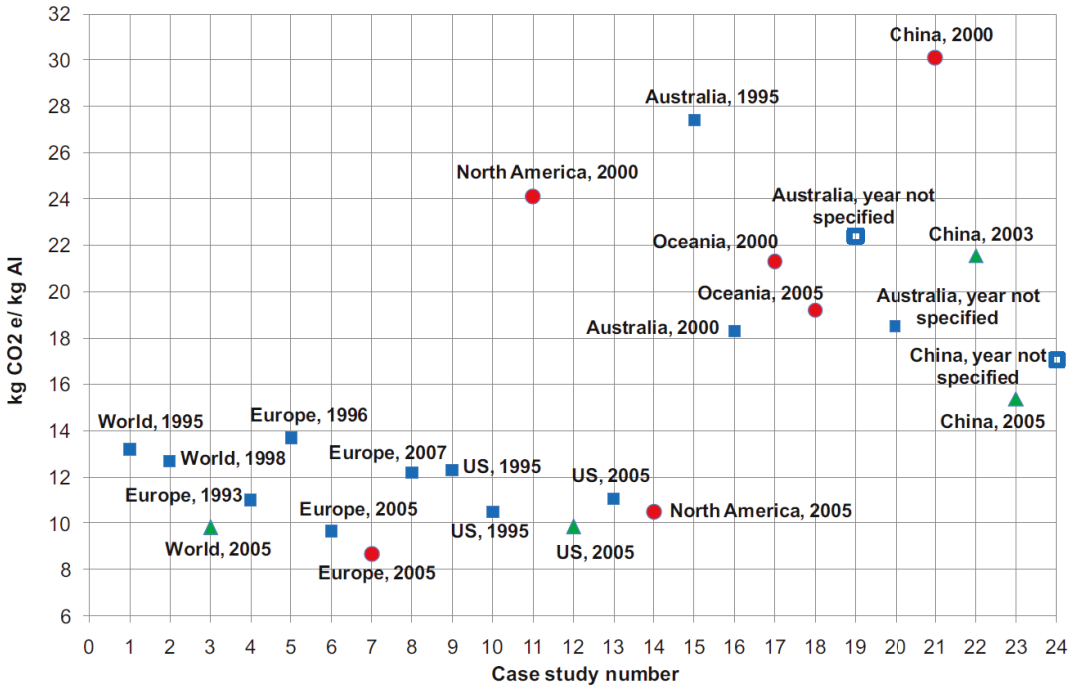

Figure 16. Variability of GHG emissions intensity for primary aluminium production in selected studies. Shapes related to other underlying LCA data assumptions detailed in the source: [105] Copyright © 2012 Elsevier Ltd. All rights reserved.

Chapter 3. Oxidation Losses in Packaging Materials

This chapter summarises the findings published in Articles A and B; *Compaction of aluminium foil and its effect on oxidation and recycling yield* and *Characteristic properties and recyclability of the aluminium fraction of MSWI bottom ash*.

3.1 Introduction and Motivation

The aim of this research line was to investigate the influence of scrap surface area and compaction state on its susceptibility to oxidation and re-melting losses. This was done through two studies. The first one (Article A) looked at the influence of the scrap thickness and compaction state on its susceptibility to oxidation, which was evaluated by thermally treating foils and sheets of various thicknesses. The second study (Article B) evaluated the oxidation state of aluminium incinerator bottom ash (IBA) recovered after the incineration of municipal waste and whether there was a correlation between their surface area, oxide content, and metal composition for different IBA particle size fractions and countries of origin. Finally, both studies tested, through laboratory-scale experiments, the influence of the presence of oxides and/or the compaction state on the re-melting yield and the coalescence when re-melting in salt-flux. The observations identified trends which highlight the importance of the size/surface area properties of the scrap on its re-melting losses due to oxidation and entrapment in salt-slag. In addition, Article A proved the benefits of compacting thin, clean scrap to avoid these losses. The findings are relevant for optimising the recycling process of aluminium scrap of high specific surface areas, such as packaging, foils, industrial shavings/shreddings and IBA.

3.2 Experimental Materials and Methods

3.2.1 Shredding, Compacting, and Oxidising Foils/Sheets

The characteristics of the foils/sheets used in the study are displayed in Table 6. The compositions of the 15 and 30 μm thick materials (household and laboratory foil respectively) were measured with a portable XRF analysis with an error of ±0.4. The specifications of the sheets of AA8006 alloy of thickness 100-300 μm were provided by the producer.

Table 6. Thickness and composition (wt%) of foils/sheets.

Thickness	Al	Fe	Si	Mg	Mn	Cu	Zn	Remaining
15 μm	98.6 ± 0.4	0.73	0.53	<0.16				<0.05
30 μm	98.9 ± 0.4	0.8	0.11	<0.17				<0.15
100, 200, 300 μm	95.9-98.5	1.2-2	0.4	0.10	0.3-1	0.3	0.10	<0.15

The materials were shredded using a Getecha RS 1600-A1.1.1, and the size of the resulting chips was unified using two sieves of square mesh size 2 and 5 mm^2. The average mass per chip after sieving was 6, 12.3, 12.4, 18.2, and 21.8 mg for the 15, 30, 100, 200, and 300 μm thick material, respectively. The chips were subsequently compressed into cylindrical briquettes of 4 cm diameter, each weighing 20 g, using a hydraulic press MTS 311. Three different compaction methods were tested: uniaxial pressure, moderate-pressure-torsion (MPT), and Hot MPT at 450 °C. The MPT method consists of applying torque and uniaxial pressure simultaneously. After reaching the desired compressive force, torque was applied by 4 revolutions at 1.2 rpm. For the Hot MPT method, the mould was pre-heated by induction (EFD induction device MINAC 6/10) to 450 °C before implementing the uniaxial pressure and torque. The internal porosity of the briquettes was characterised by computed-tomography scans (CT). A subset of the chips and briquettes was directly re-melted, while another subset was first thermally treated at 650 °C for one hour in a Nabertherm electric furnace featured with air circulation, to promote oxidation. The weight gain during the thermal treatment was measured and calculated according to:

$$\%\, Weight\ increase = \frac{m_f - m_i}{m_i} * 100 \qquad \text{(Eq. 12)}$$

Where m_i is the initial mass of the samples (approx. 20 g) and m_f the final weight reached after the thermal treatment. The average values were calculated from three repetitions for each sample type/route.

3.2.2 Characterisation of Incinerator Bottom Ash

The aluminium fractions of bottom ash were dry sorted from municipal waste incinerator plants in the USA, UK, and Denmark (DK). The samples from the USA and UK were received in three size ranges (2–6, 6–12, 12–30 mm) while samples from Denmark were produced in two size ranges (2–12, 12–30 mm). Table 7 summarises the characteristics of each of the sample categories. The average aspect ratio was analysed by image analysis for images taken of random batches weighing 50 g (typically 20–150 pieces), and the average weight was calculated from weighing 20 random samples per category.

Table 7. Characteristics of bottom ash for different size fractions and sources.

Country	UK			USA			DK	
Size fraction (mm)	2-6	6-12	12-30	2-6	6-12	12-30	2-12	12-30
Av. weight (g)	0.21	1.25	4.31	0.24	1.07	3.89	0.65	5.04
STD (g)	0.12	0.66	2.36	0.25	0.61	3.44	0.37	5.10
Aspect ratio	0.533	0.471	0.619	0.488	0.611	0.594	0.635	0.527
STD	0.31	0.24	0.16	0.27	0.18	0.20	0.19	0.09
Av. Axis length (mm)	8	11.5	18.4	9	12.1	19.1	11.8	18.3
STD (mm)	2.1	2.1	5.2	2.1	2.9	4.1	3.1	6.6

For the characterisation of oxide thickness and composition of bottom ash, three random samples were picked from each of the eight sample groups. The 24 random samples were mounted in epoxy and sectioned for oxide layer characterisation. The thickness of the oxide was measured at 18 points per sample (6 points in 3 images) using a Scanning Electron Microscope (Zeiss Ultra 55LE FEG-SEM). EDS was used for approximate analysis of the oxide and metal composition for each piece. The Kruskal-Wallis method [106] was used to analyse whether the different size fractions could be considered statistically as identical populations.

3.2.3 Re-melting in Salt-flux

The aluminium foil/sheets and the bottom ash were re-melted using a similar procedure under protective salt flux. The crucibles filled with the mixed salts (68.6 wt% NaCl, 29.4 wt% KCl, and 2 wt% CaF_2) were first introduced into a resistance furnace pre-heated to 800 °C. The melting point of a mixture of 30 wt% KCl and 70 wt% NaCl is approximately 690 °C, and the small additions of CaF_2 increase it by 20–30 °C [107]. Once the salt was melted (after approximately 30 minutes), the aluminium samples were charged into the crucibles. The briquettes were re-melted using 80 g of salt flux (4:1 salt/metal ratio), whereas 150 g of salt flux was used when re-melting the loose chips and 100 g when re-melting the IBA (2:1 salt/metal ratio). Although this salt/metal ratios are far higher than the industrial, they were chosen so that the salt could completely cover the charged materials in the static crucible setup. The density of the molten salt flux was approximately 1.5 g/cm^3 and it was observed that briquettes with lower bulk densities floated just below the surface, whereas the denser briquettes quickly sank into the crucible. After charging the samples, the muffle furnace was closed and held at 800 °C for 10 minutes for the foil/sheets study, with no stirring applied. For the IBA study, the materials (50 g per trial) were charged in 4 batches separated by 15 minutes, and at the end of each experiment, manual stirring was applied for 5 s. Then crucibles were taken out and cooled down at room temperature. The metal and salt were separated in all cases by crushing in a mortar and washing in water on a sieve of 800 square-mesh size µm. During re-melting, typically most of the material coalesced into a main rounded-shaped piece and a few small pieces (Figure 17).

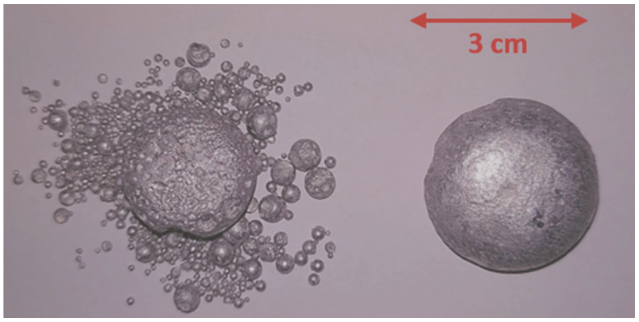

Figure 17. Aluminium recovered from two crucibles. Right: the material coalesced into one piece, so m_r=m_c. Left:m_c (mass of the biggest piece) is smaller than m_r.

The percentage of input material that successfully melted into one piece was defined as coagulation efficiency or coalescence and it is crucial in the industrial recycling operations, where the small pieces tend to remain trapped into the salt slag. The metal yield and coalescence/coagulation efficiency were calculated as follows:

$$Metal\ Yield\ [\%] = \left(\frac{m_r}{m_i}\right) * 100 \qquad \text{(Eq. 13)}$$

$$Coalescence\ [\%] = \left(\frac{m_{droplets>s}}{m_i}\right) * 100 \qquad \text{(Eq. 14)}$$

where m_r is the sum of the masses of the pieces recovered, $m_{droplets \geq s}$ is the mass of the pieces that coalesced into sizes equal to or above certain size limit (s), and m_i is the initial mass of the scrap charged into the crucible. In the foils/sheet study, s was chosen as the size of the largest piece recovered per trial, while in the bottom ash study it was the upper size limit of each size-fraction category; 6 mm, 12 mm and 30 mm for the size fractions 2-6 mm, 6-12 mm, and 12-30 respectively.

3.3. Results

3.3.1 Briquetting Foils and Thin Sheets

A study on the compressibility of the chips was carried out by Philipson [108] as part of a master thesis within the same research project. The compressive forces necessary to achieve similar briquette bulk densities across samples vary due to the different thickness and stiffness of the materials. Philipson defined the shredding and compression parameters required to obtain chips and briquettes of similar characteristics for the five types of foils/sheets tested in the study. The compressive stress required to achieve briquette bulk densities 0.8 g/cm^3, 1.4 g/cm^3 and 2-2.1 g/cm^3 are plotted below in Figure 18 for all the materials, and for a wider range of densities for the two thinner foils in Figure 19.

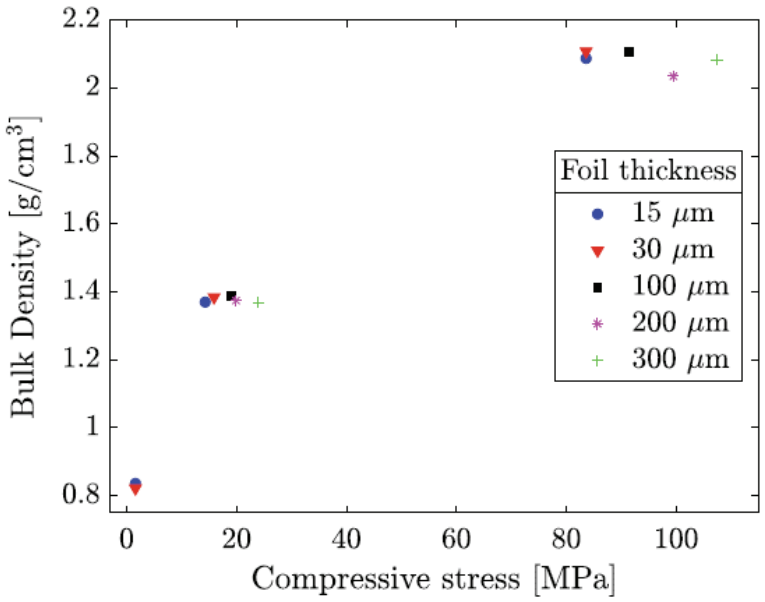

Figure 18. Uniaxial stress versus briquette bulk density for sheet/foil of varied thickness.

Figure 18 shows that the required pressure to achieve the same bulk densities increases with the thickness of the materials. Figure 19 shows how the density increases logarithmically with the applied uniaxial pressure for the thinner foils and stabilises in a plateau around 2-2.2 g/cm^3. Applying torque in addition to the uniaxial pressure by the MPT method was an effective way to drastically increase the density. For example, if the MPT method is used while applying 56 MPa of uniaxial pressure to the materials of 15, 30 and 300 µm thickness, the briquette density increases from 1.8-2 g/cm^3 to 2.5-2.6 g/cm^3. If the mould was heated in addition (Hot MPT method), the bulk density increased to 2.63-2.65 g/cm^3.

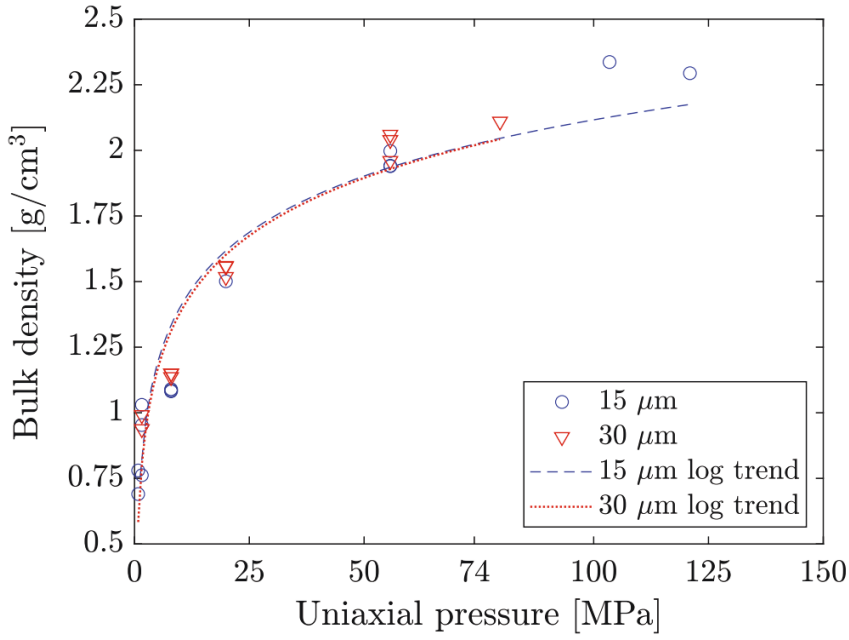

Figure 19. Compressibility curve for the 15 and 30 µm gauge foils, showing a logarithmic behaviour in the uniaxial pressure versus density.

Table 8 shows the internal porosity of several briquettes analysed by CT.

Table 8. Average internal porosity for sheet thickness and density of briquette ranges, measured by CT, in (%).

Thickness	0.8-0.9 g/cm^3	1.1-1.2 g/cm^3	2.0-2.1 g/cm^3	2.4-2.5 g/cm^3
15 µm	57	29	10	4
30 µm	57	45	15	4
100 µm	-	-	17	6
300 µm	-	-	18	4

The relationship between porosity and bulk density was found to be approximately linear; higher bulk densities have lower internal porosity. For briquettes of similar densities, the lowest porosity was achieved for the thinnest foil, but the porosity differences between materials of different thickness significantly decreased for the highly compacted briquettes.

3.3.2 Effect of Compaction on Oxidation and Re-melting Losses

Figure 20 shows the weight increase due to oxidation for briquettes with various material thicknesses and bulk densities when exposed to air atmosphere at 650 °C for 1 hour.

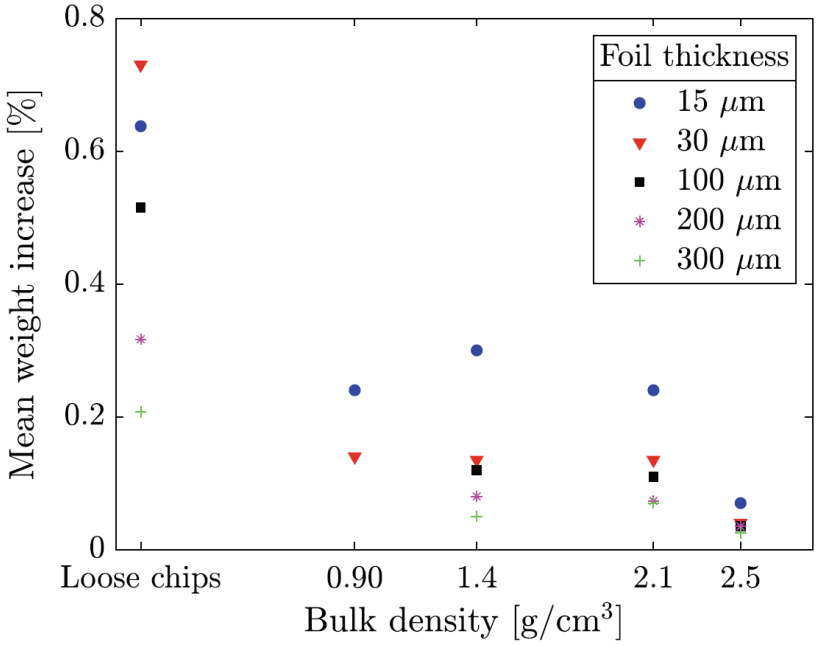

Figure 20. Weight increase after thermal treatment of the chips and briquettes. The bulk density of the loose chips is considered as 0 and the samples initially weighed 20 g.

These results demonstrate that compacting the chips into briquettes is an effective strategy to reduce the susceptibility to oxidation of thin materials. Furthermore, it shows that the degree of compaction of the briquettes does not cause a significant difference between the ranges 0.9-2.1 g/cm^3. However, the implementation of torsion (MPT method) during the compaction, reaching densities of 2.5 g/cm^3 reduces the oxidation susceptibility further. This is consistent with the measured decrease in internal porosity.

Upon re-melting, the oxidation and compaction state influenced the metal yield and coalescence. This is illustrated by Figure 21 for the thermally-treated loose chips and briquettes of the 30–300 µm materials, and in Figure 22 for the 15 µm foil.

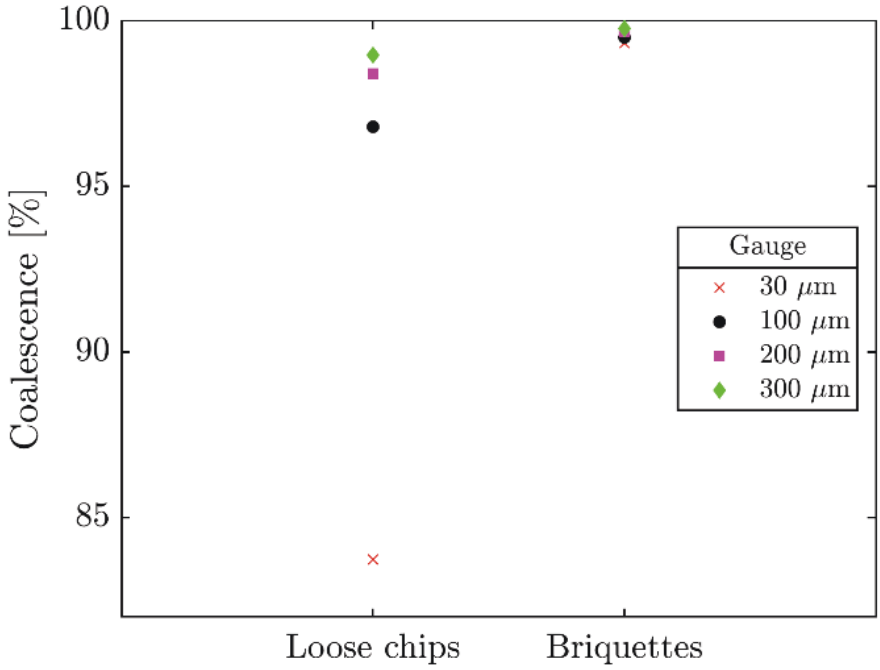

Figure 21. Re-melting coalescence for loose chips and briquettes of sheets of varied gauges.

The variations in briquette bulk density for the material gauges 30, 100, 200, and 300 µm did not have a tangible effect on the re-melting coalescence so all results were averaged. The average coalescence improved due to compaction by 15.6 %, 2.7 %, 1.3 %, and 0.8 % for the 30, 100, 200, and 300 µm materials, respectively.

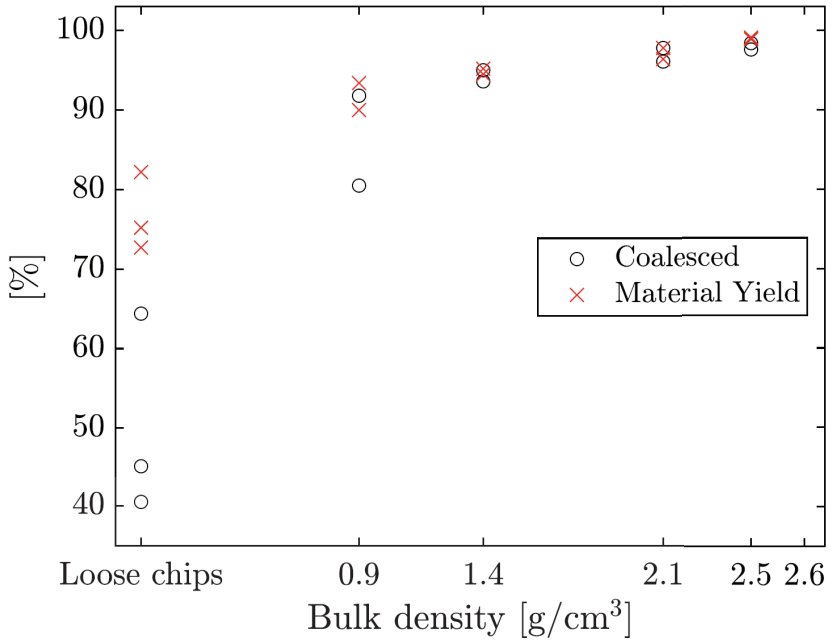

Figure 22. Material yield and coalesced recovery for household foil of 15 µm gauge compacted to different densities. Unit is wt% of the input material, which weighed 20 g.

For the 15 µm foil, the coalescence varied for different bulk densities. The average coalescence improvement when compacting 15 µm foil chips to the lowest density briquettes (0.9 g/cm^3) was 36.1 %. Thus, compaction is especially beneficial for thin household foil, even if it is to low briquette densities. The reasons might be related to several factors such as the improved contact between the chips, decrease in the specific surface area, or increase in thermal conductivity. For the non-heat-treated samples, the metal yield ranged between 98 and 100 % for all thicknesses and degrees of compaction. This indicates that the salt-flux method effectively protected the scrap from oxidation during re-melting, but this may not be the case for other re-melting processes or scrap types, where thickness and compaction could influence the yield and coalescence differently, for instance by affecting whether the scrap floats or not on top of the melt, increasing the dross formation when re-melting in reverberatory furnaces, or whether the scrap oxidises upon charging if it is not directly submerged into molten salts.

3.3.3 Recyclability of Incinerator Bottom Ash

Samples of different size-fractions and origins were analysed by SEM. Figure 23 shows an example of one of the SEM images, where the oxide layer can be differentiated.

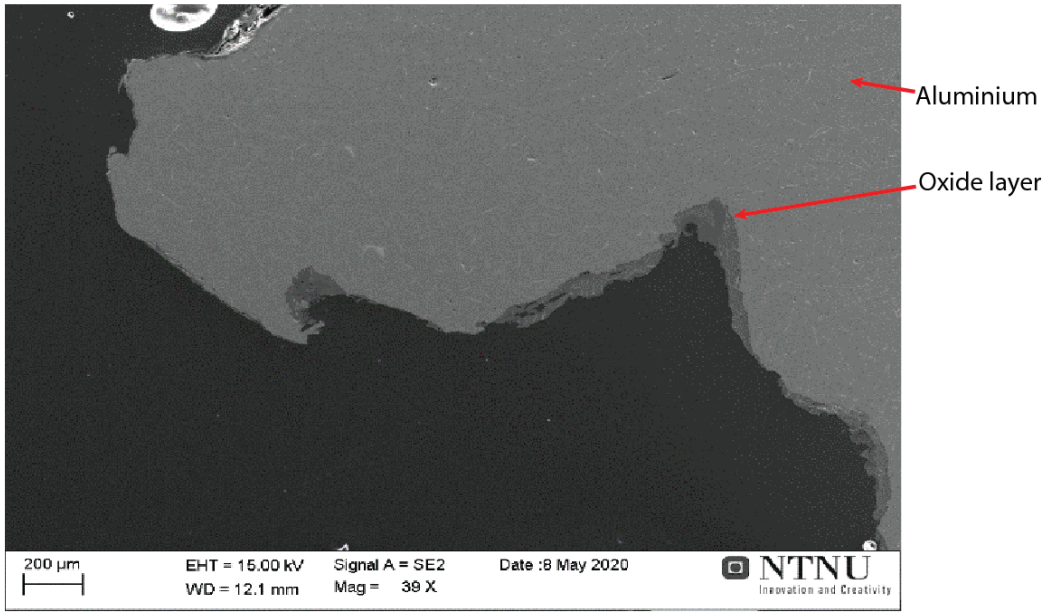

Figure 23. Secondary electron image of the cross-section of sample 24.

Figure 24 shows the oxide layer thickness values for each IBA size fraction and country of origin. Most of the samples showed heterogeneous oxide thicknesses throughout the surfaces, which is the reason behind the large standard deviations.

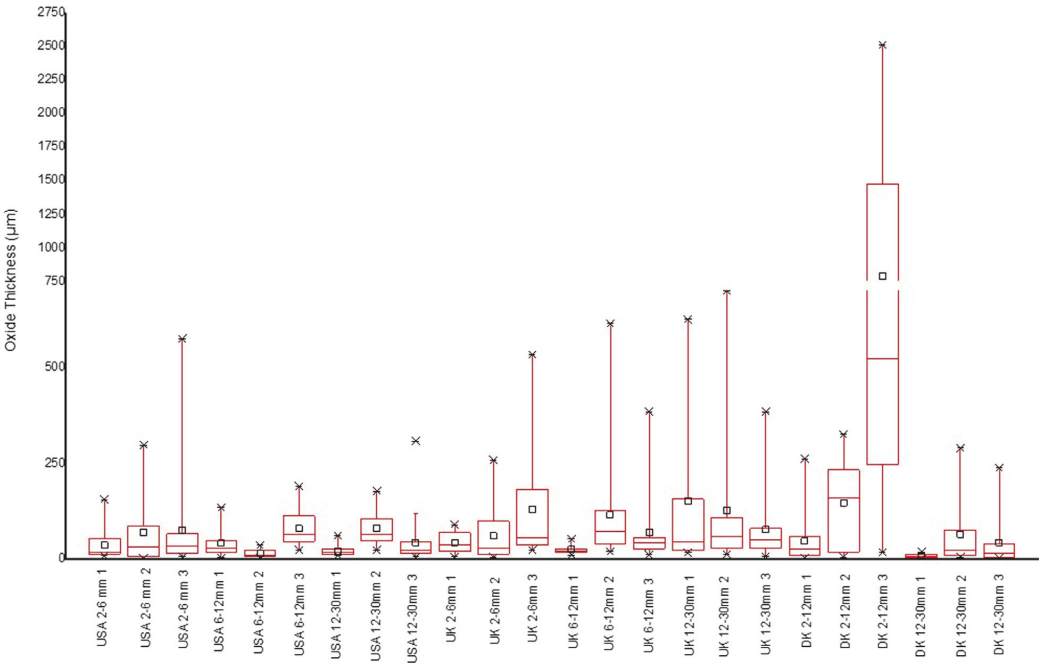

Figure 24.Oxide thickness measurements of 24 aluminium IBA samples.

Although the oxide thickness presents large variations, 80 % of measurements lay below 100 µm and 90 % were below 200 µm. The Kruskal Wallis test was conducted to analyse the statistical differences between samples, and the results can be found in Article B of this thesis [109]. Except for sample 21 which shows the larger STD, the sample groups could be treated as identical populations with a significance level of 5 %, hence the oxide thickness results (omitting sample 21) could be used to calculate an average across all samples. While there was no direct correlation between oxide thickness and magnesium content in the metal of the samples investigated, abnormally thick oxide layers were typically associated with a higher magnesium content in the oxide, illustrating the effect of local breakaway oxidation.

The re-melting trials resulted in metal yields between 76 and 93 % for the different size fractions, as presented in Figure 25.

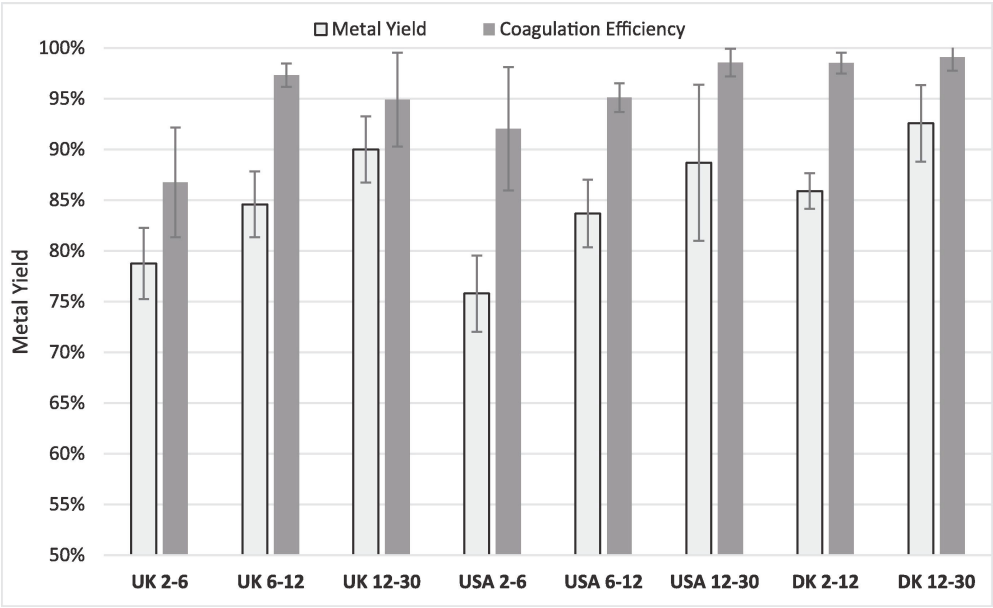

Figure 25. Metal yield and coagulation efficiency after re-melting IBA under salt flux.

The results agree with previous findings in literature: a metal yield range of 82 to 93 wt% for IBA of 5–25 mm size was reported by Gökelma [21], an average of 91.9 % for IBA between 5-50 mm sizes by Syvertsen [110], and the range 77-93 wt% was reported by Hu [19] for household waste composed of different packaging types (beverage cans, containers and foils). The difference in metal yield between the same input material size-fraction for different countries may be partly caused by plant-specific technology and waste residence time during the incineration, as discussed in [20], where residence time between feeding and extraction was 4–6 h in one plant and 9–10 h in other.

There is a direct correlation between the scrap size and its metal yield and coagulation efficiency. Smaller IBA pieces have a larger oxide/metal content because of their larger surface area to weight ratio which made them more susceptible to oxidation during incineration. In addition, the salt flux must dissolve/remove more oxide layer to release the metal from the smaller size fractions during re-melting. Thus, higher specific surface areas and oxide contents affect the metal yield and the coalescence behaviour of molten aluminium in salt-flux negatively.

A simplified model, calculating the theoretical metal yield as a function of the sample size, was proposed based on the average oxide thickness measured on the IBA samples.

In this model, all samples were assumed to have spherical shape with a real density (ρ_{metal}) of 0.918 g/cm^3 and an oxide density (ρ_{oxide}) of 3.95 g/cm^3 [21]. The theoretical metal yield was calculated according to:

$$Theoretical\ metal\ yield = \frac{m_{metal}}{m_{oxide}+m_{metal}} \qquad \text{(Eq. 15)}$$

Where:

$$m_{metal} = \rho_{metal} * \frac{4\pi(r_{sample}-oxide\ thickness)^3}{3(m_{oxide}+m_{metal})} \qquad \text{(Eq. 16)}$$

$$m_{oxide} = \rho_{oxide} * \left[\left[\frac{4}{3} * \pi\left(r_{sample}\right)^3\right] - \left[\frac{4}{3} * \pi\left(r_{sample} - oxide\ thickness\right)^3\right]\right] \qquad \text{(Eq. 17)}$$

Figure 26 shows the theoretical and experimental average metal yield (6–12: 85 %, 12–30: 90 %, USA 2–6: 76 %, 6–12: 84 %, 12–30: 89 %, DK 2–12: 86 %, 12–30: 93 %) depending on the diameter of the bottom ash.

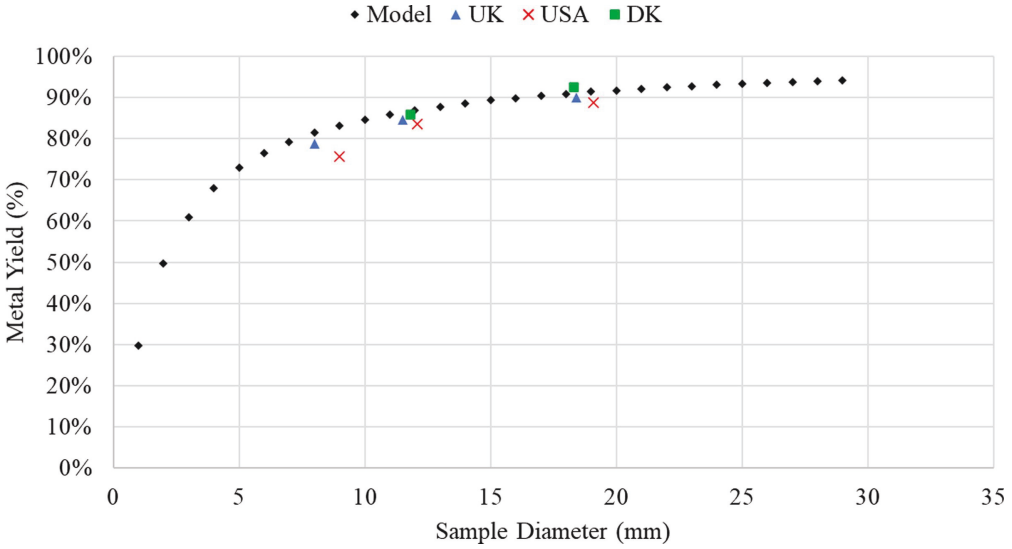

Figure 26. Comparison of the theoretical and experimental metal yield results.

The experimental diameter of the samples was estimated based on their average axis length values, displayed in Table 7. The model showed an acceptable correlation with the experimental test results, which may be used to estimate the maximum achievable yields in the industrial recycling process. The similarities between the presented experimental and modelling results indicate that the oxide thickness measurements adequately represent the entire population.

In addition to reasonable metal yield, the alloy composition is also an important factor for recycling. The ICP-MS analysis of the samples and a more in-depth discussion on the origin of the metallic elements was included in Article B [109]. The iron concentration was measured at 3590 to 6380 ppm, without notable variation trends between size fractions and material origin. The silicon concentration was also at the same level throughout the samples analysed, ranging between 2810 and 9940 ppm. The 2–6 and 6–12 mm fractions of the US bottom ash samples contained more than 1 % of zinc in the melt. This concentration level is normally not found in packaging alloys and likely originate from other Zn-containing products in the waste (such as pennies, zinc-carbon batteries, nuts, and bolts). The source of these elements (Fe, Si and Zn) may be beverage can bodies (Al 3004) aluminium screw caps and closures (Al 3105, 8011).

3.4 Conclusions and Future Work

This chapter has discussed the interaction between scrap properties (size/thickness/compaction degree), susceptibility to oxidation and re-melting yield and coalescence when recycling in salt-flux. The following conclusions were drawn:

3.4.1 Compaction of Foils/Sheets

- The MPT compaction method, which combines torsion and uniaxial compaction, produces briquettes of densities between 2.4–2.6 g/cm^3; above the density of liquid Al (2.3 g/cm^3).
- Compacting foils into briquettes reduces the specific oxidation during thermal treatment significantly, and this is more explicit the thinner the material is. The oxidation did not vary significantly for briquettes compacted uniaxially to densities between 0.86–2.12 g/cm^3. The briquettes compacted by MPT to bulk densities 2.4–2.6 g/cm^3 were the least oxidized after the heat treatment.
- Compacting the aluminium chips before the thermal treatment promoted their coalescence and material yield, and this effect increased for thinner foil gauges. For the thinnest foil (15 μm), higher degrees of compaction promoted the coalescence and metal yield. The minimum bulk density required to achieve yields and coalescence higher than 95 % for the thinnest foil was 2

g/cm^3. For the thicker materials (30–300 μm), briquetting promoted coalescence, but the effect of briquette density was negligible.

3.4.2 Recyclability of Incinerator Bottom Ash

- The average thickness of the oxide layer of the aluminium IBA recovered after incineration was 68 μm, although it can vary from <1 to several thousand μm depending on the incineration dynamics and the alloy composition of the sample.
- The re-melting metal yield increases for larger IBA sizes due to the decreasing oxide/metal ratio, which is a direct consequence of the surface area exposed during incineration. The metal yield of the different size fractions ranged from 75.8 to 92.6 %.
- A simplified model correlating particle size and remelting yield was developed for spherical samples with a diameter varying between 1 and 30 mm and a 68.12 μm oxide layer covering the sample surface, which agrees with the experimental results.
- The remelted aluminium materials from all three countries (USA, UK, DK) and size fractions displayed significant contents of Fe, Si, Cu, Mn, Mg and Zn in accordance with typical Al alloy specifications for packaging materials. Materials originating from USA showed the highest average concentrations of alloying and trace elements.

3.4.3 Future Work

Future work could test the potential benefits of compacting other types of thin aluminium products before re-melting them, e.g., thin foils recovered from batteries or from flexible packaging laminates. Furthermore, in the present work the oxidation of the materials was simulated by exposure to an air atmosphere at 650 °C, but it would be interesting to test the response to a thermal pre-treatment under industrial conditions for various compaction states, e.g., by introducing the foil/sheets together with aluminium post-consumer scrap in a rotary kiln de-coater.

The recyclability of IBA of different size fractions obtained in the study could be compared with metal yield values obtained in a rotary furnace to validate the correlation between industrial and laboratory results.

In addition, both studies could be expanded by using other re-melting methods, such as laboratory-scale studies where the scrap is charged into a molten heel without salts, or industrial-scale experiments in reverberatory or vortex furnaces. Compacting clean scrap of high specific surface areas into briquettes of higher densities could be beneficial for those re-melting setups also from the point of view that it may facilitate the submersion of scrap into the melt, and it would be interesting to test this for briquettes of bulk densities above and below the density of liquid aluminium. Finally, compacting thin post-consumer aluminium thin scrap upon disposal could also benefit the recovery rates of sorting processes.

Chapter 4. Pre-treatments for Coated Aluminium

This chapter summarises Article C; *Effect of compaction and thermal de-coating pre-treatments on the recyclability of coated and uncoated aluminium,* Article D; *Thermal de-coating pre-treatment for loose or compacted aluminium scrap and consequences for salt-flux recycling*, and Article E; *Effects of compaction and thermal pre-treatments on generation of dross and off-gases in aluminium recycling.*

4.1 Introduction and Motivation

This research investigated the mechanisms behind re-melting losses for aluminium sheets coated by organics, to determine which pre-treatment route combination (compaction and/or thermal pre-treatment) could minimise them. This was done for two different re-melting processes: with and without salt-flux.

Articles C and D investigated the optimal parameters for a thermal pre-treatment to remove the organics from the materials before re-melting. The focus was placed on evaluating the de-coating efficiency when the materials go through the thermal treatment in different compaction states, by measuring the weight changes after the treatment. The samples were re-melted to study the influence of the different pre-treatment combinations on the metal yield and coalescence when recycling with molten salts. Article E expanded the investigation of the influence of the compaction state of the scrap on the thermal de-coating process. The study focused on characterising the amount and composition of the off-gases emitted during de-coating. The samples were subsequently re-melted into a molten heel, without salts, and the percentage of dross formed, metal yield and dross metallic content were evaluated. Several compaction states were tested: loose chips and briquettes pressed by uniaxial compaction or by moderated-pressure-torsion (MPT) methods. In all re-melting investigations, for each of the compaction states, a subset of samples was re-melted after pre-treatment and another subset directly without pre-treatment.

The observations highlighted that organic contamination, such as coatings, increase the re-melting losses by hindering the coalescence of the metallic droplets when re-melting in salt-flux and by increasing the amount of dross formed in salt-free re-melting. In addition, Articles C and D illustrated the benefits of applying a thermal de-coating before re-melting with salts, reaching similar degrees of coalescence as when re-melting bare, clean sheets. Article E highlighted the presence of char residues due to the incomplete thermolysis/combustion of organics as the main factor impacting the dross formation during salt-free re-melting. Finally, the three studies concluded that the high densification of the briquettes by torsion was detrimental for the de-coating efficiency, thereby increasing the re-melting losses significantly for both recycling processes. Part of this work was included in a master thesis by Høgåsen [111].

4.2 Experimental Materials and Methods

4.2.1 Materials and Sample Preparation

The materials were two coils of aluminium sheet alloy AA8111 of 600 μm thickness, one coated and the other uncoated (bare), provided by Speira Holmestrand. The metal heel used for some of the re-melting trials was of the same alloy. Their compositions are shown below:

Table 9. Composition of the 8111 alloy sheets. Arc spark OES data from producer.

	Al (%)	Fe (%)	Si (%)	Mg (ppm)	Cu (ppm)	Ga (ppm)	V (ppm)	Ti (ppm)	Mn (ppm)	Zn (ppm)
Bare	98.37	0.86	0.59	463	361	112	195	50	368	76
Coated	98.34	0.75	0.88	6	11	117	80	107	26	18
Heel	98.15	0.81	0.94	86	64	117	124	122	209	97

The reason for using the same as-produced material with and without coating instead of post-consumer scrap was to isolate the influence of the coating on the mechanisms leading to re-melting losses. This specific alloy, used for instance in roofing applications, was selected based on production schedules and due to its low Mg

content compared to the typical alloys used in UBCs, thus minimising the influence of Mg oxidation on the results.

The samples were prepared by first shredding the sheets into chips of 2-5 mm^2 size, followed by compaction into briquettes by the uniaxial, MPT and Hot MPT methods described in the previous chapter. The samples used for the salt-flux re-melting studies (Articles C and D) weighed 20 g, while those used for the off-gas analysis and consequent re-melting in molten heel weighed 50 g. The average internal porosity of the 20 g briquettes of coated and uncoated materials was characterised by computed tomography scans.

4.2.2 Thermal De-coating Methods

In the initial study (Article C), the weight changes experienced by the chips and briquettes of coated and uncoated materials after a thermal pre-treatment were measured. The trials were conducted using a Nabertherm muffle furnace with exhaust. A subset of the samples, weighing 20 g each, were thermally treated for 1 h at 550 °C, while another subset was re-melted directly without thermal treatment. This de-coating procedure was also used to test the weight loss after treating batches of 1 kg of chips; results which were added to the discussion in Article E.

The same equipment was used to determine the optimal de-coating parameters for the material. For this set of experiments, the coated sheet was cut into rectangles of 10×5 cm, each weighing 8–9 g. A subset of these samples was thermally treated at a constant temperature of 550 °C and durations of 5, 10, 20, 30, 40, 50, and 60 min, and another subset at temperatures 450 °C, 550 °C, and 600 °C for 5 and 10 min. The de-coating performance was evaluated based on several observations: changes in mass, composition, and colour.

The off-gas characterisation during thermal de-coating was carried out at Aachen University in a pyrolysis chamber connected to a Gasmet FTIR analyser. The heating rate was 350 °C/h until reaching 550 °C and held at that temperature for 30 minutes. The flow gas amount and composition were targeted to reach stoichiometric thermolysis conditions, which means that the exact amount of oxygen needed to react with the organics present is provided throughout the treatment, thus preventing excess oxygen from oxidising the aluminium, as discussed by Steglich [32]. A gas mix with 5 % O_2 and 95 % inert gas (N_2) was set at a flow of 3 L/min after flushing the chamber

with N_2 at 180 °C. In the calculations, it was assumed that the samples contained 2 wt% organics (based on observations from the previous studies) and that the composition was 50 % epoxy and 50 % polyester, which would begin decomposing at 250 °C following the equations below:

Epoxy: $C_{21}H_{24}O_5 + 21O_2 \rightarrow 14CO_2 + 7CO + 12H_2O$ (Eq. 18)

Polyester: $C_8H_6O_4 + 6O_2 \rightarrow 5CO_2 + 3CO + 3H_2O$ (Eq. 19)

The excess gas not analysed by the FTIR was connected to a scrubbing system. Figure 27 shows a scheme of the setup:

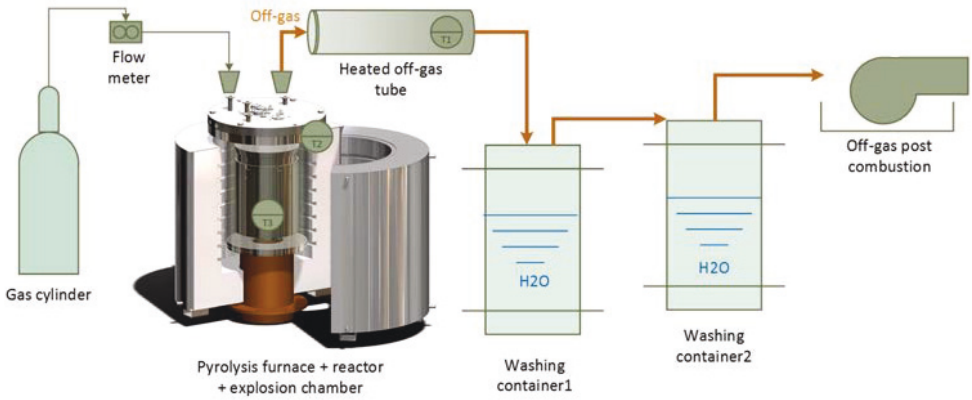

Figure 27. Pyrolysis furnace and gas scrubbing system.

4.2.3 Re-melting Methods

The re-melting of the chips and briquettes in salt-flux was carried out under similar conditions as those described in the previous chapter: the samples were charged into crucibles containing molten salts (salt-scrap ratio 4:1, salt-mix 68.6:29.4:2 wt% NaCl:KCl:CaF_2) and pre-heated to 800 °C inside a resistance furnace. No stirring was applied, and after a holding time of 10 minutes, the crucibles were taken out and cooled in air. The metal was recovered from the salts by crushing and washing with water on a sieve of 0.8 mm^2 mesh size. The coalescence of the recovered metal was calculated as follows:

$$Coalescence\ [\%] = \left(\frac{m_c}{m_i}\right) * 100 \qquad \text{(Eq. 20)}$$

Where m_i is the mass of the sample charged into the crucible (ca. 20 g), and m_c the mass of the largest metallic piece recovered.

The trials re-melting dross (Article E) were also carried out by a similar procedure in the same resistance furnace. However, in this case the salt-dross ratio was 2:1, the dross was charged in 2 batches separated by 5 minutes, the mixture was stirred after a holding time of 10 minutes and the molten materials were cast into a copper mould before crushing and washing away the salts and fine NMCs from the recovered metal on top of a sieve of 1 mm^2 mesh. The dross metal content was then calculated as:

$$Dross\ metal\ content\ [\%] = \frac{m_r}{m_d} \qquad \text{(Eq. 21)}$$

Where m_r is the mass of the metal recovered after the salt-flux re-melting and m_d the mass of the dross charged into the crucible.

The re-melting trials in a molten heel were conducted at Aachen University in crucibles inside an induction furnace operating at 2.5-3 kHz.

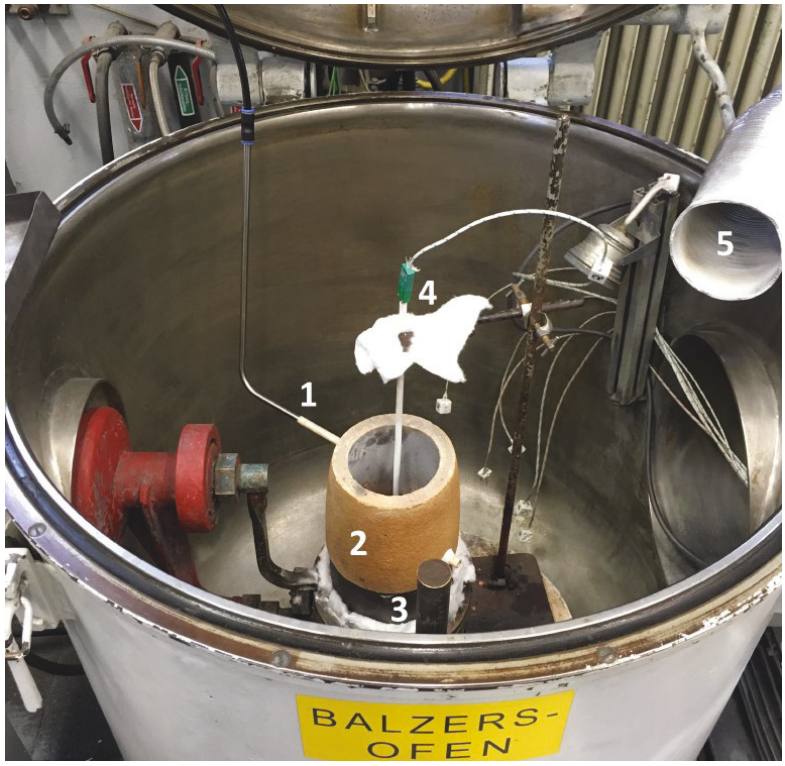

*Figure 28. Furnace setup for remelting in molten heelwhere; 1=Argon gas inlet, 2=Hood, 3=Crucible, 4=Thermocouple and 5=Exhaust pipe.*The temperature was measured by a thermocouple placed inside the melt, and the melt was flushed with argon introduced to the hood at 10 L/min. First, the crucible with approximately 1 kg of aluminium heel was heated to 780 °C. Then the furnace was turned-off to skim

the dross using a slotted spoon. The chips/briquettes (1 kg) were gradually charged into the melt at 750 °C. For the coated materials which had not been thermally pre-treated, the smoke arising from the combustion of the coating impeded the process, and the furnace had to be turned off a few times to stir and sink the samples into the melt. After charging, the melt was stirred again, and the temperature was raised to 780 °C before skimming the dross. Finally, the metal was cast at 750 °C. Once cold, the dross and the cast ingots were weighed to calculate the percentage of dross formed during re-melting and the metal yield as follows:

$$Dross\ [\%] = \frac{m_d}{m_i} * 100 \qquad \text{(Eq. 22)}$$

$$Metal\ Yield\ [\%] = \frac{m_{\ ingot}}{m_i + m_{heel}} * 100 \qquad \text{(Eq. 23)}$$

Where m_d is the mass of the dross formed, m_i is the initial mass of the samples charged, m_{ingot} the mass of the secondary ingot and m_{heel} the mass of the metal heel. Finally, the Total Metal Yield was calculated by adding the dross metal content values obtained from the re-melting of the dross in salt-flux into the equation:

$$Total\ Metal\ Yield\ [\%] = \frac{(m_i - m_d) + (dross\ metal\ content\ (\%) * m_d)}{m_i} \qquad \text{(Eq. 24)}$$

3.2.3 Characterisation Methods

The supplier did not provide the characteristics of the coating, so its composition and thickness were characterised by SEM–EDS point analysis (Zeiss Ultra 55LE FEG-SEM) and by Electron Probe Micro Analysis (EPMA). The inorganic de-coating residues remaining after the thermal treatment were analysed by X-ray diffraction (XRD) in a DaVinci X-ray diffractometer. The compositions of the metal recovered after re-melting the samples in salt-flux and of the metal recovered from the dross were analysed by ICP-MS by ALS Scandinavia.

4.3 Results and Discussion

4.3.1 Optimal Thermal De-coating

The results showed the influence of the temperature and duration of the thermal treatment on the appearance and weight losses of the coated sheets. Figure 29 displays both sides of an untreated sample next to samples treated at 550 °C for 5, 10 and 20 minutes.

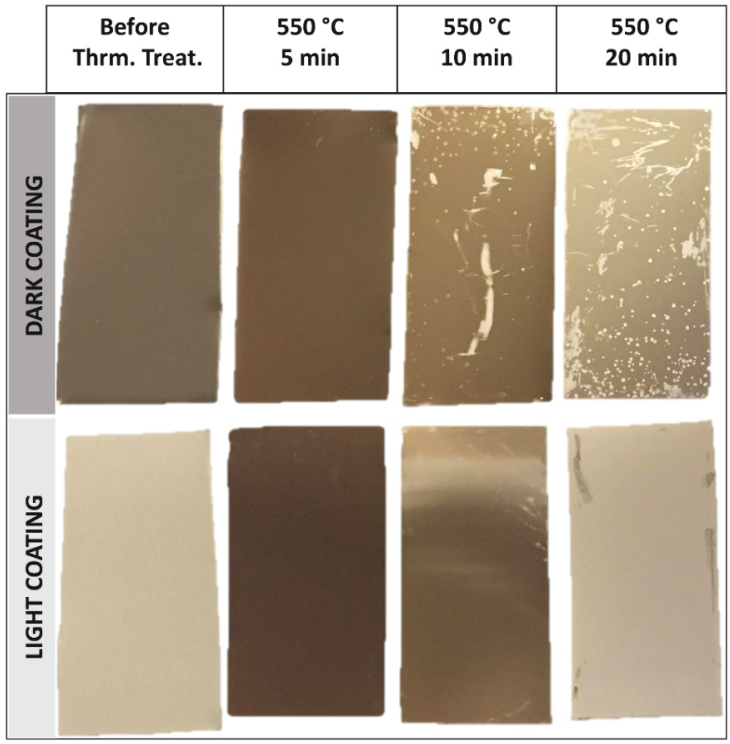

Figure 29. Coating colour variations after thermal treatment for both sides of the sheets. The terms dark/light coating simply refer to the two different sides of the sheets.

The samples thermally treated for 5 and 10 min became darker than initially, and the colour faded with increasing treatment time. For treatments of 20 min and longer, the differences in appearance were negligible, and this is why the sheets treated at 30, 40, 50 and 60 min are not displayed. Similar observations were also described by Kvithyld [112], who linked the darker colour to char formed during the initial stages of coating decomposition (scission) and the white colour to complete thermolysis without organic residues.

Figure 30 presents the weight losses of the sheets for 5 and 10 minutes at varied temperatures.

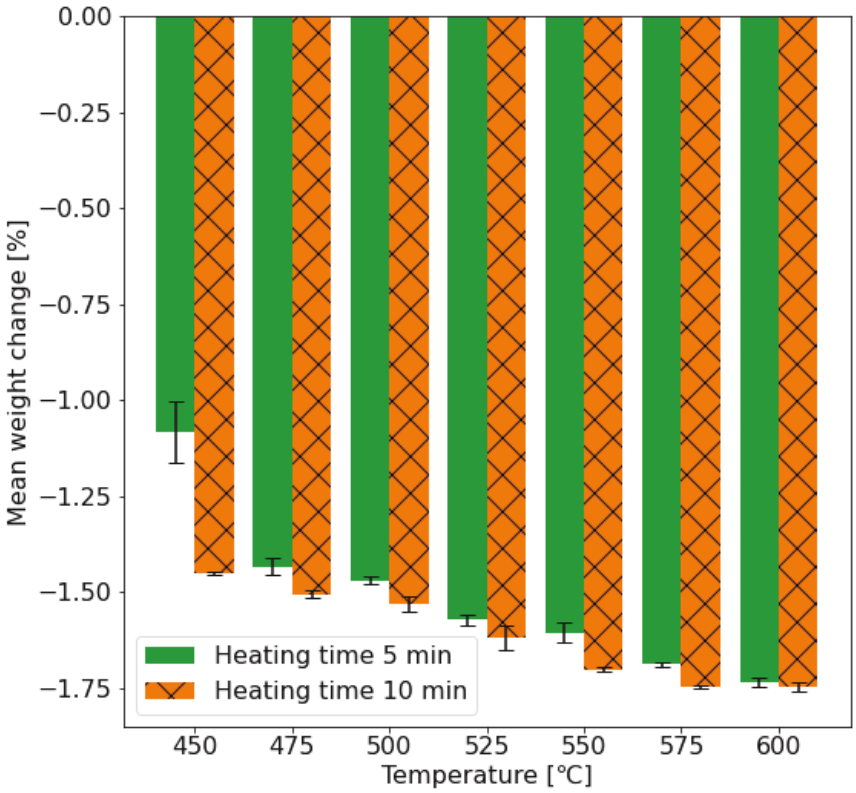

Figure 30. Weight change after de-coating at varied temperature and duration.

The bars show the average weight change as a percentage of the sheets' initial weight (8-9 g). As expected, the weight losses increase with the temperature. The most significant weight loss was obtained for 600 °C and 10 min and the least for 5 min at 450 °C. Increasing the duration of the treatment from 5 to 10 minutes promotes the weight losses, although this effect was minor at the more elevated temperatures. Since the weight changes seemed to stabilise for temperatures of 550 °C or higher, this was selected as the optimal thermal de-coating temperature. Thus, another set of samples was treated at 550 °C for various durations. Those results showed that the weight reduction increased with the treatment time up to 20 min, while after this point, it stagnated. Therefore, the treatment parameters 550 °C and 20 min were selected as optimal for these samples, leading to a weight decrease of 1.8 wt%. This represented 74.5 % of the total weight of the coating. The powder residues, visible in Figure 29, were scraped off from the surface and analysed by

XRD, identifying TiO_2, SiO_2 and $BaSO_4$. These compounds may have been added to the coating as pigments or fillers, as discussed in [113]. The XRD results agree with the EPMA elemental mapping of the cross-section of the coated sheets, displayed below. The EPMA images are semi-quantitative colour maps where the brighter colours represent a higher concentration of the elements targeted by the analysis.

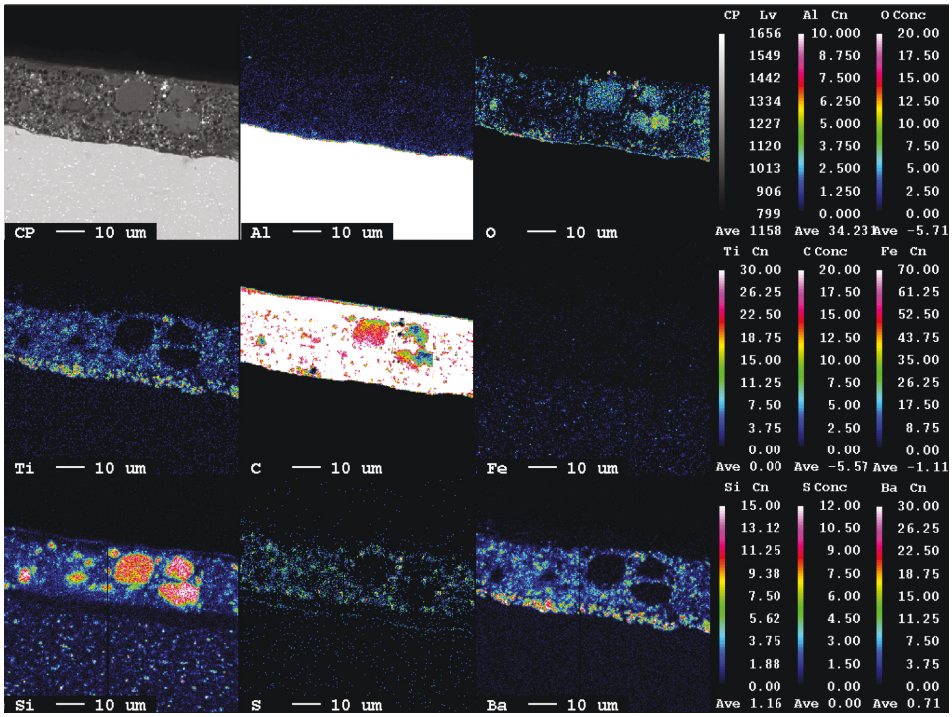

Figure 31. EPMA analysis of the cross-section of the coated sheet. Colour scale in %.

The images show higher concentrations of the elements carbon, silicon, oxygen, titanium, barium, and sulphur, suggesting that this coating is a polymeric matrix with particles of TiO_2, $BaSO_4$ and SiO_2, which, based on the de-coating results, represent roughly 25 % of the weight of the coating and are not removable by a thermal treatment.

4.3.2 Interaction between Compaction and Thermal De-coating

Table 10 below summarises the properties of the briquettes compacted through the different methods for both uncoated and coated materials.

Table 10. Average bulk density and internal porosity of the briquettes of 8111 alloy.

	UNIAXIAL		MPT		HOT MPT	
	Porosity	Density	Porosity	Density	Porosity	Density
Uncoated	16.64	1.94 ± 0.01	0.68	2.46 ± 0.01	0.04	2.60 ± 0.02
Coated	14.68	1.90 ± 0.18	4.48	2.19 ± 0.09	0.07	2.54 ± 0.07

The MPT method proved again, as in the precedent chapter, to be an effective way to increase the density and lower the internal porosity of the briquettes. Introducing moderate temperatures (450 °C) increased the density further, especially for the coated materials, possibly due to a partial de-coating.

The weight changes of the different types of briquettes due to oxidation (for the uncoated material) and de-coating (for the coated) after a thermal treatment are included in Table 11. The Hot MPT briquettes were not thermally treated since the compaction already took place at temperatures of 450 °C.

Table 11. Weight changes after thermal treatment of chips and briquettes.

	CHIPS		UNIAXIAL		MPT	
	Av. wt% change	STD	Av. wt% change	STD	Av. wt% change	STD
Uncoated	+0.02	0.01	+0.005	0.00	0.013	0.01
Coated	-1.66	0.05	-1.70	0.01	-1.52	0.05

These numbers show that the weight increase due to oxidation during the thermal de-coating was minimal even for the chips, probably due to their thickness, thus lower specific surface area compared to earlier materials (Chapter 3). In terms of de-coating efficiency, both chips and uniaxial briquettes reached similar values, close to those obtained for the optimal de-coating pre-treatment in the previous section. However, the MPT briquettes experienced a lower weight decrease, pointing to an incomplete de-coating likely linked to their low internal porosity.

Figure 32 displays the off-gas evolution for the different compaction states, measured by FTIR for batches of 500 g per trial. For clarity, the hydrocarbons are grouped according to their chemical structure as aliphatic and aromatic hydrocarbons.

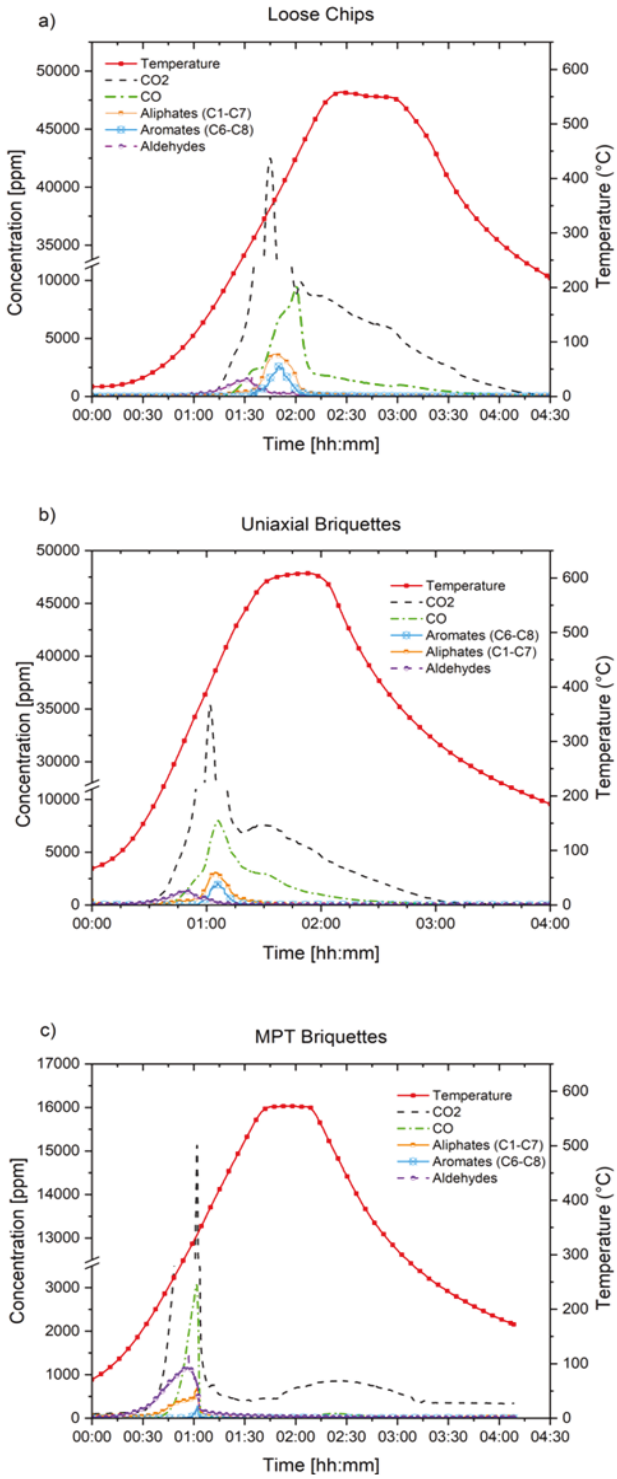

Figure 32. Off-gases emitted during the thermal treatment of a) loose chips, b) uniaxial briquettes (low compaction) and c) MPT briquettes (high compaction) plotted against time and temperature.

The results reveal that the first phase of de-coating, scission, started at temperatures between 175-190 °C and lasted until 500-515 °C. After reaching this temperature, no hydrocarbons were present in the off-gas and the second phase began: the gasification of residual carbon, releasing CO_2 and CO at a much lower rate. These two phases correspond with those described in literature for organic coatings on aluminium [112] and magnesium [114], although the off-gases were previously not analysed in such detail. The measured CO_2 peaked at 42506 ppm for loose chips, 35340 ppm for uniaxial and 24000 ppm for MPT. The same decreasing trend applied for CO, aliphatic hydrocarbons, aromatic hydrocarbons, indicating that compaction reduced all VOC emissions.

The total emissions are shown in Figure 33 together with an image of the briquette cross section.

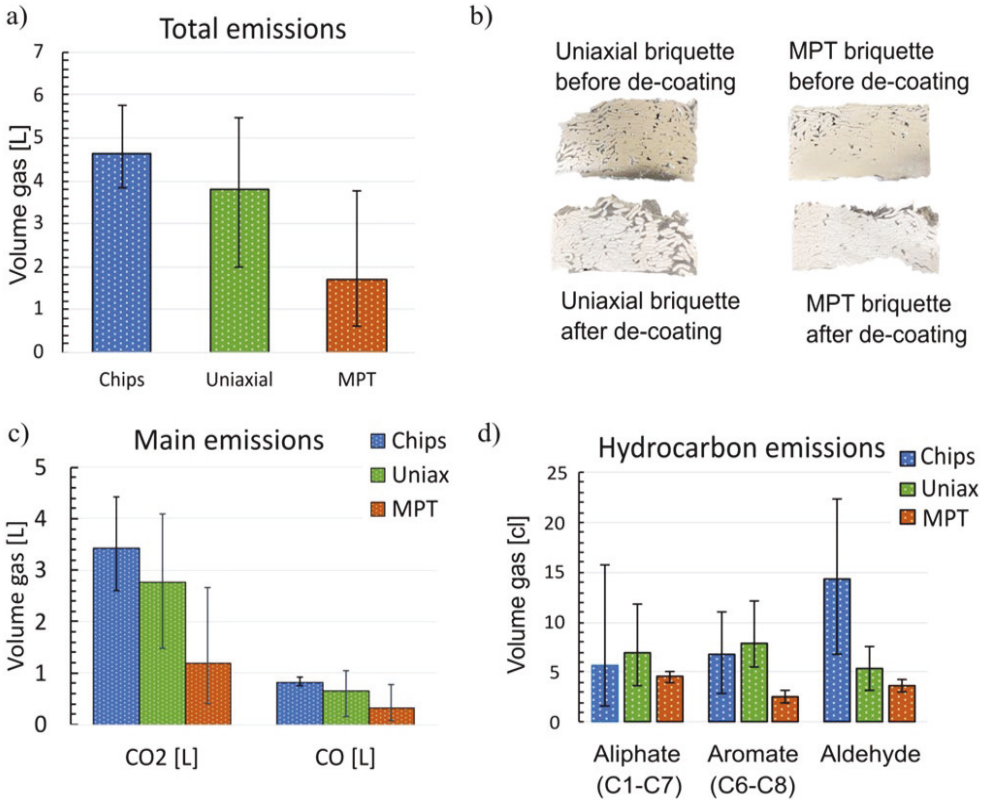

Figure 33. Off-gas released during treatment for each compaction state.Average and STD; three trials each. a) Total gas emissions. b) Cross-section of uniaxial and MPT briquettes before and after treatment. c) CO_2 and CO and d) hydrocarbons emissions.

The decreasing off-gas generation, particularly CO_2 and CO, supports the hypothesis raised in the previous section: oxygen availability is crucial for organics removal and therefore, compacting coated materials into denser briquettes limits the efficiency of the de-coating. Chamakos [87] attributed the incomplete de-coating of UBC bales in their trials to their low thermal conductivity, since the temperatures measured in the centre of the bales were below those required for de-coating. Due to the small size of the briquettes in this study, it was assumed that the temperature differences between the surface and the centre were negligible, and that insufficient gas transport inside the briquette is the main factor behind the influence of compaction on de-coating.

The ideal gas law was used to convert the volumes into mass (temperature of measurement was 180 °C). De-coating 1 tonne of the materials under the present operation conditions would generate 8.1 kg CO_2-eq per tonne scrap for the chips, 6.6 kg CO_2-eq for the briquettes and only 2.8 kg CO_2-eq for the MPT briquettes. Thus, high densifications reduce the gases released during pre-treatment. This could be beneficial from the point of view that it reduces the amount of off-gases which need to be further treated and the process direct emissions, although on the other hand, the off-gases could be reused internally to save energy, as discussed in [10]. However, there is evidence that none of these sets of de-coating trials fully removed the organic residues from the materials, since all the samples showed partially dark surfaces. This is an indication of char residue remaining after a scission phase which requires oxygen in the atmosphere to be volatilised, as illustrated in Figure 34. Although the concentration of oxygen in the off-gas and the gas flow had been calculated in order to fully remove the organics from the materials throughout the treatment, likely this was not sufficient, perhaps due to an insufficient gas transport as the samples were stacked in a crucible and the inlet and outlet gas channels were both placed on the top lid of the chamber (Figure 27).

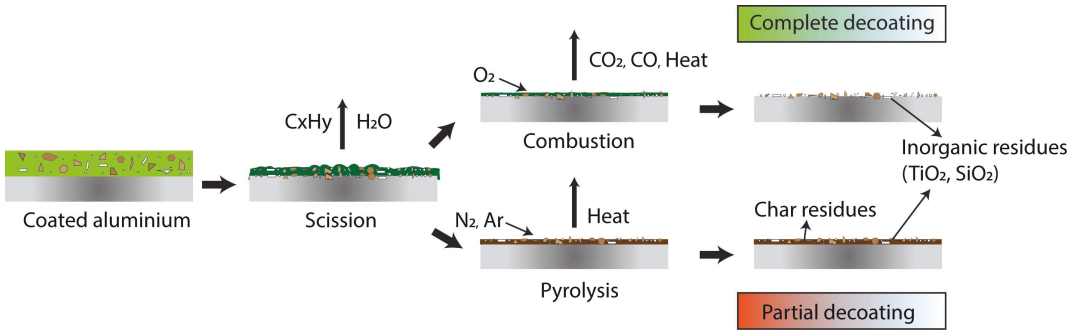

Figure 34. De-coating reaction stagesfor atmospheres with and without oxygen.

4.3.3 Impact of Pre-treatments on Salt-flux Re-melting

The metals recovered from re-melting the samples prepared by different pre-treatment routes and materials are displayed in Figure 35 below.

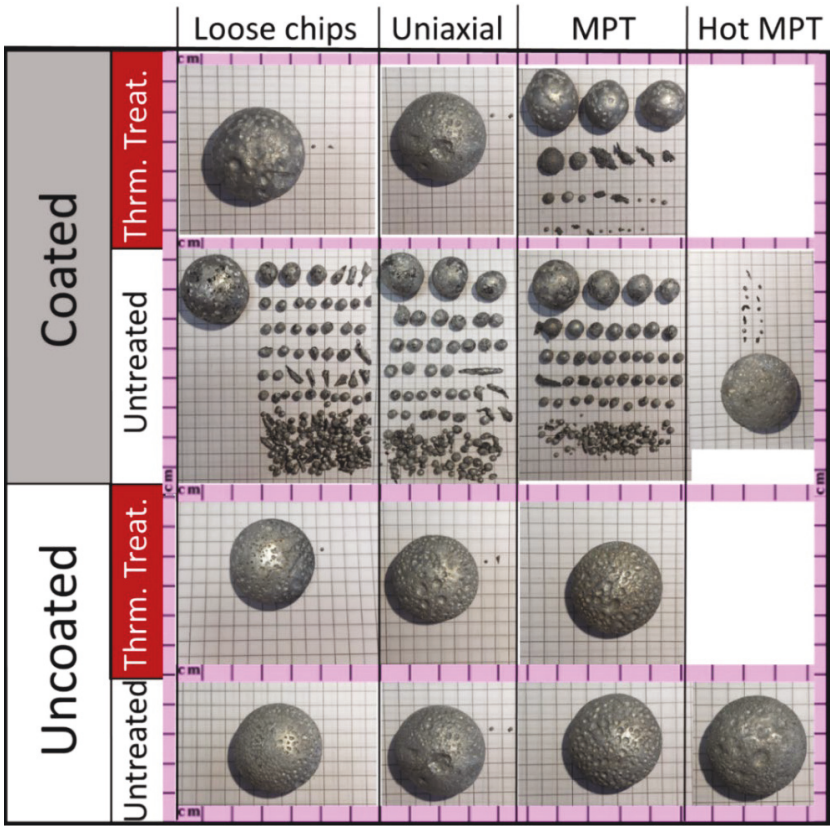

Figure 35. Appearance of the recovered metal for each pre-treatment route.

The differences in metal yield for the different pre-treatment routes were small, but the coalescence varied drastically, as visible in the images. The chips of the samples of coated material which were not thermally treated before re-melting did not coalesce, thereby forming small metal beads. The average wt% of material which coalesced into the largest piece per trial is plotted in Figure 36.

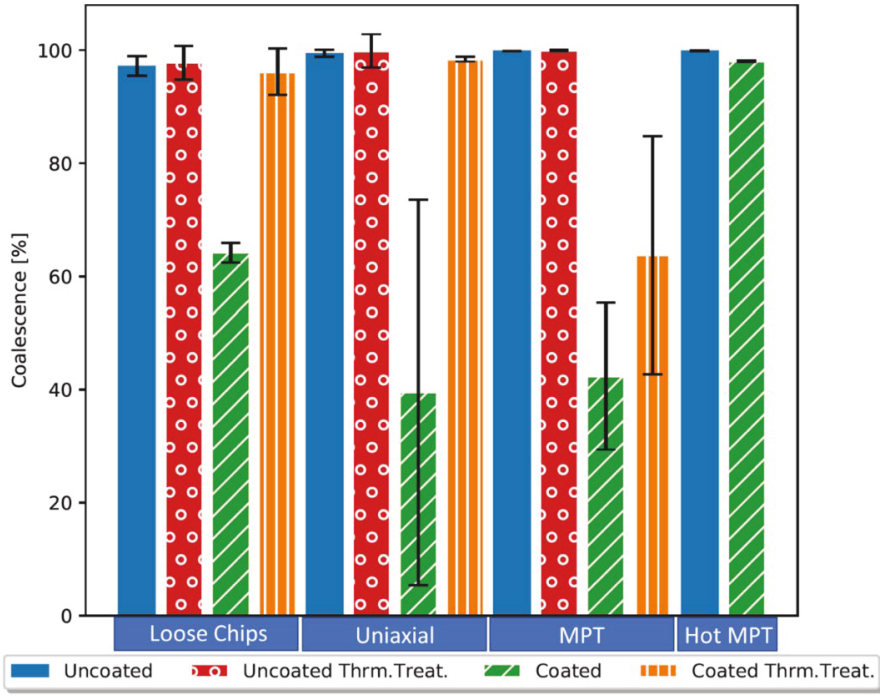

Figure 36. Average coalescence results after re-melting in salt-flux. The bars show the STD.

The graph shows that applying a thermal de-coating before re-melting increases the re-melting coalescence of the coated materials to values close to those obtained for those uncoated. However, the effect of the thermal treatment is less beneficial for the MPT briquettes, probably due to carbonaceous residues trapped inside the briquette after an incomplete de-coating. The Hot MPT briquettes reached very high coalescences both for uncoated and coated material, indicating that the compaction process parameters (pressure-torsion at 450 °C) were sufficient to successfully de-coat the chips.

4.3.4 Impact of Pre-treatments on Re-melting in Molten Heel

The average dross formation, metal yield, dross metallic content and total metal yield after recovering the metal from the dross by salt-flux re-melting are displayed in Figure 37 for each pre-treatment route.

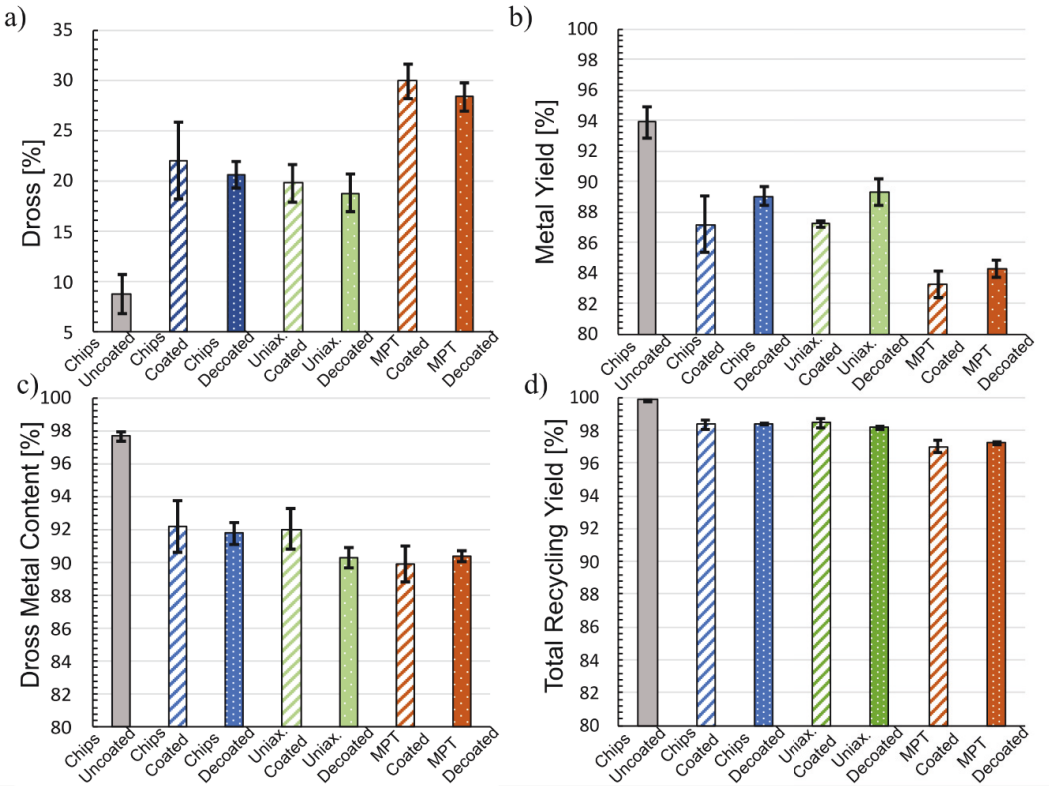

*Figure 37. Re-melting in molten heel results **a)** Dross related to wt. scrap. **b)** Metal yield from cast ingots. **c)** Dross metal content. **d)** Total recycling yield. Each bar represents the average and STD (out of 3) for each conditioning route: compaction (loose chips/uniaxial briquettes/ MPT briquettes) and thermal treatment (coated/de-coated). Chips uncoated is untreated bare Al.*

The uncoated chips generated less dross (9 wt%) than the coated samples (20-30 wt%). The benefits of applying a thermal de-coating, which had been previously observed for salt-flux re-melting, were not as clear in this study; the dross and metal yield differences between samples thermally treated or not were only around 2 wt%. This was lower than expected, as the partial removal of organic contaminants and the prevention of the combustion reactions during re-melting by thermally treating beforehand were thought to have had a larger impact. However, as discussed, the partial de-coatings left organic residues. This is coherent with the fact that the MPT

samples generated the highest amounts of dross, since they were the samples which experienced the lowest degree of de-coating, as described in the previous sections.

The presence of organic residues seems to be the major factor behind dross formation, irrespective of whether the samples were thermally pre-treated or directly charged into the aluminium melt. The organics remaining after the incomplete de-coating treatments or after the spontaneous combustion during re-melting (for the untreated samples) may consist of decomposed but not removed organics, such as carbon and non-decomposed hydrocarbons ($C_xH_yO_z$). These will likely react with the liquid aluminium during re-melting and cause metal losses due to the formation of aluminium carbide and oxide, as reported by Dittrich [40].

Figure 37c shows that the metal content of the dross was highest for the uncoated Al. The dross from the coated and the de-coated chips had similar metallic content than the coated uniaxial briquettes, and the dross from the de-coated uniaxial briquettes and MPT briquettes contained slightly lower metal. Still, these metallic contents are higher than those typically observed during secondary dross recycling [75].

Finally, the total recycling yield results in Figure 37d show that if the aluminium is recovered from the dross, recycling coated aluminium leads to slightly higher overall losses than bare aluminium, which increase if the scrap is compacted to high densities by torsion. Although these differences in metal yield may seem small, they would have a significant environmental (and economic) impact at an industrial scale, as explained in the following chapter. Furthermore, to recover the metal from the dross implies additional transport, energy, and resources to treat it in a rotary furnace and generates salt-slag residues that need to be processed.

4.5 Conclusions and Future Work

4.5.1 Conclusions

This line of research evaluated the effect of compacting coated aluminium through various methods on the thermal de-coating process, and the consequences of combining these pre-treatment routes for the performance of aluminium recycling with and without salt-flux. The following conclusions were drawn:

- Compacting materials containing organics reduced the off-gas emissions upon the decomposition of the organics during the thermal de-coating or re-melting processes.
- Compacting scrap to densities over 2.2 g/cm^3 by torsion-pressure (MPT) drastically decreased the briquette's internal porosities, which difficulted the gas transport, leading to lower de-coating efficiencies and more de-coating char residues inside the briquettes.
- The presence of carbonaceous residues was the main factor increasing the re-melting losses through both processes since it impacts the coalescence of the aluminium chips when re-melting in salt-flux and the dross formation when re-melting in a molten heel without salt additions.
- Compacting the chips into briquettes by the uniaxial compaction method did not significantly affect the re-melting performance in neither of the two processes for the studied sheets of 600 μm thickness.

4.5.2 Future Work

Future work could expand the present study by using thinner coated materials, since the material thickness can significantly influence its responses to compaction, de-coating, and re-melting, as seen in the previous chapter. A particularly interesting case would be to test the influence of thermal de-coating and compaction on the recycling performance of flexible packaging and laminates, which are deemed non-recyclable and excluded from most of the current collection systems.

Future work could also investigate the influence of food residues on recycling losses, and how different packaging designs, customer behavioural campaigns and cleaning treatments can influence the recovery/recycling of post-consumer scrap.

Since the oxygen content in the atmosphere and sufficient gas transport were proved critical for a successful de-coating, it would be advisable to carry out future studies using setups which secure this, e.g., a rotary kiln de-coater or higher gas-flows/O_2 concentrations. Furthermore, a deeper understanding of the decomposition reaction kinetics for different oxygen supplies and amount of organic matter is still lacking.

Industrially, it would be interesting to explore the potential benefits of recirculating the off-gas emitted during de-coating and re-melting for the energy efficiency and environmental impacts of the overall recycling processes.

Chapter 5. LCA of Recycling in a Rotary Furnace

This chapter summarises Article F; *LCA of recycling aluminium incineration bottom ash, dross and shavings in a rotary furnace and environmental benefits of salt-slag valorisation*.

5.1 Introduction and Motivation

There is ongoing debate in the field of metallurgy regarding the relative sustainability of different aluminium recycling routes. The process of re-melting in a tilting rotary furnace offers high energy efficiency and recycling yields, but brings potential environmental burdens linked to the use of salt-fluxes and generation of slag residues which need to be further processed. The latest EEA environmental profile report [115] outlines some of the environmental impacts from re-melting scrap in an integrated cast house. Still, it does not include detailed data related to the process of dross recycling, which generally involves re-melting in rotary furnaces with salt-flux, stating that a dedicated task force should be dedicated to this work. This chapter contributes to the current knowledge of the sustainability of the recycling processes through a life cycle assessment of re-melting a mix of partly oxidised/contaminated aluminium streams (dross, incinerator bottom ash, shavings) using salt-fluxes in a rotary furnace. The LCA results show the environmental benefits of recycling aluminium, all of which increase if the salt-slag residue is treated for recovery versus landfilling it. The analysis also allows discussing which process parameters are most critical for improved sustainability; for instance, the metal recovery, process emissions, energy consumption and recovery of byproducts from the salt-slag, and to what extent they contribute to the environmental indicators evaluated; global warming, human carcinogenic toxicity, depletion of mineral resources, etc. In addition, the impact of the metal yield assumptions on the results was tested through a sensitivity analysis, showing that increasing the metal yield from 20 to 95 wt% would reduce the

global warming contributions from -3.5 to -17 tonne CO_2-eq per tonne treated via the studied industrial process.

5.2 LCA Methodology

The study was conducted following the framework defined by ISO 14040-14044. [99, 116]

5.2.1 Goal and Scope

The main goals of the LCA were:

- To assess the environmental impacts of recycling aluminium-containing materials in a rotary furnace.
- To evaluate the benefits of the salt-slag valorisation treatment with respect to landfill.
- To identify hotspots; areas where the sustainability of the process could be improved.

The functional unit (F.U.) was 1 tonne of aluminium-containing streams (dross, IBA, shavings) ready to be recycled. The recycling route included two processes. The first one, re-melting in the rotary furnace, produces secondary aluminium, salt-slag residue and furnace off-gas. The second process, salt-slag valorisation treatment, recovers some of the salts (NaCl/KCl) and the entrapped metallic particles (aluminium concentrates) from the salt-slag, which are assumed to be fed into the next rotary furnace cycle. Other by-products are non-metallic-compounds (NMCs) and ammonium sulphate ($(NH_4)_2SO_4$), which can be further used in the construction sector as an alternative alumina source for various applications [47, 48, 117] (cement, ceramics, mineral wool) or by the chemical or agriculture industries [118]. To allocate these co-products, a system expansion approach was applied, as recommended by ISO [116]. The system boundaries were cradle-to-gate and excluded downstream impacts after aluminium has been recycled.

The two main scenarios assessed differ in the choice of salt-slag residues management:

- Scenario 1. Al recycling + salt-slag landfill
- Scenario 2. Al recycling + salt-slag treatment

Figure 38 shows the evaluated system. It was assumed that the metal entering the system had the same composition as the secondary cast alloys under demand, omitting the need to adjust it by refining or addition of alloying elements to the melt.

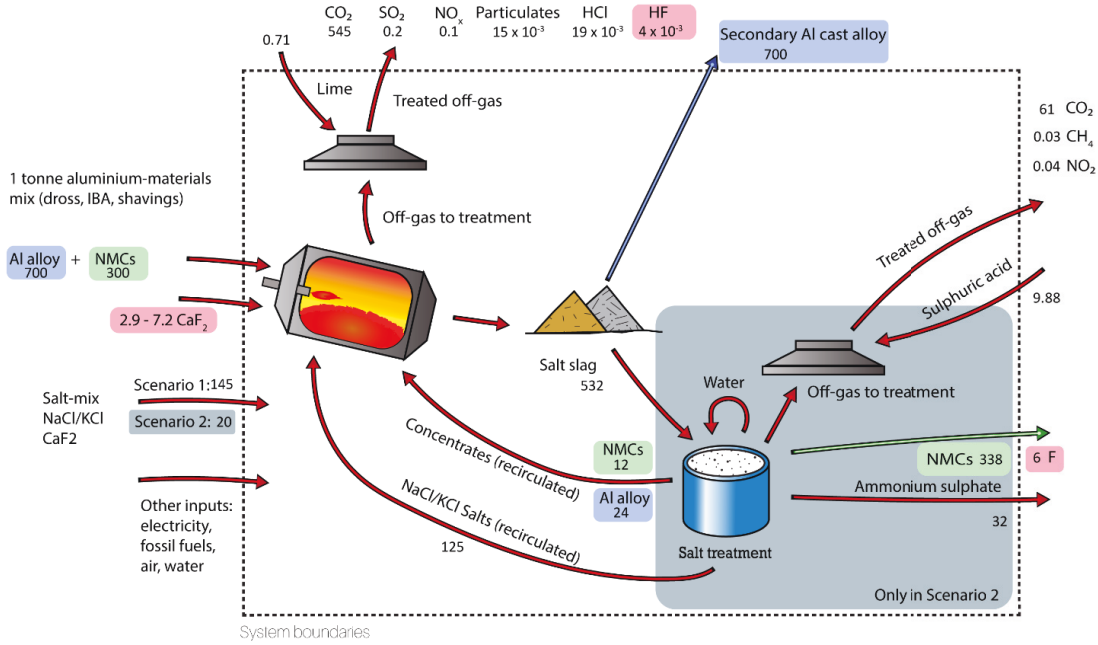

Figure 38. System considered in the LCA with inputs and outputs for the two processes: recycling 1 tonne of Al-containing material mix in a rotary furnace and salt-slag treatment. The units are kg.

The scheme shows the raw materials, the products and wastes produced, and the gas emissions monitored during the re-melting processes. For better visualisation, it excludes the energy sources and process input gases (diesel, natural gas, electricity, N_2, O_2), detailed in the LCI tables provided in Article F. The mass flows containing aluminium alloys (metal), oxides and fluorides entering and exiting the system are highlighted with colour and were calculated in Article F to discuss potential uncertainties that may not have been considered by the study, for example, due to process inefficiencies, as oxidation metal losses, or non-monitored emissions.

5.2.2 Inventory Analysis

The data was sourced from the environmental reports summarising the 2021 operations of European aluminium refining and salt-slag treatment plants. The study considered the treatment of 1 tonne of material mix consisting of 1/3 wt. incineration bottom ash (IBA), 1/3 dross, and 1/3 industrial shavings. Since the expected metal

yield of each of these material types individually was 74.6 % for IBA, 64.7 % for dross and 70.3 % for shavings, the average metal yield of the scrap mix was assumed to be 70 %. However, for the scenario where the salt-slag residues are treated, and additional aluminium concentrates are recovered, the metal yield increases to 72.3 %. The inputs and outputs to the LCI inventory are included in the appendix of Article F. The systems evaluated consider European market conditions. The impact of recycling different types of material with varied metal yield was tested through sensitivity analysis, where the global warming contributions of recycling hypothetical batches of the individual material streams were compared to other scrap types (e.g., UBCs, coated or de-coated packaging, black dross).

5.3 LCA Results

Table 12 shows the net impacts to the midpoint indicators considered when treating 1 tonne of the materials mix. The third column shows the relative improvement when implementing a salt-slag treatment with respect to landfilling the residue.

Table 12. LCA results for 18 midpoint indicators for recycling 1 tonne of aluminium-containing mix in a rotary furnace for salt-slag residue landfill or valorisation treatment and relative improvement.

Midpoint indicator	Salt-slag landfill	Salt-slag treatment	Improvement (%)	Unit
Global warming	-12,267	-13,221	7.8	kg CO_2 eq
Stratospheric ozone depletion	0	0	9.8	kg CFC11 eq
Ionising radiation	-212	-229	8.0	kBq Co-60 eq
Ozone formation, Human health	-32	-34	7.2	kg NO_x eq
Fine particulate matter formation	-26	-27	5.3	kg PM2.5 eq
Ozone formation, Terrestrial ecosyst.	-32	-34	7.0	kg NO_x eq
Terrestrial acidification	-56	-59	5.5	kg SO_2 eq
Freshwater eutrophication	-5	-5	8.6	kg P eq
Marine eutrophication	0	0	6.1	kg N eq
Terrestrial ecotoxicity	-9,254	-11,078	19.7	kg 1.4-DCB
Freshwater ecotoxicity	-350	-411	17.5	kg 1.4-DCB
Marine ecotoxicity	-483	-567	17.6	kg 1.4-DCB
Human carcinogenic toxicity	-2,616	-3,141	20.1	kg 1.4-DCB
Human non-carcinogenic toxicity	-11,340	-13,058	15.2	kg 1.4-DCB
Land use	-1,001	-1,131	13.0	m_2a crop eq
Mineral resource scarcity	-163	-203	24.6	kg Cu eq
Fossil resource scarcity	-2,596	-2,855	10.0	kg oil eq

The results show significant improvements, ranging between 5 and 25 % of impact savings when implementing a salt-slag recovery treatment. The most benefited indicators were mineral resource scarcity, human carcinogenic toxicity and terrestrial, marine, and freshwater ecotoxicity. The "Global warming potential" is the most discussed midpoint in LCA studies since, in many cases, it causes the most significant damage to the end-point indicators ecosystems, resource availability and human health. The industrial recycling route assessed in this LCA gave net savings of 12 tonnes CO_2 equivalent per tonne of treated Al if the salt-slag residue was disposed at the landfill, while valorising it increased the net savings by one additional tonne CO_2-eq. The selection of the most relevant impact categories for further assessment was based on 2 criteria: those midpoints that display a higher relevance for the endpoint categories (analysis included in Article F) and those more greatly affected by a change in scenario.

Figure 39 displays the normalised contributions of each input to the selected midpoint impacts for Scenario 1 (salt slag landfill) and 2 (salt-slag treatment).

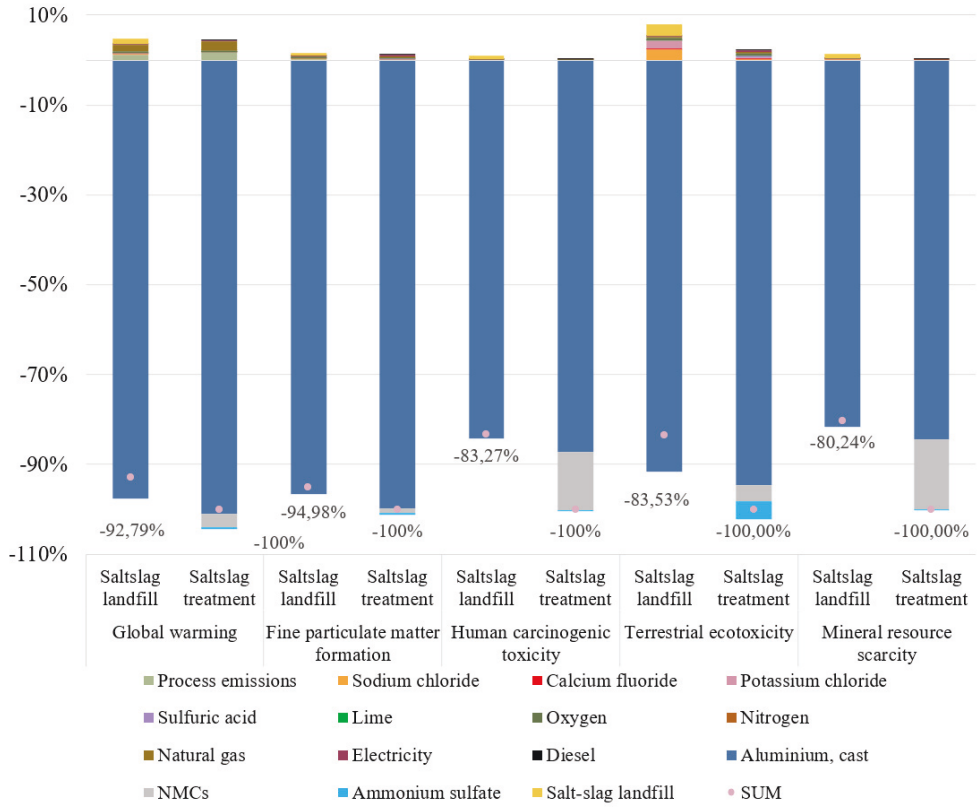

Figure 39. LCA contribution analysis to selected indicators during aluminium recycling in a rotary furnace for salt-slag landfill or valorisation. Results normalised per impact category.

The impacts from substituting primary aluminium with secondary aluminium dominate. Through the system expansion approach, it is assumed that by producing secondary aluminium, the market could avoid the production of primary aluminium, which has a high contribution to all the former impact categories, and therefore, this impact gets discounted from the total. The contribution of this substitution of primary aluminium by secondary is higher for the salt-slag treatment route because around 36 kg of aluminium concentrates are recovered from the salt-slag per tonne of scrap treated. Recovering these concentrates reduces the global warming contributions by an additional -445 kg. This is a clear example of how small increases in yield bring forth significant environmental benefits. Therefore, minimising the aluminium losses should be a priority to optimise the environmental (and economic) performance of the process, as waste management routes which manage to recover the most secondary

aluminium tend to be the most sustainable. To discuss the contributions of the rest of the inputs to the process, the figure below omits the aluminium.

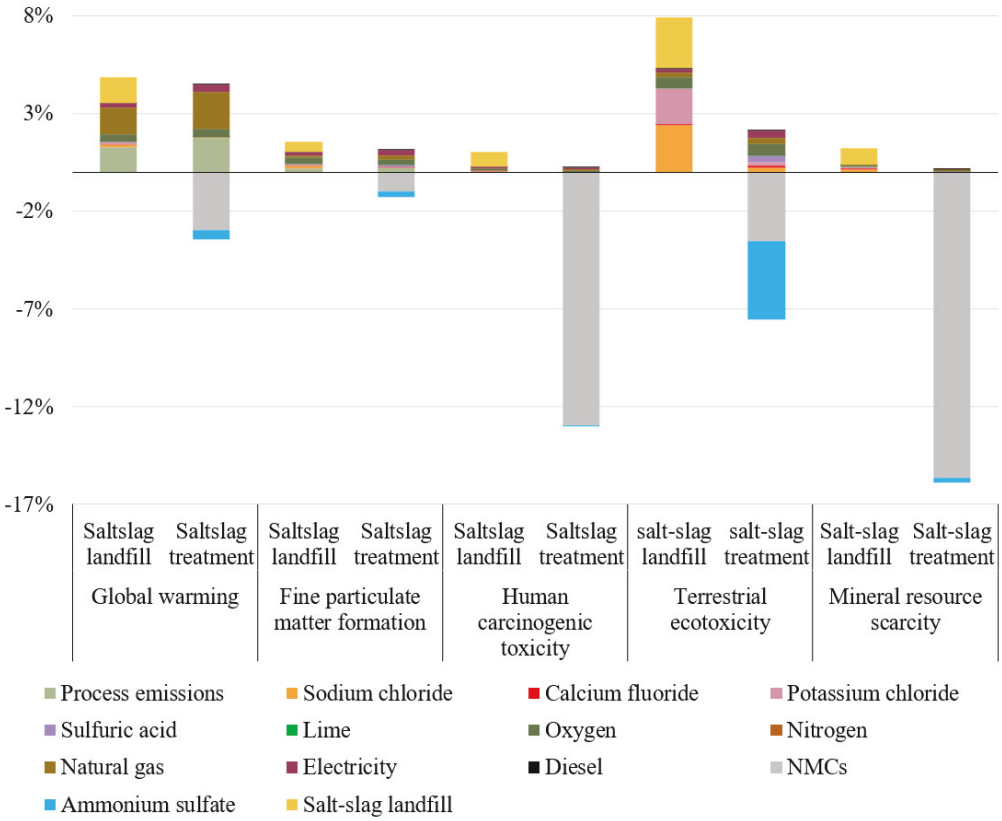

Figure 40. Contribution analysis omitting the allocation of aluminium recovered.

Figure 40 reveals the hotspots or most relevant potential areas for process improvement besides minimising metal losses. To reduce the process impacts to the midpoint "global warming", efforts should be put on minimising process emissions, reducing the use of natural gas for thermal energy, avoiding landfill, and recovering the NMCs. Recovering ammonium sulphate is also beneficial, to a lesser extent but enough to compensate for the impacts related to the use of oxygen and electricity, contributions which are also visible. For the midpoint indicator "fine particulate matter formation", the relative contributions of the process emissions, the use of oxygen, sodium chloride, electricity, natural gas, and the recovery of ammonium sulphate are of similar magnitude. The impact of the salt-slag disposal is roughly three times as high as those mentioned, and the savings from recovering NMCs are the

largest. The recovery of NMCs offers the most substantial benefits for the indicators "human carcinogenic toxicity", and "mineral resource scarcity". The impact of preventing salt-slag landfill is visible for all indicators but especially beneficial for the "terrestrial ecotoxicity". For this category, the reuse of NaCl and KCl are also significant benefits of the salt-slag treatment. Finally, the recovery of aluminium sulphate also saves substantial impacts on the "terrestrial ecotoxicity", and the impacts related to the consumption of oxygen as fuel to the furnaces are also visible across all the selected indicators, although they are not affected by the choice of recycling route. In absolute numbers, for a tonne of the material mix treated, the impacts to global warming arising from process emissions were 170 kg CO_2-eq/tonne Al treated for the salt-slag landfill route, and 234 kg CO_2-eq for the salt-slag treatment route. Using natural gas to fire the furnaces led to 183 kg CO_2-eq for salt-slag landfill and 250 kg CO_2-eq for salt-slag treatment. The impacts of electricity consumption were also lower for salt-slag landfill than for salt-slag treatment; 27 kg CO_2-eq vs. 48 kg CO_2-eq, since the salt-slag treatment uses additional fuels and energy. However, the salt-slag treatment prevents the impacts due to waste landfill (176 kg CO_2-eq). In addition, recovering NMCs saves 394 kg CO_2-eq, ammonium sulphate 63 kg CO_2-eq, and recovering and recirculating NaCl/KCl salts into the rotary furnace reduces the emissions associated with salt production by 31 kg CO_2-eq. Finally, the substitution of primary aluminium reduced the global warming impacts by 13,355 for the salt-slag treatment and 12,909 for the salt-slag landfill, and the difference of 445 kg CO_2-eq is due to the recovery of aluminium concentrates.

Damgaard [100] attributed global warming impacts of similar magnitude (between 360-1,260 kg CO_2-eq tonne^{-1} scrap treated) to the recycling processes for aluminium post-consumer scrap in refiners. In [115], there is data from an environmental assessment for secondary cast alloy production in 2010 in Europe (refining model, using the software GaBi), where the Global Warming potential of the recycling processes was 510 kg CO_2-eq tonne^{-1} secondary aluminium.

5.4 Discussion and Recommendations

The results show that the recovery of by-products from the salt-slag increases the sustainability of the recycling process, despite increasing the energy and raw materials

consumption. The main benefits of the salt-slag valorisation are the recovery of the aluminium concentrates, NMCs, ammonium sulphate, and avoiding the negative impacts of landfilling waste.

Salt-flux recycling makes it possible to recover aluminium from streams which are complicated to recycle through other re-melting methods, such as dross, thus bringing significant environmental savings compared to aluminium primary production. However, if certain scrap types could be recycled efficiently without salts, e.g., by applying a thermal pre-treatment to clean the scrap from organics before remelting in a reverberatory furnace, a specific assessment should be conducted to determine the most sustainable and profitable route. This could apply to shavings and packaging waste, but not to partly oxidised scrap as dross or IBA where salt additions are needed to liberate the metal from the oxides it is surrounded by. To improve the sustainability performance of the recycling route evaluated, the results suggest focusing the efforts firstly on preventing aluminium losses, and, secondly, on maximising energy efficiency, minimising the process emissions and optimising the recovery and usage of NMCs.

The dominance of the aluminium recovery may lead to large differences in the environmental impacts when considering different types of scrap. The metal yield depends both on the intrinsic content of non-metallic contaminants (moisture, organics, oxides) of the treated materials, and on the metal losses which take place during the high-temperatures processes, affected by factors such as the scrap specific surface area or the furnace operation, as discussed in previous chapters. Figure 41 illustrates through a sensitivity analysis the influence the metal yield considered on the global warming potential when treating 1 tonne of materials via the studied industrial route (Scenario 2).

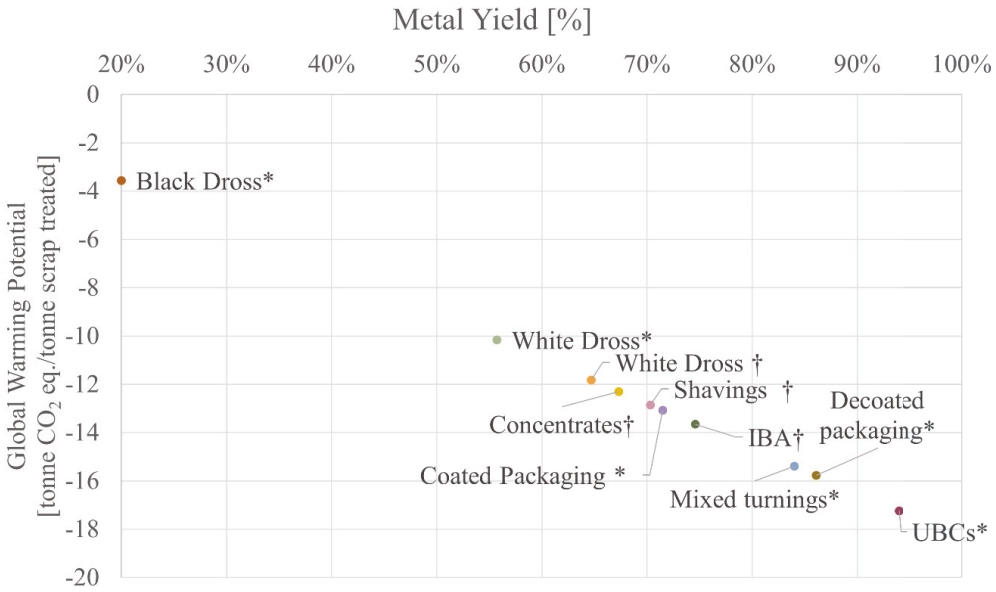

*Figure 41. Calculated global warming potentials for varying scrap types and metal yields. *Average metal yield values from Standard EN13920. †Metal yield values reported by recycling plant.*

Recycling 1 tonne of scrap with different metal yields between 55 and 94 % as illustrated in the figure, would save between ca. 10 and 17 tonnes CO_2-eq. Therefore, it is advisable that LCA studies which aim to compare recycling routes use fixed metal yield values or include a similar sensitivity analysis.

The results also show that, even for black dross with a hypothetical metal yield as low as 20 % of its weight, recycling would still be beneficial, saving 3.5 tonnes CO_2-eq/tonne treated. Another interesting fact is that recycling 1 tonne of de-coated packaging would save approximately 3 more tonnes of CO_2-eq compared to recycling coated packaging, due to the expected metal yield differences. However, the energy and emissions associated with the additional thermal de-coating pre-treatment process have not been included in the study. All considered, in view of the sensitivity analysis, it is proposed that successfully de-coating the scrap before re-melting it or preparing it in other ways that help decrease the re-melting losses, even just to a small extent, would improve the net environmental impacts of the recycling process.

5.5 Conclusions and Future Work

5.5.1 Conclusions

This LCA study described a realistic scenario for European aluminium refiners and allowed comparing the impact of two salt-flux management routes and recommending potential areas where the efforts to improve the environmental performance of recycling processes should focus. The following conclusions were drawn:

- Recycling 1 tonne of aluminium-containing streams (dross, IBA, shavings) with a metal yield of 72 % in a salt-based rotary furnace process saves 13.2 tonnes CO_2-eq of global warming contributions.
- Treating the salt-slag instead of landfilling it reduces the global warming potential by an additional tonne of CO_2-eq and brings forth significant environmental benefits (between 5-25 %) for the rest of the midpoint indicators.
- The most benefitted midpoint indicators when treating the salt-slag were, in descending order: mineral resource scarcity and human carcinogenic toxicity (due to NMCs recovery), and terrestrial ecotoxicity (due to prevention of landfill and ammonium sulphate and salts recovery).
- The main contributors to reducing the global warming potential are the recovery of aluminium concentrates, NMCs, the avoidance of landfill, and to a lower extent the recovery of ammonium sulphate.
- Further efforts to improve the environmental performance of the process should focus on minimising metal losses and optimising the recovery and usage of NMCs.
- The metal yield of the treated Al streams has a substantial effect on the environmental performance of the recycling process, e.g., yield variations between 20 and 95 % lead to global warming potentials ranging from 3.5 to 17 tonne CO_2-eq.

5.5.2 Future Work

The present study could be expanded to include a sensitivity analysis of the impact of the choice of energy source and the location of production. This could be done for the direct energy consumed in the plant, and for the substituted primary aluminium or byproducts. It would also be relevant to current industrial developments to evaluate the substitution of natural gas to obtain thermal energy by other fuels, including various types of hydrogen.

Another future study could focus on deepening the understanding of the environmental savings linked to the usage of the recovered NMCs by different

applications. For example, by evaluating actual production data from cement or ceramic producers which have implemented this type of byproducts to substitute raw materials.

Finally, since aluminium post-consumer scrap, such as used packaging, can also be recycled through other routes, such as by thermal de-coating and consequent re-melting in a reverberatory furnace without salts, it would be interesting to carry out another detailed LCA of such a process to compare the environmental performance of both recycling options for relevant materials. Another relevant continuation of the current work would be to study the impacts of mixing different types of alloys and the subsequent refining, cascading or dilution required to adjust the composition versus sorting and recycling each alloy family.

Chapter 6. Overall Conclusions

The main objectives of this thesis work were to investigate how recycling processes of aluminium packaging products can be affected by their preparation via compaction or thermal treatments, and to analyse the environmental impacts of recycling Al through the rotary furnace route. Special emphasis was placed on understanding the relationship between compacting and de-coating materials with various characteristics (thickness, coating) and the mechanisms behind metal losses when re-melting with or without salts.

From the laboratory-scale experiments studying the interaction between the scrap surface area, its susceptibility to oxidation and the consequent re-melting losses in salt-flux, the main conclusions were the following:

- Scrap with high specific surface areas, such as household foil, is more susceptible to oxidation when exposed to the high temperatures and oxidising atmospheres of industrial recycling or incineration processes.
- Compacting thin scrap into briquettes is an effective way to reduce susceptibility to oxidation and to promote the coalescence of small/thin metallic pieces when re-melting with salt-flux, thereby reducing metal losses.
- The metallic content of incineration bottom ash (IBA) of sizes between 2-30 mm ranges between 76-93 wt%. The metal content increases with IBA size, which is also a direct consequence of the lower specific surface areas exposed during incineration.
- A simplified model, assuming IBA of spherical shapes with an average oxide layer thickness of 68 μm, can be used to estimate its metallic content depending on its size.

The main conclusions from the laboratory-scale experiments studying the effect of compacting coated scrap through various methods on the thermal de-coating process,

and the consequences of combining these pre-treatment routes before re-melting with and without salt-flux, were:

- Compacting coated products reduces the off-gas emissions which take place upon the decomposition of the organics during the thermal de-coating or re-melting processes.
- High densification of materials containing organics hinders the transport of oxygen, which is necessary for the thermolysis reactions. Thermally de-coating the coated products in loose or loosely compacted states promotes their de-coating efficiency and prevent de-coating char residues inside the briquettes.
- The presence of carbonaceous residues was the main factor increasing the re-melting losses through both processes since it significantly impacts the coalescence of the aluminium chips when re-melting in salt-flux and the dross formation when re-melting in a molten heel without salt additions.

Lastly, the main findings from the LCA study of an industrial recycling process via a rotary furnace with consequent salt-slag treatment were:

- Recycling 1 tonne of aluminium-containing streams (dross, IBA, shavings) with a metal yield of 72 % through a salt-based rotary furnace process prevents substantial environmental impacts, such as 13.2 tonnes CO_2-eq of global warming contributions.
- Treating the salt-slag instead of landfilling it reduces the global warming potential by 1 tonne of CO_2-eq/tonne Al-streams treated. In addition, it is particularly beneficial for the indicators mineral resource scarcity and human carcinogenic toxicity (due to NMCs recovery), and to terrestrial ecotoxicity (due to prevention of landfill and ammonium sulphate and salts recovery).
- The metal yield assumptions are critical for the LCA results of the recycling process, e.g., yield variations between 20 and 95 % lead to global warming potentials ranging from 3.5 to 17 tonne CO_2-eq.

As seen in the LCA study, the implications of improving the metal recovery of the recycling processes, even to a small extent, has significant environmental (and economic) implications at an industrial scale. Considering these results together with

the observations from the preceding studies and the benefits of compaction for logistic transport/storage operations, the following conditioning route for recycling packaging scrap is proposed:

- Transport the scrap compacted into bales to the recycling facility.
- Loosen up or shred the bales for sorting and thermal pre-treatment with controlled air flow and off-gas treatment.
- Once the organics and volatiles are fully removed, consider compacting the scrap into bales/briquettes, particularly if it presents high specific surface area, to reduce re-melting losses and ease it's charging and sinking. High densification is not needed.
- Recover Al from dross by salt-flux recycling or other suitable treatments/uses.

Chapter 7. Future Work

Based on previous literature and the findings in this study, the suitable choice of re-melting pre-treatment, depending on the re-melting method (with or without salt) and the scrap characteristics (specific surface area, organic content) can significantly affect the performance of recycling aluminium packaging products. However, several aspects still need further research to determine the optimal pre-treatment and recycling processes for the different types of packaging scrap. Recommendations for future work are discussed below.

The potential benefits of compacting scrap with high specific surface areas but free from organics before thermal treatment and re-melting could be applied to other thin products, for example foils recovered from batteries, laminates, or primary scrap, as long as they are clean from volatiles and organics. In addition, the consequences of re-melting partially oxidised scrap (IBA, de-coated foils) through salt-free methods could be explored, through similar laboratory-scale experiments as those employed in this thesis or through industrial-scale experiments in reverberatory or vortex furnaces. Compacting clean, thin scrap into high densities, e.g., using torsion-pressure or other extrusion methods, could be beneficial for some setups. For instance, it may facilitate the submersion of scrap into the melt, in addition to reducing its exposure to oxidising atmospheres. This could be particularly relevant for primary scrap, e.g., from machining, that is re-melted via salt-free processes.

The work on recycling coated products could be expanded by using thinner materials. A particularly interesting case would be to test the influence of thermal de-coating followed by compaction on the recycling performance of flexible packaging/laminates, which are deemed non-recyclable and excluded from current collection systems. This study could be also expanded for scraps of increasing degrees of organic content, e.g., post-consumer packaging containing food residues, such as coffee capsules. Since the oxygen content in the atmosphere and sufficient gas transport were proved critical for a successful de-coating, it would be advisable to carry out future studies using setups

which ensure this. For example, by using higher gas-flows/O_2 concentrations or a rotary kiln de-coater. Furthermore, at an industrial scale it would be interesting to evaluate the potential benefits of reusing/recirculating the off gas emitted from the decomposition of the organics for the energy efficiency of the overall recycling processes.

Regarding the environmental impacts of aluminium recycling, future studies could explore the influence of different energy sources. For example, it could be especially relevant to current industrial developments to evaluate the substitution of natural gas required for the thermal energy in the rotary furnace by other fuels, including various types of hydrogen.

Finally, to determine the most sustainable route to recycle packaging products, it would be necessary to carry out another detailed LCA of a recycling route consisting of a thermal de-coating and re-melting in a reverberatory furnace without salts. This could then be compared with the LCA results from the rotary furnace and salt valorisation route studied in this thesis. More in-depth analysis of the environmental impacts of the refining processes, including the implications of mixing different types of alloys and the consequent cascading or dilution versus sorting and preparation of the scrap by alloy families is also suggested.

References

[1] IAI, "Material flow model," in "International Aluminium Institute," 2021. [Online]. Available: https://international-aluminium.org/resource/iai-material-flow-model-2021-update/

[2] V. Milani and G. Timelli, "Solid Salt Fluxes for Molten Aluminum Processing - A Review," *Metals*, vol. 13, no. 5*,* doi: 10.3390/met13050832.

[3] "Proposal for a revision of EU legislation on packaging and packaging waste. Environment Directorate, EU Comission ", 2022. [Online]. Available: https://environment.ec.europa.eu/publications/proposal-packaging-and-packaging-waste_en

[4] A. Tabereaux and R. Peterson, "Aluminum production.," in *Treatise on process metallurgy*, S. Seetharaman Ed. Boston: Elsevier, 2014, ch. 2.5, pp. 839-917.

[5] CEWEP, "Bottom ash fact sheet," Confederation of European Waste to Energy Plants. [Online]. Available: https://www.cewep.eu/bottom-ash-factsheet/

[6] "Mineral commodity summaries 2023," in "Mineral Commodity Summaries," Reston, VA, Report 2023, 2023. [Online].Available: https://pubs.usgs.gov/publication/mcs2023

[7] W. M. Mayes *et al.*, "Advances in Understanding Environmental Risks of Red Mud After the Ajka Spill, Hungary," *Journal of Sustainable Metallurgy,* vol. 2, no. 4, pp. 332-343, 2016/12/01 2016, doi: 10.1007/s40831-016-0050-z.

[8] S. Morsali and F. Yildirim, "Environmental impact assessment of red mud utilization in concrete production: a life cycle assessment study," *Environment, Development and Sustainability,* 2023/08/16 2023, doi: 10.1007/s10668-023-03767-z.

[9] J. Thonstad, *Aluminium Electrolysis: Fundamentals of the Hall-Héroult Process*. Aluminium-Verlag, 2001.

[10] J. Haraldsson and M. T. Johansson, "Review of measures for improved energy efficiency in production-related processes in the aluminium industry – From electrolysis to recycling," *Renewable and Sustainable Energy Reviews,* vol. 93, pp. 525-548, 2018/10/01/ 2018, doi: 10.976/j.rser.2018.05.043.

[11] Eurostat, "Packaging waste by waste management operations," 19/10/2023 Available:https://ec.europa.eu/eurostat/databrowser/view/env_waspac__custom_7988850/default/table?lang=en

[12] Reloop, "Global Deposit Book 2022," 2022. Available: https://www.reloopplatform.org/wp-content/uploads/2022/11/RELOOP_Global_Deposit_Book_11I2022_P1.pdf

[13] R. Warrings and J. Fellner, "Current status of circularity for aluminum from household waste in Austria," *Waste Management,* vol. 76, pp. 217-224, 2018/06/01/ 2018, doi: 10.1016/j.wasman.2018.02.034.

[14] M. S. Skramstad, Martin; Kvithyld, Anne, "Aluminium packaging flows in Norway," SINTEF, 2021. [Online]. Available: https://sintef.brage.unit.no/sintef-xmlui/handle/11250/2767866

[15] Infinitum, "Infinitum Annual Report 2022," 2022. [Online]. Available: https://infinitum.no/annual-reports/

[16] D. Blasenbauer *et al.*, "Legal situation and current practice of waste incineration bottom ash utilisation in Europe," *Waste Management,* vol. 102, pp. 868-883, 2020/02/01/ 2020, doi: 10.1016/j.wasman.2019.11.031.
[17] M. Šyc *et al.*, "Metal recovery from incineration bottom ash: State-of-the-art and recent developments," *Journal of Hazardous Materials,* vol. 393, p. 122433, 2020/07/05/ 2020, doi: 10.1016/j.jhazmat.2020.122433.
[18] R. Bunge, "Recovery of metals from waste incinerator bottom ash," UMTEC, 2019.Available:https://www.umtec.ch/fileadmin/user_upload/umtec.hsr.ch/Dokumente/Metals_from_MWIBA_6_2019.pdf
[19] Y. Hu, M.C. Bakker and P.G. de Heij, "Recovery and distribution of incinerated aluminum packaging waste," Waste Manag. 2011 Dec; 31(12):2422-30. doi: 10.1016/j.wasman.2011.07.021.
[20] L. Biganzoli and M. Grosso, "Aluminium recovery from waste incineration bottom ash, and its oxidation level," Waste Management & Research 31: 954–959. doi:10.1177/0734242X13493956.
[21] M. Gökelma, I. Meling, E. Soylu, A. Kvithyld, and G. Tranell, "A Method for Assessment of Recyclability of Aluminum from Incinerated Household Waste," in *Light Metals 2019*. C. Chesonis (ed.), The Minerals, Metals & Materials Series. Springer, Cham. doi:10.1007/978-3-030-05864-7_168
[22] M. E. Schlesinger, *Aluminium recycling*. CRC Press, Taylor & Francis Group, 2007. ISBN 0-8493-9662-X.
[23] G. Coates and S. Rahimifard, "Modelling of post-fragmentation waste stream processing within UK shredder facilities," *Waste Management,* vol. 29, pp. 44-53, 2009, doi: 10.1016/j.wasman.2008.03.006.
[24] D. B. Spencer, "The High-Speed Identifi cation and Sorting of Nonferrous Scrap," *JOM,* vol. 57, pp. 46-51, 2005, doi: 10.1007/s11837-005-0081-6.
[25] R.K. Wyss and P.B. Schultz, "Color Sorting Aluminium Alloy Scrap for Recycling," Light Metals 1999. p. 1093-1098, C. Edward Eckert (ed.), The Minerals, Metals & Materials Series.
[26] S. Sander, G. Schubert, and H.-G. Jäckel, "The fundamentals of the comminution of metals in shredders of the swing-hammer type," *International journal of mineral processing,* 2004, doi: 10.1016/j.minpro.2004.07.038.
[27] S. Capuzzi and G. Timelli, "Preparation and melting of scrap in aluminium recycling: A review," *Metals,* vol. 8, p. 249, 2018, doi: 10.3390/met8040249.
[28] H. Rossel, "Fundamental investigations about metal loss during remelting of extrusion and rolling fabrication scrap," in *Light Metals 1990*, C. M. Bickert (ed.), The Mineras, Metals & Materials Series.
[29] H. Puga, J. Barbosa, D. Soares, F. Silva, and S. Ribeiro, "Recycling of aluminium swarf by direct incorporation in aluminium melts," *Journal of Materials Processing Technology,* vol. 209, no. 11, pp. 5195-5203, 2009/06/21/ 2009, doi: 10.1016/j.jmatprotec.2009.03.007.
[30] P. Klingauf. (2018) RUF briquetting system contributes to increased economic efficiency at Metal Trade Comax. *ERZMETALL*. 280-282. Available: https://www.recycling-magazine.com/2018/05/10/refiner-optimises-yield-through-briquetting/
[31] J. Steglich, R. Dittrich, G. Rombach, M. Rosefort, B. Friedrich, and A. Pichat, "Dross Formation Mechanisms of Thermally Pre-Treated Used Beverage Can

Scrap Bales with Different Density," in Ratvik, A. (eds) *Light Metals 2017*, p. 1105-1113. The Minerals, Metals & Materials Series. Springer, Cham. doi:10.1007/978-3-319-51541-0_133.

[32] J. Steglich, B. Friedrich, and M. Rosefort, "Dross Formation in Aluminum Melts During the Charging of Beverage Can Scrap Bales with Different Densities Using Various Thermal Pretreatments," *JOM,* 72, 3383-3392 (2020). doi: 10.1007/s11837-020-04268-4.

[33] B. McAvoy, J. McNeish "The alcan decoater process for UBC decoating," in *Second International Symposium – Recycling of Metals and Engineered Materials*, J. H. L. van Linden, D.L. Stewart, Y. Sahai (eds), 1990, pp. 203-214.

[34] A. van Schaik and M. A. Reuter, "Material-Centric (Aluminium and Copper) and Product-Centric (Cars, WEEE, TV, Lamps, Batteries, Catalysts) Recycling and DfR Rules," in *Handbook of Recycling*, E. Worrell and M. A. Reuter (eds). Elsevier, 2014, ch. 22. ISBN 9780123964595, doi:10.1016/B978-0-12-396459-5.00022-2

[35] W. Bateman, G. Guest, and R. Evans, "Decoating of aluminium products and the environment," in *Light Metals 1999*, C. E. Eckert (eds), The Minerals, Metals & Materials Society, pp. 1099-1105.

[36] J. Muñiz Lerma, PhD Thesis: "Recycling of Aerospace Aluminium Components into New Valuable Products," McGill University, Montreal, QC, 2016.

[37] W. Stevens and F. Tremblay, "Fundamentals of UBC decoating / delaquering for efficient melting," Light Metals 1997, R. Huglen (eds), pp 709-713. The Minerals, Metals & Materials Society.

[38] S. Capuzzi, A. Kvithyld, G. Timelli, A. Nordmark, E. Gumbmann, and T. A. Engh, "Coalescence of Clean, Coated, and Decoated Aluminum for Various Salts, and Salt–Scrap Ratios," *Journal of Sustainable Metallurgy,* vol. 4, no. 3, pp. 343-358, 2018/09/01 2018, doi: 10.1007/s40831-018-0176-2.

[39] M. Gökelma, F. Diaz, I. E. Öner, B. Friedrich, and G. Tranell, "An Assessment of Recyclability of Used Aluminium Coffee Capsules," in Tomsett, A. (eds) Light Metals 2020. The Minerals, Metals & Materials Series. Springer, Cham. doi:10.1007/978-3-030-36408-3_149

[40] R. Dittrich, B. Friedrich, G. Rombach, J. Steglich, and A. Pichat, "Understanding of Interactions Between Pyrolysis Gases and Liquid Aluminum and Their Impact on Dross Formation," In: Ratvik, A. (eds) Light Metals 2017. The Minerals, Metals & Materials Series. Springer, Cham. https://doi.org/10.1007/978-3-319-51541-0_174.

[41] A. Kvithyld, A. Nordmark, D. Dispinar, S. Ghaderi, and K. Lapointe, "Quality Comparison between Molten Metal from Remelted Sheets; Mill Finish and Coated," in *Light Metals 2012*, C. E. Suarez (eds), pp. 1031-1035. The Minerals, Metals & Materials Series. Springer, Cham. https://doi.org/10.1002/9781118359259.ch179

[42] A. Kvithyld, T. A. Engh, and R. Illés, "Decoating of aluminium scrap in various atmospheres," In: *Light Metals 2002,* pp. 1055-1060. ISBN:0-87339-519-0

[43] S. Capuzzi, A. Kvithyld, G. Timelli, A. Nordmark, and T. A. Engh, "Influence of Coating and De-Coating on the Coalescence of Aluminium Drops in Salt,"

In: Ratvik, A. (eds) *Light Metals 2017*. The Minerals, Metals & Materials Series. Springer, Cham. doi:10.1007/978-3-319-51541-0_134

[44] K. Fujisawa, T. Kogishi, O. Kenji; T. Nakamura, "A basic study on development of a swell-peeling method in UBC recycling system," in *4th Int. Symp. Recycl. Met. Eng. Mater.*, D. L. Stewart, R. Stephens and J.C. Daley, (eds), The Minerals, Metals & Materials Society, 2000, pp. 835-844.

[45] C. Paitoni, L. Benedini (2004) Rotary smelting furnace. *Diecasting Technology*. 52-54.

[46] G. Cusano, M. Rodrigo Gonzalo, F. Farrell, R. Remus, S. Roudier, and L. Delgado Sancho, "Best Available Techniques (BAT) Reference Document for the Non-Ferrous Metals Industries," *Industrial Emissions Directive 2010/75/EU,* vol. EUR 28648 EN, 2017, doi: 10.2760/8224.

[47] G. Sua-iam and N. Makul, "Use of recycled alumina as fine aggregate replacement in self-compacting concrete," *Construction and Building Materials,* vol. 47, pp. 701-710, 2013/10/01/ 2013, doi: 10.1016/j.conbuildmat.2013.05.065.

[48] M. López-Alonso, M. J. Martinez-Echevarria, L. Garach, A. Galán, J. Ordoñez, and F. Agrela, "Feasible use of recycled alumina combined with recycled aggregates in road construction," *Construction and Building Materials,* 195, pp. 249-257, 2019, doi: 10.1016/j.conbuildmat.2018.11.084.

[49] J. Wu, F. Djavanroodi, C. Gode, S. Attarilar, and M. Ebrahimi, "Melt refining and purification processes in Al alloys: a comprehensive study," *Materials Research Express,* vol. 9, no. 3, p. 032001, 2022/03/24 2022, doi: 10.1088/2053-1591/ac5b03.

[50] P. Waite, "A technical perspective on molten aluminium processing," In: W. Schneider (eds) *Light metals 2002, TMS-AIME* p. 841.

[51] T. A. Engh, G. K. Sigworth, and A. Kvithyld, *Principles of Metal Refining and Recycling*. Oxford University Press, 2021. doi: 10.1093/oso/9780198811923.001.0001.

[52] J. Campbell, "Entrainment defects," *Materials Science and Technology,* vol. 22, no. 2, pp. 127-145, 2006/02/01 2006, doi: 10.1179/174328406X74248.

[53] C. E. Eckert, "The origin and identification of inclusions in foundry alloys," presented at the 3rd International Conference on Molten Aluminium Processing, Orlando, Florida, 1992. pp. 17-50.

[54] T. A. Utigard, "The properties and uses of fluxes in molten aluminum processing," *JOM,* vol. 50, no. 11, pp. 38-43, 1998/11/01 1998, doi: 10.1007/s11837-998-0285-7.

[55] T. Hiraki, T. Miki, K. Nakajima, K. Matsubae, S. Nakamura, and T. Nagasaka, "Thermodynamic Analysis for the Refining Ability of Salt Flux for Aluminum Recycling," (in eng), *Materials,* vol. 7, no. 8, pp. 5543-5553, 2014, doi: 10.3390/ma7085543.

[56] R. R. Roy and Y. Sahai, "Coalescence behavior of aluminium alloy drops in molten salts," *Materials Transactions, JIM,* vol. 38, no. 11, pp. 995-1003, 1997. Doi: 10.2320/matertrans1989.38.995

[57] B. Wan, W. Li, F. Liu, T. Lu, S. Jin, K. Wang, A. Yi, J. Tian, W. Chen, "Determination of fluoride component in the multifunctional refining flux used for recycling aluminum scrap," *Journal of Materials Research and*

Technology, vol. 9, no. 3, pp. 3447-3459, 2020/05/01/ 2020, doi: 10.1016/j.jmrt.2020.01.082.

[58] J. A. Soares Tenorio, M. Carboneri Carboni, and D. C. Romano Espinosa, "Recycling of aluminum – effect of fluoride additions on the salt viscosity and on the alumina dissolution," *Journal of Light Metals,* vol. 1, no. 3, pp. 195-198, 2001/08/01/ 2001, doi: 10.1016/S1471-5317(01)00013-X.

[59] J. A. Soares Tenorio and D. C. Romano Espinosa, "Effect of salt/oxide interaction on the process of aluminum recycling," *Journal of Light Metals,* vol. 2, no. 2, pp. 89-93, 2002/05/01/ 2002, doi: 10.1016/S1471-5317(02)00027-5.

[60] M. Shi and Y. Li, "Performance Improvement in Aluminum Alloy Treated by Salt Flux with Different Fluorides," *Journal of Materials Engineering and Performance,* 32, 3065-3072, 2023, doi: 10.1007/s11665-022-07306-1.

[61] J. Ye and Y. Sahai, "Interfacial behavior and coalescence of aluminium drops in molten salts," *Materials Transactions, JIM,* vol. 37, no. 2, pp. 175-180, 1996.

[62] A. Bergin, "Ceramic Foam Filters (CFFs) for Aluminium Melt Filtration - Stability, Compression, and Performance," PhD Thesis, NTNU, Trondheim, 2022.

[63] G. A. Wolstenholme, "Aluminum Extraction," in *Molten Salt Technology*, D. G. Lovering Ed. Boston, MA: Springer US, 1982, pp. 13-55.

[64] L. Zhang, J. Gao, L. N. W. Damoah, and D. G. Robertson, "Removal of Iron From Aluminum: A Review," *Mineral Processing and Extractive Metallurgy Review,* vol. 33, no. 2, pp. 99-157, 2012/03/01 2012, doi: 10.1080/08827508.2010.542211.

[65] X. Cao and J. Campbell, "Effect of precipitation and sedimentation of primary α-Fe phase on liquid metal quality of cast Al–11.1Si–0.4Mg alloy," *International Journal of Cast Metals Research,* vol. 17, no. 1, pp. 1-11, 2004/01/01 2004, doi: 10.1179/136404604225014792.

[66] A. Flores-V, M. Sukiennik, A. H. Castillejos-E, F. A. Acosta-G, and J. C. Escobedo-B, "A kinetic study on the nucleation and growth of the Al8FeMnSi2 intermetallic compound for aluminum scrap purification," *Intermetallics,* vol. 6, no. 3, pp. 217-227, 1998/01/01/ 1998, doi: 10.1016/S0966-9795(97)00073-3.

[67] X. Zhenming, L. Tianxiao, and Z. Yaohe, "Elimination of Fe in Al-Si cast alloy scrap by electromagnetic filtration," *Journal of Materials Science,* vol. 38, no. 22, pp. 4557-4565, 2003/11/01 2003, doi: 10.1023/A:1027393820932.

[68] J.-H. Kim and E.-P. Yoon, "Elimination of Fe element in A380 aluminum alloy scrap by electromagnetic force," *Journal of Materials Science Letters,* vol. 19, no. 3, pp. 253-255, 2000/02/01 2000, doi: 10.1023/A:1006727212353.

[69] P. Le Brun, C. Kräutlein, G. Rombach, P. Pouly, P. Vries, and J. Luyten, "Removal of intermetallic particles for the purification of aluminum alloys," *TMS Light Metals,* pp. 657-664.

[70] G. J. Sloan and A. R. McGhie, *Techniques of Melt Crystallization. Techniques of Chemistry Volume XIX*. Wiley Interscience, 1988. ISBN 10: 0471078751.

[71] K. Qiu, W. Duan, and Q. Chen, "Basic principles of control of continuous crystallizer in metal refining," *Mineral Processing and Extractive Metallurgy,*

vol. 110, no. 3, pp. 161-164, 2001/12/01 2001, doi: 10.1179/mpm.2001.110.3.161.
[72] W. H. Sillekens, J. A. F. M. Schade Van Westrum, O. S. L. Bruinsma, B. Mehmetaj, and M. Nienoord, "Refining Aluminum Scrap by Means of Fr4Ctional Crystallisation: Basic Experimental Investigations," in *Recycling of Metals and Engineered Materials*, 2000, pp. 963-977. doi: 10.1002/9781118788073.ch85
[73] S. Venditti, D. Eskin, and A. Jacot, "Fractional Solidification for Purification of Recycled Aluminium Alloys," in A. Tomsett (eds), Light Metals 2020. The Minerals, Metals & Materials Series. Springer, Cham. doi:10.1007/978-3-030-36408-3_150
[74] D. C. Curtolo, "Design and investigation of a fractional crystallization-based method using an immersed roational crystallizer for the production of high purity alloy," PhD Thesis, IME, RWTH Aachen, Aachen, 2022.
[75] Alcycle, "Aluminium Dross Processing: A Global Review," 2020. Available: https://www.alcircle.com/specialreport/306/drossprocessing
[76] *EN 13920-1:2003 Aluminium and aluminium alloys scrap*, CEN, 2003.
[77] *EN 13920-10:2003 Aluminium and aluminium alloys scrap*, CEN, 2003.
[78] *EN 13920-14:2003 Aluminium and aluminium alloys scrap*, CEN, 2003.
[79] *EN 13920-15:2003 Aluminium and aluminium alloys scrap*, CEN, 2003.
[80] Y. Xiao and M. A. Reuter, "Recycling of distributed aluminium turning scrap," *Minerals Engineering,* vol. 15, no. 11, Supplement 1, pp. 963-970, 2002/11/01/ 2002, doi: 10.1016/S0892-6875(02)00137-1.
[81] M. Thoraval and B. Friedrich, "Metal Entrapment in Slag during the Aluminium Recycling Process in Tilting Rotary Furnace," in *European Metallurgy Conference*, 2015.
[82] R. M. Xiao Y, Boin U, "Aluminium recycling and environmental issues of salt slag treatment," *J Environ Sci Health A Tox Hazard Subst Environ Eng,* vol. 40, no. 10, pp. 1061-75, 2005, doi: 10.1080/10934520500183824.
[83] S. Capuzzi, G. Timelli, L. Capra, and L. Romano, "Study of fluxing in Al refining process by rotary and crucible furnaces," *International Journal of Sustainable Engineering,* vol. 12, no. 1, pp. 38-46, 2019/01/02 2019, doi: 10.1080/19397038.2017.1393022.
[84] G. O. Verran and U. Kurzawa, "An experimental study of aluminum can recycling using fusion in induction furnace," *Resources, Conservation and Recycling,* vol. 52, no. 5, pp. 731-736, 2008/03/01/ 2008, doi: 10.1016/j.resconrec.2007.10.001.
[85] H. Amini Mashhadi, A. Moloodi, M. Golestanipour, and E. Z. V. Karimi, "Recycling of aluminium alloy turning scrap via cold pressing and melting with salt flux," *Journal of Materials Processing Technology,* vol. 209, no. 7, pp. 3138-3142, 2009/04/01/ 2009, doi: 10.1016/j.jmatprotec.2008.07.020.
[86] H. Puga, J. Barbosa, and C. S. Ribeiro, "Factors Affecting the Metal Recovery Yield during Induction Melting of Aluminium Swarf," *Materials Science Forum,* vol. 730-732, pp. 781-786, 2013.
[87] N. Chamakos *et al.*, "Towards the Efficient Recycling of Used Beverage Cans: Numerical Study and Experimental Validation," in *Light Metals 2023*, S. Broek Ed. Cham: Springer Nature Switzerland, 2023, pp. 942-948.

[88] D. Doutre and A. Kvithyld, "Aluminium," in *Handbook of Recycling*, E. W. Christina Meskers, Markus A. Reuter Ed.: Elsevier, 2023, ch. 20, pp. 319-337.
[89] S. Van den Eynde *et al.*, "Forecasting global aluminium flows to demonstrate the need for improved sorting and recycling methods," *Waste Management,* vol. 137, pp. 231-240, 2022/01/01/ 2022, doi: 10.1016/j.wasman.2021.11.019.
[90] A. N. Løvik and D. B. Müller, "A Material Flow Model for Impurity Accumulation in Beverage Can Recycling Systems," in *Light Metals 2014*, J. Grandfield Ed. Cham: Springer International Publishing, 2016, pp. 907-911.
[91] E. Sevigné-Itoiz, C. M. Gasol, J. Rieradevall, and X. Gabarrell, "Environmental consequences of recycling aluminum old scrap in a global market," *Resources, Conservation and Recycling,* vol. 89, pp. 94-103, 2014/08/01/ 2014, doi: 10.1016/j.resconrec.2014.05.002.
[92] M. B. G. Castro, J. A. M. Remmerswaal, M. A. Reuter, and U. J. M. Boin, "A thermodynamic approach to the compatibility of materials combinations for recycling," *Resources, Conservation and Recycling,* vol. 43, no. 1, pp. 1-19, 2004/12/01/ 2004, doi: 10.1016/j.resconrec.2004.04.011.
[93] International Aluminium Institute. Primary Aluminium Smelting Energy Intensity [Online] Available: https://international-aluminium.org/statistics/primary-aluminium-smelting-energy-intensity/
[94] G. Saevarsdottir, S. K. Padamata, B. N. Velasquez, and H. Kvande, "The Way Towards Zero Carbon Emissions in Aluminum Electrolysis," in *Light Metals 2023*, Cham, S. Broek, Ed., 2023// 2023: Springer Nature Switzerland, pp. 637-645.
[95] Environmental Protection Agency, "European Waste Catalogue and Hazardous Waste List ", 2002. Accessed: November 2023. [Online]. Available: https://archive.org/details/ewccodebook
[96] T. Tolaymat and X. Huang, "Secondary Aluminum Processing Waste: Salt Cake Characterization and Reactivity," U.S. Environmental Protection Agency, Washington D.C.,2015.[Online].Available: http://nepis.epa.gov/Exe/ZyPDF.cgi?Dockey=P100NRFR.pdf
[97] P. E. Tsakiridis, P. Oustadakis, and S. Agatzini-Leonardou, "Aluminium recovery during black dross hydrothermal treatment," *Journal of Environmental Chemical Engineering,* vol. 1, no. 1, pp. 23-32, 2013/06/01/ 2013, doi: 10.1016/j.jece.2013.03.004.
[98] I. Padilla, M. Romero, S. López-Andrés, and A. López-Delgado, "Sustainable Management of Salt Slag," *Sustainability*, vol. 14, no. 9, doi: 10.3390/su14094887.
[99] "ISO 14040:2006 Environmental management Life cycle assessment Principles and framework." [Online]. Available: https://www.iso.org/obp/ui/#iso:std:iso:14040:ed-2:v1:en.
[100] A. Damgaard, A. W. Larsen, and T. H. Christensen, "Recycling of metals: accounting of greenhouse gases and global warming contributions," *Waste Management & Research,* vol. 27, no. 8, pp. 773-780, 2009/11/01 2009, doi: 10.1177/0734242X09346838.
[101] G. Olivieri, A. Romani, and P. Neri, "Environmental and economic analysis of aluminium recycling through life cycle assessment," *International Journal of Sustainable Development & World Ecology,* vol. 13, no. 4, pp. 269-276, 2006/08/01 2006, doi: 10.1080/13504500609469678.

[102] C. Vadenbo, S. Hellweg, and T. F. Astrup, "Let's Be Clear(er) about Substitution: A Reporting Framework to Account for Product Displacement in Life Cycle Assessment," *Journal of Industrial Ecology,* vol. 21, no. 5, pp. 1078-1089, 2017/10/01 2017, doi: 10.1111/jiec.12519.

[103] S. Manfredi, D. Tonini, and T. H. Christensen, "Environmental assessment of different management options for individual waste fractions by means of life-cycle assessment modelling," *Resources, Conservation and Recycling,* vol. 55, no. 11, pp. 995-1004, 2011/09/01/ 2011, doi: 10.1016/j.resconrec.2011.05.009.

[104] C. A. McMillan and G. A. Keoleian, "Not All Primary Aluminum Is Created Equal: Life Cycle Greenhouse Gas Emissions from 1990 to 2005," *Environmental Science & Technology,* vol. 43, no. 5, pp. 1571-1577, 2009/03/01 2009, doi: 10.1021/es800815w.

[105] G. Liu and D. B. Müller, "Addressing sustainability in the aluminum industry: a critical review of life cycle assessments," *Journal of Cleaner Production,* vol. 35, pp. 108-117, 2012/11/01/ 2012, doi: 10.1016/j.jclepro.2012.05.030.

[106] E. Ostertagová, O. Ostertag, and J. Kováč, "Methodology and Application of the Kruskal-Wallis Test," *Applied Mechanics and Materials,* vol. 611, pp. 115-120, 2014. [Online]. Available: https://www.scientific.net/AMM.611.115.

[107] C. Schmitz, *Handbook of Aluminium Recycling: Mechanical Preparation, Metallurgical Processing, Heat Treatment*. Vulkan-Verlag, 2014.

[108] H. Philipson, "The effect of thickness and compaction on the recovery of aluminium in recycling of foils in salt flux," Materials Science and Engineering, KTH and NTNU, 2020. Available: https://ntnuopen.ntnu.no/ntnu-xmlui/handle/11250/2785300

[109] M. Gökelma, A. Vallejo-Olivares, and G. Tranell, "Characteristic properties and recyclability of the aluminium fraction of MSWI bottom ash," *Waste Management,* vol. 130, pp. 65-73, 2021/07/01/ 2021, doi: 10.1016/j.wasman.2021.05.012.

[110] M. Syvertsen, T. Ludwig, S. Rist, and K. Ellingsen, "Use of Incinerator Bottom Ash (IBA) in Aluminium Recycling," in *Light Metals 2022*, Cham, D. Eskin, Ed., 2022// 2022: Springer International Publishing, pp. 1051-1055.

[111] S. Høgåsen, "The effect of compaction and thermal treatment in the recovery of coated aluminium scrap through FTIR off-gas analysis and remelting in molten heel," 2022. [Online]. Available: https://ntnuopen.ntnu.no/ntnu-xmlui/handle/11250/3028711

[112] A. Kvithyld, C. E. M. Meskers, S. Gaal, M. Reuter, and T. A. Engh, "Recycling light metals: Optimal thermal de-coating," *JOM,* vol. 60, no. 8, pp. 47-51, 2008/08/01 2008, doi: 10.1007/s11837-008-0107-y.

[113] C. Meskers, "Coated magnesium - designed for sustainability?," PhD Thesis, TU Delf, 2008.

[114] C. E. M. Meskers, M. A. Reuter, U. Boin, and A. Kvithyld, "A Fundamental Metric for Metal Recycling Applied to Coated Magnesium," *Metallurgical and Materials Transactions B,* vol. 39, no. 3, pp. 500-517, 2008/06/01 2008, doi: 10.1007/s11663-008-9144-8.

[115] EEA, "Environmental profile report - Life-cycle inventory data for aluminium production and transformation processes in Europe," no. Brussels, 2018.

[116] "ISO 14044:2006 Environmental management - Life cycle assessement - Requirements and guidelines." [Online]. Available: https://www.iso.org/obp/ui/#iso:std:iso:14044:ed-1:v1:en.
[117] W. Shang *et al.*, "Production of glass-ceramics from metallurgical slags," *Journal of Cleaner Production,* vol. 317, p. 128220, 2021/10/01/ 2021, doi: 10.1016/j.jclepro.2021.128220.
[118] K. Mikula *et al.*, "From hazardous waste to fertilizer: Recovery of high-value metals from smelter slags," *Chemosphere,* vol. 297, p. 134226, 2022/06/01/ 2022, doi: 10.1016/j.chemosphere.2022.134226.

Supplements to the thesis

Article A

Compaction of Aluminium Foil and Its Effect on Oxidation and Recycling Yield

Alicia Vallejo-Olivares, Harald Philipson, Mertol Gökelma, Hans J. Roven, Trond Furu, Anne Kvithyld, and Gabriella Tranell

Abstract

One of the problems when recycling aluminium is its oxidation and consequent metal loss. This is especially critical for the thin sheet/foil materials used for food packaging applications. Compacting the scrap into briquettes may partly reduce such losses in addition to facilitate transport and storage. Shredded aluminium materials of different thicknesses (15–300 μm) were compacted into cylindrical briquettes of 4 cm diameter, each weighing 20 g by uniaxial pressure or moderate-pressure torsion. A subset of briquettes and chips was subsequently oxidized at 650 °C, while a subset was left untreated. Finally, all samples were re-melted under molten protective salt flux. Compacting reduced the specific oxidation during the heat treatment and promoted the coalescence and yield for the heat-treated materials. Both effects were most significant for the thinnest foil in the study (15 μm). The material thickness influenced the porosity and surface roughness of the resultant briquette as well as the pressure required to reach a given bulk density.

Keywords

Aluminium foil • Recycling • Compaction • Thickness

Introduction

About one-third of the aluminium (Al) currently produced is coming from recycling of either industrial or post-consumer waste, which brings forth substantial economic and environmental benefits [1]. Primary aluminium production is very energy intensive [2, 3] and of the overall energy that is utilized by the aluminium industry annually (7.6 Exajoules), the electrolysis process is by far the most energy intensive, using more than ten times the energy that is used to re-melt scrap (5.0 vs. 0.4 Exajoules) [4]. One of the challenges during recycling is the scrap oxidation and consequent metal loss. The yield and quality of the metal obtained greatly depend on scrap properties and re-melting/pre-treatment methods. Xiao and Reuter showed in several studies the relevance of scrap type, size, surface conditions, and cleanliness on the re-melting losses [5, 6]. One of the results especially relevant for this study was the observation of increasing re-melting losses with decreasing scrap size [7]. Rossel [8] investigated the effect of material thickness on re-melting, and showed that the dross formation was higher for the thinnest material (2 mm), especially for the alloys with high Mg content. Scrap with higher Mg content is generally more susceptible to oxidation [9, 10]. Despite the high reactivity of pure Al with oxygen, aluminium products present excellent corrosion resistance, thanks to the passivating effect of the oxide layer in most environments [11]. This together with good barrier properties against gases, moisture and light, excellent malleability and formability, flexibility, surface resilience, and aesthetic properties makes it a popular choice for food packaging [12]. Of the total Al consumption in 2019 (almost 90 Mt), 8% was for packaging applications [13]. Due to its short life time, the recyclability of packaging is particularly relevant from a circular economy perspective. For example, assuming a Used Beverage Can (UBC) lifetime of 6 months and recovery and recycling rates of 97%, the cumulative material losses would be 84% after 10 years [14]. In order to overcome yield losses for thin

The original version of this chapter was revised: On page no. 736, the line "68.6% *KCl*, 29.4% *NaCl*" has been updated as "68.6% *NaCl*, 29.4% *KCl*". The correction to this chapter is available at https://doi.org/10.1007/978-3-030-65396-5_133

A. Vallejo-Olivares (✉) · H. Philipson · M. Gökelma · H. J. Roven · G. Tranell
NTNU Materials Science and Engineering Department, Alfred Getz vei 2B, 7034 Trondheim, Norway
e-mail: alicia.v.olivares@ntnu.no

T. Furu
NTNU Materials Science and Engineering Department and Norsk Hydro, Alfred Getz vei 2B, 7034 Trondheim, Norway

A. Kvithyld
SINTEF, Alfred Getz vei 2B, 7034 Trondheim, Norway

L. Perander (ed.), *Light Metals 2021*, The Minerals, Metals & Materials Series, https://doi.org/10.1007/978-3-030-65396-5_96

scrap, compacting the scrap into denser pieces such as briquettes or bales may be a solution. This is already an established practice for pre-consumed scrap (e.g. chips from extrusion and machining), since it facilitates storage and transport and prevents the small chips from floating when added into the molten Al pool [15]. Several authors have studied scrap compaction either as a re-melting pre-treatment step [16, 17] or for solid-state recycling, which would allow using the compacted pieces directly without re-melting [18–20]. The aim of this study was to have a closer look at the compaction properties of thin Al materials, and to evaluate the role of briquetting in oxidation and re-melting losses for the different foil thicknesses. The materials studied were non-coated aluminium foil/sheet of five different thicknesses (15, 30, 100, 200, and 300 μm), and the compaction methods uniaxial, moderate-pressure-torsion (MPT), and moderate-pressure-torsion at 450 °C (Hot MPT). The results in this study were part of a Master Thesis carried out at NTNU by Philipson [22].

Experimental Materials and Procedure

Table 1 summarizes the thickness and chemical composition of the materials. Norsk Hydro provided the aluminium sheet alloy AA8006 in gauges of 100, 200, and 300 μm. The 15 μm foil is regular household foil, and the 30 μm a laboratory foil. Their compositions were measured with a portable XRF analyser with and an error of $\pm$ 0.4*.

Shredding and Briquetting

The foils were shredded using a Getecha RS 1600-A1.1.1 shredding machine, which operates with three rotary blades at a rotor revolution of 240 rpm. Depending on the thickness and stiffness of the material, the resulting chips differed in size and level of deformation. Two sieves (square mesh 5 and 2 mm^2) were used to unify the size, keeping only the chips that fell within this range, hence discarding 10–20 wt% of the material. The average mass per chip after sieving was measured to be 6, 12.3, 12.4, 18.2, and 21.8 mg for the 15, 30, 100, 200, and 300 μm thick material, respectively. The chips were subsequently compressed into cylindrical briquettes of 4 cm diameter, each weighing 20 g, using a hydraulic press MTS 311. Since the loose chips occupy more volume than the mould, they were added in several batches and pressed manually until the 20 g was able to fit into the mould space. The chips were compacted by uniaxial pressure, MPT, and Hot MPT at 450 °C. The goal was to obtain briquettes pressed to a wide range of bulk densities, to evaluate both material's compaction behaviour and the influence of the resultant bulk density, porosity, and surface roughness on the re-melting yield. The internal porosity was characterized with a computed-tomography scan (CT) and the surface roughness with an optical 3D-microscope (Alicona 3D-microscope).

Thermal Pre-treatment and Re-melting

The aluminium was melted under protective salt flux, a common procedure in industry for dealing with highly contaminated and oxidized scrap. The salt flux protects the molten metal from further oxidation, captures the oxides and impurities, and promotes the coalescence of the metal drops. [23] A subset of the chips and briquettes was directly re-melted, while another subset was first heat treated at 650 °C for 1 h in a Nabertherm electric furnace featured with air circulation, to promote oxidation, simulating a thermal de-coating pre-treatment. This process is sometimes applied industrially when recycling scrap containing organic coatings or contaminants [24]. The oxidation temperature was chosen based on the work by Capuzzi et al. [23] that showed that by pre-treating the scrap at 600 °C, a complete de-coating was achieved that increased the coalescence of the metal droplets. The weight gain during heat treatment was measured to evaluate whether oxidation is dependent on foil thickness and degree of compaction. The re-melting experiments were performed in ceramic crucibles (Al_2O_3–SiO_2) placed into a muffle furnace. The furnace was pre-heated, and the crucibles filled with the mixed salts (68.6% $NaCl$, 29.4% KCl, and 2% CaF_2) were introduced when the furnace temperature reached 800 °C. The melting point of a mixture of 30% KCl and 70% $NaCl$ is approximately 690 °C, and the small additions of CaF_2 increase it by 20–30 °C [25]. Although the furnace temperature was 800 °C when the crucibles were put inside, it took around 30

Table 1 Composition and thickness of the materials studied

Foil gauge	Al	Fe	Si	Mg	Mn	Cu	Zn	Remain
15μm	98.6 $\pm$ 0.4*	0.73	0.53	<0.16				<0.05
30μm	98.9 $\pm$ 0.4*	0.8	0.11	<0.17				<0.15
100, 200, 300 μm	95.9–98.5	1.2–2	0.4	0.10	0.3–1	0.3	0.10	<0.15

minutes for the salt to melt due to its low thermal conductivity, and some of the salt evaporated. Once the salt melted, the briquettes were dropped into the crucibles using steel tongs. The briquettes were re-melted using 80 g of salt flux (4:1 salt/metal ratio), whereas 150 g of salt flux was used when re-melting the loose chips. Although this salt/metal ratios are far higher than the industrial, they were chosen so that the salt could completely cover the chips. The present re-melting laboratory setup is static, without stirring, in contrast to the industrial rotary furnaces. The density of the melted salt flux was approximately 1.5 g/cm^3 and it was observed that briquettes with lower bulk densities floated just below the surface, whereas the denser briquettes quickly sank into the crucible. After inserting the samples, the muffle furnace was closed and held at 800 °C for 10 minutes, and the crucibles were then taken out and cooled down at room temperature. The aluminium was recovered from the crucible by crushing and dissolving the solidified salt with water against an 800 μm mesh-size sieve. The Al pieces with a smaller diameter than 800 μm were considered as losses and not counted into the weight of the recovered material. During re-melting, typically most of the material coalesced into a main rounded-shaped piece and few small pieces (Fig. 1). The percentage of input material that successfully melted into one piece was defined as coalesced recovery and it is as crucial as the metal yield in the industrial recycling operations, where the small pieces tend to remain trapped into the salt slag. The material yield and coalescence recovery were calculated using Equations 1 and 2:

$$Material\ Yield\ [\%] = (m_r/m_i) * 100 \quad (1)$$

$$Coalescence\ [\%] = (m_c/m_i) * 100 \quad (2)$$

where m_r is the sum of the masses of the pieces (of diameter >800 μm) recovered, m_c is the mass of the biggest piece, and m_i is the initial mass of the briquette or batch of chips.

Results and Discussion

Compaction

Fig. 2 compares the stress needed to compact the materials of different thicknesses to three density ranges. The material thickness influenced the compaction behaviour, and the chips of thin foil were more easily compacted, while thicker materials demanded higher pressure. The lowest and highest achievable bulk densities also differed between materials. In Fig. 3, compressibility curves for the 15 and 30 µm foils are shown. For these materials, it was possible to obtain briquettes with bulk densities as low as 0.8–0.9 g/cm^3 by applying 1.6 MPa (2 kN force). For increasing pressures, the bulk densities increase logarithmically until stabilizing at a plateau around 2.2–2.3 g/cm^3, just below the density of liquid aluminium. A similar plateau was observed in previous investigations [17, 21]. For the 100, 200, and 300 μm sheets, it was not possible to obtain densities lower than 1.35–1.4 g/cm^3 since the chips would not hold together. The comparison between the three compaction methods is plotted in Fig. 4. Combining uniaxial pressure with torsion (MPT) proved to be a very effective compaction method, which allowed reaching densities above the values of the uniaxial plateau at relatively low uniaxial pressures. For example, just by turning the die 180° after applying 200 kN of force, a higher density was reached (2.69 g/cm^3) than for 500 kN uniaxially (2.58 g/cm^3) for the 300 µm material. Turning the die 360° four times while compacting uniaxially at 56 MPa (70 kN) increased the bulk density 29, 24, and 37% for the 15, 30, and 300 μm foils, respectively, reaching densities around 2.5 g/cm^3. Finally, the Hot MPT method (450 °C) increased the bulk density by 33, 32, and 47% for the 15, 30, and 300 μm materials, giving bulk densities above 2.6 g/cm^3, just below the density of solid aluminium (2.7 g/cm^3). The Hot MTP method aimed to simulate

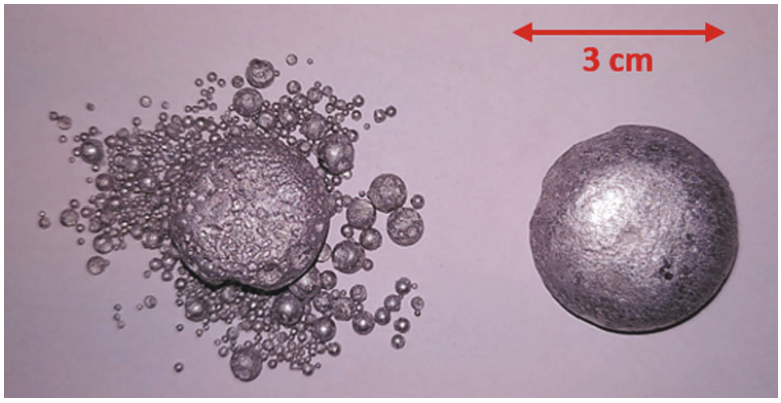

Fig. 1 Aluminium recovered from two crucibles. Right: the material coalesced completely into one piece, so m_r=m_c. Left: m_c (mass of the biggest piece) is smaller than m_r

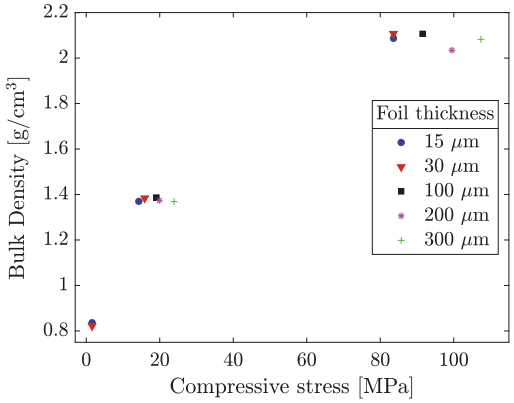

Fig. 2 Uniaxial stress versus briquette bulk density for shredded chips of the materials of different thicknesses

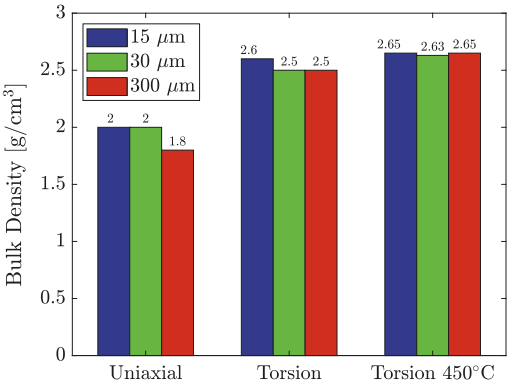

Fig. 4 Mean briquette bulk densities for the 15, 30, and 300 μm gauge materials obtained when compacted with uniaxial pressure (56 MPa), MPT (56 MPa + 4 turns), and Hot MPT (56 MPa + 4 turnings at 450 °C). (Color figure online)

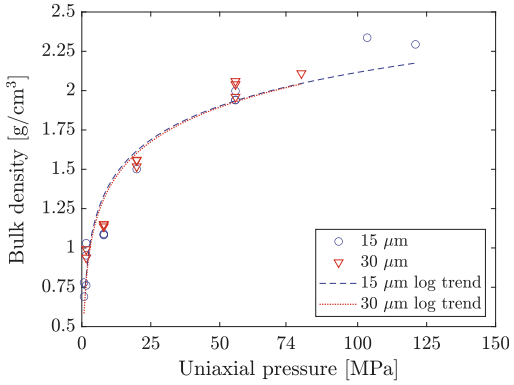

Fig. 3 Compressibility curve for the 15 and 30 μm gauge foils, showing a logarithmic behaviour in the uniaxial pressure versus bulk density. (Color figure online)

solid-state recycling technologies, such as the screw-extrusion process, which bonds shredded scrap into a solid piece of aluminium without the need of re-melting. It was seen that for a given foil thickness, the bulk density increased significantly by adding torsion, while heating to 450 °C on top of that only increased the compaction slightly.

Porosity and Surface Roughness

The porosities of several briquettes were analysed by CT and are summarized in Table 2. The relationship between porosity and bulk density was found to be approximately linear; higher bulk densities have lower internal porosity. For briquettes of similar densities, the lowest porosity was achieved for the thinnest foil, but the porosity differences between materials of different thickness significantly decreased for the highly compacted briquettes. For instance, in the column to the right (Table 2), which corresponds to samples compacted by MPT, the difference in porosity between samples is less than 2%. Figure 5 shows how the MPT method successfully reduced the internal porosity.

Oxidation

After heat treatment in air at 650 °C for 1 h, the weight of the briquettes and loose chips increased due to oxidation. Each briquette and batch of chips weighted 20 g initially, and Fig. 6 shows the mean percentages of weight increase. The results show a correlation between the degree of oxidation and material thickness. Chips and briquettes of thinner material oxidize more, since they display a higher surface to mass ratio. For the five studied materials in order of increasing thickness, the area of foil/sheet in 20 g is approximately 494, 247, 74, 37, and 25 cm^2 (values calculated assuming all materials have the density of pure Al 2.7 g/cm^3). The oxidation differences between materials are reduced when compacting the chips uniaxially, likely due to more similar values of surface area exposed when compacted. For the MPT briquettes, the oxidation differences between materials are almost negligible. Compacting the chips reduced the % wt. gains by 50% or more for all the materials. However, the degree to which they were compacted did not seem to have a significant effect, and all the briquettes compacted uniaxially (bulk density range 0.8–2.1 g/cm^3) resulted in similar weight increases, despite the

Table 2 Average internal porosity (%) measured by CT for different material thicknesses and briquette bulk density ranges

	0.8–0.9 g/cm^3	1.1–1.2 g/cm^3	2.0–2.1 g/cm^3	2.4–2.5 g/cm^3
15 μm	57	29	10	4
30 μm	57	45	15	
100 μm			17	6
300 μm			18	4

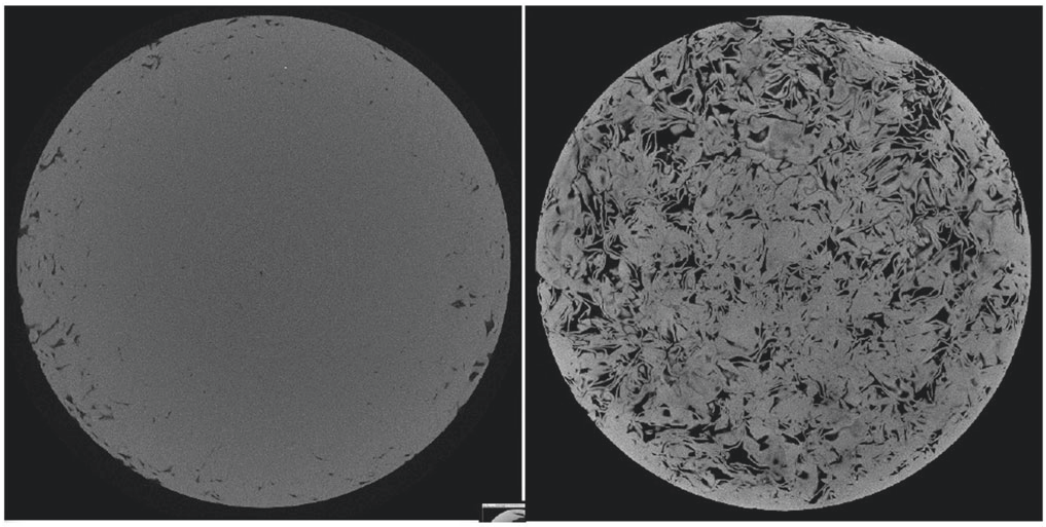

Fig. 5 Briquettes of 100 μm foil. Left: MPT sample with bulk density 2.48 g/cm^3 compacted with 90 kN and 4 torsion turns. Right: Sample compacted with 115 kN (91.5 MPa) uniaxially to bulk density 2.09 g/cm^3

CT analysis revealing large porosity variations within the briquettes and the optical microscopy analysis showing reductions of the surface roughness after high compactions. A further reduction in the % wt. gain did occur for the briquettes compacted by MPT to 2.5 g/cm^3. A hypothesis is that the MPT method achieves a certain level of solid-state bonding which inhibits the oxygen from penetrating through the briquette. On the contrary, the briquettes compacted uniaxially were more porous and the oxygen would still partially oxidize some of the surfaces between the chips.

Re-melting

Fig. 7 shows the coalescence differences between heat-treated loose chips and briquettes for the 30–300 μm materials, and Fig. 8 shows the coalescence and yield versus bulk density for the 15 μm foil. The coalescence differences between loose chips and briquettes are 15.6, 2.7, 1.3, and

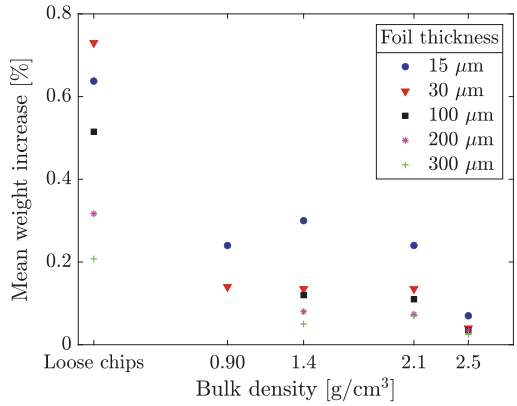

Fig. 6 Mean percentage of weight increase after heat treating 20 g samples of the five different materials in five bulk densities. The bulk density of the loose chips is considered as 0

0.8% for the 30, 100, 200, and 300 μm materials, respectively. The results showed that compacting the chips improved the coalescence, but this effect decreased for increasing material thickness. The variations in briquette bulk density for the material gauges 30, 100, 200, and 300 μm did not have a tangible effect in re-melting, thus all the results were averaged. For the 15 μm foil, the coalescence did vary for different values of bulk density and therefore the results are plotted separately in Fig. 8. The reduction when compacting 15 μm foil chips to the lowest density briquettes (0.9 g/cm^3) was 36.1 g/cm^3.

The reasons why coalescence improved with increasing bulk density for the thinnest foil might be related to several factors such as the breakage of the oxide thickness, decrease in the specific surface area, or increase in thermal conductivity. This hypothesis is discussed in more detail in [22]. The understanding of these mechanisms at a more fundamental level will be the focus of future investigations. For the non-heat-treated samples, the material yield ranged between 98 and 100% for all thicknesses and degrees of compaction. Thus, the pre-existing oxide layer (before re-melting) appears in this case to be more relevant than the oxidation developed during re-melting. It is important to remember that the experimental setup consisted of adding clean scrap directly into a crucible at 800 °C filled with a bath of molten salt flux. The salt-flux method effectively protected the scrap from oxidation, but this may not be the case for other re-melting processes or scrap properties, where thickness and compaction could influence the yield and coalescence differently.

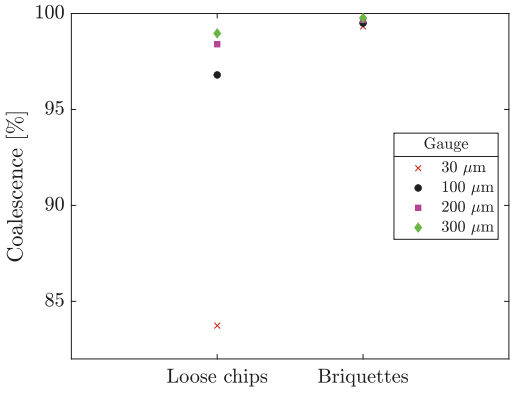

Fig. 7 Coalesced recovery after re-melting loose chips and the briquettes for the 30–300 μm material

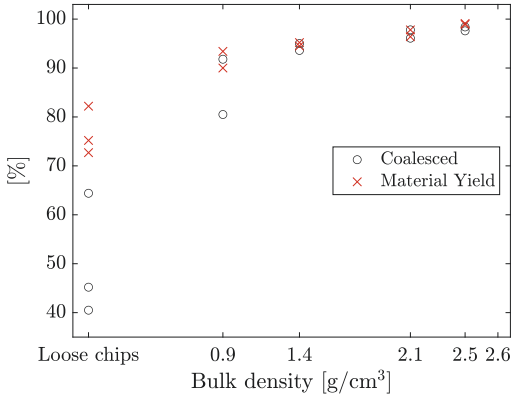

Fig. 8 Material yield and coalesced recovery for 15 μm foil compacted to different densities. Unit is % wt. of the input material, which weighted 20 g. (Color figure online)

Conclusions

The aim of the present work was to study the compaction of thin Al (15–300 μm) foil as a recycling pre-treatment. The relationship between foil thickness, briquette bulk density, oxidation during heat treatment, and recycling yield and coalescence was investigated. The following conclusions were drawn from the results of the study:

Compaction

- Material thickness plays an essential role in the compaction step. Thicker materials required higher pressures to reach a given bulk density, and higher bulk densities for the briquettes to hold together.
- For equivalent bulk densities, the internal porosity was higher for thicker materials. This dependency on thickness decreased for higher bulk densities. Higher compaction reduced the briquette's porosity and surface roughness.
- The MPT method allowed reaching densities close to the bulk density of aluminium at relatively low uniaxial pressures, and the Hot MPT method gave slightly higher densities: 2.5 and 2.6 g/cm^3, respectively.

Oxidation

- Compacting foils into briquettes reduces the specific oxidation during heat treatment significantly, and this is more explicit the thinner the material is.
- The degree of oxidation did not vary for different bulk densities within the range 0.86–2.12 g/cm^3, which corresponded with the uniaxial compaction method. The

briquettes compacted with MPT to bulk densities 2.4–2.6 g/cm^3 were the least oxidized after the heat treatment.

Re-melting

- Compacting the aluminium chips before the heat treatment promoted their coalescence and material yield, and this effect increased for thinner foil gauges.
- For the thinnest foil (15 μm), the degree of compaction of the briquettes influenced coalescence and material yield. The lowest bulk density achieving yields higher than 95% was 2 g/cm^3. For the thicker materials (30–300 μm), the difference between degree of compaction was negligible and all achieved yields higher than 98%.
- Re-melting the non-heat-treated chips and briquettes resulted in material yields above 98% for all the materials.

Acknowledgements The authors would like to gratefully acknowledge the Research Council of Norway and the partners of Alpakka—Circular Aluminium Packaging in Norway (NFR Project nr. 296276) for funding the project; Norsk Hydro Holmestrand for the materials; and the Department of Materials Science and Engineering at NTNU, Trondheim, for the experimental equipment and support, especially to Pål C. Skaret, Berit V. Kramer, Dmitry Slizovskiy, and Ole T. Buset.

References

1. Schlesinger ME (2007) Aluminium Recycling. CRC Press, Cleveland
2. Tabereaux, AT, Peterson, RD (2014) Aluminium Production. Elsevier, New York
3. Lumley RN (2010) Fundamentals of aluminium metallurgy: production, processing and applications. Elsevier, New York
4. Allwood JM, Cullen JM (2008) Sustainable materials with both eyes open. UIT Cambridge, UK
5. Xiao Y et al. (2000) Experimental study on aluminium scrap recycling. Paper presented at the 4th International Symposium on Recycling Metals and Engineered Materials, TMS Lead Zinc, 1075–1087, Pittsburg, USA
6. Xiao Y, Reuter MA, Boin U (2005) Aluminium recycling and environmental issues of salt slag treatment. J Environ Sci Heath A Tox Hazard Subst Environ Eng, 40(10):1861. https://doi.org/10.1080/10934520500183824
7. Xiao Y, Reuter MA (2002) Recycling of distributed aluminium turning scrap. Minner Eng 15:963–970. https://doi.org/10.1016/S0892-6875(02)00137-1
8. Rossel, H (1990) Fundamental investigations about metal loss during remelting of extrusion and rolling fabrication scrap- In: Subodh, KD (ed) Light Metals 1990, p. 721–729. The Minerals, Metals & Materials Society, Pittsburgh; Springer, New York
9. Field DJ, Scamans GM, Butler EP (1987) The high temperature oxidation of Al-4.2 Wt Pct Mg alloy. Metall Mater Trans A 18, 463–472. https://doi.org/10.1007/BF02648807
10. Kim DH, Yoon EP, Kim JS (1996) Oxidation of an aluminium-0.4 wt% magnesium alloy, J. Mater Sci Lett 15:16 p 1429–1431. https://doi.org/10.1007/BF00275297
11. Lyle JP, Granger DA, Sanders RE (2000) Aluminium alloys. In: Ullmann's Encyclopedia of Industrial Chemistry, Wiley-VCH Verlag GmbH & Co. KGaA, Weinheim
12. Marsh K, Bugusu B (2007) Food packaging - Roles, materials and environmental issues: scientific status summary. J Food Sci 72:3. https://doi.org/10.1111/j.1750-3841.2007.00301.x.
13. Hydro (2019) In: Hydro Annual Report 2019, p 44 https://www.hydro.com/Document/Index?name=Annual report 2019 web.pdf&id=506433 Accessed 1 Sept 2020.
14. Reichel A, De Schoenmakere M, Gillabel J (2016) Circular economy in Europe. Developing the knowledge base. EEA report No2/2016. https://doi.org/10.2800/51444
15. Wells PA, Peterson PD (1990) Transient three dimensional briquette preheater model, in Proc. Second International Symposium - Recycling Metals and Engineered Materials, p. 221–236
16. Puga H, Barbosa J, Soares D, Silva F, Ribeiro S (2009) Recycling of aluminium swarf by direct incorporation in aluminium melts. J Mater Process Technol 209:7, 3138–3142. https://doi.org/10.1016/j.jmatprotec.2008.07.020
17. Amini Mashhadi H, Moloodi A, Golestanipour M, Karimi EZ (2009) Recycling of aluminium alloy turning scrap via cold pressing and melting with salt flux, J. Mater. Process. Technol. 209:7, 3138–3142. https://doi.org/10.1016/j.jmatprotec.2008.07.020
18. Krolo B, Lela B, Dumanic (2019) Statistical analysis of the combined ecap and heat treatment for recycling aluminium chips without remelting, Metals (Basel). 9:6. https://doi.org/10.3390/met9060660
19. Shamsudin S, Lajis MA, Zhong ZW (2016) Solid-state recycling of light metals: a review. Adv Mech Eng 8:8, p 1–23. https://doi.org/10.1177/1687814016661921
20. Cui J, Kvithyld A, Roven HJ (2010) Degreasing of aluminium turnings and implications for solid state recycling. In: Johnson, JA (ed) Light Metals 2010, p. 675–678. The Minerals, Metals & Materials Society, Pittsburgh; Springer, New York
21. Fogagnolo JB, Ruiz-Navas EM, Simón MA, Martinez MA (2003) Recycling of aluminium alloy and aluminium matrix composite chips by pressing and hot extrusion, J. Mater. Process. Technol. 143–144:1, 792–795. https://doi.org/10.1016/S0924-0136(03)00380-7
22. Philipson H (2020) The effect of thickness and compaction on the recovery of aluminium in recycling of foils in salt flux, MsC Thesis, Norwegian University of Science and Technology, Trondheim, Norway
23. Capuzzi A, Kvithyld A, Timelli G, Nordmark A, Gumbmann E, Engh TA (2018) Coalescence of Clean, Coated and Decoated Aluminium for Various Salts, and Salt-Scrap Ratios, J. Sustain. Metall 4:3, 343.358. https://doi.org/10.1007/s40831-018-0176-2
24. Capuzzi S, Timelli G (2018) Preparation and melting of scrap in aluminium recycling: a review, metals (Basel). 8:4. https://doi.org/10.3390/met8040249
25. Schmitz CJ (2014) Handbook of aluminium recycling: mechanical preparation, metallurgical processing, heat treatment. Vulkan-Verlag GmbH, Essen, Germany.

Article B

Waste Management 130 (2021) 65–73

Contents lists available at ScienceDirect

Waste Management

journal homepage: www.elsevier.com/locate/wasman

Characteristic properties and recyclability of the aluminium fraction of MSWI bottom ash

Mertol Gökelma [a,b,*], Alicia Vallejo-Olivares [b], Gabriella Tranell [b]

[a] Department of Materials Science and Engineering, Izmir Institute of Technology, 35430 Izmir, Turkey
[b] Department of Materials Science and Engineering, Norwegian University of Science and Technology, 7491 Trondheim, Norway

ARTICLE INFO

Article history:
Received 18 February 2021
Revised 9 May 2021
Accepted 11 May 2021

Keywords:
Aluminium
Recycling
Bottom ash
Incineration
MSWI

ABSTRACT

The increasing use of aluminimum in packaging applications results in many different aluminium-based products ending up in consumer mixed-waste bins. This waste is typically incinerated, generating an aluminium-containing bottom ash. The current work investigates the recyclability of the aluminium fraction in the bottom ash from waste incineration plants in the USA, UK and Denmark. Incinerated Al-samples from different size fractions (2–6 mm, 6–12 mm and 12–30 mm) were characterized in terms of inherent oxide thickness, re-melting yield/coagulation and composition. The measured average oxide thickness on Al particles was 68 μm (SD=100), with the metal yield and coagulation efficiency measured to between 76 and 92% and 87–99% respectively. Larger particle size fractions resulted in a higher metal yield due to their higher mass to surface ratio. A simplified model correlating metal yield and particle size was proposed. The aluminium content of the melted material was determined to between 95.6 and 98.5% with main impurities being Fe, Si, Mn, Zn, Mg and Cu, corresponding to major aluminium alloying elements and waste charge components.

1. Introduction

The production of aluminium has increased rapidly over the last decades due to an increasing consumer population and new application areas of this versatile metal. The global aluminium consumption in 2019 was 89.9 million mt (Hydro Annual Report, 2019), of which 26% was used for transport, 24% for construction, 11% for each of the categories electrical goods and machinery, 8% for each of the packaging and foil stock applications and 6% for consumer durables. Packaging products have a relatively short lifetime, and their waste management has been the focus of recent environmental regulations in Europe (Directive (EU) 2018/852), which state that by 2025 at least 50% by weight of the aluminium packaging must be recycled; 60% by 2030.

A part of the used aluminium packaging materials is collected and recycled with the help of deposit-refund systems and/or sorted household curb-side collection. However, in many countries, and particularly those with a low collection rate, household packaging scrap is thrown in the waste bin and end up at incineration facilities or landfills, depending on the regulations of the corresponding country (Hoornweg & Bhada-Tata, 2012). 47.4% of municipal waste was recycled in the European Union in 2018. The highest recycling rate was achieved in Germany with 67.3% while 49.9% was recycled in Denmark, and 44.1% in United Kingdom (Eurostat, 2020). The recycling rate of municipal waste in the USA is approximately 25% (2017) which is lower than the average rate in the EU. Approximately 139.6 MT municipal solid waste was landfilled in the USA, which is over 50% of the total amount (EPA, 2021).

Incinerating household waste is a way to reduce landfilling while generating thermal energy that could be converted to electricity or used for heating. During the predominant type of incineration, the waste is conveyed through an incineration zone, burning its organic content and generating temperatures as high as 1100 °C (Bunge, 2016). Grate-firing technology is the most common incineration method however the fluidized bed is also used in the US (20%) and Europe (5%) (Leckner and Lind, 2020). After incineration, the bottom ash is sorted out for utilisation/recycling into different fractions: minerals (50-70 wt%), glass and ceramics (10-30 wt%), ferrous metals (5-15 wt%) and non-ferrous metals (1-5 wt%) (Šyc et al., 2020). About 16.5 Mt incineration bottom ash (IBA) is generated per year as a result of roughly 84.5 Mt incinerated municipal solid waste in the EU (Blasenbauer et al., 2020).

Up to 2.2% of the overall mass of incineration bottom ash consists of aluminium (Šyc et al., 2018). Recovering the aluminium from the IBA makes economic and environmental sense, since the energy consumption and related greenhouse emissions of

* Corresponding author at: Department of Materials Science and Engineering, Izmir Institute of Technology, 35430 Izmir, Turkey.
E-mail address: mertolgokelma@iyte.edu.tr (M. Gökelma).

https://doi.org/10.1016/j.wasman.2021.05.012
0956-053X/

recycling aluminium via re-melting are considerably lower than that of primary Al production (Rüttinger et al., 2016). However, the recyclable aluminium content is not well established due to the high oxygen affinity of aluminium and subsequent oxidation/metal loss during incineration (Hu et al., 2011). Warrings and Fellner (2018) reported that approximately 11% of the aluminium mass is oxidized during incineration, while Bunge (2016) stated that a third of the mass of used beverage cans (UBCs) is oxidized if they undergo this process. The oxidation of aluminium alloys is a time and temperature dependent phenomenon (Smith et al., 2018b ; Thiele, 1962). The exposure to high temperatures and a heterogenous furnace atmosphere due to variable incinerator charges, causes a wide range of oxidation behaviours, as well as losses due to the formation of aluminium nitride (Bunge, 2016). In addition to temperature and atmosphere, the degree of oxidation may also be affected by different scrap parameters such as thickness, surface area, coatings/contamination and alloy chemical composition. Numerous studies have shown the critical effect of magnesium content (Field et al., 1987 ; Kim et al., 1996 ; Rossel, 1990; Tabereaux and Peterson, 2014), as well as thickness and surface area (Rossel, 1990; Xiao and Reuter, 2002; Xiao et al., 2000) on the recyclability of aluminium.

Since the melting point of pure aluminium is 660 °C (Totten et al., 2018), the scrap melts during incineration and solidify into different shapes and sizes, which are typically sieved into different size fractions and commercialized separately due to their differences in recyclability (Biganzoli et al., 2014; Gökelma et al., 2019; Hu and Bakker,2015). The reason behind such differences might be higher specific oxide content in the smaller pieces. Another factor could be the chemical composition or surface area of the initial scrap that form each fraction. According to Hu and co-workers, the type of scrap determines the bottom ash particle size, e.g. 86% of the UBCs end up in the + 6 mm size fraction (Hu et al., 2011). Therefore, hypothetically a higher % magnesium content could be expected in this fraction, since the alloy 3004, which is high in magnesium, is used generally for the lids which constitutes 25% of the mass of the UBCs (Totten et al., 2018). Household foil on the other hand, which generally has a low recycling yield attributed to its thickness (Hu et al., 2011; Schlesinger, 2017), mostly ends up in the 2–6 mm fraction.

The goal of the current work was to investigate the correlation between particle size, level of oxidation, impurity element content and recyclability of the aluminium fraction from IBA generated in three different countries (USA, UK and Denmark) with the size fractions of 2–6, 6–12, and 12–30 mm.

2. Materials and methods

2.1. Materials

Dry sorted aluminium fractions of bottom ash from MSWI plants were received from a European recycling company. The eight IBA samples (5 kg each) were received from incineration plants in the USA, UK and Denmark. The samples from the USA and UK were received in three size ranges (2–6, 6–12, 12–30 mm) while samples from Denmark were produced in two size ranges (2–12, 12–30 mm).

To ease the comparison with the UK and USA samples, 0.5 kg of the DK size fraction 2–12 mm was sieved with a 6 mm mesh size. This revealed that 2/3 of the mass fell within the size range 2–6 mm and 1/3 within 6–12 mm. However, the remaining original fraction DK 2–12 (4.5 kg) was kept for the experimental study as provided by industry since the manual sorting in the laboratory might not represent the machine sorting used in the industry.

2.2. Aspect ratio and mass analysis of bottom ash

The aluminium pieces in all size ranges can be found in a large variety of shapes. Aspect ratio [A_R = min ferret/max ferret (Merkus, 2010)] is a common method to identify the shape characteristics of an object. Pictures of 50 g (typically 20–150 pieces) of each sample size were taken and processed by using the image analysis software ImageJ (Schneider et al.). The minimum and maximum axis of each sample was measured and the A_R was calculated accordingly. Furthermore, the average mass of the bottom ash samples was calculated by weighing 20 random samples from each group (UK 2–6, 6–12, 23–30, USA 2–6, 6–12, 23–30, DK 2–12-12–30).

2.3. Characterisation of oxide thickness and composition of bottom ash

Three random samples were picked from each of the eight sample groups. The 24 random samples were mounted in epoxy and sectioned into mirrored pieces for oxide layer characterization by the SEM (Zeiss Ultra 55LE FEG-SEM). The oxide layer thicknesses were measured in at least 15 different positions of each sample. EDS was used for approximate analysis of the oxide and metal composition for each piece. The Kruskal-Wallis method (Ostertagová et al., 2014) was used to analyse whether the different size fractions could be considered statistically as identical populations.

2.4. Re-melting setup and procedure

A resistance heating furnace and a ceramic crucible (Al_2O_3-SiO_2) was used for the re-melting experiments. The re-melting was carried out under a salt flux mixture to break the oxide layer, protect against further oxidation and coalesce the aluminium (Besson et al., 2011; Sydykov et al., 2002). 100 g of the salt flux with a composition of 49 wt% NaCl, 49 wt% KCl and 2 wt% CaF_2 was melted in the crucible. After the salt bath reached 800 °C, 50 g of bottom ash sample was added into the bath in four portions of equal mass. Between each charge, the melt was held for 15 min to ensure that the aluminium pieces melted, and that the salt bath again reached 800 °C before adding a new charge. At the end of each experiment, manual stirring was applied for 5 s before the furnace was shut down. The metal and salt were separated by crushing in mortar and washing in water. After the salt was washed out, the metal part was sieved out and separated into two fractions which were coagulated and non-coagulated by measuring the upper size limit of the droplet (usl). The usl of each size fraction was taken as the lowest size of a coagulated droplet and coagulation efficiency (CE) was calculated accordingly.

$CE = \frac{m_{droplets>usl}}{m_{total}} * 100$ (1) where, $m_{droplets\ >\ usl}$ is the weight of particles larger than 6, 12 and 30 mm for the size ranges 2–6, 6–12 and 12–30 mm respectively and m_{total} is the total mass of recovered metal after the re-melting.

In addition, metal yield was calculated after each experiment to assess how much metal can be recovered by re-melting.

Metal Yield $= \frac{m_{total}}{m_{inputmaterial}} * 100$ (2) where, $m_{input\ material}$ is the charged bottom ash scrap for the re-melting.

The same procedure was applied for each sample group and in total 26 re-melting experiments were performed including at least 3 repetitions for each trial. After the re-melting procedure, the solidified samples were cut by a diamond wheel into pieces (1.5–2 g) and the chemical composition of the samples with the closest metal yield to the average value of each fraction were analysed by ICP-MS. The samples were digested with HCl and HNO_3.

3. Results

3.1. Characterization of the bottom ash samples

3.1.1. Physical properties

The results of measurements (25 samples for each fraction) of average weight, axis length and aspect ratio are summarized in Table 1. An increase in the average weight and the axis length was observed with increasing size range as expected. The deviation in aspect ratio and weight between different samples can be explained by the irregular shape of the samples and their behaviour during the sieving process.

3.1.2. Oxide layer thickness

Samples from each size fraction of the materials from USA, UK and Denmark were analysed by SEM. Fig. 1 shows the oxide layer thickness values for each size fraction and country. The graph was plotted by using 437 measurements in 24 random samples. The largest deviation between different samples was observed in the bottom ash from Denmark in which the thickness ranged from < 1 μm up to approximately 2.5 mm. The smallest differences were observed in the samples from the USA. Furthermore, most of the individual samples also showed a heterogeneous oxide thicknesses throughout the surfaces as it can be seen in Fig. 1 by the scattered analysis result per sample.

Table 2 summarises the minimum, maximum and mean thickness values of the oxide layer measured in each of the 24 samples, as well as the sample diameter (maximum axis of the surface analysed by SEM) and the magnesium content of the matrix measured by EDS point analysis.

The mean oxide thicknesses of each sample are shown in Table 2 as a function of measured magnesium content in the matrix. Most of the measurements lay below the 100 μm and the oxide/metal ratio increased with decreasing size fraction. The oxide/metal ratio is the ratio between the mass of the oxide and the mass of the metal. No direct correlation was observed between the mean oxide layer thickness and the magnesium content in the alloy, as elaborated in the discussion. Sample 21, which had a relatively high

Table 1
Characteristics of bottom ash samples for different size fractions and sources.

Country	UK			USA			DK	
Size fraction (mm)	2–6	6–12	12–30	2–6	6–12	12–30	2–12	12–30
Av. weight (g)	0.21	1.25	4.31	0.24	1.07	3.89	0.65	5.04
St. Dev. (g)	0.12	0.66	2.36	0.25	0.61	3.44	0.37	5.10
Aspect ratio	0.533	0.471	0.619	0.488	0.611	0.594	0.635	0.527
St. Dev.	0.31	0.24	0.16	0.27	0.18	0.20	0.19	0.09
Av. axis length (mm)	8	11.5	18.4	9	12.1	19.1	11.8	18.3
St. Dev. (mm)	2.1	2.1	5.2	2.1	2.9	4.1	3.1	6.6

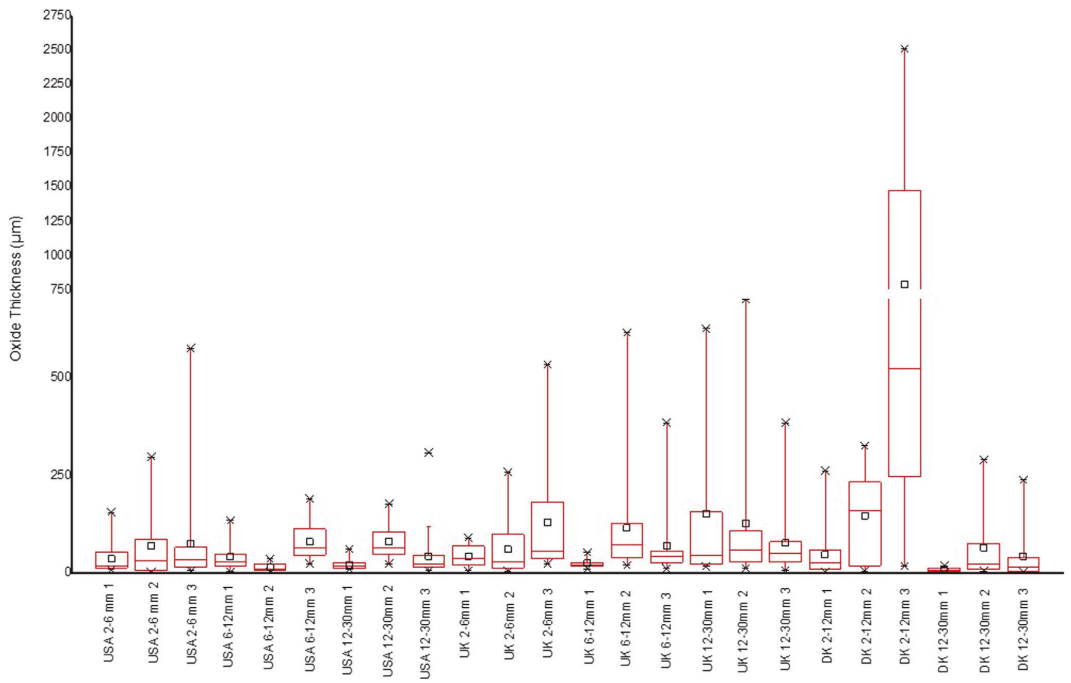

Fig. 1. Oxide thickness measurements of 24 random aluminium IBA samples.

Table 2
Summary of oxide thickness measurements and magnesium content, as measured by EDS in the SEM of each sample.

Sample	Country	Size fraction (mm)	Max axis of the actual particle (mm)	Oxide thickness (μm)			Mg in the alloy (wt%)
				min	max	mean	
1	USA	2–6	6	8.3	155.5	36.2	0.8
2		2–6	7	2.1	297.6	68.8	0.8
3		2–6	7.5	5.9	575.3	74.7	0.9
4		6–12	14.5	3.7	135	41.3	1.8
5		6–12	11	1.4	36.2	13.4	0.9
6		6–12	10.5	23.5	189.7	79.3	0.8
7		12–30	22	8.3	61.2	21.6	2.5
8		12–30	14.5	24	177.4	80.7	1.2
9		12–30	20	6	55.9	42.6	0.8
10	UK	2–6	5	6.1	89.5	46.2	0.8
11		2–6	3	4	258.4	60.5	0.8
12		2–6	3.5	23.6	533.7	129	1.5
13		6–12	11	10.6	52.4	24.4	1.3
14		6–12	11	20	614.4	115.7	0.9
15		6–12	14	12	383.8	69.3	0.9
16		12–30	20.5	16.4	625.3	151	1.2
17		12–30	17	12.3	699.4	127.2	0.9
18		12–30	15.8	6.3	384.4	76.4	1.3
19	DK	2–12	6.6	2.3	261.2	46.5	0.9
20		2–12	6.2	4.5	325.8	146.2	0.9
21		2–12	8.4	17	2512.1	790	1.9
22		12–30	15.7	0.9	18.9	7.4	0.7
23		12–30	13.3	5.1	289.3	65	1
24		12–30	11	2.5	238.5	43.1	1

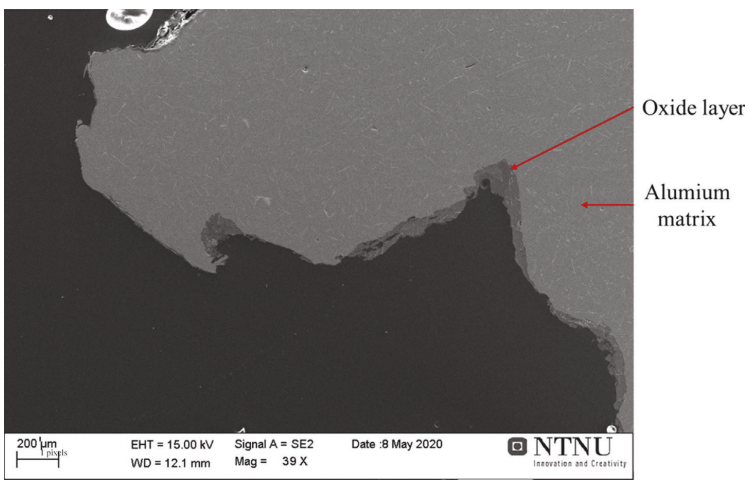

Fig. 2. SEM image of the cross-section of sample 24.

magnesium content, has the largest average oxide thickness value (790 μm) due to a particular heavily oxidized region of the sample. On the other hand, sample 7 with the highest magnesium content had only an average oxide thickness of (22 μm).

Fig. 2 shows sample 24 (DK 12–30) with an average oxidation . The oxide layer (darker part) on the aluminium matrix (lighter part) can be observed clearly in the picture. SEM-EDS analysis was performed to determine the elemental composition of the oxide layer for samples 3, 10, 11, 12 and 23 (from the groups USA 2–6 and UK 2–6) to compare the oxidation behaviour between different samples. Magnesium was found in the range between 0.37 and 0.95 wt% in oxide form and the heavier oxidizied samples generally had higher MgO content in the dross. Exothermic reactions during the incineration may cause an inhomogeneous distribution of oxide growth depending on the position and the surroundings of the samples.

3.2. Re-melting

The metal yield and coagulation efficiency results with mean values and standard deviations (3–5 repetitions for each sample group) are shown in Fig. 3. Metal yield is the most critical parameter to recyclability because it indicates the recyclable metal content in the scrap after subtracting the oxide losses. A clear increase in the metal yield was observed with increasing size range of the samples. The coagulation efficiency of the 2–6 mm samples was, as expected, typically lower than the 6–12 mm and 12–30 mm fractions for the samples from UK and USA. The coagulation

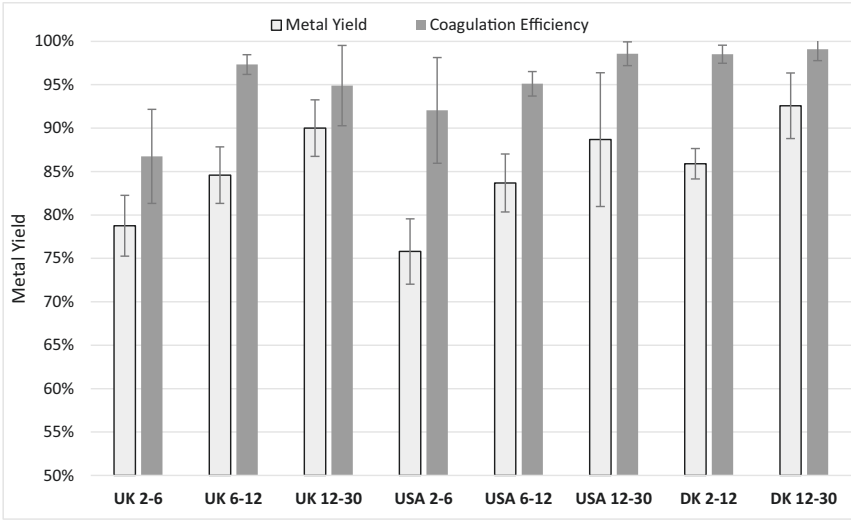

Fig. 3. Metal yield and coagulation efficiency results after re-melting the bottom ash samples under salt flux.

Table 3
Elemental composition (ICP-MS) of remelted aluminium fraction.

Elements (ppm)	UK 2–6 mm	UK 6–12 mm	UK 12–30 mm	USA 2–6 mm	USA 6–12 mm	USA 12–30 mm	DK 2–12 mm	DK 12–30 mm
Cr	133	111	217	198	284	65	210	131
Cu	2240	1630	805	9180	3620	2950	2670	1250
Fe	6080	3900	5680	5860	6380	3780	5020	3590
K	9	5	<0.4	7	33	<0.4	30	<0.8
Mg	357	1020	756	240	654	495	468	1350
Mn	5860	4310	5910	5870	6380	3800	5380	3860
Na	11	8	4	10	33	2	34	4
Ni	71	71	59	277	135	187	74	50
Pb	264	58	169	492	1630	146	418	104
S	2	50	14	15	13	12	18	23
Si	3610	2810	2200	9940	8850	8610	4460	3490
Sn	67	70	9	105	38	36	25	30
Ti	197	232	198	237	219	255	206	130
Y	0.3	0.3	0.5	0.6	0.5	0.8	0.7	0.4
Zn	1880	1010	557	11,100	12,500	1530	3240	2370
Al %	97.9	98.5	98.3	95.6	95.9	97.8	97.8	98.4

efficiency of the two size fractions of DK samples did not deviate significantly from each other.

The aluminium purity was measured by ICP-MS between 95.6 and 98.5 wt%. The elemental composition shows a high variation between the samples and size fractions (Table 3). However, some compositional trends can be observed. As can be expected given typical aluminium alloys, all materials display high concentrations in Cu, Fe, Mg, Mn, Si and Zn. For all three countries, the Cu content is highest in the finest size fraction while the Mg content is highest in the middle fraction. The Si content in all fractions from the US is more than double that of fractions from UK and Denmark. The Ni and Zn contents are also significantly higher in the US material compared to the European materials. Of note is also the seemingly high Pb content in all samples.

4. Discussion

4.1. Physical properties

The shape and weight of aluminium scraps after incineration generally become very irregular. The sorting is done through sieving the aluminium fraction of the bottom ash into different size fractions at the handling/recycling facility. Homogenity of the size fractions depend on the behaviour of particles during the sieving process. The deviation in aspect ratio of the samples in this study was calculated between 0.09 and 0.31. This illustrates that each individual particle does not necessarily fit a given fraction when all three dimensions are taken into account which is a consequence of the sieving process. This heterogene-

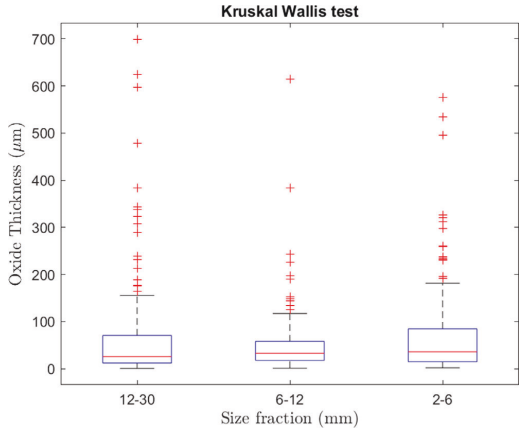

Fig. 4. Kruskal Wallis test graph for size fractions 12–30, 6–12 and 2–6 mm. *The overall average oxide thickness was calculated as 68.12* (SD=100 μm) *for the 413 measurements of 23 samples.*

ity within fractions also causes a variation in the mass of the particles in every size fraction.

4.2. Oxide layer thickness

Although the oxide layer thickness of samples varies, 80% of measurements lay below 100 μm and 90% were below 200 μm of oxide thickness. Fig. 4 presents the Kruskal Wallis test results of the remaining 413 measurements (Chi-square = 2.41, p = 0.229) where the boxes show the interquartile range for each size fraction and the line in the box represents the median of the measurements. As the resultant chi-sq value is below 5.99 and the p value is above 0.05, there is no indication that the sample groups are of a different population. The sample groups can be treated as identical populations with a significance level of 5% and the oxide thickness results can be used to calculate an average. The Kruskal Wallis test showed that the oxide thickness variations are comparable across the different sample groups except for the measurements from the sample 21. Therefore the measurements of sample 21 were not considered for calculating the average.

The magnesium content of the samples did not show a significant correlation to oxide thickness, i.e, the oxide thickness did not increase with increasing magnesium content (Table 2). This indicates that materials containing magnesium do not necessarily over-oxidize during the incineration process. The degree of oxidation can vary depending on the type of waste materials and gases generated around the particle. Protective gases, such as CO_2 form in the process due to the combustion of organic waste products, significantly inhibit the oxidation of magnesium-containing Al alloys (Smith et al., 2018a) . While there was no direct correlation between oxide thickness and magnesium content in the metal of investigated samples, abnormally thick oxide layers were typically associated with a higher magnesium content in the oxide, illustrating the effect of local breakaway oxidation.

4.3. Re-melting

Between 76 and 93% of aluminium was recovered by re-melting of incinerated aluminium fractions for the different size fractions. The results agree with the previous work which focused on the incinerated Norwegian municipal waste where (Gökelma et al., 2019) reported a metal yield of 82 to 93 wt% for the 5–25 mm size fraction. Similar results were reported by other researchers: Biganzoli et al (2014) reported a yield range of 76 to 87 wt% for the size fraction greater than 5 mm aluminium samples from an incineration plant in Italy. Hu and Bakker (2015) stated that the yield of aluminium from household waste composed of different packaging types (beverage cans, containers and foils) ranged between 77 and 93 wt%. Biganzoli and Grosso (2013) studied the operation of two incineration plants and reported that the residence time of the municipal waste between the feeding and the bottom ash extraction was 4–6 h in one plant and 9–10 h in another one. The difference in metal yield between the same input material fraction for different countries may hence be partly caused by plant-specific technology and waste residence time during the incineration.

The increasing metal yield with the increasing size fraction is mainly caused by a decreasing oxide/metal mass ratio. The coagulation efficiency showed an increasing trend with decreasing oxide/metal ratio similar to the metal yield; the salt flux has to dissolve/remove more oxide layer in smaller size fractions because the surface area is larger in smaller size fractions. The larger surface area and oxide/metal ratio may affect the metal yield and the coagulation behaviour negatively. Both coagulation efficiency and metal yield however depend on the recycling method, and thus, an industrial comparison of metal yield should be done for different size fraction materials to verify the laboratory results.

A simplified model, calculating the metal yield as a function of the sample size, is proposed based on the calculated average oxide thickness on the particles. In our model, all samples are assumed to have spherical shape with a real density (ρ_{metal}) of 0.918 g/cm^3 and an oxide density (ρ_{oxide}) of 3.95 g/cm^3 (Gökelma et al., 2019).

$$\text{Theoretical metal yield} = \frac{m_{metal}}{m_{oxide} + m_{metal}}$$

where the mass of the metal was calculated for spherical samples with a diameter varying between 1 and 30 mm and the mass of the oxide was calculated for an 68.12 μm oxide layer covering the corresponding sample surface, using equations (4) and (5).

$$m_{metal} = \rho_{metal} * [4/3 * \pi(r_{sample} - \text{oxidethickness})^3] \quad (4)$$

$$m_{oxide} = \rho_{oxide} * [[4/3 * \pi(r_{sample})^3] - [4/3 * \pi(r_{sample} - \text{oxidethickness})^3]] \quad (5)$$

Fig. 5 shows the theoretical and experimental (UK 2–6: 79%, 6–12: 85%, 12–30: 90%, USA 2–6: 76%, 6–12: 84%, 12–30: 89%, DK 2–12: 86%, 12–30: 93%) results for the metal yield of bottom ash samples. The average axis length values of samples, shown in Table 1, were taken as sample diameter in the model. Although simple, the model shows an acceptable correlation with the experimental test results, which may be used to estimate expected maximum yield in the industrial recycling process.

Most of the theoretical data is slightly above the experimental data which may be due to the metal losses during the re-melting procedure. Similar experimental (re-melting of approximately 3000 pieces) and modelling results indicate that the oxide thickness measurements adequately represent the entire population.

In addition to reasonable metal yield, the alloy composition is also an important factor for recycling. The iron concentration was measured at 3590 to 6380 ppm, without notable variation trends between size fractions and material origin. The silicon concentration was also at the same level throughout the samples analyzed, ranging between 2810 and 9940 ppm. Zinc is found in aluminium beverage can bodies up to 0.25 wt% which may explain the high zinc concentration in the samples. The source of these three elements (Fe, Si and Zn) may be the beverage can bodies

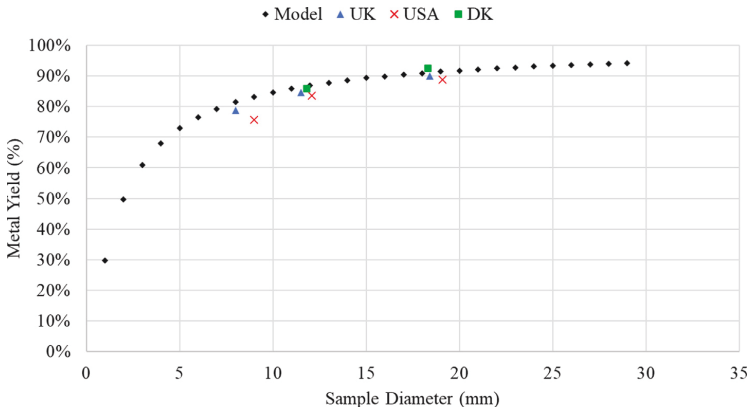

Fig. 5. Comparison of the theoretical and experimental metal yield results.

(Al 3004) and the aluminium screw caps and closures (Al 3105, 8011). The 2–6 and 6–12 mm fractions of the US bottom ash samples contained more than 1% of zinc in the melt. This concentration level is normally not found in packaging alloys and likely originate from Zn evaporation from other Zn-containing materials in the waste charge (such as pennies, zinc-carbon batteries, nuts and bolts).

More statistical data of the aluminium household waste in the different countries is needed in order to explain the compositional differences of the recovered metal. A possible approach is to study the sieving behaviour of the main types of aluminium scrap, and look for correlations between the composition of that type of products and the composition of the remelted metal of the expected size fraction where they would end up. Hu et al. studied the sieving behaviour of aluminium foil containers, beverage cans and thin foil, and found out that 86% of the UBCs end up in the 6–20 mm size fraction (Hu and Bakker,2015). Therefore, hypothetically a higher % magnesium content due to incinerated beverage cans could be expected in the 6–12 mm fraction, since the alloy 5182, which is high in magnesium, is generally used for the lids and constitutes 25% of the mass of the UBCs (Totten et al., 2018). The high magnesium concentration is also reflected in the presented ICP-MS results for the IBA from UK and US. This did not apply to the DK samples, which is explained by the fact that in the DK fraction 2–12 mm, the particles with sizes + 6 mm constituted only 1/3 of the weight. Accordingly, results from Hu et. al showed that most of the thin foils, produced typically from 8011 alloy with a certain iron and silicon concentrations,would end up in the < 2 mm or 2–6 mm fractions. This could explain the slightly higher iron and silicon content found in the ICP-MS results for most of the 2–6 mm fractions.

Manganese is added between 0.5 and 1.5 wt% in 3000 series alloys which are used as sheet products, rigid foil containers and beverage cans (Hu et al., 2011). These alloy materials can be found in almost every size fraction in the bottom ash and subsequently, the manganese concentration was measured to between 3800 and 6380 ppm in all samples. Chromium is present in some of the alloys as a minor element up to 1000 ppm in Al5182 and 500 ppm in Al8011 (Papadopoulou et al., 2020) which are also used in beverage cans and foils respectively (Shi and Shen, 2018). Titanium is typically used as grain refiner and a normal level of addition is approximately 100 ppm. In addition, titanium is found in many wrought alloys as minor element from 100 to 3500 ppm (Sigworth and Kuhn, 2007).

Unpredictable deviations in trace elements is the most important problem for the recycling of complex secondary resources. In the current case, the lead concentrations were considerable with the highest concentration in the 6–12 mm size fraction of the USA sample measuring 1630 ppm. Lead is not commonly alloyed in aluminum however, aluminium alloy 2011 containing up to 0.6 wt% lead is used for making fasteners, fittings, nuts, bolts etc. due to its excellent machinability. Through EU regulations, the permissible level of Pb concentration as trace element in Al alloys has been set at 0.1 wt% (allowing exceptions to the regulation for contents up to 0.4 wt% if the Pb is used as an alloying element) (EC Directive 2015/863/EU) and similar limitations have been set in other countries too. The limitations in the USA market is 0.5 wt% lead in aluminium alloys (Senel, 2019). This may be the reason for higher lead concentrations detected in USA bottom ash samples. Given the legislative limitations, investigations into production of lead free aluminium alloys have been conducted in different research groups (Koch and Antrekowitsch,2011 ;Timelli and Bonollo,2011). Consequently, it is expected that the lead content in bottom ash originating from Al alloys will continuously decrease in the future. As lead has a low melting point and high vapor pressure at elevated temperatures, non-aluminium origins for the measured lead content in the bottom ash is also a possiblity.

The main copper sources in the bottom ash may be the Al5052 and Al8011, used for easy-open lids and foils, which contain copper up to 1000 ppm, the Al2011 and Al3004 containing up to 6 and 0.25 wt% copper respectively. A higher copper concentration was detected in smaller sizes in samples from each country. The copper concentration in the 2–6 mm fraction may be due to the small sized nuts, bolts and fasteners and in the 6–12 mm fraction due to the used beverage cans.

5. Conclusions

Aluminium bottom ash samples from MSWI of different size fraction and country of origin were investigated for characteristic properties and recyclability. The following conclusions were drawn from the investigation:

- The thickness of oxides on the surface of the aluminium samples after incineration can vary from < 1 to several thousand μm depending on the incineration dynamics and the alloy composition of the sample. The thickness measured after incinera-

tion was 68 μm in average over the entire population of samples investigated and oxide thickness has no direct correlation with the size of the particle or country of origin.

- The re-melting metal yield increases with the increasing particle size due to the decreasing oxide/metal ratio. The yield was calculated to between 75.8 and 92.6% with a standard deviation of 3.8%. The USA 2–6 mm samples showed the lowest yield and the DK 12–30 mm resulted in the highest metal yield after re-melting. A simplified model correlating particle size and re-melting yield was developed for spherical samples with a diameter varying between 1 and 30 mm and an 68.12 μm oxide layer covering the sample surface.
- Although magnesium is an important influencing factor for oxidation, the oxide thickness of samples with high magnesium content did not deviate significantly from other samples, which may be due to protective gases, such as CO_2, during the combustion of organic materials surrounding the metal scrap.
- The remelted aluminium materials from all three countries (USA, UK, DK) and size fractions displayed significant contents of Fe, Si, Cu, Mn, Mg and Zn in accordance with typical Al alloy specifications for packaging materials. Materials originating from USA typically showed the highest average concentrations of alloying and trace elements.

The results of the current study may aid in a better understanding of achievable recyclability of incinerated aluminium in terms of metal yield and composition. This is important in e.g the development of improved MFA/LCA models of the aluminium life cycle as well as for operators of aluminium recycling plants.

Declaration of Competing Interest

The authors declare that they have no known competing financial interests or personal relationships that could have appeared to influence the work reported in this paper.

Acknowledgement

The authors wish to thank staff at Blue Phoenix Group for supplying bottom ash samples. Funding was partially provided by the Norwegian Centre for Research-Based Innovation (SFI Metal Production, NFR Project Number 237738.

References

Besson, S.; Pichat, A.; Xolin, E.; Chartrand, P.; Friedrich, B. Improving coalescence in Al-Recycling by salt optimization. In Proceedings of the European Metallurgical Conference, Dusseldorf, Germany, 26–29 June 2011; pp. 1–16. Available online: http://www.metallurgie.rwth-aachen.de/new/images/pages/publikationen/besson_emc2011_id_8928.pdf

Biganzoli, L., Grosso, M., 2013. Aluminium recovery from waste incineration bottom ash, andits oxidation level. Waste Manage. Res. 31 (9), 954–959. https://doi.org/10.1177/0734242x13493956.

Biganzoli, L., Grosso, M., Forte, F., 2014. Aluminium Mass Balance in Waste Incineration and Recovery Potential From the Bottom Ash: A Case Study. Waste Biomass Valorization 5 (1), 139–145. https://doi.org/10.1007/s12649-013-9208-0.

Blasenbauer, D., Huber, F., Lederer, J., Quina, M.J., Blanc-Biscarat, D., Bogush, A., Bontempi, E., Blondeau, J., Chimenos, J.M., Dahlbo, H., Fagerqvist, J., Giro-Paloma, J., Hjelmar, O., Hyks, J., Keaney, J., Lupsea-Toader, M., O'Caollai, C.J., Orupõld, K., Pająk, T., Simon, F.-G., Svecova, L., Šyc, M., Ulvang, R., Vaajasaari, K., Van Caneghem, J.o., van Zomeren, A., Vasarevičius, S., Wégner, K., Fellner, J., 2020. Legal situation and current practice of waste incineration bottom ash utilisation in Europe. Waste Manage. 102, 868–883. https://doi.org/10.1016/j.wasman.2019.11.031.

Bunge, R. (2016). Recovery of metals from waste incinerator bottom ash. https://vbsa.ch/wp-content/uploads/2016/07/Studie-Bunge-Internetversion.pdf

Directive (EU) 2018/852 of the European Parliament and of the Council of 30 May 2018 amending Directive 94/62 / EC on packaging and packaging waste (Text with EEA relevance). (2018). EUR-Lex. https://eur-lex.europa.eu/eli/dir/2018/852/oj

Field, D.J., Scamans, G.M., Butler, E.P., 1987. The high temperature oxidation of Al-4.2 wt pct Mg alloy. Metall. Trans. A 18 (4), 463–472. https://doi.org/10.1007/bf02648807.

Gökelma, M., Meling, I., Soylu, E., Kvithyld, A., Tranell, G., 2019. A Method for Assessment of Recyclability of Aluminum from Incinerated Household Waste. Light Metals 2019, 1359–1365. https://doi.org/10.1007/978-3-030-05864-7_168.

Hoornweg, D., & Bhada-Tata, P. (2012). WHAT A WASTE A Global Review of Solid Waste Management. Urban development series;knowledge papers. http://documents1.worldbank.org/curated/en/302341468126264791/pdf/68135-REVISED-What-a-Waste-2012-Final-updated.pdf

Hu, Y., Bakker, M.C.M., 2015. Recovery of Aluminum Residue from Incineration of Cans in Municipal Solid Waste. J. Residuals Sci. Technol. 12 (3), 157–163 https://doi.org/10.12783/issn.1544-8053/12/3/6.

Hu, Y., Bakker, M.C.M., de Heij, P.G., 2011. Recovery and distribution of incinerated aluminum packaging waste. Waste Manage. 31 (12), 2422–2430. https://doi.org/10.1016/j.wasman.2011.07.021.

Hydro annual report. (2019). https://www.hydro.com/Document/Index?name=Annual%20report%202019%20web.pdf&id=506433

Kim, D.H., Yoon, E.P., Kim, J.S., 1996. Oxidation of an aluminum-0.4 wt% magnesium alloy. J. Mater. Sci. Lett. 15 (16), 1429–1431. https://doi.org/10.1007/bf00275297.

Koch, S., Antrekowitsch, H., 2011. Alloying Behaviour of Cu, Mg and Mn in Lead-free Al-Cu Based Alloys Intended for Free MachiningAuswirkungen der Legierungselemente Cu, Mg und Mn in bleifreien Al-Cu-Automatenlegierungen. BHM Berg- Huettenmaenn. Monatsh. 156 (1), 22–27. https://doi.org/10.1007/s00501-011-0621-z.

Leckner, B., Lind, F., 2020. Combustion of municipal solid waste in fluidized bed or on grate – A comparison. Waste Manage. 109 (2020), 94–108.

Merkus, H.G., 2010. Particle Size Measurements: Fundamentals, Practice, Quality (Particle Technology Series, 17) (Softcover reprint of hardcover. Springer.

Ostertagová, E., Ostertag, O., Kováč, J., 2014. Methodology and Application of the Kruskal-Wallis Test. Applied Mechanics and Materials 611, 115–120. https://doi.org/10.4028/www.scientific.net/amm.611.115.

Papadopoulou, S., Kontopoulou, A., Gavalas, E., Papaefthymiou, S., 2020. The Effects of Reduction and Thermal Treatment on the Recrystallization and Crystallographic Texture Evolution of 5182 Aluminum Alloy. Metals. 10 (10), 1380. https://doi.org/10.3390/met10101380.

Recycling rate of municipal waste. (2020). Eurostat. https://ec.europa.eu/eurostat/databrowser/view/sdg_11_60/default/table

Rossel H. (1990) Fundamental investigations about metal loss during re-melting of extrusion and rolling fabrication scrap. Light Metals 1990, ed. C.M. Bickert, TMS, 721-729, 5. SECAT Press Release.

Rüttinger,L.,Treimer,R.,Tiess,G.,&Griestop,L.(2016).Umwelt-undSozialauswirkungenderBauxitgewinnungundAluminiumherstellunginPará,Brasilien.adelphi.https://www.umweltbundesamt.de/sites/default/files/medien/378/dokumente/umsoress_fallstudie_bauxit_brasilien_finale_version.pdf

Schlesinger, M.E., 2017. Aluminum Recycling. CRC Press.

Senel E., What you need to know about lead-free aluminium alloys. (2019, September 26). Shapes by Hydro. https://www.shapesbyhydro.com/en/material-science/what-you-need-to-know-about-lead-free-aluminium-alloys/

Sigworth, G.K., Kuhn, T.A., 2007. Grain Refinement of Aluminum Casting Alloys. Inter Metalcast 1 (1), 31–40. https://doi.org/10.1007/BF03355416.

Shi, C., Shen, K., 2018. Twin-roll casting 8011 aluminium alloy strips under ultrasonic energy field. International Journal of Lightweight Materials and Manufacture 1 (2), 108–114. https://doi.org/10.1016/j.ijlmm.2018.06.001.

Smith, N., Gleeson, B., Saidi, W.A., Kvithyld, A., Tranell, G., 2018a. Mechanism behind the Inhibiting Effect of CO2 on the Oxidation of Al–Mg Alloys. Ind. Eng. Chem. Res. 58 (3), 1434–1442. https://doi.org/10.1021/acs.iecr.8b04691.

Smith, N., Kvithyld, A., Tranell, G., 2018b. The Mechanism Behind the Oxidation Protection of High Mg Al Alloys with Beryllium. Metallurgical and Materials Transactions B 49 (5), 2846–2857. https://doi.org/10.1007/s11663-018-1340-6.

Šyc, M., Krausová, A., Kameníková, P., Šomplák, R., Pavlas, M., Zach, B., Pohořelý, M., Svoboda, K., Punčochář, M., 2018. Material analysis of Bottom ash from waste-to-energy plants. Waste Manage. 73, 360–366. https://doi.org/10.1016/j.wasman.2017.10.045.

Šyc, M., Simon, F.G., Hykš, J., Braga, R., Biganzoli, L., Costa, G., Funari, V., Grosso, M., 2020. Metal recovery from incineration bottom ash: State-of-the-art and recent developments. J. Hazard. Mater. 393, 122433. https://doi.org/10.1016/j.jhazmat.2020.122433.

Sydykov, A., Friedrich, B., Arnold, A. (2002) Impact of parameter changes on the aluminium recovery in a rotary kiln, in: Schneider, W. A. (ed.), Proceedings of the technical sessions presented by the TMS Aluminium, Light Metals 2002, 131st TMS Annual Meeting, Warrendale, Pennsylvania, USA, pp 1045–1052.

Tabereaux, A.T., Peterson, R.D., 2014. Treatise on Process Metallurgy. Elsevier, 839–917. https://doi.org/10.1016/B978-0-08-096988-6.00023-7.

Thiele, W. (1962). Die Oxydation von Aluminium- und Aluminiumlegierungs-Schmelzen. Erscheinungsort nicht ermittelbar.

Timelli, G., Bonollo, F., 2011. Influence of tin and bismuth on machinability of lead free 6000 series aluminium alloys. Mater. Sci. Technol. 27 (1), 291–299. https://doi.org/10.1179/026708309x12595712305799.

Warrings, R., Fellner, J., 2018. Current status of circularity for aluminum from household waste in Austria. Waste Manage. 76, 217–224. https://doi.org/10.1016/j.wasman.2018.02.034.

Xiao, Y., Reuter, M.A., 2002. Recycling of distributed aluminium turning scrap. Miner. Eng. 15 (11), 963–970. https://doi.org/10.1016/s0892-6875(02)00137-1.
Totten, G.E., Tiryakioğlu, M., & Kessler, O. (Eds.). (2018). Encyclopedia of Aluminum and Its Alloys (1st ed.). CRC Press. https://doi.org/10.1201/9781351045636
Xiao, Y., Reuter, M., Vonk, P., Voncken, J., Orbon, H., Probst, Th.,Boin, U.,(2000). Experimental study on aluminium scrap recycling.In: Stewart Jr., D.L., Daley, J. C., Stephens, R.L., (Eds.), Proceed-ings of the Fourth International Symposium on Recycling of Metals and Engineered Materials, 22–25 October, USA, pp. 1075–1087
National Overview: Facts and Figures on Materials, Wastes and Recycling. (2021). United States Environmental Protection Agency (EPA). https://www.epa.gov/facts-and-figures-about-materials-waste-and-recycling/national-overview-facts-and-figures-materials

Article C

Effect of Compaction and Thermal De-coating Pre-treatments on the Recyclability of Coated and Uncoated Aluminium

Alicia Vallejo-Olivares, Solveig Høgåsen, Anne Kvithyld, and Gabriella Tranell

Abstract

Scrap pre-treatments, such as compaction and thermal de-coating, are standard industrial practices for recycling aluminium post-consumer scrap. This study compares the recyclability of a coated and uncoated 8111 alloy under the application of compaction and/or thermal de-coating pre-treatments. Sheets of 600 μm thickness were shredded into chips and compacted by uniaxial pressure, moderate pressure torsion (MPT), or MPT at 450 °C (Hot MPT) into briquettes of 4 cm diameter. A subset of briquettes and loose chips was subsequently heat-treated for 1 h at 550 °C, while the other set was left untreated. The effectiveness of the heat treatment for the different compaction methods was examined by mass balance and the internal porosity of the briquettes by computed tomography. Re-melting the samples under molten salt-flux showed that the coalescence of the coated material significantly improves with the thermal de-coating pre-treatment, especially for the loose chips and briquettes compacted uniaxially. Lower coalescences were obtained for the de-coated MPT briquettes, as a result of an incomplete de-coating.

Keywords

Compaction • De-coating • Salt-flux • Recycling • Aluminium

Introduction

Aluminium food packaging scrap is often coated and/or contaminated with organic materials, which decreases the quantity and quality of the aluminium recovered. Applying a thermal pre-treatment is a common industrial practice to prevent issues associated with the moisture and organic content of this scrap [1]. Another challenging aspect in the recycling of aluminium packaging is the oxidation losses [2]. Compacting thin scrap into bales or briquettes reduces its specific surface area, an important parameter [3] on its susceptibility to oxidation during re-melting. This is already being done for some scrap types, e.g. chips from machining [4, 5] and used beverage cans (UBCs), since it facilitates storage and transport and, in the case of the chips, prevents them from floating when charged into the furnace. However, the importance of the degree of compaction (bulk density) on the oxidation losses is not yet clear. In a previous study, Vallejo-Olivares et al. observed that for clean aluminium foils compacted to briquettes of varied densities, compaction significantly reduced the oxidation during heat-treatment, especially for the thinnest materials. [6] For the current study, the research question is if "too much" compaction would negatively affect the de-coating process and if so, what consequences would this have on scrap re-melting?

De-coating pre-treatments are beneficial in many ways, such as lower dross generation and improved process control and melt cleanliness [7]. Furthermore, re-melting un-treated packaging scrap could be the source of safety hazards such as the formation of H_2S (g), PH_3 (g), H_2 (g), or CH_4 (g), which are toxic, explosive, or combustible [8]. The EN 139 standard [9] describes an average re-melting yield of 71.5% for coated packaging and of 86.1% for de-coated scrap. However, to compare these values, one must first carefully read the definitions. The metal yield is the percentage of metal gained from the total mass of the scrap. In contrast, the metal recovery represents the percentage of metal gained from the metallic mass of the scrap. Another

A. Vallejo-Olivares (✉) · S. Høgåsen · G. Tranell
Norwegian University of Science and Engineering (NTNU), Trondheim, Norway
e-mail: alicia.v.olivares@ntnu.no

A. Kvithyld
SINTEF, Trondheim, Norway

D. Eskin (ed.), *Light Metals 2022*, The Minerals, Metals & Materials Series,
https://doi.org/10.1007/978-3-030-92529-1_134

parameter often addressed in research is the coalescence efficiency. It describes the ability of the individual aluminium pieces to merge, which is critical for a successful re-melting operation without too much metal loss to small metal droplets dispersed in the salt. It is however difficult to directly infer coalescence results from laboratory experiments to industrial set-ups, which may consist of rotary furnaces, magnetic stirring, etc.

Many researchers have studied the thermal de-coating pre-treatment to define the optimal time, temperature and atmosphere that secure an efficient de-coating while minimising aluminium oxidation. Kvithyld et al. [10] stated that there is a fine line between too little de-coating, exactly enough, and too much de-coating leading to oxidation. According to their weight loss analysis of a polyester coating, the complete combustion occurs at 550 °C, and higher temperatures just oxidise the aluminium. Capuzzi et al. [11] heat-treated and re-melted coated and uncoated aluminium disks under different salt-flux compositions and temperatures. They concluded that disks thermally de-coated at 600 °C reached equivalent coalescence to those uncoated, while the treatments at 400 and 500 °C were not as effective. Gökelma [12] assessed the recyclability of used aluminium coffee capsules, one of the packaging examples with higher organics/metal ratio, and obtained higher metal yield and coalescence efficiencies for the capsules that had been thermally pre-treated at 500 °C. The work performed by Steglich [13–16] constitutes one of the few research lines that include bale density as a parameter for thermal pre-treatment and re-melting. The most recent study [16] covers the recycling of UBC bales with different densities, organic content, and pre-treatment conditions in a multi-chamber furnace process. It showed that lower bale densities promote the removal of organics during heat treatment and that this results in a lower dross formation during re-melting. This partly answers our previously placed question: for aluminium scrap containing organics, denser bales can lead to a less effective heat treatment and, therefore, more re-melting losses. The present study aims to cast some more light into this matter by evaluating the interaction between the compaction, thermal de-coating and re-melting processes of an AA8111 aluminium sheet with and without coating. It is a continuation of the previous publication on the compaction, oxidation and re-melting of clean aluminium foil. [6]

Experimental Materials and Procedure

Two coils of aluminium sheet alloy AA8111 with 600 μm gauge were provided by Speira Holmestrand. One was coated with a lacquer, and this material will be referred to as «coated», while the other will be referred to as «uncoated». Table 1 contains the chemical composition of the produced alloy. Information on the coating composition and thickness was not available, so it was measured with a portable XRF analyser and SEM–EDS.

One side of the coating was thinner (5 μm) and light in appearance, while the other was five times thicker (25 μm) and dark grey. As shown in Fig. 1, the coating consists of a matrix and filler particles. An SEM–EDS point analysis taken in one of these particles revealed a composition of 21.26 wt% O, 20.75 wt% Ca, 12.30 wt% Ti, 4.76 wt% Si, and 23.81 wt% C. Although these analyses do not provide the exact composition of the coatings, they indicate that they consist of a polymeric matrix with filler particles of CaO, TiO, and SiO_2. Figure 1d shows the dark coating after the heat treatment. The darker area shows a void (2 μm wide) surrounded by the oxide fillers that remained loosely adhered to the aluminium surface after the combustion of the organic matrix.

Table 1 Thickness and composition (wt%) of the materials and coatings studied

Material	Thickness	Al	Fe	Si	Mg	Mn	Cu	Zn	Ti	S	C	Remain
AA8111 alloy[1]	600 μm	98.371	0.865	0.587	0.046	0.037	0.036	0.007	0.005	–	–	<0.05
Dark side (XRF)[2]		87.2 ± 6.1	0.68	4.56	–	–	–	0.017	5.43	2.03	–	
Light side (XRF)[2]		94.5 ± 0.5	0.69	2.55	–	–	–	0.01	2.01	0.19	–	
Dark coating[3]	25 μm	0.35	0.04	18.28	0.15	–	0.1	0.18	2.13		57.84	
Light coating[3]	5 μm	1.41	0.15	7.18	0.1	–	0.1	0.18	2.07		64.77	

[1]Coil composition provided by Speira Holmestrand. [2]Both sides of the coated material composition were analysed by a portable XRF SPECTRO xSORT. [3]The coating composition was analysed by SEM–EDS Zeiss Ultra 55LE FEG-SEM

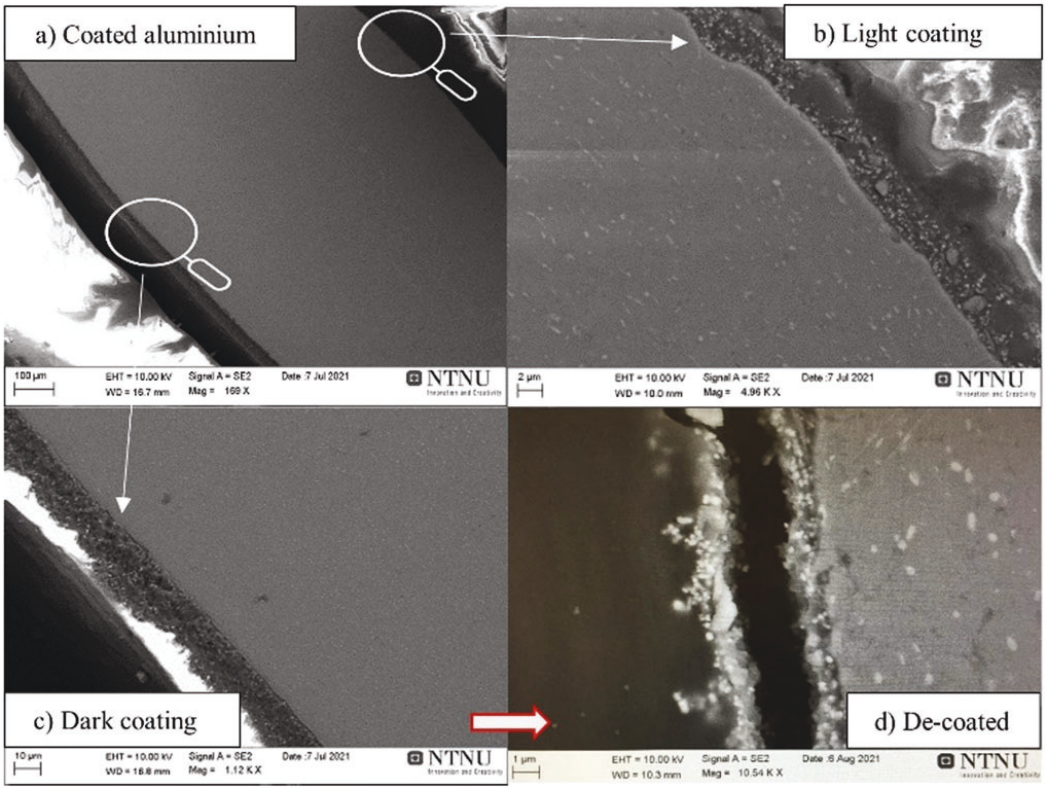

Fig. 1 SEM images **a** Coated material. **b** Higher magnification image of the light coating. **c** Higher magnification image of the dark coating. **d** Dark coating after thermal de-coating for 1 h at 550 °C

Shredding and Sieving

The coated and uncoated sheets were shredded into chips using a Getecha RS 1600-A1.1.1 with a grate of 8 mm diameter. Two sieves of square mesh 5 and 2 mm^2 were used to unify the size of the chips to this range, hence discarding 40–50%wt of the material. Image analysis of 700 sieved fragments with the software ImageJ revealed an average area of 0.26 cm^2 and median area of 0.24 cm^2 for the uncoated chips and 0.26 cm^2 average and 0.23 cm^2 median for the coated chips, with a standard deviation of 0.14 cm^2 for both materials. The average weight per chip was estimated by dividing the weight of the chips analysed by their number. The mean weight was 49.0 mg for the uncoated and 48.4 mg for the coated chips.

Compaction into Briquettes

The chips were compressed into cylindrical briquettes of 4 cm diameter, each weighing 20 g, using a hydraulic press MTS 311. A subset was compacted by holding a 100 kN (80 MPa) uniaxial force during 5 s. This method will be referred to as uniaxial. Another subgroup was compacted by moderate pressure torsion (MPT), where the piston applied a uniaxial force of 70 kN (56 MPa), while the mould rotated 360° four times for 200 s. Finally, a third subset was compacted by moderated pressure torsion under 450 °C (Hot MPT). Half of the briquettes compacted uniaxially and by MPT were heat-treated. No heat treatment was applied to the Hot MPT samples to evaluate whether the Hot MPT method would simultaneously serve as both de-coating and

compaction. Figure 2 summarises the experimental procedure. The number of repetitions was 3 for each sample group, except for the Hot MPT with two repetitions. One sample from each subgroup was analysed by computed tomography (CT), giving a set of slices used to measure the internal porosity and reconstruct a 3D image.

Thermal De-coating

The heat treatment was performed in a Nabertherm Muffle Furnace with exhaust for 1 h at 550 °C in air atmosphere. The samples were introduced into the furnace once the desired temperature was reached. A preliminary study was performed on sheets cut to 10 × 5 cm before selecting the above parameters, which also agrees with the values recommended in the literature [10, 11, 13]. Three temperatures were evaluated: 450, 550, and 650 °C. Due to partial melting of the sheets at 650 °C and incomplete de-coatings at 450 °C, the temperature of 550 °C was confirmed. The treatment was also tested for 1 h, 2 h, and 3 h at this temperature. No significant improvements were observed for 2 h, and the weight increased after 3 h due to oxidation.

Re-melting

The re-melting experiments were carried out in a Nabertherm resistance furnace. Three ceramic crucibles (Al_2O_3-SiO_2) of 20 cl volume, filled with 80 g of mixed salts with composition ratios (%wt) of 68.6:29.4:2.0 $NaCl : KCl : CaF_2$ were placed in the furnace at 800 °C. The aluminium samples were added into the crucibles once the salt was molten (after approx. 40 min). The crucibles were held in the closed furnace for 10 min at 800 °C, removed and naturally cooled in air. For the chips and briquettes of coated material that had not been thermally pre-treated, the spontaneous combustion of the coating generated flames and dark smoke for around 30 s. The furnace lid was kept open until the end of this combustion. Once the crucibles were at room temperature, the salt was separated from the metal by crushing and washing it with water on an 800 microns sieve, discarding any smaller particles. After drying, the metal pieces were weighted, and the metal yield, metal recovery, and coalescence were calculated using Eqs. 1, 2, and 3.

$$\%Metal\ Yield = \frac{m_{recov}}{m_{input}} * 100 \quad (1)$$

$$\%Metal\ Recovery = \frac{m_{recov}}{m_{metalinput}} * 100 \quad (2)$$

$$\%Coalesced = \frac{m_{coalesced}}{m_{input}} * 100 \quad (3)$$

$$m_{metal\ input} = m_{input} - m_{input} * \%\, average\ weight\ loss \quad (4)$$

where m_{recov} is the sum of the masses of the pieces recovered, m_{input} is the mass of the briquette or batch of chips

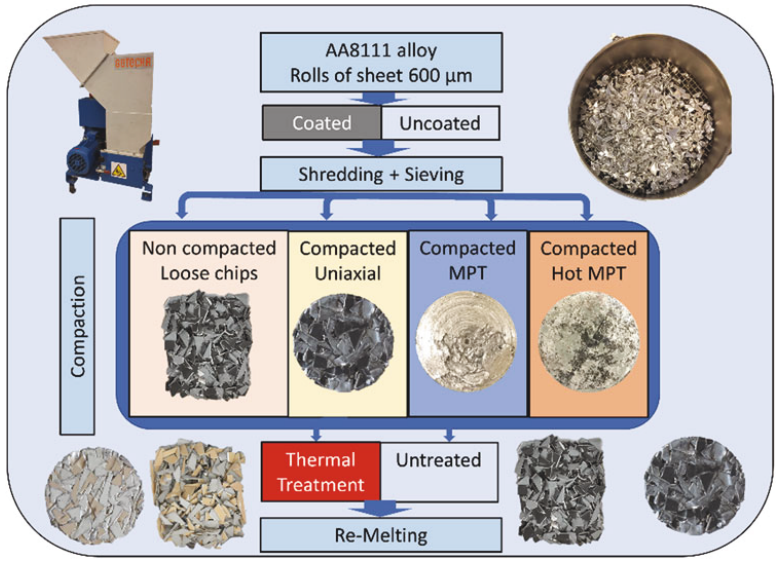

Fig. 2 Experimental procedure

before re-melting, $m_{coalesced}$ is the mass of the biggest piece, and $m_{metal\ input}$ is calculated based on the average weight loss results for each compaction route: 1.66% for loose chips, 1.70% for uniaxial, and 1.52% for MPT briquettes. This way, we can estimate the metal content of the sample before re-melting and calculate metal recovery values. It is assumed that after heat-treatment, the samples are 100% metal, so for the uncoated and the de-coated samples, metal yield is equal to metal recovery.

Results and Discussion

Compaction

Table 2 presents the average bulk densities after briquetting by the different compaction methods and the briquette's internal porosity of both untreated and thermally treated briquettes. The internal porosity was measured by CT for one sample from each group. The analysis was performed slice by slice using the software ImageJ, first adjusting a threshold to differentiate between material and void and then conducting a porosity measure. The values presented for each sample are the average of between 80 and 250 images and the standard deviation within sample ranged between 0 and 3%. Slices close to the top and bottom of the briquettes showed higher porosity values, but they were omitted since they represent the external porosity.

The bulk densities reached for the coated chips were lower than for the uncoated. This could be due to a lower adhesion of the coatings, higher thickness leading to stiffer chips, or both. Coated briquettes sometimes fell apart completely. In most cases, some loose chips fell off when taking them out of the mould and in further handling, especially for the briquettes compacted by the uniaxial method. The internal porosity drastically decreases when compacting by the MPT method, from the range 14.7–18.3% to 0.7–5%, and down to 0.04–0.07 for the Hot MPT method. The porosity is higher for the uncoated material than for the coated material compacted uniaxially but higher for the coated material that had been compacted by MPT and Hot MPT. Both coated and uncoated materials present higher porosity after the thermal treatment, which could be attributed to the elimination of the coating and other volatiles or to a slight re-arrangement of the position of the chips due to thermal expansion during the treatment. These porosities are lower than those found in Steglich's [13] study on UBC bales (range 59–83%), which correspond with today's industrial values.

During MPT of coated chips, some metal got stuck in the piston resulting in weight loss of the briquette and an uneven surface. Loose chips rarely fell off or got stuck for the uncoated briquettes, and the surfaces were smooth. These differences between the compaction methods are shown in the CT 3D reconstructions in Fig. 3.

Thermal De-coating

The coated chips and briquettes experienced a colour change, shown in Fig. 2, and became very fragile after thermal treatment. The uncoated briquettes showed no visible change and held together also after the treatment. Figure 4 shows the average weight change due to thermal treatment for coated and uncoated chips and briquettes.

For the coated material, the uniaxially compacted briquettes lost, on average, almost the same weight as the loose chips: 1.70 versus 1.66%. The coated MPT briquettes lost less weight on average: 1.52%. This indicates that uniaxial compaction does not reduce the effectiveness of the thermal de-coating, in contrast to MPT compaction. All samples increased in weight for the uncoated briquettes due to oxidation, and the loose chips experienced the highest average weight increase: 0.02%. Still, the weight increases due to oxidation are two orders of magnitude lower than the weight decreases due to the de-coating. Therefore, the heat treatment parameters (1 h, 550 °C) seem to offer the pursued effects: effective coating removal and low oxidation. The oxidation results agree with some of the conclusions from the previous study [6], where briquettes were observed to oxidise less than loose chips. A lower oxidation for MPT than for uniaxial compression was expected, based on the lower internal porosity of the MPT briquettes. While the results indicate the opposite, the standard deviation in the

Table 2 Average briquette bulk density (g/cm^3) and internal porosity (%) for different compaction routes

	Uniaxial		MPT		Hot MPT	
	Porosity	Density	Porosity	Density	Porosity	Density
Uncoated	16.64	1.94 ± 0.01	0.68	2.46 ± 0.01	0.04	2.60 ± 0.02
Coated	14.68	1.90 ± 0.18	4.48	2.19 ± 0.09	0.07	2.54 ± 0.07
Uncoated Thrm. Treat	18.28		1.39			
Coated Thrm. Treat	15.89		4.75			

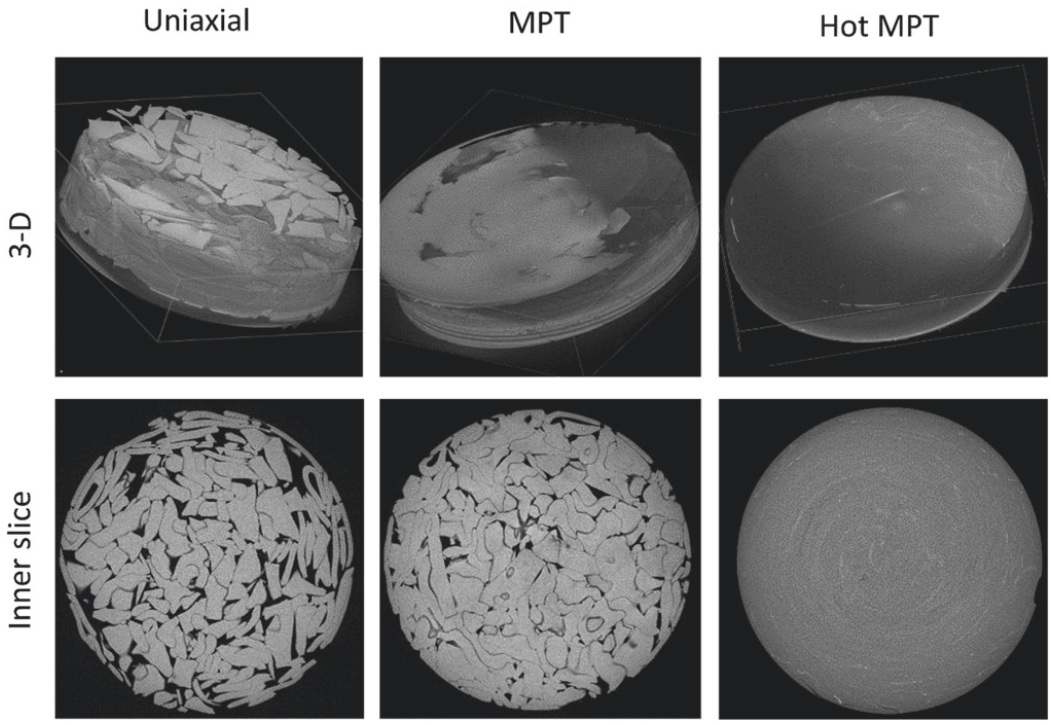

Fig. 3 Computed tomography of briquettes of coated material compacted by Uniaxial, MPT, and Hot MPT method. **Top row:** 3D reconstruction. **Bottom row**: one of the inner planes captured showed the chips' internal porosity and deformation

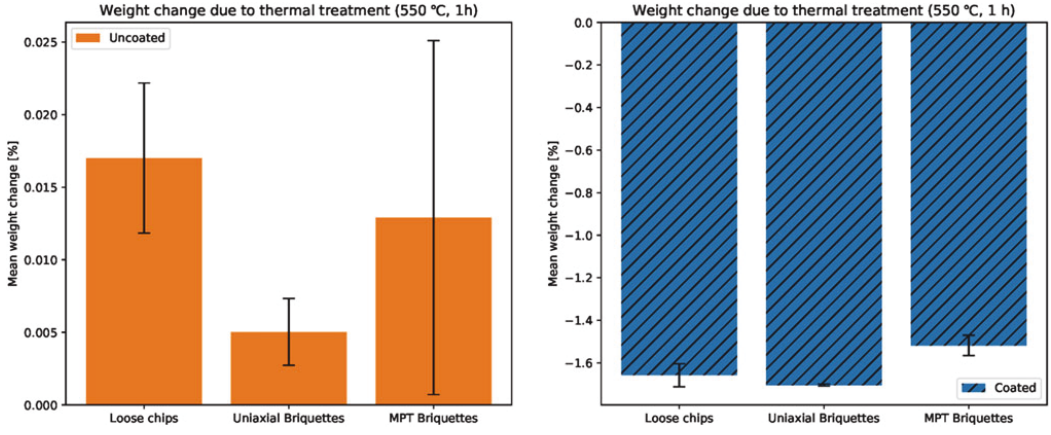

Fig. 4 Average weight changes due to thermal treatment for the uncoated (left) and coated (right) material. The bars show the std. dev between the three repetitions. Note the difference in the y-axis scale between both graphs

data is large, making the result tentative. Finally, the fact that the uniaxial compaction, even up to densities of 2 g/cm^3, does not affect the heat treatment compared to the loose chips seems to oppose some of Steglich' s observations, where bales compacted to lower densities generated higher dross, attributed to an incomplete de-coating. Crucial differences in their experimental method (re-melting without salt-flux) and material type (post-consumer scrap) may be the cause for the deviating observations.

Re-melting

Coalescence

The material recovered after re-melting showed various degrees of coalescence. Good coalescence leads to most of the chips merging into one round piece. On the contrary, poor coalescence leads to multiple small pearls distributed in the salt. A coalescence analysis can be done by comparing the recovered metal images in Fig. 5a and the average coalescences for the different routes in Fig. 5b. The results are collected in Table 3, in the following sub-section, together with the metal yield and metal recovery values.

The surfaces of the metal recovered from the coated, untreated samples appear rougher and darker because of the spontaneous combustion that took place during their re-melting. On the contrary, the re-melted uncoated and de-coated materials look smooth and shiny. The average coalescence results demonstrate (in agreement with literature [11, 12]) that applying a thermal de-coating pre-treatment has a great effect on improving the coated materials' coalescence. Regarding the compaction route, thermally de-coating either loose chips or uniaxial briquettes resulted in similar coalescences to those of the uncoated materials. However, the coalescence was lower for the de-coated MPT briquettes. The reason may be that the MPT briquettes are so tightly compacted that they inhibit part of the de-coating process, leaving some carbonaceous materials trapped inside the briquette and limiting the ability of chips to coalesce together, as previously observed by Steglich. This is consistent with the results from the previous section. The uncoated material reached almost perfect coalescences regardless of the pre-treatment routes. However, a slight increase can be observed for the MPT and Hot MPT samples.

Metal Yield and Metal Recovery

Table 3 collects the coalescence, metal yield, and metal recovery results for all re-melting experiments. As mentioned in the introduction, these are different ways of reporting recycling efficiency. For comparisons between samples with different non-metallic content, metal recovery values would be more accurate than metal yield. For most of the samples of this study, though, the recycling yield and recovery are the same. Therefore, some of the cells in the table are merged and present one value for both.

The calculated metal recovery is just 1–2% higher than the yield for the untreated coated samples. The difference would be more relevant when recycling materials with higher organics content, such as post-consumer scrap. Regarding coalescence, while the difference between coalescence and yield/recovery values is very small or

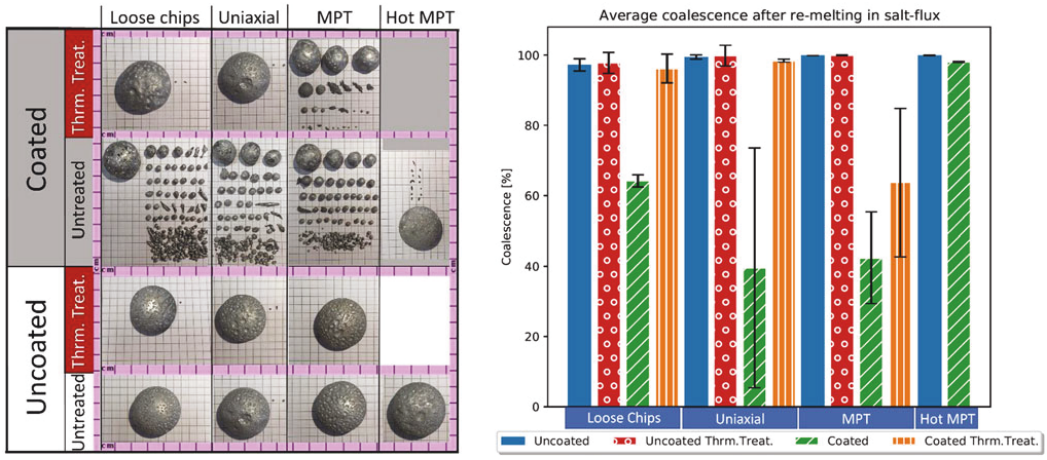

Fig. 5 Left: **a** Example of the recovered metal for each of the compaction and thermal pre-treatment routes. Right: **b** Coalescence results for all re-melting experiments. The bars show the standard deviation between repetitions

Table 3 Coalescence (C), Metal Yield (Y), and Metal Recovery (R) results

	Loose chips			Loose chips Thrm.Treat			Uniaxial			Uniaxial Thrm.Treat			MPT			MPT Thrm.Treat			Hot MPT		
	C	Y	R	C	Y	R	C	Y	R	C	Y	R	C	Y	R	C	Y	R	C	Y	R
Uncoated	95	95		94	94		100	100		103	103		100	100		100	100		100	100	
Uncoated	98	98		100	100		100	100		100	100		100	100		100	100		100	100	
Uncoated	99	99		100	100		99	99		96	96		100	100		100	100		–		
Average	97	97		98	98		99	100		100	100		100	100		100	100		100		
Std. Dev	1.7	1.6		3.0	3.0		0.6	0.6		3.0	3.0		0.0	0.0		0.1	0.1		0.0		
Coated	65	96	97	90	100		85	95	96	98	98		29	96	98	62	97		98	98	
Coated	62	94	96	99	99		3	96	98	99	99		60	96	98	91	95		98	98	
Coated	66	97	99	99	99		30	94	95	99	99		39	96	97	39	96		–		
Average	64	96	97	96	99		40	95	96	98	98		42	96	98	64	96		98		
Std. Dev	1.8	1.3	1.4	4.0	0.4		34.0	1.1	1.1	0.4	0.4		13.0	0.1	0.1	21.0	0.6		0.1		

non-existent for the uncoated and the de-coated samples, it can become as high as 90% for the most extreme cases of coated untreated samples. Thus, in this study, coalescence is the most relevant parameter. If only the recovery or yield were evaluated, all the re-melting results would lay within the ranges 94–100%. This would not explain the differences between the products obtained via the different pre-treatment routes, shown in Fig. 5a.

Conclusions

This work has investigated the compaction of coated and uncoated chips of aluminium sheet alloy AA8111 with 600 μm gauge by three different methods: uniaxial, moderate pressure torsion (MPT), and Hot MPT at 450 °C. The performance of thermal de-coating and re-melting in salt flux of these materials has been investigated. The following conclusions were drawn:

- The uncoated material was easier to compact than the coated, meaning more densely packed briquettes.
- The internal porosity of the briquettes drastically decreases when adding torsion to the compaction process and even further by adding temperature.
- A thermal de-coating of 1 h at 550 °C removed the organics while keeping the oxidation low; the weight of the coated samples decreased by 1.5–1.7%, and it increased by less than 0.02% for the uncoated.
- The coalescence of the coated samples improved due to the thermal de-coating: by 32% for the loose chips, 58% for uniaxially compacted briquettes, and 22% for the MPT compacted briquettes.
- Re-melting de-coated chips and uniaxial briquettes resulted in similar coalescences to those of the uncoated materials.
- An incomplete de-coating is crucial for coalescence, as observed for the de-coated MPT briquettes; just a slightly lower de-coating weight loss (0.18%) than the uniaxial but 35% lower coalescence.
- Average metal yields lay between 95 and 100, and recoveries between 97 and 100%.
- While it is possible to observe small differences between the yield and recovery results (averages below 98% for the coated non-heat-treated samples, uncoated loose chips, and de-coated MPT briquettes), the coalescence is more representative of the recycling efficiency in the present study.

Acknowledgements The authors would like to gratefully acknowledge the Research Council of Norway and the partners of *Alpakka—Circular Aluminium Packaging in Norway* (NFR Project nr. 296276) for funding the project, Speira Holmestrand for the materials, and the Department of Materials Science and Engineering at NTNU, Trondheim, for the experimental equipment and support, especially to Pål C. Skaret for his help with the compactions.

References

1. Capuzzi, S., Timelli, G. (2018) Preparation and melting of scrap in aluminum recycling: A review. Metals 8(4):249. https://doi.org/10.3390/met8040249
2. Tabereaux, A. T., Peterson, R. D. (2014) Aluminium Production. Elsevier, New York
3. Rossel, H. (1990) Fundamental investigations about metal loss during remelting of extrusion and rolling fabrication scrap. In: Bickert, C. M. (eds) Light Metals 1990, p. 721–729. The Minerals, Metals & Materials Series. Springer, New York

4. Wells P. A., Peterson. P. D. (1990) Transient three-dimensional briquette preheater model, in Proc. Second International Symposium - Recycling Metals and Engineered Materials, p. 221–236
5. Tucholski, G., Ruf, U. (2013) Chips versus briquettes: How the aluminium industry can effectively and efficiently recycle scrap. Int. Alum. J., 89(1/2):87–88
6. Vallejo-Olivares, A. et al (2021) Correction to: Compaction of Aluminium Foil and Its Effect on Oxidation and Recycling Yield. In: Perander L (eds) Light Metals 2021. The Minerals, Metals & Materials Series. Springer, Cham. https://doi.org/10.1007/978-3-030-65396-5_133
7. Kvithyld, A. (203) Thermal Decoating of Aluminium Scrap. Ph.D. thesis, Norwegian University of Science and Technology
8. Van Schaik, A., Reuter, M. A., (2014) Material-Centric (Aluminium and Copper) and Product-Centric (Cars, WEEE, TV, Lamps, Batteries, Catalyst) Recycling and DfR Rules. In: Worrel, E, Reuter M. A (eds) Handbook of Recycling 2014, Elsevier, https://doi.org/10.1016/B978-0-12-396459-5.00022-2
9. CEN, "EN 13920–1:2003 E," in Aluminium and aluminium alloys - Scrap, 2003.
10. Kvithyld, A., Meskers, C. E. M., Gaal, S. et al. (2008) Recycling light metals: Optimal thermal de-coating (2008) JOM 60(8):47–51 https://doi.org/10.1007/s11837-008-0107-y
11. Capuzzi, S., Kvithyld, A., Timelli, G. et al. (2018) Coalescence of Clean, Coated, and Decoated Aluminium for Various Salts, and Salt-Scrap Ratios. J. Sustain. Metall 4:343–358 https://doi.org/10.1007/s40831-018-0176-2
12. Gökelma, M., Diaz, F., Öner, I. E., Friedrich, B., Tranell, G. (2020) An Assessment of Recyclability of Used Aluminium Coffee Capsules. In Tomsett A. (eds) Light Metals 2020. The Minerals, Metals & Materials Series. Springer, Cham. https://doi.org/10.1007/978-3-030-36408-3_149
13. Steglich J., Matthies C., Rosefort M., Friedrich B. (2018) Behavior of Mg-Si-Rich Phases in Aluminium Can Sheets and Their Impact on Metal Oxidation During Industrial Thermal Pre-treatment. In: Martin O. (eds.) Light Metals 2018. The Minerals, Metals & Materials Series. Springer, Cham. https://doi.org/10.1007/978-3-319-72284-9_146
14. Steglich J., Dittrich R., Rombach G., Rosefort M., Friedrich B., Pichat, A. (2017) Dross Formation Mechanisms of Thermally Pre-Treated Used Beverage Can Scrap Bales with Different Density. In: Ratvik, A. (eds) Light Metals 2017. The Minerals, Metals & Materials Series. Springer, Cham. https://doi.org/10.1007/978-3-319-51541-0_133
15. Steglich J., Buchholz A., Gültekin R., Dittrich R., Rombach G., Friedrich B., Pfeifer H. (2015) Conductive heat transfer in used beverage can scrap. Paper presented at the conference Advances In Materials And Processing Technologies, 14–17 Dec 2015 in Madrid.
16. Steglich, J., Friedrich, B., Rosefort, M. Dross Formation in Aluminium Melts During the Charging of Beverage Can Scrap Bales with Different Densitie Using Various Thermal Pretreatments. JOM 72, 3383–3392 (2020). https://doi.org/10.1007/s11837-020-04268-4

Article D

Journal of Sustainable Metallurgy
https://doi.org/10.1007/s40831-022-00612-x

THEMATIC SECTION: REWAS 2022: DEVELOPING TOMORROW'S TECHNICAL CYCLES

Thermal De-coating Pre-treatment for Loose or Compacted Aluminum Scrap and Consequences for Salt-Flux Recycling

Alicia Vallejo-Olivares[1] · Solveig Høgåsen[1] · Anne Kvithyld[2] · Gabriella Tranell[1]

Received: 9 June 2022 / Accepted: 6 October 2022

Abstract
In aluminum recycling, thermal de-coating pre-treatments remove moisture and organic contamination before re-melting. If the scrap is compacted into bales or briquettes before the thermal treatment and re-melting processes, less surface area is exposed to oxidation in contact with air. However, compaction may also limit the efficiency of the de-coating process. In this study, coated sheets of aluminum were thermally de-coated at varied temperatures and durations. Observations of changes in coating thickness, mass, color, and composition revealed a maximum de-coating efficiency of close to 75% wt due to remaining oxide residues. The relationship between de-coating and compaction was investigated by thermally treating loose shreddings (chips) and briquettes of various densities. The briquettes were compacted by three methods: uniaxial, moderate-pressure torsion (MPT), and MPT at 450 °C (Hot MPT); and the de-coating efficiency was calculated from the mass loss. Subsequently, the samples were re-melted under salt-flux and compared with another set of samples which were re-melted without thermal pre-treatment. The results showed that thermal de-coating significantly promotes the coalescence of loose chips and briquettes compacted uniaxially, up to similar coalescences than initially uncoated aluminum samples. Thermally treating the MPT briquettes, which were more densely compacted, led to less de-coating, and subsequently lower coalescences. The analysis of re-melted material revealed that the coating residues did not significantly affect the composition, while the compaction prevented Mg loss for the uncoated materials.

The contributing editor for this article was Zhi Sun.

✉ Alicia Vallejo-Olivares
alicia.v.olivares@ntnu.no

[1] Norwegian University of Science and Technology (NTNU), Trondheim, Norway

[2] SINTEF, Trondheim, Norway

Published online: 28 October 2022

Graphical Abstract

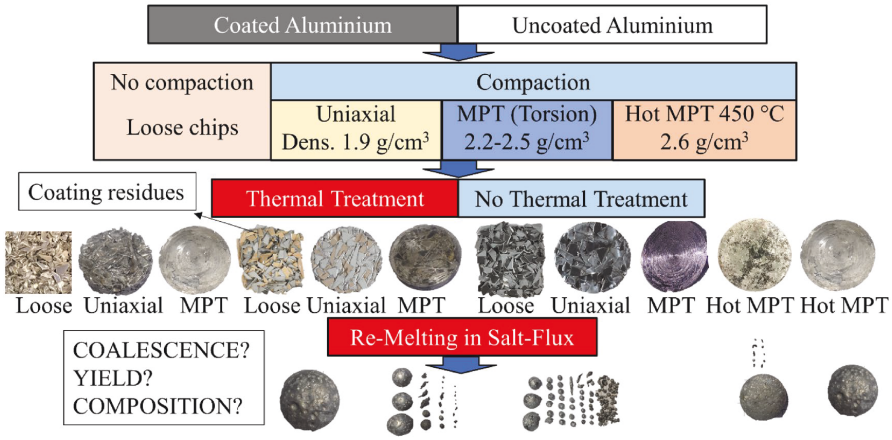

Keywords Recycling · Aluminum · Pre-treatment · Compaction · De-coating · Salt-flux

Introduction

In aluminum recycling, a thermal pre-treatment is often applied to post-consumer scrap in order to remove coatings, moisture, and other organics before re-melting [1]. Thermal pre-treatments are beneficial in many ways, such as lower dross generation, higher re-melting yield, and improved process control and melt cleanliness. Furthermore, re-melting contaminated scrap without treatment could lead to the formation of H_2S (g), PH_3 (g), H_2 (g), CH_4 (g) or dioxins, which are toxic, explosive or combustible [2]. An ideal thermal pre-treatment should remove the moisture and organic materials without oxidizing the metals while operating at the lowest possible cost and energy consumption. Regarding the process parameters, low temperatures may reduce metal oxidation and energy consumption but at the expense of an incomplete removal of the organics or longer times for completion. Kvithyld et al. [3] showed that the optimal parameters also depend on the chemical composition of the coating, the atmosphere (especially oxygen availability) and the heating rate.

Compacting the scrap into bales or briquettes is another standard recycling pre-treatment, since it facilitates storage and transport. A previous study [4] showed that compaction could reduce the oxidation of thin scrap, which has a high specific surface area. The correlation between scrap thickness and re-melting losses was previously described by Rossel [5]. However, the scrap bales are often broken down back into loose pieces before the sorting and thermal pre-treatments [6, 7]. Whether the scrap is loose or compacted during the thermal treatment may affect the removal of organics as it may alter scrap heat transfer and exposure to oxygen. Steglich [8] thermally treated bales of used beverage cans (UBCs) and foils and observed a correlation between the thermal conductivity of the bales and their density and porosity. According to Wells [9], the heat transferred through bales of UBCs is much lower than through a block of solid aluminum. In a later study, Steglich [10] re-melted UBC bales with different densities, organic content, and pre-treatment conditions. The results indicated that bales compacted more loosely formed less dross during re-melting, for a set-up consisting of a multi-chamber furnace with molten aluminum heel.

Another common method to re-melt post-consumer scrap is the use of rotary furnaces with salt-flux. The salt-flux, a mix of NaCl and KCl with small additions of fluorides, helps separating the molten metal from the oxides and contamination, promoting the coalescence of the metal droplets and preventing the melt from oxidation [1, 7]. The coalescence efficiency describes the ability of the individual aluminum pieces to merge into a macro phase. This is critical for a successful re-melting operation without too much metal loss trapped in the salt slag residues. Several studies have used the coalescence efficiency as an indicator for recyclability, and showed that it is influenced by furnace operation conditions [11, 12], the salt/scrap ratio [13], the concentration of fluorides [14], and non-metallic particles [15] in the salts and the surface area and contamination of the scrap [12, 16, 17]. Furthermore, the work of Capuzzi on small coated disks [14] and Gökelma

on coffee capsules [18] showed that thermal de-coating promoted the coalescence of coated scrap when re-melting under salt-flux, and in both cases, the results were better for the samples treated at higher temperatures (600 °C and 500 °C, respectively).

Another critical aspect of aluminum recycling is metal quality. Even if the thermal de-coating removes most organic and volatile elements from the scrap, some residues (e.g., oxides) remain and can act as a source of impurities or inclusions in the melt. For example, white inorganic pigments of TiO_2 are commonly found in aluminum packaging. Wang et al. [19], Li and Qui [20], and Önem [21] demonstrated the presence of these oxide residues on the the surface of UBCs after thermal de-coating. Wang also observed that the thermal de-coating removed up to 93% of the weight of the coating, in contrast to a 100% removal by chemical treatment. Whether the de-coating residues will accumulate in the melt or end up in the slag or salt-cake after re-melting was investigated by Meskers for magnesium alloys based on thermodynamic and kinetic mechanisms [22, 23] and by Rombach [24] for aluminum. Hiraki [25] evaluated the refining ability of salt-flux on aluminum secondary melts based on a thermodynamic model, and concluded that only Ho, Dy, Li, La, Mg, Gd, Ce, Yb, Ca, and Sr could be removed from the melt by reaction with chloride salts. Oosumi [26] studied the accumulation of Ti experimentally by re-melting (without salt-flux) UBCs after thermal or chemical de-coating treatments, observing higher Ti concentrations for the recycled aluminum that had been thermally de-coated than the chemically de-coated. The concern over the accumulation of impurities and alloying elements in aluminum recycling is associated with the lack of successful refining methods. Løvik et al. [27] argued that the impurity accumulation would be a challenge even with closed-loop recycling systems such as that of UBCs. Several researchers, such as Castro [28] and Reuter [29], have emphasized the criticality of optimizing scrap collection and sorting techniques, as well as proposing a design-for-recycling approach in an attempt to overcome these metallurgical challenges for the circular economy.

To contribute to the state of the art, this study evaluates the de-coating efficiency of coated aluminum sheets at various temperatures and durations by measuring the changes in weight and coating thickness, and the composition of the de-coating residues. The relationship between the compaction state of the scrap and the de-coating efficiency and re-melting losses in salt-flux is further investigated, comparing coated and uncoated sheets of clean, as-produced aluminum. Finally, the recycled metal is analyzed to determine whether the application of thermal de-coating or compaction routes influences its chemical composition.

Materials and Method

This study is divided into two parts. The first aims to find the optimal thermal de-coating parameters for the coated sheet by testing a range of temperatures and durations, and the second part investigates the effects of combining mechanical and thermal pre-treatments before re-melting under salt-flux. The materials were two coils of aluminum sheet alloy AA8111 of 600 µm thickness, one coated and the other uncoated. The main alloying elements for both sheets are displayed in Table 1, and the detailed composition including trace elements in Table 4, where it is also compared to the compositions of the samples after re-melting.

Thermal De-coating Optimization: Time and Temperature Variations

For the optimisation study, the coated sheet was cut into rectangles of an area of 10×5 cm, weighing 8–9 g. A subset of these samples was thermally treated at a constant temperature of 550 °C and durations of 5, 10, 20, 30, 40, 50, and 60 min, and the second subset at temperatures 450 °C, 550 °C, and 600 °C for 5 and 10 min. The samples were introduced into a pre-heated Nabertherm muffle furnace with exhaust and were taken out to cool down at room temperature after the treatment. The efficiency of the de-coating treatment was assessed based on several observations: changes in mass, coating thickness, elemental composition, and the visual appearance, particularly the color when comparing the samples before and after the treatment. Part of the coating remained adhered to the aluminum after the thermal treatment. For one of the sheets, all coating rests were removed by washing with ethanol. The dry and clean sheet weighed 0.22 g less than before the thermal treatment. This value was accepted as the standard coating mass for the sheet samples, and the de-coating efficiencies were calculated as the percentage ratio of the mass loss to the standard coating mass. Calculating the de-coating efficiencies makes it possible to compare with other de-coating methods used in literature, such as acid leaching in Wang et al. [19]

Table 1 Compositions of the aluminum sheets analyzed by ICP-MS

	Al (%)	Fe (%)	Si (%)	Mg (ppm)	Cu (ppm)	Ga (ppm)	V (ppm)	Ti (ppm)	Mn (ppm)	Zn (ppm)
Coated	96.87	0.75	0.23	7	11	114	84	99	27	23
Uncoated	98.10	0.81	0.23	404	340	106	208	53	377	75

Combination of Compaction and Thermal Pre-treatments

Both coated and uncoated aluminum were used to study the influence of compaction in the thermal pre-treatment. The sample preparation began by shredding the sheets into chips and sieving them to unify their size. Next, some chips were compacted by one of the three routes described below, and some were left uncompacted (referred to as "loose chips"). Half of the samples were then thermally treated, and finally, all the samples were re-melted under salt-flux. The experimental procedure is shown schematically in the graphical abstract.

Shredding

The shredding machine was a Getecha RS 1600-A1.1.1 with a grate of 8 mm diameter. The shredded chips were sieved with two square mesh sieves of 2–5 mm^2. Image analysis of 700 sieved fragments with the software ImageJ revealed an average area of 0.26 cm^2 and median area of 0.24 cm^2 for the uncoated chips and 0.26 cm^2 average and 0.23 cm^2 median for the coated chips, with a standard deviation of 0.14 cm^2 for both materials. The average weight per chip was estimated by dividing the weight of the chips analyzed by their number. The mean weight was 49.0 mg for the uncoated and 48.4 mg for the coated chips.

Compaction

The chips were compressed into cylindrical briquettes of 4 cm diameter, each weighing 20 g, using a hydraulic press MTS 311. One subset was compacted by holding a 100 kN (80 MPa) uniaxial force during 5 s. This method is referred to as "uniaxial." Another sub-group was compacted by moderate-pressure torsion (MPT), where the piston applied a uniaxial force of 70 kN (56 MPa), while the mold rotated 360° four times for 200 s. Finally, a third subset was compacted by MPT under 450 °C (Hot MPT).

One briquette sample from each sub-group was analyzed by computed tomography (CT), giving a set of slices used to measure the internal porosity. The analysis was performed using the software ImageJ; this procedure was described in a previous study [30]. Table 2 presents the average bulk densities and the briquette internal porosities. The porosity presented for each sample is the average of between 80 and 250 images, and the standard deviation within a sample is also displayed. Slices close to the top and bottom of the briquette were omitted.

The bulk densities of the coated chips were lower than for the uncoated. In most cases, some loose chips fell off when taking them out of the mold and in further handling, especially for the briquettes compacted by the uniaxial method. The internal porosity was significantly lower when compacting by the MPT method and essentially non-existent by Hot MPT.

Thermal De-coating

No treatment was applied to the Hot MPT briquettes since the method, reaching temperatures of 450 °C, would simultaneously serve as thermal treatment and compaction. Out of the rest of the samples, half were treated by the procedure described above but with constant parameters of 1 h and 550 °C and half were left untreated.

Re-melting

The re-melting was carried out in a Nabertherm resistance furnace. Three ceramic crucibles (Al_2O_3–SiO_2) of 20 cl volume, filled with 80 g of mixed salts with composition ratios (%wt) of 68.6:29.4:2.0 NaCl:KCl:CaF_2 were placed in the furnace at 800 °C. The amount of salt-flux used relative to the non-metallic content of the scrap is significantly higher than those typically used in industrial rotary furnaces, as reported by Capuzzi [13]. For the present static set-up, a salt/scrap ratio of 4 was required so that the chips would be completely covered by the molten salts and protected from oxidation. The aluminum samples, either briquettes or batches of loose chips weighing 20 g each, were added to the crucibles once the salt was molten (after approx. 40 min). The crucibles were then held in the closed furnace for 10 min at 800 °C, removed, and cooled in air. Stirring was not applied. For the chips and briquettes of coated material that had not been thermally pre-treated, the spontaneous combustion of the coating generated flames and dark smoke for around 30 s. The furnace was kept open until the end of this combustion. Once the crucibles were at room temperature, the salt was separated from the metal by crushing and washing it with water on an 0.8 mm sieve. After drying, the metal pieces were weighed, and the metal yield and coalescence were calculated using Eqs. 1 and 2.

Table 2 Average briquette bulk density (g/cm^3) and internal porosity (%) for the different compaction routes

	Uniaxial		MPT		Hot MPT	
	Porosity	Density	Porosity	Density	Porosity	Density
Uncoated	16.64 ± 1.37	1.94 ± 0.01	0.68 ± 0.84	2.46 ± 0.01	0.04 ± 0.04	2.60 ± 0.02
Coated	14.70 ± 1.43	1.90 ± 0.18	4.48 ± 1.65	2.19 ± 0.09	0.06 ± 0.11	2.54 ± 0.07

$$\%\text{Metal Yield} = \frac{m_{\text{recov}}}{m_{\text{input}}} * 100, \quad (1)$$

$$\%\text{Coalesced} = \frac{m_{\text{coalesced}}}{m_{\text{input}}} * 100, \quad (2)$$

where m_{recov} is the sum of the masses of the pieces recovered, m_{input} is the mass of the briquette or batch of chips before re-melting, and $m_{\text{coalesced}}$ is the mass of the largest piece recovered (shown in Fig. 6a).

Characterization Methods

The composition and thickness of the coating were studied by scanning electron microscopy (SEM) and optical microscopy (OM). On one side of the sheet, the coating was thinner (5 µm) and light in appearance, while on the other side, the coating was five times thicker (25 µm) and dark gray. The cross-sections of the dark coating were analyzed by SEM–EDS point analysis (Zeiss Ultra 55LE FEG-SEM) and by Electron Probe Micro Analysis (EPMA), for several samples before and after the thermal treatment. This way, it was possible to study the influence of the treatment time and temperature in the removal of specific elements. The de-coating residues formed a white/yellowish powder, which was analyzed by X-Ray Diffraction (XRD) in a DaVinci 1 X-ray Diffractometer using angles between 15° and 80° and a scan time of 30 min, and the qualitative phase identification was carried out with the software DIFFRAC.EVA. Finally, slices weighing approximately 1 g were cut from the re-melted metals and from the original sheets and sent for ICP-MS elemental analysis to ALS Scandinavia. The coated sheet was thermally treated at 550 °C for 1 h and cleaned with ethanol to remove the coating, and all samples were pre-digested with HCl and HNO_3.

Results and Discussion

Thermal De-coating Optimisation: Time and Temperature Variations

The results showed that heating duration and temperature affect the weight change, the coating thickness, and composition. Figure 1 shows an untreated sample, placed in the far left, next to samples treated at 550 °C with increasing treatment durations to the right.

A color change occurred for the coatings on both sides of the samples. For the samples thermally treated for 5 and 10 min, the color became darker than the original color. For treatments of 20 min and longer the differences were minor, therefore sheets treated at 30, 40, 50 and 60 min are not shown in Fig. 1. Similar color changes were also described by Kvithyld [3], who attributed the darker color to char residues from the decomposition of the coating by scission and the white color as a sign of a complete combustion of the carbon residues. When handling the samples, it was also observed that longer times resulted in the coating more easily flaking off. Note that the sheets were stored in sample bags before the pictures were taken; therefore, the flaking seems more intense than it was right after the treatment. Figure 2a presents the weight losses during de-coating after the treatments at 550 °C, and Fig. 2b for the 5- and 10-min treatments at varied temperatures. The bar graphs show the mean weight loss as a percentage of the sheets' initial weight and the variations within the three repetitions.

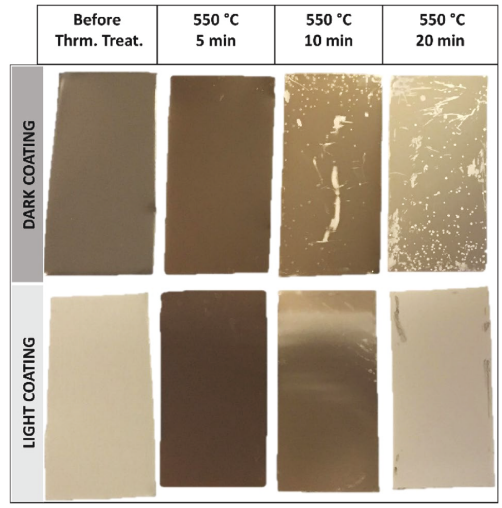

Fig. 1 Variations in dark side coating (above) and light side coating color (below) after thermal treatment

For the experimental series at 550 °C (Fig. 2a), the weight reduction increased with the treatment time up to 20 min, while after this point, the difference stagnated. The subset thermally treated for 20 min experienced the most significant weight decrease: − 1.8% wt. This was 74.5% of the total weight of the coating, meaning that this coating has a higher ratio of inorganic components than the UBCs studied by Wang [19]. Since the weight change did not increase for longer durations than 20 min, this seems to be the optimal treatment duration for the sheets. This is supported by the visual inspection of the samples in Fig. 1; the color differences after 20 min were minor. The results suggest that around 25% wt of this coating is not removable by thermal treatment. The treatments at 5 and 10 min removed 66.7% and 70.7% wt of the coating (corresponding to sheet's weight

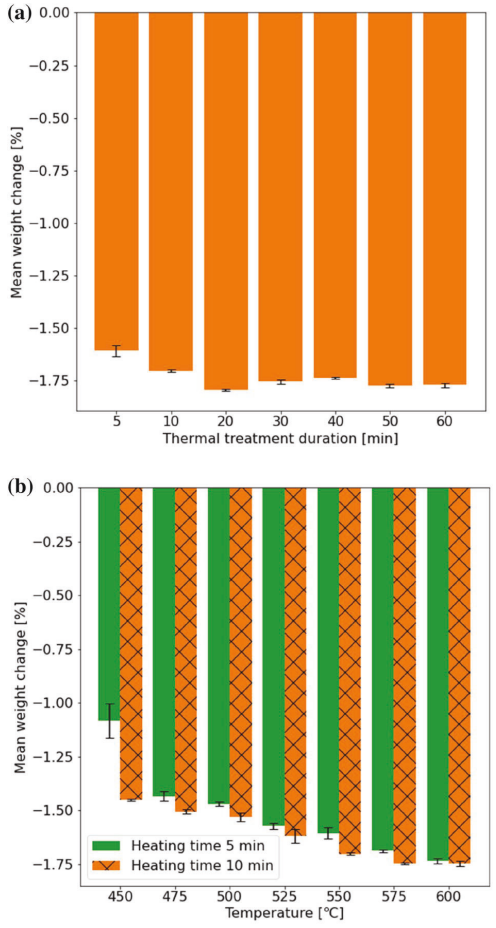

Fig. 2 Left: **a** Weight change due to thermal treatment at 550 °C and durations between 5 and 60 min. Right: **b** Weight change due to thermal treatment for 5 and 10 min at temperatures from 450 to 600 °C. Three repetitions each trial

changes − 1.6% and − 1.7% wt), which indicated that the thermal treatment was still incomplete. Figure 2b shows the result for the second subset of experiments that explored the possibilities of achieving complete de-coatings at 5 or 10 min by varying the temperature. The results show larger weight changes as temperatures increase. The largest de-coating efficiency was obtained at 600 °C and 10 min: 72.1%, corresponding to a weight loss of -1.8%. However, this is still slightly lower than for the samples treated 20 min at 550 °C in the first series of experiments. The sheets treated for 5 min at 450 °C led to the lowest de-coatings efficiency: 45.0% (− 1.1% wt decrease). Another trend was

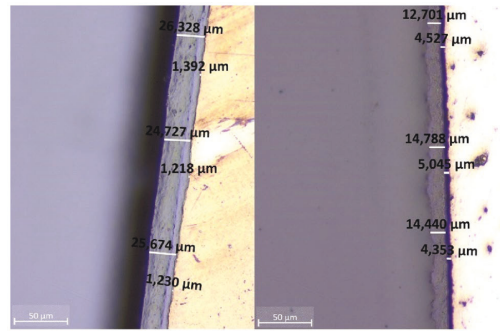

Fig. 3 Coating and void thickness measured by OM for an untreated sample (left) and a sample treated at 550 °C for 60 min (right)

that the difference in weight change between 5- and 10-min treatment times was more pronounced at lower temperatures. Figure 3 shows optical microscope images used to measure the thickness of the dark coating before and after thermal treatment. The images confirmed the partial removal of the coating after thermal treatment, as the coating is thinner in the treated samples than in the non-treated (untreated) sample. This analysis, performed on the samples treated at 550 °C, showed no significant differences between the treatment durations. The thickness decreased, on average, from an initial 25 µm before thermal treatment to 14 µm. This average was calculated out of 21 measurements, 3 in each sample. Treatments of 5, 10, 20, 30, 40, and 50 min are not shown in Fig. 3 but were included in the averages. It was also possible to observe a void between the aluminum surface and the coating, measuring on average 4 µm for the treated samples.

In both SEM (displayed in [30]) and EPMA images, it was observed that the coating was composed of a polymeric matrix and oxide filler particles. An SEM–EDS point analysis taken in one of the particles revealed a composition of 21.3% wt O, 20.8% wt Ca, 12.3% wt Ti, 4.8% wt Si, and 23.8% wt C. The carbon composition is uncertain in this analysis, but the findings suggest the presence of pigments or filler particles such as TiO_2, CaO, and SiO_2. In addition, the EPMA analysis of the coating before thermal treatment, displayed in Fig. 4, revealed that the coating is composed of higher concentrations of the elements carbon, silicon, oxygen, titanium, barium, and sulfur. The EPMA images are a semi-quantitative color mapping where brighter white, green, and red colors represent a higher concentration than black and blue.

These concentrations did not change after the thermal treatment, except for oxygen and carbon, shown in Fig. 5.

Changes in oxygen and carbon concentrations can be observed already after a 5-min treatment. This is likely

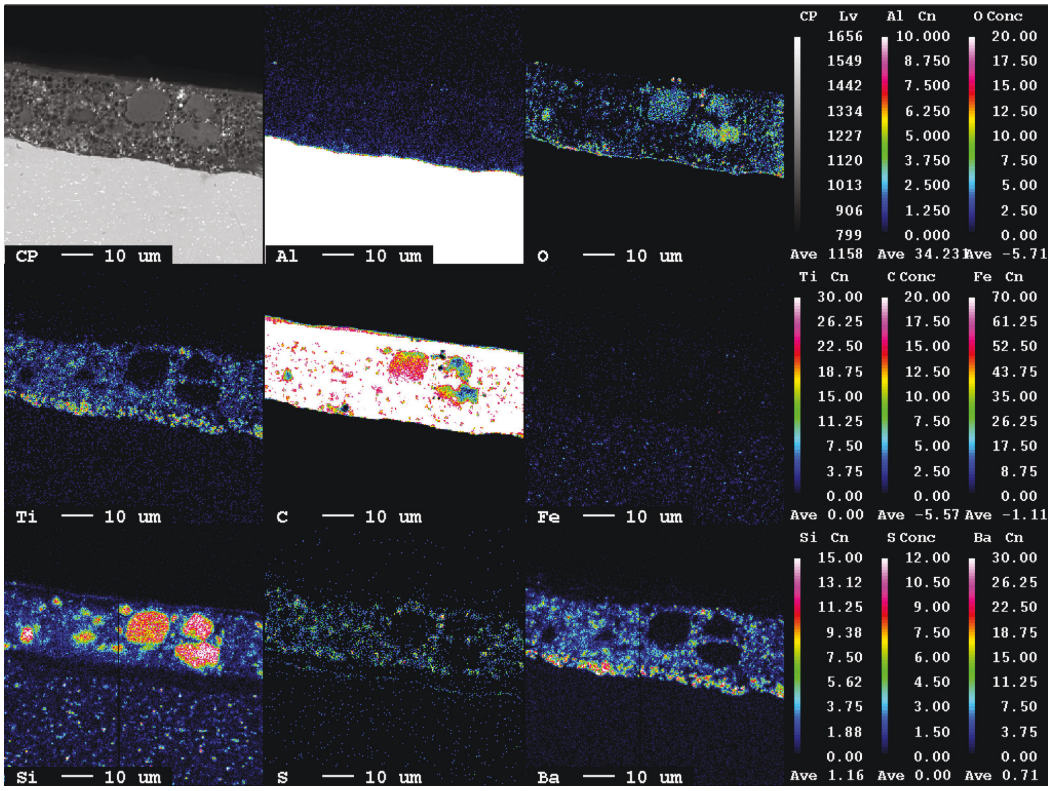

Fig. 4 EPMA analysis of the cross-section of the coated aluminum sheet. The color scale is in % (Color figure online)

related to the release of hydrocarbons or the formation of combustion gas products such as CO or CO_2. Still, after treatments of 60 min, high concentrations of C and O remain, possibly as oxide and carbide residues. Note that the carbon-containing epoxy resin used for sample preparation can affect the results.

An XRD analysis of the powder residue scraped off the samples treated for 5, 10, and 60 min at 550 °C identified the three main phases as $BaSO_4$, TiO_2, and SiO_2. The three analysis gave similar results, and one of the XRD patterns can be found in the supplementary material. $BaSO_4$ and TiO_2 have been previously highlighted as common components in organic coatings of magnesium alloys [31], as well as SiO_2, CaO, and Cr_2O_3 which are sometimes found in both organic and conversion/anodizing coatings. In a recent study, Önen et al. [21] characterized the coatings of several aluminum packaging products (UBCs, coffee capsules, and cosmetic cream tubes) and their thermal de-coating behavior. They observed that for those scraps, containing inner and outer coatings of thicknesses between 5 and 20 µm, a treatment of 500 °C and 15 min was sufficient to remove most of the organics leaving an apparently clean outer surface. However, even if the surface appeared clean after thermal treatment, the study also identified the presence of carbon and titanium residues by XRD analysis. One of the applications of the sheets in the current study is roofing plates, and the coating composition may thus differ from the typical coatings applied to packaging products and subsequently display different residues after thermal treatment.

Combination of Compaction and Thermal Pre-treatments

Thermal De-coating

The uniaxially compacted briquettes lost, on average, the same weight as the loose chips: 1.7% wt, and the weight loss for the MPT briquettes was smaller: 1.5% (out of initial weights of 20 g). Therefore, the results suggest that the uniaxial compaction did not affect the thermal de-coating, while

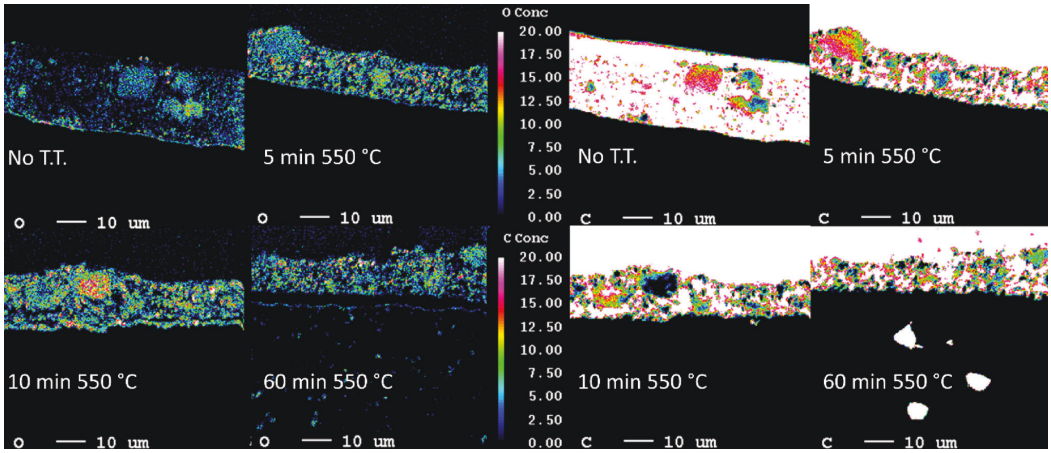

Fig. 5 Change in oxygen (left) and carbon (right) concentration from EPMA analysis. The color scale is in % (Color figure online)

MPT compaction slightly reduced the de-coating efficiency. The fact that the uniaxial compaction, even up to densities of 2 g/cm^3, does not affect the heat-treatment compared to the loose chips opposes some of Steglich's [10] observations, where bales compacted uniaxially to higher densities (1.11 g/cm^3) generated higher dross than those compacted to lower densities (0.69 g/cm^3) which was explained by an incomplete de-coating. Crucial differences in re-melting method (submersion in aluminum melt without salt-flux) and material (UBC post-consumer scrap) may cause the deviating observations. The weight change of the uncoated samples during treatment was also measured in a previous study [30]. All uncoated samples experienced a weight increase lower than 0.02%, which is attributed to oxidation and considered negligible compared to the de-coating weight loss in the coated samples.

Re-melting Coalescence

The material recovered after re-melting showed various degrees of coalescence. Good coalescence leads to most of the re-melted material merging into one round piece. On the contrary, poor coalescence leads to multiple tiny pearls distributed in the salt. A coalescence analysis can be done by comparing the images in Fig. 6a or the average coalescences for the different routes in Fig. 6b. All coalescence results are displayed in Table 3, in the following sub-section, together with the metal yield values.

The surfaces of the metal recovered from the coated, untreated samples appear rougher and darker because of the spontaneous combustion during their re-melting. On the contrary, the re-melted uncoated, and de-coated materials look smooth and shiny. The results prove, in agreement with literature [14, 18], that applying a thermal de-coating pre-treatment greatly improves the coalescence of the coated materials. Regarding the compaction route, thermally de-coating either loose chips or uniaxial briquettes resulted in similar coalescences to those of the uncoated materials. However, the coalescence was lower for the de-coated MPT briquettes. The reason may be that the MPT briquettes are so tightly compacted that oxygen cannot penetrate into the briquette, partly inhibiting the de-coating, as previously suggested by Steglich [32], and consequently, the resulting residues limit the ability of chips to coalesce together as also suggested by Capuzzi [14]. These results are consistent with the previous section. The uncoated material reached almost perfect coalescences regardless of the pre-treatment routes and a slight increase can be observed for the MPT and Hot MPT samples.

Re-melting Metal Yield

Table 3 contains the coalescence and metal yield results for all re-melting experiments. For comparisons between samples with significantly different non-metallic contents, comparing the metal recovery values may be more representative. For the present materials, however, the organic content was less than 2%, and therefore, the difference between metal recovery and metal yield would be approximately 1–2%, as calculated in [30].

The metal yield differences between pre-treatment routes are very small. If only the metal yields were evaluated, all the re-melting results would lie within 94–100%. These results would not explain the apparent differences observed

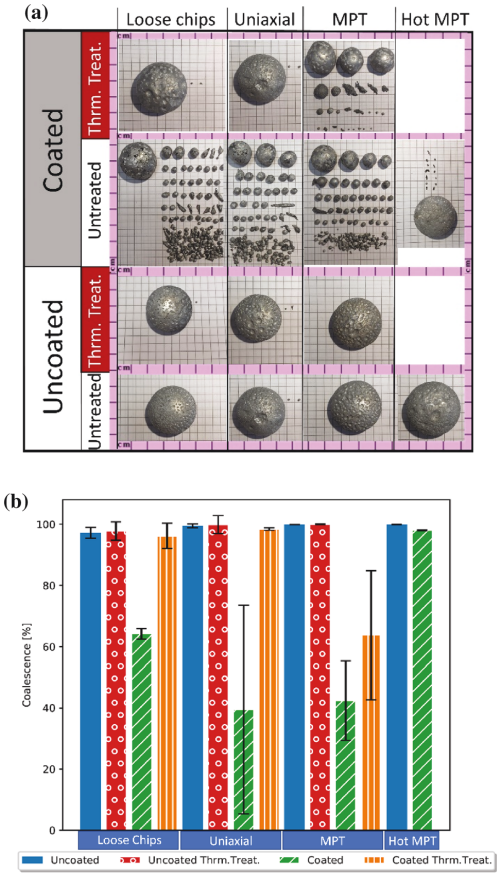

Fig. 6 Left: **a** Example of the recovered metal for each compaction and thermal pre-treatment routes. Right: **b** Average coalescence results for all re-melting experiments. The bars show the standard deviation (2 repetitions for Hot MPT, 3 for the rest)

on the re-melting products obtained via the different pre-treatment routes (Fig. 6a). In contrast, the coalescence variations can become as high as 90% when comparing coated thermally treated or coated untreated samples.

Composition of Recycled Metal

The ICP-MS analysis aimed to evaluate whether the choice of different compaction or thermal pre-treatment routes would affect the composition of the recovered aluminum. Table 4 contains the average results for both coated and uncoated material, and the number of repetitions per sample type is also indicated. For the coated re-melted samples, two had been thermally pre-treated before re-melting and two had not. Out of the three re-melted uncoated samples analyzed, two had been thermally treated, and one had not. Since it was not possible to observe any trend related to the application of the thermal pre-treatment or not, samples were classified by their compaction state. Some concentrations were lower than their detection limits for this analysis, so Li (< 5 ppm), Ca (< 200 ppm), Ba (< 10 ppm), In (< 0.1 ppm, Hg (< 0.04 ppm), Be (< 0.02 ppm) ,and Cd (< 0.03 ppm) are not displayed. For the coated aluminum, this was also the case for the Mg results in 5 samples (< 20 ppm) for two uniaxial briquettes, two MPT briquettes, and the one Hot MPT briquette. Thus, the results of Mg come from only two repetitions for both the uniaxial and MPT briquettes in the coated Al.

For the coated materials, there was a minor increase of some alloying elements after re-melting (Fe, Mn, Cu, Cr, and Mg), which is lower for the more compacted samples than for the loose samples. However, the standard deviations are larger than the differences between sample types and hence no firm conclusion may be drawn as to whether the inorganic coating residues contaminate the aluminum melt during re-melting with salt-flux. The Ti accumulation

Table 3 Coalescence (C) and metal yield (Y) results

Compaction	Loose chips				Uniaxial				MPT				Hot MPT	
Therm. Tr	No		Yes		No		Yes		No		Yes		No	
result	C	Y	C	Y	C	Y	C	Y	C	Y	C	Y	C	Y
Uncoated	95	95	94	94	100	100	103	103	100	100	100	100	100	100
Uncoated	98	98	100	100	100	100	100	100	100	100	100	100	100	100
Uncoated	99	99	100	100	99	99	96	96	100	100	100	100	–	
Average	97	97	98	98	99	100	100	100	100	100	100	100	100	
Std. dev	1.7	1.6	3.0	3.0	0.6	0.6	3.0	3.0	0.0	0.0	0.1	0.1	0.0	
Coated	65	96	90	100	85	95	98	98	29	96	62	97	98	98
Coated	62	94	99	99	3	96	99	99	60	96	91	95	98	98
Coated	66	97	99	99	30	94	99	99	39	96	39	96	–	
Average	64	96	96	99	40	95	98	98	42	96	64	96	98	
Std. dev	1.8	1.3	4.0	0.4	34.0	1.1	0.4	0.4	13.0	0.1	21.0	0.6	0.1	

Table 4 Averages and standard deviation of the 29 composition analyses by ICP-MS

	Coated aluminum					Uncoated aluminum				
Re-melted	No	Yes				No	Yes			
Sample	Sheet	Loose chips	Uniaxial briquettes	MPT briquettes	Hot MPT briquette	Sheet	Loose chips	Uniaxial briquettes	MPT briquettes	Hot MPT briquette
Nr. rep	3	4	4	4	1	3	3	3	3	1
Al (wt%)	96.87 ± 0.94	99.10 ± 0.80	99.13 ± 0.71	97.02 ± 0.65	96.00	98.10 ± 1.56	98.43 ± 0.95	98.1 ± 2.33	98.10 ± 0.83	99.50
Fe (%)	0.75 ± 0.01	0.80 ± 0.05	0.78 ± 0.03	0.76 ± 0.02	0.76	0.81 ± 0.01	0.83 ± 0.01	0.82 ± 0.03	0.83 ± 0.01	0.85
Si (%)	0.23 ± 0.03	0.23 ± 0.02	0.21 ± 0.02	0.21 ± 0.02	0.21	0.23 ± 0.02	0.16 ± 0.00	0.15 ± 0.01	0.15 ± 0.01	0.15
B (ppm)	7.30 ± 0.23	8.58 ± 4.80	6.81 ± 1.06	5.55 ± 0.75	2.35	4.78 ± 0.13	4.47 ± 0.41	4.19 ± 0.14	3.69 ± 0.29	3.41
Cd (ppm)	0.02 ± 0.00	0.10 ± 0.07	0.17 ± 0.08	0.10 ± 0.06	< 0.03	0.10 ± 0.01	0.15 ± 0.01	0.27 ± 0.11	0.19 ± 0.10	0.123
Co (ppm)	1.82 ± 0.04	1.92 ± 0.10	1.91 ± 0.07	1.77 ± 0.04	1.76	2.86 ± 0.07	2.83 ± 0.07	2.74 ± 0.06	2.84 ± 0.11	2.78
Cr (ppm)	7.78 ± 0.17	17.93 ± 3.19	15.58 ± 3.45	14.85 ± 4.24	8.56	15.60 ± 0.16	19.33 ± 4.67	17.73 ± 2.47	18.27 ± 0.87	19
Cu (ppm)	10.93 ± 0.40	32.43 ± 8.29	25.80 ± 4.27	22.50 ± 6.67	14.5	340.00 ± 6.38	348.00 ± 12.75	339.33 ± 4.11	354.67 ± 16.21	372
Ga (ppm)	114.00 ± 1.41	113.00 ± 6.04	111.75 ± 5.31	109.00 ± 6.75	103	106.33 ± 1.70	106.07 ± 6.09	103.30 ± 5.95	106.67 ± 4.03	98.8
Mg (ppm)	6.90 ± 0.16	16.09 ± 6.90	15.05 ± 3.55	13.15 ± 1.35	< 20	404.00 ± 5.35	131.00 ± 27.80	234.33 ± 48.61	267.00 ± 28.33	251
Mn (ppm)	26.63 ± 0.49	34.78 ± 2.40	32.25 ± 1.44	30.45 ± 2.21	29.2	366.00 ± 6.16	376.67 ± 3.09	367.00 ± 1.63	370.00 ± 1.41	383
Ni (ppm)	39.80 ± 0.22	42.50 ± 3.53	40.68 ± 1.99	38.53 ± 1.23	39.9	30.20 ± 0.94	31.93 ± 1.31	30.77 ± 0.66	31.40 ± 2.08	32.3
P (ppm)	3.64 ± 0.41	2.01 ± 0.20	3.15 ± 1.47	3.00 ± 0.59	2.54	1.93 ± 0.11	1.66 ± 0.22	2.93 ± 1.42	2.35 ± 0.86	2.19
Pb (ppm)	9.53 ± 0.13	10.59 ± 1.05	9.67 ± 0.33	9.29 ± 0.27	9.99	14.43 ± 0.12	14.87 ± 0.47	15.03 ± 0.05	15.03 ± 0.58	15.4
Sn (ppm)	1.93 ± 0.01	2.59 ± 0.74	2.04 ± 0.06	1.94 ± 0.07	1.94	2.45 ± 0.50	8.90 ± 7.92	3.35 ± 0.14	3.24 ± 0.11	3.44
Sr (ppm)	0.15 ± 0.01	0.59 ± 0.71	0.36 ± 0.21	0.16 ± 0.05	0.16	0.28 ± 0.08	0.74 ± 0.00	0.21 ± 0.13	0.10 ± 0.02	0.211
Ti (ppm)	99.37 ± 1.16	102.48 ± 4.54	101.10 ± 7.75	99.65 ± 1.93	105	53.03 ± 1.62	57.53 ± 3.74	56.70 ± 2.27	53.33 ± 0.69	56.5
V (ppm)	83.77 ± 1.87	82.90 ± 7.27	82.83 ± 4.94	84.70 ± 1.86	86	207.67 ± 0.94	212.00 ± 2.16	219.33 ± 4.19	213.00 ± 2.16	211
Zn (ppm)	22.50 ± 1.84	24.58 ± 1.41	25.60 ± 2.41	24.28 ± 2.05	23.5	74.40 ± 2.48	79.60 ± 2.84	79.43 ± 1.76	77.53 ± 3.90	80.6
Zr (ppm)	15.83 ± 0.40	17.88 ± 1.43	18.13 ± 1.75	18.35 ± 2.09	20.6	6.82 ± 0.27	7.33 ± 0.55	7.56 ± 0.76	7.65 ± 0.83	8.77

observed by Oosumi in UBC re-meltings without salt-flux [26] could not be replicated.

For the uncoated material, Fig. 7 shows the normalized concentration differences, calculated by subtracting the average concentration of each re-melted sample group from the average of the original sheets, and dividing it by the concentration of the original sheets. Decreases in specific elements after re-melting could indicate their removal from the melt due to reaction with the molten salt-flux.

If the initial concentrations were very low, increases of just a few ppm would stand out in the normalized comparison. Therefore, elements of concentrations lower than 10 ppm were not included in the graph. Figure 7 shows that Mg decreases during re-melting of the uncoated samples and that the Mg loss can be reduced by compacting the material. Figure 7 also shows a consistent decrease in the Si concentration after re-melting, regardless of the compaction. As for the rest of the results, the slight increases observed cannot be explained by the contamination from the coating since these samples were not coated. Furthermore, by looking again at Table 4, the standard deviations between the samples are of the same magnitude as the difference between samples.

In conclusion, the most significant result is that compaction leads to lower Mg reduction. This is supported by Hiraki's [25] thermodynamic analysis, showing the tendency of Mg to be refined from aluminum secondary melts by reaction with the salt-flux. The results suggest that by compacting the loose chips, the surface area exposed to the salt-flux is reduced, and as a result, Mg loss is partially prevented. The influence of compaction in the removal of Mg during salt-flux re-melting was also observed in [33]. Mg loss is a challenge during industrial re-melting operations, and the effect of compacting clean, Mg containing scrap, or even the Mg chips added during re-melting operations should be explored at a larger scale.

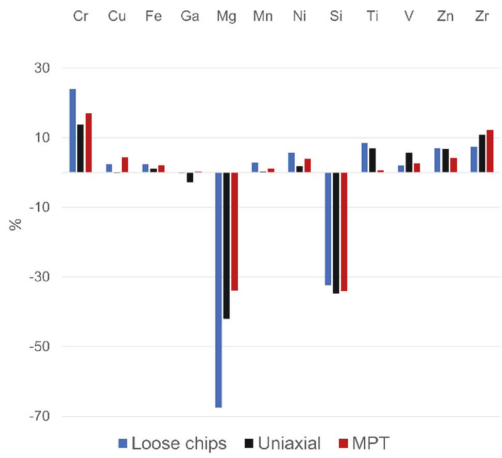

Fig. 7 Normalized concentration changes for the uncoated samples

Conclusions

The current work has investigated the interaction between the compaction and thermal de-coating pre-treatments for coated and uncoated aluminum. The performance of thermal de-coating and re-melting in salt-flux was assessed in terms of recycling metal yield, coalescence, and composition, leading to the following conclusions:

- Observations of changes in coating thickness, mass, color, and composition revealed a maximum de-coating efficiency of close to 75% wt, achieved after 20 min of treatment at 550 °C.
- The thermal de-coating was not affected by compacting the briquettes uniaxially (1.9 g/cm^3 density), but MPT compaction (2.2 g/cm^3 density) decreased the de-coating efficiency.
- The coalescence of the coated samples significantly improved due to the thermal de-coating similarly for the loose chips and uniaxially compacted briquettes (over 95%), but to a lower extent for the MPT compacted briquettes (64%).
- All metals yield results ranged between 94 and 100% for the different pre-treatment routes.
- Oxide residues (Ti, Si, S, Ba) remained attached to the material after thermal de-coating but were not associated with an increase in impurity concentration in the re-melted metal.
- Compaction may reduce Mg losses during salt-flux re-melting.

Supplementary Information The online version contains supplementary material available at https://doi.org/10.1007/s40831-022-00612-x.

Acknowledgements The authors would like to gratefully acknowledge the Research Council of Norway and the partners of *Alpakka—Circular Aluminium Packaging in Norway* (NFR Project nr. 296276) for funding the project, Speira Holmestrand for the materials, and the Department of Materials Science and Engineering at NTNU, Trondheim, for the experimental equipment and support. On behalf of all authors, the corresponding author states that there is no conflict of interest.

Funding Open access funding provided by NTNU Norwegian University of Science and Technology (incl St. Olavs Hospital - Trondheim University Hospital).

References

1. Capuzzi S, Timelli SG (2018) Preparation and melting of scrap in aluminum recycling: a review. Metals 8(4):249. https://doi.org/10.3390/met8040249
2. van Schaik A, Reuter M (2014) Material-centric (aluminum and copper) and product-centric (cars, WEEE, TV, lamps, batteries, catalysts) recycling and DfR rules. In: Worrel E, Reuter M (eds) Handbook of recycling: state-of-the-art for practitiones, analyst and scientists. Elsevier, Amsterdam
3. Kvithyld A, Meskers C, Gaal S, Reuter M, Engh T (2008) Recycling light metals: optimal thermal de-coating. JOM 60:47–51. https://doi.org/10.1007/s11837-008-0107-y
4. Vallejo-Olivares A, Philipson H, Gökelma M, Roven HJ, Furu T, Kvithyld A, Tranell G (2021) Compaction of aluminium foil and its effect on oxidation and recycling yield. In: Perander L (ed) Light metals 2021. Springer, Cham
5. Rossel H (1990) Fundamental investigations about metal loss during remelting of extrusion and rolling fabrication scrap. In: Bickert CM (ed) Light metals 1990. Springer, Cham, pp 721–729
6. Peterson RD (1995) Issues in the melting and reclamation of aluminum scrap. JOM 47(2):27–29. https://doi.org/10.1007/BF03221402
7. Schmitz CJ (2014) Handbook of aluminium recycling: mechanical preparation, metallurgical processing, heat treatment. Vulkan-Verlag GmbH, Essen
8. Steglich J, Buchholz A, Aluminium H, Dittrich R, Friedrich B (2015) Conductive heat transfer in used beverage can scrap. In: Proceedings advances in materials & processing technologies, Madrid December 2015
9. Wells PA, Peterson RD (1990) Transient three-dimensional briquette preheater model. In: van Linden J, Stewart D, Sahai Y (eds) Proc. Second international symposium - reclying metals and engineered materials, Springer, Cham, pp 221–236
10. Steglich J, Friedrich B, Rosefort M (2020) Dross formation in aluminum melts during the charging of beverage can scrap bales with different densities using various thermal pretreatments. JOM 72:3383–3392. https://doi.org/10.1007/s11837-020-04268-4
11. Boin U, Reuter MA, Probst T (2004) Measuring - modelling: understanding the Al scrap melting processes inside a rotary furnace. World Metall ERZMETALL 57(5):266–271
12. Zhou B, Yang Y, Reuter MA, Boin UMJ (2006) Modelling of aluminium scrap melting in a rotary furnace. Miner Eng 19:299–308. https://doi.org/10.1016/j.mineng.2005.07.017
13. Capuzzi S, Timelli G, Capra L, Romano L (2019) Study of fluxing in Al refining process by rotary and crucible furnaces. Int J Sustain Eng 12(1):38–46. https://doi.org/10.1080/19397038.2017.1393022
14. Capuzzi S, Kvithyld A, Timelli G, Nordmark A, Gumbmann E, Engh TA (2018) Coalescence of clean, coated, and decoated aluminum for various salts, and salt-scrap ratios. J Sustain Metall 4:343–358. https://doi.org/10.1007/s40831-018-0176-2S
15. Thoraval DM, Friedrich B (2015) Metal entrapment in slag during the aluminium recycling process in tilting rotary furnace. In: Proceedings of EMC 2015, pp 359–367. https://doi.org/10.13140/RG.2.1.3436.8887
16. Xiao Y, Reuter MA, Boin U (2005) Aluminium recycling and environmental issues of salt slag treatment. J Environ Sci Heal 40(10):1861–1875. https://doi.org/10.1080/10934520500183824
17. Xiao Y, Reuter MA (2002) Recycling of distributed aluminium turning scrap. Miner Eng 15(11):963–970. https://doi.org/10.1016/S0892-6875(02)00137-1
18. Gökelma M, Diaz F, Öner IE, Friedrich B, Tranell G (2020) An assessment of recyclability of used aluminium coffee capsules. In: Tomsett A (ed) Light metals 2020. Springer, Cham
19. Wang M, Do Woo K, Kim DK, Ma L (2007) Study on de-coating used beverage cans with thick sulfuric acid for recycle. Energy Convers Manag 48(3):819–825. https://doi.org/10.1016/j.enconman.2006.09.008
20. Li N, Qiu K (2013) Study on delacquer used beverage cans by vacuum pyrolysis for recycle. Environ Sci Technol 47(20):11734–11738. https://doi.org/10.1021/es4022552
21. Önen R, Gökelma M (2022) Characteristics and behaviuor of coated aluminium scraps during thermal pre-treatment. In: Proceedings of ALUS 10th international aluminium symposium, pp 2016–210
22. Meskers C, Reuter M, Boin U, Kvithyld A (2008) A fundamental metric for metal recycling applied to coated magnesium. Metall Mater Trans B 39:500–517. https://doi.org/10.1007/s11663-008-9144-8
23. Meskers C, Xiao Y, Boom R, Boin U, Reuter M (2007) Evaluation of the recycling of coated magnesium using exergy analysis. Miner Eng 20(9):913–925. https://doi.org/10.1016/j.mineng.2007.02.006
24. Rombach G (2000) Verhalten mineralischer Pigmente beim Aluminiumrecycling. World Metall - Erzmetall 2(53):98–104
25. Hiraki T, Miki T, Nakajima K, Matsubae K, Nakamura S, Nagasaka T (2014) Thermodynamic analysis for the refining ability of salt flux for aluminum recycling. Materials (Basel) 7(8):5543–5553. https://doi.org/10.3390/ma7085543
26. Oosumi K (1994) Influence of paint on recycling of aluminum used beverage cans. In: Symposium K: environment conscious materials of the 3rd IUMRS international conference on advanced materials 1993, pp 197–200, https://doi.org/10.1016/B978-1-4832-8381-4.50051-2
27. Løvik NA, Müller DB (2014) A material flow model for impurity accumulation in beverage can recycling systems. In: Grandfield J (ed) Light metals 2014. Springer, Cham
28. Castro M, Remmerswaal J, Reuter M, Boin U (2004) A thermodynamic approach to the compatibility of materials combinations for recycling. Resour Conserv Recycl 43(1):1–19. https://doi.org/10.1016/j.resconrec.2004.04.011
29. Reuter MA, Van Schaik A, Gutzmer J, Bartie N, Abadías-Llamas A (2019) Challenges of the circular economy: a material, metallurgical, and product design perspective. Annu Rev Mater Res 49:253–274. https://doi.org/10.1146/annurev-matsci-070218-010057
30. Vallejo-Olivares A, Høgåsen S, Kvithyld A, Tranell G (2022) Effect of compaction and thermal de-coating pre-treatments on the recyclability of coated and uncoated aluminium. In: Eskin D (ed) Light metals 2022. Springer, Cham
31. Meskers CM (2008) Coated magnesium - designed for sustainability? PhD Thesis. ISBN: 978-9-064643-05-7
32. Steglich J, Dittrich R, Rombach G, Rosefort M, Friedrich B, Pichat A (2017) Dross formation mechanisms of thermally pretreated used beverage can scrap bales with different density, pp 1105–1113
33. Amini Mashhadi H, Moloodi A, Golestanipour M, Karimi EZV (2008) Recycling of aluminium alloy turning scrap via cold pressing and melting with salt flux. J Mater Process Technol

209(7):3138–3142. https://doi.org/10.1016/j.jmatprotec.2008.07.020

Article E

Journal of Sustainable Metallurgy
https://doi.org/10.1007/s40831-023-00773-3

RESEARCH ARTICLE

Effects of Compaction and Thermal Pre-treatments on Generation of Dross and Off-Gases in Aluminium Recycling

Alicia Vallejo-Olivares[1] · Tom Gertjegerdes[2] · Solveig Høgåsen[1] · Bernd Friedrich[2] · Gabriella Tranell[1]

Received: 11 August 2023 / Accepted: 25 November 2023

Abstract
Organic coatings are a challenge for aluminium packaging recycling since they tend to increase the re-melting metal losses. A solution is de-coating the scrap via a thermal pre-treatment to burn-off the organics before re-melting. Due to logistic benefits, the scrap is often pressed into bales. This study evaluates the influence of compaction on the de-coating efficiency and off-gas emissions, and its consequences for dross formation and recycling metal yield. Loose chips and two types of briquettes, one loosely compacted by uniaxial pressure and the other compacted by moderated-pressure-torsion to higher densities, were heated to 550 °C while analysing the off-gas emissions using FTIR. The briquettes were subsequently re-melted into a molten heel. Re-melting coated scrap multiplied the % wt of dross by a factor of 2 or 3, depending on the compaction pre-treatment, compared to re-melting uncoated aluminium. The densest briquettes emitted less than half the CO_2 and CO gases during de-coating and formed significantly more dross. Compaction to the lower densities showed no tangible effects. The effect of de-coating compacted materials or not was small ($\pm 2\%$ wt dross), which was attributed to carbonaceous residues remaining after the thermal treatment. In conclusion, high compactions by torsion limit the de-coating reactions, which depend on factors such as temperature and gas transport. A complete removal of the organic residues is critical for a more sustainable recycling with less dross generated.

The contributing editor for this article was Markus Reuter.

✉ Alicia Vallejo-Olivares
Alicia.v.olivares@ntnu.no

Tom Gertjegerdes
TGertjegerdes@metallurgie.rwth-aachen.de

Bernd Friedrich
BFriedrich@metallurgie.rwth-aachen.de

Gabriella Tranell
Gabriella.tranell@ntnu.no

[1] Department of Materials Science and Engineering, Norwegian University of Science and Technology, Alfred Getz Vei 2, 7018 Trondheim, Norway

[2] Department of Process Metallurgy and Metal Recycling, RWTH Aachen University, Intzestraße 3, 52072 Aachen, Germany

Published online: 12 December 2023

Graphical Abstract

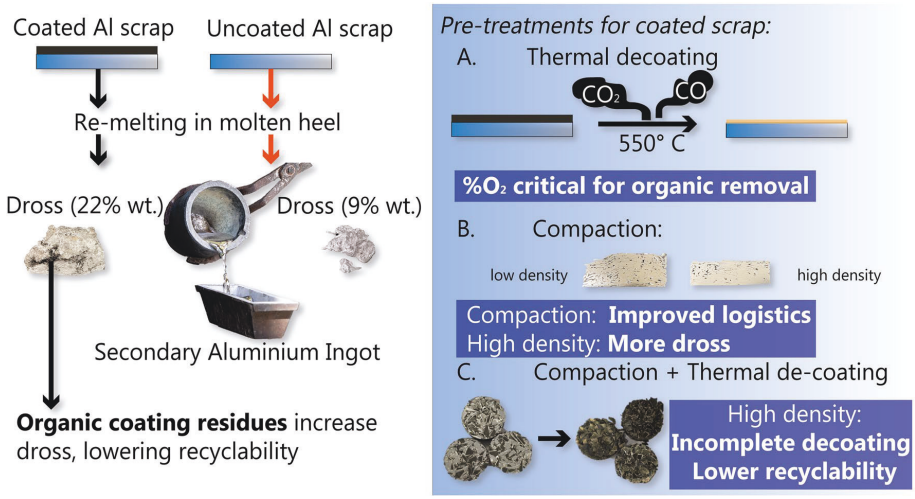

Keywords Aluminium · Recycling · Coating · Dross · Compaction · De-coating

Introduction

Efficient and sustainable recycling processes are critical to meet the increasing demand for aluminium while lowering production costs and environmental impacts. Recycling aluminium is less energy-intensive than primary production, which is one of the main reasons behind its associated lower emissions and environmental impacts [1]. The energy required to produce 1 tonne of secondary aluminium, based on European data, can vary between 2 and 9 GJ [2]. Damgaard [3] reported that recycling 1 tonne of aluminium-containing scrap and using the secondary metal produced to substitute primary aluminium saves between 5 and 19 tonne CO_2 equivalent of global warming contributions. These variations in energy efficiency and emissions of the secondary route depend on the energy sources, the type and quality of the scrap and the consequent choice of pre-treatment, re-melting and refining processes.

In 2019, the International Aluminium Association registered a record global intake of post-consumer scrap for recycling of 20 million tonnes. The heaviest proportion, 5.3 million tonnes, was used packaging [4]. The main drivers of recycling packaging are their short lifetimes and the valuable wrought alloys they are made of. However, recycling thin sheet packaging materials can be complex due to their high surface-to-mass ratio and the presence of organic residues, coatings, and labels [5]. Thin shapes are more exposed to the atmosphere and oxidized during high-temperature processes, as demonstrated in [6, 7] for aluminium fabrication scrap and [8] for incineration bottom ash. Additionally, larger surface areas imply having more coatings, labels, and other surface-contaminants, which increase the aluminium losses and off-gas emissions during its re-melting. The aluminium losses are induced by reactions between the contaminants and the melt, forming oxides, sulphides (e.g., Al_2S_3) or carbides (e.g., Al_4C_3) [9].

Mixing oxidized or contaminated scrap with salts in rotary furnaces is a common practice, since the salt-flux protects the metal from oxidation and separates it from the non-metallic contaminants [10, 11]. However, using salts leads to salt slag residue, a toxic hazardous waste [12]. In contrast, salt-free re-melting processes require cleaner scrap and generate dross—a mix of oxides and entrapped Al—as residue, which is then recycled in rotary furnaces with salts, although alternative processes have been proposed [13]. Producing 1 tonne of secondary Al can generate up to 500 kg salt slag if re-melting in a rotary furnace with salt-fluxes or up to 80 kg dross if re-melting in a closed well furnace [2]. Decreasing the dross and salt slag residue quantities would be highly beneficial for the costs and environmental impacts of recycling. The presence of organic contamination on the scrap, as shown in [6, 14, 15], has a significant impact.

Preconditioning the scrap with a thermal treatment is an established method which makes it possible to re-melt initially dirty scrap without salts, described by e.g. in [16].

The thermal pre-treatment aims to remove as much moisture and organic contamination as possible without oxidizing the metal. According to the European Aluminium Scrap Standard EN 13920 coated packaging contains 71.5% metal, significantly less than the 86.1% of de-coated packaging [17], since most of the organics and volatiles (moisture, food residues, coatings and labels) are removed by the de-coating treatment. The thermal treatment also reduces the risks of health and safety hazards during re-melting, such as the generation of toxic, poisonous, or combustible gases (H_2S, PH_3, H_2 and CH_4) [9, 18]. Moreover, in salt-recycling processes, de-coating promotes the coalescence of the metal droplets, potentially reducing the amount of metal entrapped in the salt slag residue [19–21]. However, the volatile organic compounds (VOC's) and other gases generated during the thermal de-coating pre-treatments can also pose health, safety and environmental risks and must be handled adequately, e.g. through afterburner and off-gas treatment, as discussed by Bateman [22]. The organic gases developed during de-coating or re-melting can also be utilised in several ways to improve the process energy efficiency [23].

A typical thermal de-coating of aluminium scrap can be divided into two phases. When the material is exposed to a sufficiently high temperature (above 250 °C), rapid decomposition of the organic molecules takes place (cracking). This releases volatile components such as short-chain hydrocarbons. The decomposition leaves a carbon-rich residue, which is gasified in the second stage, provided there is oxygen as a reaction partner in the gas atmosphere [24, 25]. To secure a complete removal of the organics during de-coating, the process parameters (temperature, atmosphere, duration) must be carefully controlled. Studies showed that treatments under inert gas-atmospheres and low temperatures can leave pyrolysis residues [26] which lead to re-melting losses by increasing the amount of dross generated in salt-free processes [25] or by lowering the coalescence of aluminium droplets and thus increasing the amount of aluminium entrapped in the salt slag residues when recycling in rotary furnaces [19]. On the other hand, using higher temperatures and O_2-rich atmospheres increases the risk of oxidizing the scrap.

Pre-conditioning scrap by compaction into bales or briquettes can benefit recycling by facilitating transport, storage and charging operations. Research has also shown that compacting clean, dry aluminium swarf [27, 28] into briquettes increases its recycling efficiency in a salt-free process. Furthermore, briquetting thin aluminium foil can prevent high-temperature-oxidation and the consequent entrapment of small beads by the salt residues [29]. The benefits of compaction could be explained by, depending on the process, the reduction of the surface area exposed to oxidation, the higher density allowing the scrap to sink into the melt, or the enhanced metal–metal contact. However, for contaminated scrap, compacting may sometimes have negative consequences. A previous study showed that pressing coated aluminium chips into briquettes of low densities did not affect its recycling in salts. However, compacting to higher densities by the moderate-pressure torsion (MPT) method limited the de-coating efficiency and metal coalescence [21]. Steglich [25] re-melted used beverage cans (UBCs) without salt-flux and concluded that a thermal de-coating would reduce dross if conditions for stoichiometric thermolysis were applied for at least 30 min at 550–570 °C. The concept of stoichiometric thermolysis means that the exact amount of oxygen needed to react with the organics present is provided throughout the treatment. Steglich's investigations argue that if conditions are not met, the char residues remaining when the total oxygen supply is too low (sub-stoichiometric conditions) or the oxidized aluminium due to too much oxygen (over-stoichiometric conditions) may lead to more dross and metal losses. One of the challenges of this approach is that it requires knowing the amount and composition of the organics present. In addition, the results suggested that the compaction state of the scrap also plays a role on the de-coating efficiency, being lower bale densities beneficial. Chamakos [30] thermally treated bundles of UBC bales and measured large differences between the temperature at the surface and centre of the bales as well as lower de-coating degrees inside, indicating that compaction may hinder de-coating by limiting heat transfer. Steglich and Chamakos investigated the recycling of UBCs, made of alloys with higher concentrations of Mg, which makes them more susceptible to oxidation, as demonstrated by Rossel [7].

The main contributions to knowledge in aluminium recycling by the current study is the detailed characterization of the de-coating off-gases during the thermal pre-treatment in different compaction states, and the consequences that the different thermal and compaction pre-treatment combinations can have on metal losses when re-melting without salts. The present study uses sheets of an alloy low in Mg, as it is the case for packaging materials as foils, laminated materials or flexible tubes, made of 8XXX and 1XXX alloys [31]. The stoichiometric thermolysis hypothesis proposed by Steglich [25] was used to test whether this estimate would give the optimal de-coating parameters.

Materials and Method

Materials

The materials were two coils of aluminium sheet AA8111 alloy with a thickness of 600 µm; one bare (uncoated) and one coated. The heel used in the re-melting experiments was of the same alloy. These sheets were fabricated to be used for roofing and they were chosen due to its low Mg content,

which allows omitting the effect of Mg on oxidation metal losses during the de-coating and re-melting processes. The composition of the material's production batches are provided in Table 2 in the Appendix. By using as-produced coated sheets instead of scrap, it was possible to isolate the influence that the coating and coating residues have for recycling from other contaminants, e.g., oil or food residues. The coating was dark grey and thicker (ca. 25 µm) on one side, light grey and thinner (5 µm) on the other. A preceding study [21] revealed that 75% wt of the coating (equal to 1.7 wt% of the sheet weight) was removable by a thermal treatment of 20 min at 550 °C under air. The residual 25% wt were oxides ($BaSO_4$, TiO_2 and SiO_2) loosely adhered.

Shredding and Compaction Pre-treatment

The sheets were first shredded into chips, and then sieved with two square mesh sieves of 2 and 5 mm^2. A subset of the chips was compacted into cylindrical briquettes of 4 cm diameter, each weighing 50 g, using a hydraulic press MTS 311. A subset was compacted by applying a uniaxial force of 100 kN for 5 s. Another subset was compacted by moderate-pressure-torsion (MPT), applying a compression load of 100 kN for 200 s while rotating the mould 4 times (speed of 1.2 rpm). The average density of the briquettes after compaction was 2.04 ± 0.04 g/cm^3 for the uniaxial method and 2.22 ± 0.08 g/cm^3 for the MPT method (just below the liquid Al density of 2.3 g/cm^3). The height of the uniaxial briquettes was 1.96 ± 0.03 and of the MPT briquettes 1.80 ± 0.08 cm. Table 1 shows the experimental matrix of the materials and pre-treatment combinations.

Thermal De-coating Pre-treatment: Off-Gas Emissions

The samples were thermally treated in batches of 500 g inside a closed induction furnace connected to a Gasmet FTIR analyser. The heating rate was 350 °C/h and the temperature was held for 30 min at the top temperature of 550 °C. Since excess oxygen could lead to combustion and oxidation of the aluminium, the flow gas amount and composition were targeted to reach stoichiometric thermolysis conditions. The oxygen was calculated so that the hydrocarbon compounds contained in the organic matter would be converted to CO_2 and CO in a ratio of 2:1. The gas mix with 5% O_2 and 95% inert gas (N_2) was set at a flow of 3 L/min after flushing the chamber with N_2 at 180 °C. In the calculations it was assumed that the samples contained 2% wt organics and that the composition was 50% epoxy and 50% polyester, which would begin decomposing at 250 °C following Eqs. 1 and 2 respectively for 1 h and 22 min. These assumptions were based on the literature [32] and on a previous study [21] since the supplier did not provide information on the coating composition due to commercial considerations.

$$C_{21}H_{24}O_5 + 21O_2 \rightarrow 14CO_2 + 7CO + 12H_2O \quad (1)$$

$$C_8H_6O_4 + 6O_2 \rightarrow 5CO_2 + 3CO + 3H_2O \quad (2)$$

The top of the furnace chamber was water-cooled, and the outlet gas pipes had filters for particles larger than 1 µm, which were washed with ethanol between trials. The excess gas which was not analysed by the FTIR was connected to a scrubbing system and the residue collected in the outlet gas filters were analysed by gas chromatography and mass spectrometry (GS/MS).

Table 1 Experimental matrix of the pre-treatment routes (three repetitions for each)

Material	Compaction	Thermal de-coating
Uncoated	No (loose chips)	No
Coated	No (loose chips)	No
Coated	Low (uniaxial)	No
Coated	High (MPT)	No
Coated	No (loose chips)	Yes
Coated	Low (uniaxial)	Yes
Coated	High (MPT)	Yes

Re-melting in Molten Heel: Dross Formation

The re-melting trials were conducted in an induction furnace operating at 2.5–3 kHz. The temperature was measured by a thermocouple placed inside the melt, and the melt was flushed with argon introduced to the hood at 10 L/min. First, the crucible with approximately 1 kg of aluminium heel was heated to 780 °C. Then the furnace was turned-off to skim the dross using a slotted spoon. The chips/briquettes (1 kg) were gradually charged into the melt at 750 °C using a small scoop. The power input to the induction furnace was adjusted to keep the temperature stable. Charging times ranged between 6 and 12 min. For the coated materials which had not been thermally pre-treated, the smoke arising from the combustion of the coating impeded the process, and the furnace power had to be turned off a few times to stir and sink the samples into the melt. After charging the melt was stirred again, and the temperature was raised to 780 °C before skimming the dross. Finally, the metal was cast at 750 °C. Once cold, the dross and the cast ingots were weighted to calculate the percentage of dross formation during re-melting (Eq. 3) and the metal yield (Eq. 4). For the first nine re-melting trials, the average weight of the dross skimmed-off the heel was $18.5\ g \pm 2.9$ ($1.73\% \pm 0.26$ of its weight), and the Al casting residues remaining in the crucible weighed 15.0 ± 1.8 g. Both were considered negligible for the calculations.

$$Dross[\%] = \frac{Wt.Dross}{Wt.Scrap\ charged} * 100 \quad (3)$$

$$Metal\ Yield[\%] = \frac{Wt.\ cast\ ingots}{Wt.of\ Scrap\ charged + Wt.heel} * 100 \quad (4)$$

Dross Re-melting in Salt-Flux: Dross Metal Content

The dross was re-melted in a resistance furnace. The salt-flux/dross ratio was 2:1 so that the dross would be completely submerged in the salt-flux, and the dross was sawed into pieces so that it would fit the crucible. First, the crucible filled with the mixed salts (68.6 wt% NaCl, 29.4 wt% KCl and 2 wt% CaF_2, purchased separately and mixed before each trial) was placed inside the furnace at 800 °C. Once the salt was molten (after approximately 30 min) the dross was charged in two batches separated by 5 min. Manual stirring was applied during 5 s using a graphite stick, and the temperature was held for 10 min more after the second charge. The molten metal and salts were subsequently cast into a copper mould. The salts were washed away with water and the recovered metal weighed. The metal content of the dross was calculated using Eq. 5 and the total recycling yield with Eq. 6:

$$Dross\ metal\ content[\%] = \frac{Metal\ recovered}{wt.dross\ charged\ to\ salt} \quad (5)$$

$$Total\ Metal\ Yield[\%] = \frac{(wt.scrap(g) - wt.dross(g)) + (dross\ metal\ content(\%) * wt.dross(g))}{wt.scrap(g)} \quad (6)$$

Dross Characterization Methods

Pieces of dross were polished and examined using Scanning Electron Microscope and Electron Probe Micro Analysis (SEM-EPMA). This allows distinguishing the phases and identifying some of the elements present. The equipment was a JEOL JXA-6500F Field Emission Electron Probe Micro-analyzer. A small piece of the metal recovered from the dross re-melting, weighing approximately 1 g, was sent to ALS Scandinavia for ICP-MS trace element analysis.

Results and Discussion

Thermal Treatment

Figure 1 shows pictures of the chips and uniaxial briquettes before and after the thermal treatment. According to a prior study on the same material [21], a light brown/yellow colour is characteristic of the oxide residues remaining after a complete de-coating, while darker colours reveal the presence of carbonaceous residues.

For brevity in the discussion of the results, often when referring to the materials and briquettes tested, their names will be shortened to loose, uniaxial and MPT. The weight of the loose aluminium chips decreased after the thermal treatment by 1.51% ± 0.04, 1.43% for the uniaxial briquettes and 1.32% for the MPT briquettes. These values are the average and standard deviation of 2 trials for the chips, and the results of one trial for each of the briquette types. Based on the weight changes and the colour of the coating before and after the treatment, the uniaxially-compacted briquettes experienced a lower degree of de-coating than the loose chips, and the torsion-compacted briquettes (MPT) had the least degree of de-coating of the three compaction methods. This can be explained by the lower surface area and lower internal porosity of the MPT briquettes, limiting gas transport and the contact between oxygen and organics. A yellow/brown residue was condensed in the furnace lid and the filters of the outlet pipes. This was sent for GC/MS analysis at SINTEF Industry, identifying the components Phthalimide ($C_8H_5NO_2$) and 1,2-Benzenedicarboxylic acid ($C_8H_6O_4$) with a match factor of 99.4 and 99.5% respectively. The weight losses are smaller than those measured in the previous study using the same material, which were 1.7% wt for chips and uniaxial briquettes and 1.5% wt for MPT briquettes [33]. However, those trials were conducted in a muffle furnace in air, and the present trials in a thermolysis

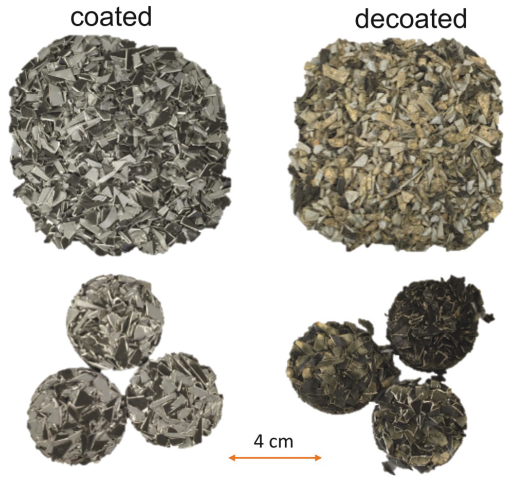

Fig. 1 Aluminium chips and uniaxial briquettes before and after the thermal treatment

furnace with a lower oxygen concentration (5%). In addition, the amount of material treated per trial in this study is significantly higher than the previous study: 500 g vs. 60 g. To check the weight losses expected after a complete de-coating that does not leave dark carbonaceous residues, two more trials were conducted on chips using a different set-up. For each trial a tray with approximately 1 kg of chips was introduced in a muffle furnace at 550 °C. After 30 min, there were still dark residues in the chips, so the holding time was extended to 1 h. The average weight loss measured was $1.59 \pm 0.02\%$, only slightly higher than measured from the chips treated in the thermolysis furnace. Thus, de-coating coated sheet industrially could lead up to 16 kg of weight losses per tonne of scrap treated. Assuming that all those volatiles are 50/50% wt epoxy/polyester, and the decomposition follows the thermolysis reactions described in Eqs. 1 and 2, fully de-coating 1 tonne of this coated chips would generate approximately 24 kg of CO_2 and 8 kg of CO gases.

Although the time, temperature, gas flow and oxygen concentrations needed for the stoichiometric reactions to volatilize all organics had been calculated, dark residues remained for all trials. This suggests that the oxygen supplied, time or temperature were not sufficient to react with all the organics present. Alternatively, it could point to the unsuitable placement of the gas pipes. Both the inflow and outflow piping were connected through the furnace lid, while the materials were placed below, stacked inside a crucible. Future investigations should ensure optimal transport of gases with a moving material bed, e.g., use a rotary kiln while still ensuring briquette integrity.

De-coating Off-Gas Analysis

Figure 2 shows the off-gases generated during the thermal pre-treatment for all compaction types.

For clarity, the hydrocarbons are grouped according to their chemical structure as aliphatic and aromatic hydrocarbons. Aliphatic hydrocarbons include methane, ethane, propane, heptane, ethene and propene. The aromatic hydrocarbons include benzol, styrene and phenol. Additionally, two aldehydes, formaldehyde and acetaldehyde, were measured.

The results reveal that the CO_2 concentration decreases significantly with increased compaction. The measured CO_2 peaked at 42,506 ppm for loose chips, 35,340 ppm for uniaxial and 24,000 ppm for MPT. The same trend applies for CO (Loose: 9448 ppm, Uniaxial: 7995 ppm, MPT: 5800 ppm), aliphatic hydrocarbons (Loose: 3660 ppm, Uniaxial: 3118 ppm, MPT: 1722 ppm) and aromatic hydrocarbons (Loose: 2644 ppm, Uniaxial: 2146 ppm, MPT: 1630 ppm). The gas evolution started at temperatures between 175 and 190 °C. The emission of CO_2, CO and hydrocarbons peaked after 1 h at around 320 °C for MPT and 400 °C for chips and uniaxial briquettes. The first phase, scission, and

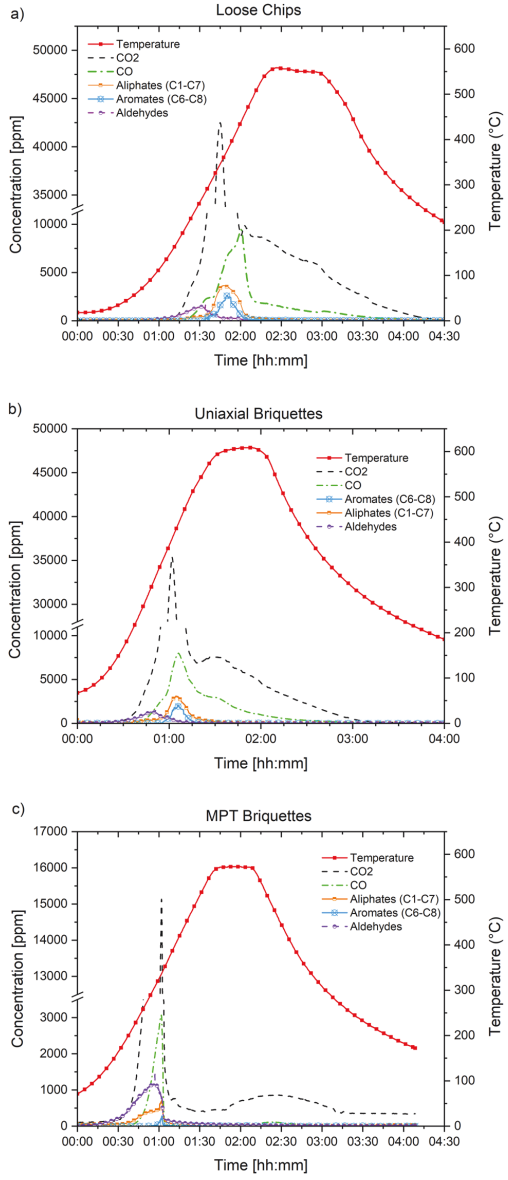

Fig. 2 Off-gases evolved against time and temperature during the thermal pre-treatment of **a** loose chips, **b** uniaxial briquettes (low compaction) and **c** MPT briquettes (high compaction)

decomposition of organics, lasted until 500–515 °C. After this temperature was reached, no hydrocarbons were present in the off-gas and the second phase began: the gasification of residual carbon, releasing CO_2 and CO at a much slower

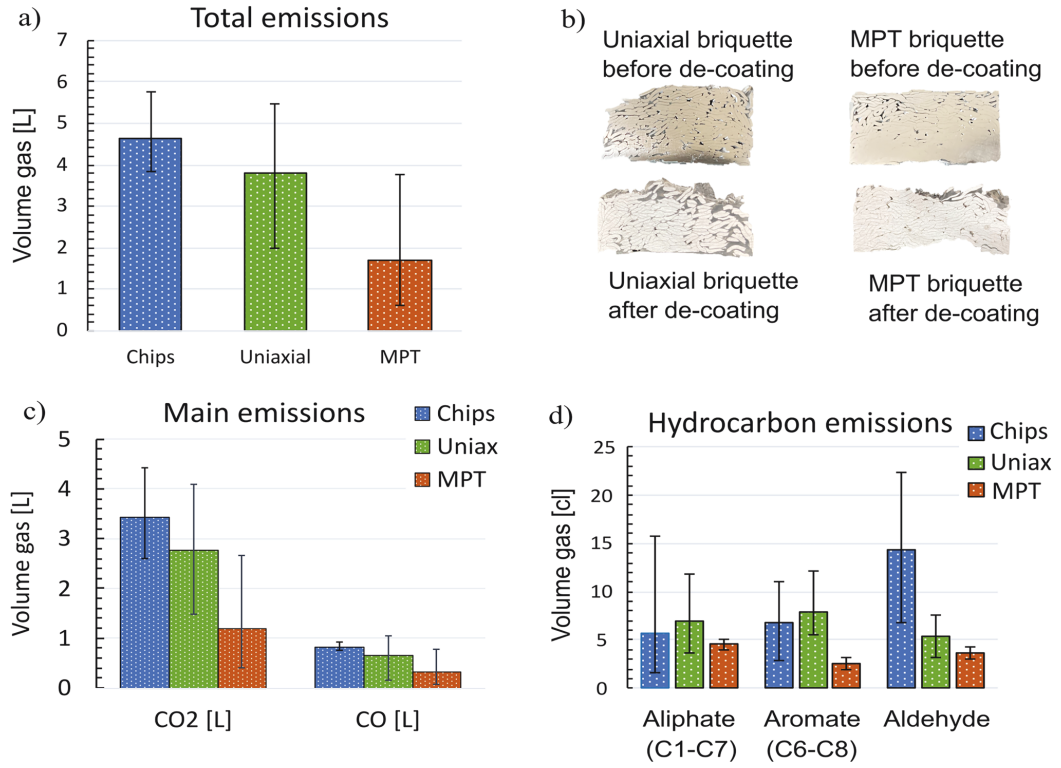

Fig. 3 **a** Total gas emissions released during thermal treatment for each compaction type. Average and STD; three trials each. **b** Cross-section of uniaxial and MPT briquettes before and after treatment. **c** Average CO_2, CO released and **d** Average volatile hydrocarbons released

rate. These two phases (although the off-gases were previously not analysed in such detail) correspond with those described in literature for organic coatings on aluminium [24] and magnesium [34]. The de-coating gas evolution has also been monitored by Al Mahmood [35] and Gökelma [20] when treating polymer-laminated thin aluminium (coffee capsules), although in those cases the furnace atmosphere was inert.

To correlate the findings with the theoretical concept of stochiometric thermolysis, the total gas volumes were calculated from the FTIR measurements and averaged for each pre-treatment route. The calculation of released gases refers to the time period where the sample is above 175 °C, starting from the initial heating phase where the first volatile components are measured by the FTIR and then until cooling down below 175 °C. This temperature range/profile differs from that reported for the decomposition of other coatings (commencing at 250 °C) reported in literature. This could be due to temperature differences between the samples and the thermocouple. To correctly calculate the total amount of gas, the time interval in which the gases were measured by FTIR was chosen. Accordingly, the total generation of gaseous components was calculated by Eq. 7:

$$V_{i,total} = \sum_{t_0}^{t_1} c_i * \dot{V} \tag{7}$$

$V_{i,total}$: Total volume of generated gaseous component i [L].
t_0 : point in time where the sample reaches 175 °C [min]
t_1 : point in time where the sample falls below 175 °C [min]
c_i : concentration of gaseous component i at specific time [%] $\dot{V}$: gas flow [L/min].

The results are summarized in Fig. 3. The total volume of gas generated decreased with compaction. This applies to CO_2 and CO as well as to organic volatile compounds. Treating 500 g of loose chips generated 3.44 litres (± 0.978 L) while the uniaxial briquettes released 2.77 L (± 1.33 L) and the MPT briquettes only produced 1.2 L (± 1.47 L). Hydrocarbons (aliphatic and aromatic) volumes were similar when treating loose or uniaxial briquettes but lower for the MPT

briquettes. Aldehydes were predominantly released during the thermal pre-treatment of loose chips with up to 0.143 L (±0.08 L). However, the estimated variability is larger than the differences between compaction states. This may be because part of the briquettes fell apart during handling, as shown in the briquettes cross-sections of Fig. 3b.

The ratio between the average total CO_2 and CO released was higher (4.2) for chips and uniaxial briquettes than for the MPT briquettes (3.7). Higher values indicate a higher degree of combustion during the de-coating reactions. The decreasing off-gas generation, particularly CO_2 and CO, as well as the decreasing CO_2/CO ratio for the denser briquettes (MPT), supports the hypothesis raised in the previous section: oxygen availability is crucial for organics removal, and therefore compacting coated materials into briquettes of lower surface areas limits the efficiency of the de-coating. The internal porosity of the briquettes was measured in a previous study [33] as 15% for uniaxial and 5% for MPT. Therefore, gas transport was very limited inside the MPT. Chamakos [30] attributed the incomplete de-coating of UBC bales to their low thermal conductivity, since the temperatures measured in the center of the bales were below those required for de-coating. But due to the small size of the briquettes in this study, it is assumed that the temperature differences between the surface and the centre are negligible and that insufficient gas transport is the main factor behind the influence of compaction on de-coating.

The ideal gas law was used to convert the volumes into mass, considering that the temperature of the off-gases was 180 °C during measurement. De-coating 1 tonne of the materials under the present operation conditions would generate 8.1 kg CO_2 eq. per tonne scrap for the chips, 6.6 kg CO_2 eq. for the briquettes and only 2.8 kg CO_2 eq. for the MPT briquettes. Thus, high densifications reduce the gases from

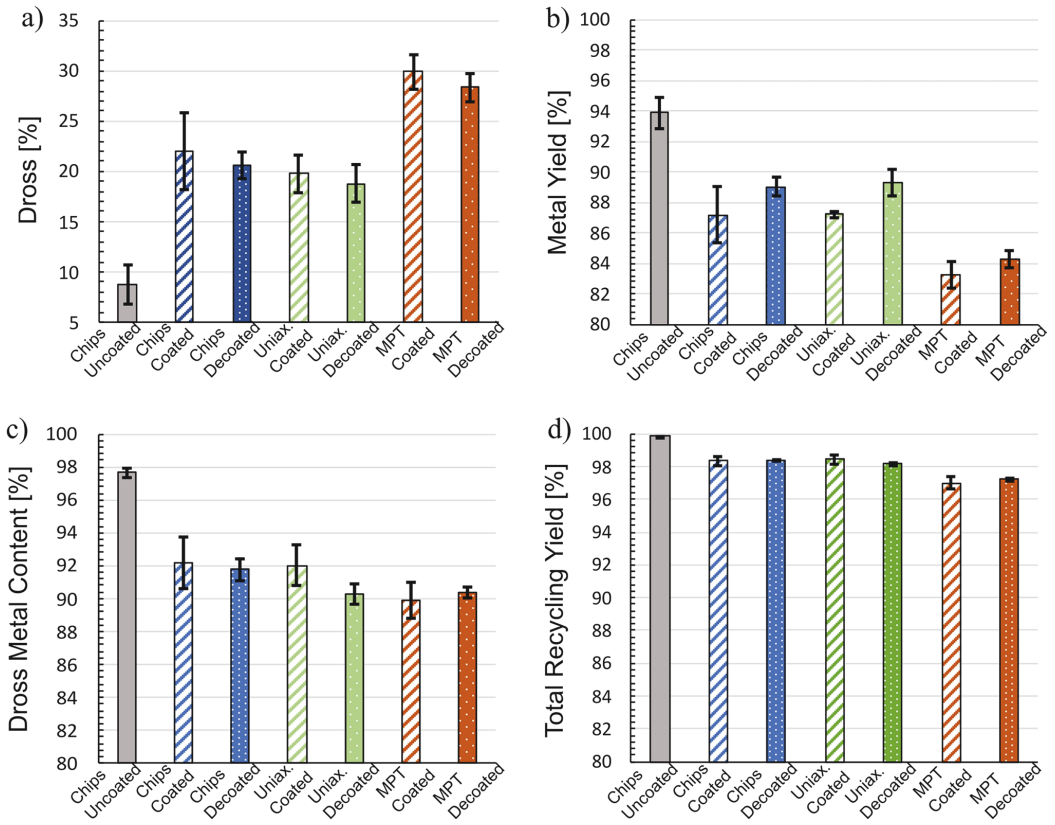

Fig. 4 **a** Dross related to wt scrap. **b** % wt Metal Yield from cast ingots. **c** Dross metal content **d** Total recycling yield. Each bar represents the average and STD for each conditioning route: compaction (loose chips/uniaxial briquettes/MPT briquettes) and thermal treatment (coated/de-coated). Chips uncoated is untreated bare Al

re-melting/pre-treatment. This could be beneficial from the point of view that it reduces the amount of off-gases which need to be further treated and the process direct emissions, although on the other side the off-gases could be reused internally to save energy, as discussed in [23]. The next section investigates the implications for the performance of the re-melting process.

Re-melting

The coated samples behaved very differently depending on whether they had been thermally treated or not. If untreated, they burned as soon as they were charged to the furnace, while those thermally pre-treated did not. When comparing the untreated samples in various compaction states, the most compacted briquettes (MPT) produced less smoke and flames. Thus, in industrial processes which re-melt dirty scrap without pre-treatment (e.g., in rotary furnaces with salts), compacting the bales to higher densities could be beneficial for process control and safety.

Figure 4 shows the dross generation relative to the initial weight of the scrap (Eq. 3) and the average metal yield (Eq. 4) for each pre-treatment route. Re-melting the uncoated, bare chips generated the least amount of dross (9% wt). Even if the weight of the coating was less than 2% of the scrap charged, the presence of the coating led to at least twice as much dross generation for all cases: values around 20–30 wt% of the scrap charged. The differences between the thermally treated and untreated coated samples were ~ 2% wt. This difference was lower than expected, as the removal of organic contaminants and the prevention of the combustion reactions during re-melting were thought to have a larger impact. However, as discussed, the thermal treatment only removed part of the organics. Regarding the effect of the degree of compaction, re-melting chips and uniaxial briquettes generated similar amounts of dross relative to the weight of scrap charged (~ 19–22%), while the MPT samples generated higher relative amounts of dross (28–30% wt). The metal yield results follow the inverse trend; higher metal yield (94% wt) for the uncoated material, lower for the chips and uniaxial briquettes (87–89% wt), lowest for the MPT briquettes (83–84% wt), and ~ 2% wt differences due to thermal treatment. The de-coating weight losses presented in the previous section were used to estimate the initial metal content of the samples before re-melting and the metal recovery: ratio of metal recovered with respect to the metal charged into the furnace. The average numbers for metal recovery slightly reduced the differences between the thermal pre-treatment route and directly melting. All the re-melting data is provided in the online supplementary material.

The presence of organic residues seems to be the major factor behind dross formation, irrespective of pre-treatment of the chips and briquettes or by just adding to the aluminium melt. The results show that the combustion of the coating during melting of the chips or briquettes produced the same amount of dross as the de-coated chips and briquettes. The coating residues may consist of decomposed but not removed products of thermal pre-treatment, such as carbon and non-decomposed long chain hydrocarbons ($C_xH_yO_z$). These will likely react with the liquid aluminium during re-melting and cause dross formation and metal losses due to the formation of aluminium carbide and oxide (see Eqs. 8 & 9). Additionally, re-oxidation of aluminium with CO_2 and CO can occur (see Eqs. 10 & 11). This has also been reported in previous studies [36].

$$\mathrm{Al} + \frac{3}{4}\mathrm{C} = \frac{1}{4}\mathrm{Al_4C_3} \quad \Delta G(1023K) = -43\mathrm{kJ/mol} \tag{8}$$

$$\mathrm{Al} + \frac{3}{4}\mathrm{C} = \frac{1}{4}\mathrm{Al_4C_3} \quad \Delta G(1023K) = -43\mathrm{kJ/mol} \tag{9}$$

$$\mathrm{Al} + \frac{3}{2}\mathrm{CO_2} = \frac{1}{2}\mathrm{Al_2O_3} + \frac{3}{2}\mathrm{CO} \quad \Delta G(1023K) = -379\mathrm{kJ/mol} \tag{10}$$

$$\mathrm{Al} + \frac{3}{2}\mathrm{CO} = \frac{1}{2}\mathrm{Al_2O_3} + \frac{3}{2}\mathrm{C} \quad \Delta G(1023K) = -367\mathrm{kJ/mol} \tag{11}$$

The metal content of the dross, obtained by re-melting it in salt-flux, is represented in Fig. 4c). The results confirm the expected high metallic content of the dross from re-melting uncoated Al: 97.7 ± 0.3%. The dross from the coated and the thermally treated chips gave similar metal yields (92.2 ± 1.6% and 91.8 ± 0.7% respectively) to the

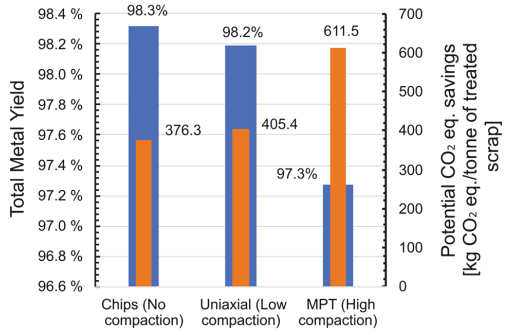

Fig. 5 Potential for improving the CO_2-savings compared to total metal yields of 100% when re-melting material with varying degree of compaction

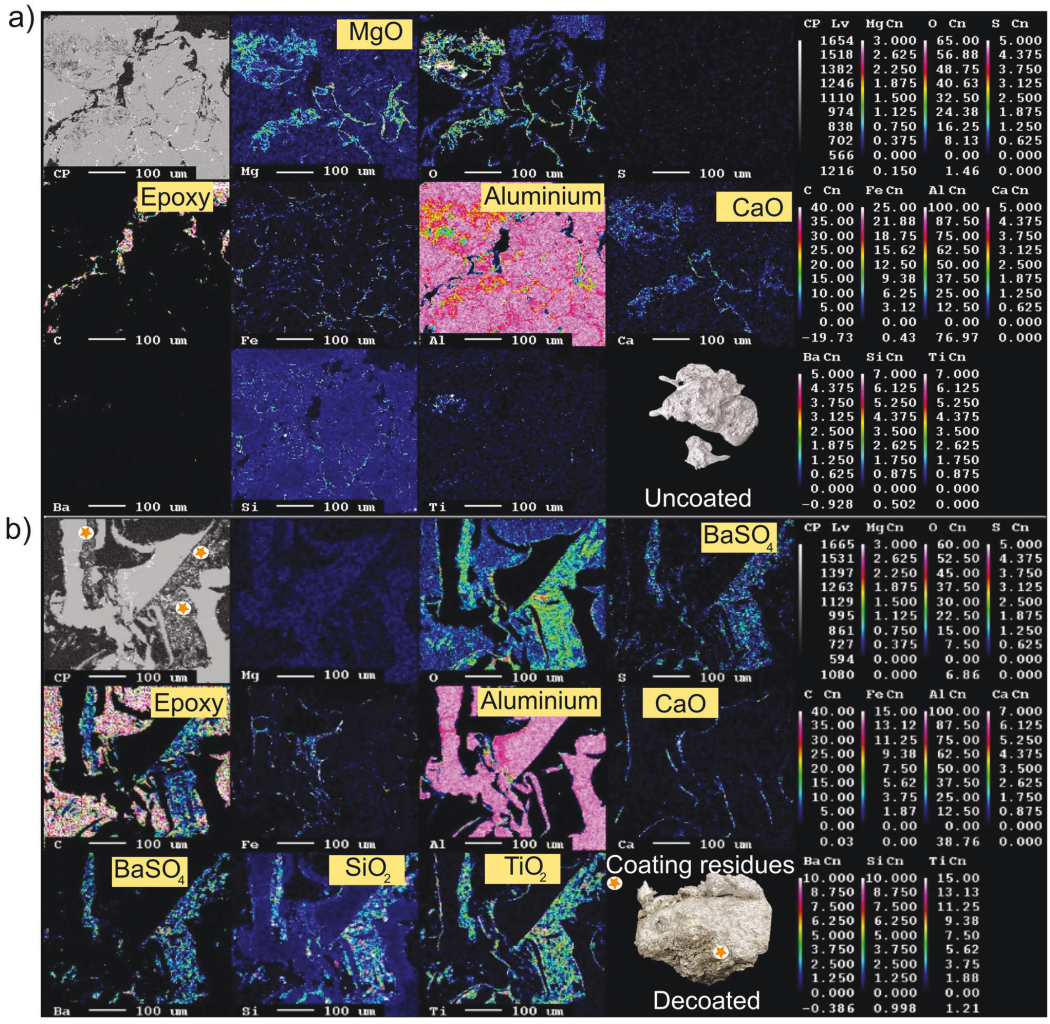

Fig. 6 SEM/EPMA elemental mapping of dross samples. Bright colours (white, pink, and yellow) = high concentrations. Dark colours = low concentrations. **a** Dross from re-melting uncoated Al. **b** Dross from re-melting thermally de-coated Al

coated uniaxial briquettes (92.0 ± 1.2%). The dross from thermally treated uniaxial briquettes, MPT untreated and the MPT treated briquettes contained less metal (90.3 ± 0.3%, 89.9 ± 1.1% and 90.4 ± 0.3% respectively).

Finally, the total recycling yield in Fig. 4d) shows that, if the aluminium from the dross is recovered, recycling coated aluminium leads to slightly higher overall losses than bare aluminium, which increase if the scrap is compacted to high densities by torsion. Although these differences may seem small, at an industrial scale they would have a significant environmental and economic impact. Due to the higher energy-intensity and environmental impacts associated with primary aluminium production compared to recycling [1], the optimization of the recycling processes is key for a more sustainable Al production. For the studied process, high densification decreased the metal yield by 4–5%. Assuming the aluminium would be recovered from the dross by a salt-flux process as efficient as these re-melting trials at laboratory scale, the increase in total metal yield when melting loose chips instead of highly compacted MPT briquettes

corresponds to 10.5 kg per tonne of treated material. With a CO_2 equivalent of 22.4 kg/kg of primary aluminium [37] not recovering that aluminium would correspond to loosing potential CO_2 savings of 235.2 kg/tonne of treated scrap. As the degree of compaction of the scrap increases, the total metal yield decreases, raising the carbon footprint of the re-melting process. Figure 5 relates the total metal yield for the compaction routes to the potential CO_2 savings which could be achieved if the Metal Yield of the process would be improved to 100%.

Furthermore, to recover the metal from the dross implies additional transport, energy, and resources to treat it in a rotary furnace and generates salt-slag residues that need to be processed as well [2]. Thus, minimising the amount of organic contamination introduced into the melt by applying a successful thermal pre-treatment in loose/loosely compacted scrap would reduce the metal lost to the dross, bringing large environmental and economic savings.

Dross Characterization

The SEM/EPMA analysis of the dross samples is displayed in Fig. 6. The square in the top left of each bundle of images shows the secondary electron image and the rest are qualitative colour maps of the concentration of specific elements. Approximate concentrations can be deduced using the colour scales.

All dross samples contained mostly aluminium. The dross from the uncoated material (Fig. 6a) contains magnesium and calcium oxides, as well as silicon and iron phases expected in the alloy. In contrast, the dross from the coated samples (both thermally treated (Fig. 6b) and untreated) contained titanium, silicon, barium, sulphur, and calcium. Most of these elements were arranged into layers and agglomerates. This agrees with previous analysis [21] which identified $BaSO_4$, TiO_2, and SiO_2 as residues in the coating which are not removable by thermal treatment, and remain loosely adhered to the surface. Meskers [38] observed TiO_2, CaO, $BaSO_4$ and SiO_2 residues as well on magnesium scrap. They are added as pigments or fillers. Since the samples were embedded in epoxy it was not possible to identify whether carbon-containing coating residues were also present. There were no significant compositional differences between the dross from re-melting de-coated samples or from directly charging them into the melt. The elemental composition of the metal recovered from the dross is displayed in Table 3 in the Appendix.

The results suggest that the salt-flux separates the coating oxide residues from the metal as there is no significant increase of neither titanium, barium nor silicon when comparing the results to the initial alloy composition (Table 1). There was an increase in sodium, likely from the NaCl present in the salt-flux, and a decrease in Mg for the uncoated material. Magnesium could have been evaporated or oxidized during the first re-melting or removed by reaction with the salt-flux. This is consistent with published experimental [21] and thermodynamic [39] recycling studies for aluminium and magnesium [34].

Since scrap compaction brings logistic and operational benefits, the authors propose the following practice for recycling packaging scrap in a more environmentally friendly way, minimizing dross:

1. Transport the scrap compacted into bales to the recycling facility.
2. Loosen up or shred the bales for sorting and thermal pre-treatment with controlled air flow and off-gas treatment.
3. Once the organics and volatiles are fully removed, consider compacting the scrap into briquettes to ease its charging and sinking (not necessary for furnaces with vortex). High densification is not needed.
4. Recover Al from dross by salt-flux recycling or other suitable treatments/uses.

Conclusions

This study investigated the effects of compacting coated aluminium chips of an alloy low in Mg on the efficiency of the thermal de-coating and re-melting processes by comparing dross generation, de-coating off-gases and overall metal yield. The following conclusions were drawn:

Thermal De-coating Pre-treatment

- Oxygen availability is crucial for maximising the gasification of carbon from coatings.
- A thermal pre-treatment of 30 min at 550 °C under a 5% O_2–95% N_2 atmosphere, only partly removed the organic components of the coating, possibly due to a low O_2 residence time inside the furnace. Further work should investigate the optimal transport of gases, e.g., in a rotary kiln with a moving material bed.
- Compaction into briquettes of high densities by torsion lowers the de-coating efficiency due to limiting the gas transport inside the briquette, due to the briquette's lower surface area and internal porosity.

- The main gaseous products were CO_2 and CO, and their emission decreased for higher compactions, as well as the CO_2/CO ratio decreasing. The loose chips released 3.44 L of VOCs, uniaxially compacted briquettes 2.77 L and the densest briquettes (MPT) 1.2 L.
- Other gas emissions included aliphatic hydrocarbons (methane, ethane, heptane, ethene and propene), aromatic (benzol, styrene and phenol) hydrocarbons and aldehydes (formaldehyde and acetaldehyde).

Re-melting

- Applying a thermal de-coating pre-treatment prevents flames and smoke during re-melting, making the process safer and more stable.
- The organic residues from the coating after pre-treatment were the main factor increasing dross and lowering recycling yield. The incomplete de-coating did not reduce the dross generated or improve the recycling yield significantly compared to re-melting without de-coating, despite avoiding combustion gases above the molten aluminium.
- The briquettes compacted to higher densities by torsion (MPT) produced the highest amount of dross (29% wt of the charged samples) and the lowest total recycling yield (97% wt), due to the compaction limiting the burn-off of the organic residues. This has economic and sustainability implications at the industrial scale.
- Melting loose material results in the highest total metal yields. This potentially saves environmental impacts, as it reduces the demand for primary aluminium. In this context, the melting of loose material provides an estimated reduction of 235 kg CO_2 eq/tonne of treated scrap compared to the highly densified (MPT) briquettes.
- Removing the organics from aluminium scrap before re-melting helps minimising the production of dross, hereby reducing efforts for an additional re-melting process in salt-flux. Reducing the amount of dross accounts for a decrease in total energy, resources and salt-slag residues associated with the recycling process.

Appendix

See Tables 2 and 3.

The composition of the coated material was calculated from 9 samples, 4 of which had been thermally treated before the molten heel re-melting, and 5 from samples without thermal treatment. The uncoated material composition was calculated from 2 samples. There were no evident differences attributable to the application of different compaction or thermal pre-treatment routes. Therefore, the averages

Table 2 Composition of the AA8111 alloy sheets. Arc spark OES data from producer

	Al (%)	Fe (%)	Si (%)	Mg (ppm)	Cu (ppm)	Ga (ppm)	V (ppm)	Ti (ppm)	Mn (ppm)	Zn (ppm)	Na (ppm)	Ca (ppm)	Cr (ppm)
Coated	98.34	0.75	0.88	6	11	117	80	107	26	18	1	4	7
Uncoated	98.37	0.86	0.59	463	361	112	195	50	368	76	10	35	16
Heel	98.15	0.81	0.94	86	64	117	124	122	209	97	4	11	14

Table 3 Average composition (and standard deviation) of the aluminium recovered from dross

	Al (%)	Fe (%)	Si (%)	Mg (ppm)	Cu (ppm)	Ga (ppm)	V (ppm)	Ti (ppm)	Mn (ppm)	Zn (ppm)	Na (ppm)	Ba (ppm)	Ca (ppm)	Cr (ppm)
Coated	97.34	0.77	0.64	11	38	108	114	131	130	60	146	4	32	16
STD (±)	1.61	0.07	0.05	3	5	6	14	17	23	15	88	1	15	3
Uncoated	96.55	0.78	0.47	96	198	108	198	100	340	66	183	0	33	19
STD (±)	0.09	0.00	0.01	12	3	2	4	9	14	5	40	0	1	1

were calculated based on the initial aluminium sheet composition used for the samples (coated or uncoated).

Supplementary Information The online version contains supplementary material available at https://doi.org/10.1007/s40831-023-00773-3.

Acknowledgements The authors would like to gratefully acknowledge the Research Council of Norway for funding the projects Extreme-Alloys and Coatings for Space and other Extreme Applications (NFR Project nr. 310048) and Alpakka—Circular Aluminium Packaging in Norway (NFR Project nr. 296276), to Speira Holmestrand for the materials and to the departments of Process Metallurgy and Metal Recycling (IME) at RWTH Aachen University, and Materials Science and Engineering (IMA) at NTNU for the experimental equipment and support. The authors acknowledge Anders Brunsvik (SINTEF) for GC/MC analysis, Morten Peder Raanes (NTNU) for SEM-EPMA analysis and Anne Kvithyld (SINTEF) for the valuable discussions.

Funding Open access funding provided by NTNU Norwegian University of Science and Technology (incl St. Olavs Hospital - Trondheim University Hospital).

Declarations

Conflict of interest The authors declare that they have no conflict of interest.

References

1. Olivieri G, Romani A, Neri P (2006) Environmental and economic analysis of aluminium recycling through life cycle assessment. Int J Sust Dev World 13(4):269–276. https://doi.org/10.1080/13504500609469678
2. Cusano G, Rodrigo Gonzalo M, Farrell F, Remus R, Roudier S, Delgado Sancho L (2017) Best available techniques (bat) reference document for the non-ferrous metals industries. Ind Emiss Dir. https://doi.org/10.2760/8224
3. Damgaard A, Larsen AW, Christensen TH (2009) Recycling of metals: accounting of greenhouse gases and global warming contributions. Waste Manage Res 27(8):773–780. https://doi.org/10.1177/0734242X09346838
4. IAI (2021) Material flow model. URL: https://international-aluminium.org/resource/iai-material-flow-model-2021-update/
5. Tabereaux AT, Peterson RD (2014) Ch. 2.5 Aluminum production. In: Seetharaman S (ed) Treatise on process metallurgy. Elsevier, Boston, pp 839–917

6. Xiao Y, Reuter MA (2002) Recycling of distributed aluminium turning scrap. Miner Eng 15(11):963–970. https://doi.org/10.1016/S0892-6875(02)00137-1
7. Rossel H (1990) Fundamental investigations about metal loss during remelting of extrusion and rolling fabrication scrap. In: Bickert CM (ed) Light metals 1990. Springer, Cham
8. Gökelma M, Vallejo-Olivares A, Tranell G (2021) Characteristic properties and recyclability of the aluminium fraction of mswi bottom ash. Waste Manage 130:65–73. https://doi.org/10.1016/j.wasman.2021.05.012
9. van Schaik A, Reuter MA (2014) Ch. 22 Material-centric (aluminium and copper) and product-centric (cars, weee, tv, lamps, batteries, catalysts) recycling and dfr rules. In: Worrell E, Reuter MA (eds) Handbook of recycling. Elsevier, Amsterdam
10. Milani V, Timelli G (2023) Solid salt fluxes for molten aluminum processing—a review. Metals. https://doi.org/10.3390/met13050832
11. Schmitz C (2014) Handbook of aluminium recycling: mechanical preparation, metallurgical processing, heat treatment. Vulkan-Verlag, Essen
12. Tsakiridis PE, Oustadakis P, Agatzini-Leonardou S (2013) Aluminium recovery during black dross hydrothermal treatment. J Environ Chem Eng 1(1):23–32. https://doi.org/10.1016/j.jece.2013.03.004
13. Ünlü N, Drouet MG (2002) Comparison of salt-free aluminum dross treatment processes. Resour Conserv Recycl 36(1):61–72. https://doi.org/10.1016/S0921-3449(02)00010-1
14. Xiao Y, Reuter MA, Boin U (2005) Aluminium recycling and environmental issues of salt slag treatment. J Environ Sci Health 40(10):1861–1875. https://doi.org/10.1080/10934520500183824
15. Bao S, Kvithyld A, Bjørlykke GA, Sandaunet K (2023) Recycling of aluminum from aluminum food tubes. In: Broek S (ed) Light metals 2023. Springer, Cham, pp 960–966
16. Capuzzi S, Timelli G (2018) Preparation and melting of scrap in aluminium recycling: a review. Metals 8:249. https://doi.org/10.3390/met8040249
17. Boin UMJ, Bertram M (2005) Melting standardized aluminum scrap: a mass balance model for Europe. JOM 57(8):26–33. https://doi.org/10.1007/s11837-005-0164-4
18. Stark TD, Martin JW, Gerbasi GT, Thalhamer T, Gortner RE (2012) Aluminum waste reaction indicators in a municipal solid waste landfill. J Geotech Geoenviron Eng 138(3):252–261. https://doi.org/10.1061/(ASCE)GT.1943-5606.0000581
19. Capuzzi S, Kvithyld A, Timelli G, Nordmark A, Engh TA (2017) Influence of coating and de-coating on the coalescence of aluminium drops in salt. In: Ratvik AP (ed) Light metals 2017. Springer, Cham, pp 1115–1121
20. Gökelma M, Diaz F, Öner IE, Friedrich B, Tranell G (2020) An assessment of recyclability of used aluminium coffee capsules. In: Tomsett A (ed) Light metals 2020. Springer, Cham, pp 1101–1109
21. Vallejo-Olivares A, Høgåsen S, Kvithyld A, Tranell G (2022) Thermal de-coating pre-treatment for loose or compacted aluminum scrap and consequences for salt-flux recycling. J Sustain Metall 8(4):1485–1497. https://doi.org/10.1007/s40831-022-00612-x
22. Bateman W, Guest G, Evans R (1999) Decoating of aluminium products and the environment. In: Eckert CE (ed) Light metals. Springer, Cham, pp 1099–1105
23. Haraldsson J, Johansson MT (2018) Review of measures for improved energy efficiency in production-related processes in the aluminium industry—from electrolysis to recycling. Renew Sustain Energy Rev 93:525–548. https://doi.org/10.1016/j.rser.2018.05.043
24. Kvithyld A, Meskers CEM, Gaal S, Reuter M, Engh TA (2008) Recycling light metals: optimal thermal de-coating. JOM 60(8):47–51. https://doi.org/10.1007/s11837-008-0107-y
25. Steglich J, Friedrich B, Rosefort M (2020) Dross formation in aluminum melts during the charging of beverage can scrap bales with different densities using various thermal pretreatments. JOM 72(10):3383–3392. https://doi.org/10.1007/s11837-020-04268-4
26. Steglich J, Dittrich R, Rombach G, Rosefort M, Friedrich B, Pichat A (2017) Dross formation mechanisms of thermally pretreated used beverage can scrap bales with different density. In: Ratvik AP (ed) Light metals 2017. Springer, Cham, pp 1105–1113
27. Puga H, Barbosa J, Soares D, Silva F, Ribeiro S (2009) Recycling of aluminium swarf by direct incorporation in aluminium melts. J Mater Process Technol 209(11):5195–5203. https://doi.org/10.1016/j.jmatprotec.2009.03.007
28. Puga H, Barbosa J, Ribeiro CS (2013) Factors affecting the metal recovery yield during induction melting of aluminium swarf. Mater Sci Forum 730–732:781–786
29. Vallejo-Olivares A, Philipson H, Gökelma M, Roven HJ, Furu T, Kvithyld A et al (2021) Compaction of aluminium foil and its effect on oxidation and recycling yield. In: Perander L (ed) Light metals 2021. Springer, Cham, pp 735–741
30. Chamakos N, Koklioti M, Tzevelekou T, Fiampouri A, Contopoulos I, Anestis A et al (2023) Towards the efficient recycling of used beverage cans: numerical study and experimental validation. In: Broek S (ed) Light metals 2023. Springer, Cham, pp 942–948
31. Piergiovanni L, Limbo S (2016) Food packaging materials. In: Salvatore Parisi RP (ed) Chemistry of foods Springer briefs in molecular science, 1st edn. Springer, Cham
32. Steglich J (2020) Krätzebildung in aluminiumschmelzen durch rückstände der thermischen vorbehandlung von getränkedosenschrotten. Schriftenreihe des IME, Aachen
33. Vallejo-Olivares A, Høgåsen S, Kvithyld A, Tranell G (2022) Effect of compaction and thermal de-coating pre-treatments on the recyclability of coated and uncoated aluminium. In: Eskin D (ed) Light metals 2022. Springer, Cham, pp 1029–1037
34. Meskers CEM, Reuter MA, Boin U, Kvithyld A (2008) A fundamental metric for metal recycling applied to coated magnesium. Metall Mater Trans B 39(3):500–517. https://doi.org/10.1007/s11663-008-9144-8
35. Al Mahmood A, Hossain R, Sahajwalla V (2020) Investigation of the effect of laminated polymers in the metallic packaging materials on the recycling of aluminum by thermal disengagement technology (tdt). J Clean Prod 274:122541. https://doi.org/10.1016/j.jclepro.2020.122541
36. Dittrich R, Friedrich B, Rombach G, Steglich J, Pichat A (2017) Understanding of interactions between pyrolysis gases and liquid aluminum and their impact on dross formation. In: Ratvik AP (ed) Light metals 2017. Springer, Cham, pp 1457–1464
37. Norgate TE, Jahanshahi S, Rankin WJ (2007) Assessing the environmental impact of metal production processes. J Clean Prod 15(8):838–848. https://doi.org/10.1016/j.jclepro.2006.06.018
38. Meskers CEM, Xiao Y, Boom R, Boin U, Reuter MA (2007) Evaluation of the recycling of coated magnesium using exergy analysis. Miner Eng 20(9):913–925. https://doi.org/10.1016/j.mineng.2007.02.006
39. Hiraki T, Miki T, Nakajima K, Matsubae K, Nakamura S, Nagasaka T (2014) Thermodynamic analysis for the refining ability of salt flux for aluminum recycling. Materials 7(8):5543–5553. https://doi.org/10.3390/ma7085543

Article F

LCA of recycling aluminium incineration bottom ash, dross and shavings in a rotary furnace and environmental benefits of salt-slag valorisation

Alicia Vallejo Olivares[a], Elisa Pastor-Vallés[b], Johan Berg Pettersen[b] and Gabriella Tranell[a]

[a] Department of Materials Science (IMA), NTNU Norwegian University of Science and Technology. Alfred Getz vei 2B, 7034 Trondheim, Norway.
[b] Industrial Ecology Programme, Department of Energy and Process Engineering, NTNU Norwegian University of Science and Technology. Kolbjørn Hejes vei 1B, 7034 Trondheim, Norway.
Corresponding author: alicia.v.olivares@ntnu.no **Under review**

Abstract. Recycling aluminium in a rotary furnace with salt-fluxes allows recovering valuable alloys from hard-to-recycle waste/side-streams such as packaging, dross and incinerator bottom ash. However, this recycling route generates large amounts of salt-slag/salt-cake hazardous wastes which can pose critical environmental risks if landfilled. To tackle this issue, the metallurgical industry has developed processes to valorise the salt-slag residues into recyclable salts and aluminium concentrates, while producing by-products such as ammonium sulphate and non-metallic compounds (NMCs), with applications in the construction or chemical industries. This study aims to assess through LCA the environmental impacts of recycling aluminium in rotary furnaces for both salt-slag management routes: valorisation or landfill. It was found that this recycling process brings forth considerable net environmental profits, which increase for all the considered impact categories if the salt-slag is valorised. The main benefits arise from the production of secondary cast aluminium alloys, which is not unexpected due to the high energy intensity of aluminium primary production. However, the LCA results also identify other hotspots which play a significant role, and which should be considered for the optimisation of the process based on its environmental performance, such as the production of by-products, the consumption of energy/fuels and the avoidance of landfilling waste. Additionally, the assessment shows that the indicators for mineral resource scarcity, human carcinogenic toxicity and terrestrial ecotoxicity are particularly benefited by the salt-slag valorisation. Finally, a sensitivity analysis illustrates the criticality of the metal yield assumptions when calculating the global warming potential of aluminium recycling routes.

Keywords: **Aluminium; Recycling; LCA; Rotary furnace; Salt-slag; Waste valorisation**

1 Introduction

Recycling aluminium is considerably more sustainable than its primary production, both environmentally and economically (Damgaard et al., 2009; Olivieri et al., 2006). The main reason is that primary production consumes vast quantities of energy and resources during the initial stages of mining the raw

materials and extracting from them the aluminium metal (first aluminium oxide is extracted from bauxite mineral through the Bayer process, and subsequently, the oxide is reduced into aluminium metal through the Hall-Héroult process). Another critical benefit of recycling is avoiding the generation of bauxite residue commonly known as "red mud", which can pose significant environmental risks (Mayes et al., 2016). According to a recent study, producing 1 tonne of primary Al releases between 14 and 17 metric tonnes of CO_2 equivalent from the bauxite mine to casting the metal. From these, the dominating part of the emissions are indirect, released in electricity production for electrolysis, and will therefore highly depend on the source of electricity (Saevarsdottir et al., 2023). The Hall-Héroult electrolytic process is the most energy-intensive step of primary production, with approximately 14 MWh of energy consumed per tonne of Al produced (IAA, 2022). The secondary production route consumes much less energy in comparison, and it consists of re-melting aluminium-containing scrap at temperatures around 700-750 °C, adjusting the melt composition, and solidifying the metal as slabs or ingots which can then be shaped into new products. According to the current Best Available Techniques in Europe (Delgado Sancho, 2017), the process of re-melting aluminium scrap in a rotary furnace uses 0.55-0.70 MWh (2–2.5 GJ) of energy per tonne of produced Al, and the total energy required for producing 1 tonne of secondary aluminium ranges between 0.55-2.50 MWh (2-9 GJ), depending on the quality of the scrap and the processes involved. The standard re-melting processes are carried out in reverberatory furnaces or rotary furnaces fired with natural gas, and in the second case mixed with substantial amounts of salts (NaCl/KCl/ fluorides) (Schlesinger, 2007).

This study assesses the environmental impacts of re-melting via a rotary furnace. This process is suitable for contaminated or oxidised scrap, since the molten salts separate the contaminants (e.g., oxides, carbides) from the molten metal, promote the coalescence of the droplets of molten metal and protect it from oxidation (Milani and Timelli, 2023). The usage of salts allows recovering the

aluminium present in some internal wastes from production (dross, skimmings, shavings), or in post-consumer scrap such as incineration bottom ash (IBA) or food and drink packaging. However, a downside is the generation of salt slag – a mixture of non-metallic compounds (NMCs) such as oxides, carbides and nitrides, salt, and residual droplets of aluminium metal. These residues are classified as hazardous waste (European-Comission, 2015) and they can lead to significant environmental risks if disposed into landfills (EPA., 2015). An alternative to tackle this issue is to valorise the salt slag residues by crushing and dissolving the salts in water (Delgado Sancho, 2017). Examples of salt-slag valorisation processes have been previously investigated in (Padilla et al., 2022) (Li et al., 2013). The present study considers the industrial valorisation of the salt-slag into, on one side, salts and Al concentrates which can be fed back into the rotary furnace, and on the other side ammonium sulphate with application in fertilizers (Rodrigues et al., 2022) and NMCs which the chemical or construction industries can use. The main constituent of the recovered NMCs is alumina (Lucheva and Petkov, 2005), that can be used for example to replace fine aggregates in self-compacting concrete (Sua-iam and Makul, 2017), which is more sustainable than traditional concrete (Joseph and Tretsiakova-McNally, 2010), showing acceptable performances even at 1:1 substitution (Sua-iam and Makul, 2013). Alumina waste can also be used in the production of refractories, mineral wool, or in road construction (López-Alonso et al., 2019), where it improves the long-term mechanical performance of roads made of recycled aggregates. The implementation of industrial wastes/by-products in construction is gaining popularity, since it reduces the environmental burdens associated with the manufacturing of materials and landfill of waste while also tackling the challenge of the shortage and increased prices of traditional construction raw materials, as discussed in (Joseph and Tretsiakova-McNally, 2010).

In the aluminium industry, there is an ongoing discussion regarding whether aluminium re-melting in rotary furnaces is the most sustainable recycling process or whether it merely displaces the environmental burden to the

production of salts and generation of salt-slag (Xiao Y, 2005). A recent environmental profile report (European-aluminium, 2018) contains environmental indicators of re-melting scrap in an integrated cast house. Still, it does not include detailed data regarding the process of recycling the dross generated during re-melting, which is done by re-melting in rotary furnaces with salt-flux (mixed with other aluminium-containing waste/side-streams), stating that a dedicated task force should be dedicated to this work. Thus, this study delves into this topic and provides an assessment of the potential environmental impacts of an industrial process to recycle a mix of hard-to-recycle aluminium streams (dross, IBA, shavings) in a rotary furnace with salts based on production data from 2021. The study also compares scenarios where salt-slag residues are either treated for recovery or landfilled.

There are several published environmental life cycle assessments (LCA) of aluminium production and recycling processes. A recurrent takeaway is that recycling brings forth significant environmental benefits (Damgaard et al., 2009; Olivieri et al., 2006). This is mainly due to the assumption that by producing secondary aluminium, the need for primary production and its associated energy use and emissions (e.g., CO_2, PAHs, and PFCs) is mitigated. This approach is defined as system expansion (substitution), and is recommended by the ISO guidelines when dealing with multifunctional processes, or those that provide multiple functions such as recycling systems (which treat waste while producing materials), as long as further subdivision of the system is not possible (ISO, 2006a). By expanding the system, the impacts of the alternative production of the secondary function in the most likely way of producing it (primary production of aluminium in this study) are discounted from the total impact. As discussed in (Vadenbo et al., 2017) the choice of such underlying assumptions is critical for the interpretation of the results, since the avoided burdens credited based on the expected displacement of other product systems can dominate the overall results, as it occurs for aluminium in the assessment of waste management options by Manfredi (Manfredi et al., 2011). The assumptions

related to the energy source can also play an important role in the interpretation of the LCA, as shown by the aluminium primary production emissions presented by McMillan (McMillan and Keoleian, 2009), with regional variances between 7.07 and 21.9 kg CO_2 eq. kg $^{-1}$ metal in 2005. A critical review by Liu (Liu and Müller, 2012) also highlights the energy use as a source of uncertainties in LCAs in the aluminium industry. In this review, the emissions associated with producing a tonne of primary aluminium across regions varied as much as from 5.92 to 41.10 tonnes CO_2 equivalent. Other mentioned challenges include the use of industry-wide inventory data, different system boundaries and diverse assumptions for the allocation of recycling (e.g., recyclability, product lifetime). Damgaard (Damgaard et al., 2009) concluded that recycling aluminium brings forth large overall reductions of Global Warming Factors, but since these highly depend on the type and amount of energy used and its sourcing, the reductions can vary between 5.0 to 19.3 tonne CO_2 tonne $^{-1}$ aluminium scrap processed. The current LCA study attempts to minimise these uncertainties by using data from a recycling plant instead of generic data and by carrying out a sensitivity analysis of one of the process determining assumptions: the recycling metal yield (mass of metal recovered per initial mass of the scrap treated), which varies for each type of scrap and waste management route.

2 Material and methods

The framework to develop this LCA is the International Standard Organization (ISO) framework 14040-14044 (ISO, 2006a, b). It consists of four phases: the definition of the goal and scope, in which the context and modelling aspects are defined; the inventory analysis, where inputs and outputs to the process are accounted for; the life cycle impact assessment, with the calculations of associated potential environmental impact; and finally, the life cycle interpretation phase, where results are analysed, and recommendations are drawn.

2.1 Goal and scope definition

The main goals of this research are:

- To conduct an LCA of recycling hard-to-recycle aluminium containing side/waste streams (dross, IBA, shavings) in a rotary furnace.
- To assess the environmental impacts of the usage of salts and the treatment or disposal to landfill of the salt-slag residues.
- To identify hotspots or potential areas where the environmental sustainability of the process could be improved.

The functional unit (F.U.) selected for comparison is 1 tonne of aluminium containing material ready to be recycled. The recycling route includes two processes. The first one, re-melting in the rotary furnace, produces secondary aluminium and salt-slag residue, as well as furnace off-gas. The second process, the salt-slag valorisation treatment, allows recovering some of the salts (NaCl/KCl) and the entrapped metallic particles (aluminium concentrates), which are reused internally by feeding them again into the next rotary furnace cycle. In addition, other by-products recovered from the salt-slag treatment are non-metallic-compounds (NMCs) and ammonium sulphate ($(NH_4)_2SO_4$). To allocate these co-products, a system expansion approach is applied, the procedure recommended by the ISO (ISO, 2006b). However, the allocation of the input of aluminium containing material (dross, IBA, and shavings) is considered burden-free, because as it is defined hard-to-recycle, this flow does not currently have an alternative use. To facilitate the comparison with other published studies which use 1 tonne of aluminium alloys produced as F.U., the main results were re-calculated for this F.U. and are presented in the Appendix.

The two main scenarios, which only differ in the choice of salt-slag residues management, are:

Scenario 1. Al recycling + salt-slag landfill

Scenario 2. Al recycling + salt-slag treatment

The system boundaries of this study are cradle-to-gate, considering the stages from the raw material extraction to the production of the semi-finished product (secondary cast aluminium ingots). This is a common choice for LCA studies focused on metallurgical or mining processes, due to the uncertainty around the subsequent life-stages (Santero and Hendry, 2016). For instance, an aluminium ingot can be used for multiple applications, as household appliances or car components. On the contrary, when assessing finished products, e.g. cookware, a holistic cradle-to-grave approach, including the transport, usage, and disposal stages, is recommended.

Figure 1 shows the system considered, illustrating an example input material mix with 70% metallic content and an output of secondary aluminium. It is here assumed that all the metal present in the scrap is recovered after re-melting (process metal yield 100%), and that the aluminium alloys entering the system are the same as the secondary cast alloys produced, omitting the need for adjusting the melt composition by refining, dilution, or addition of alloying elements.

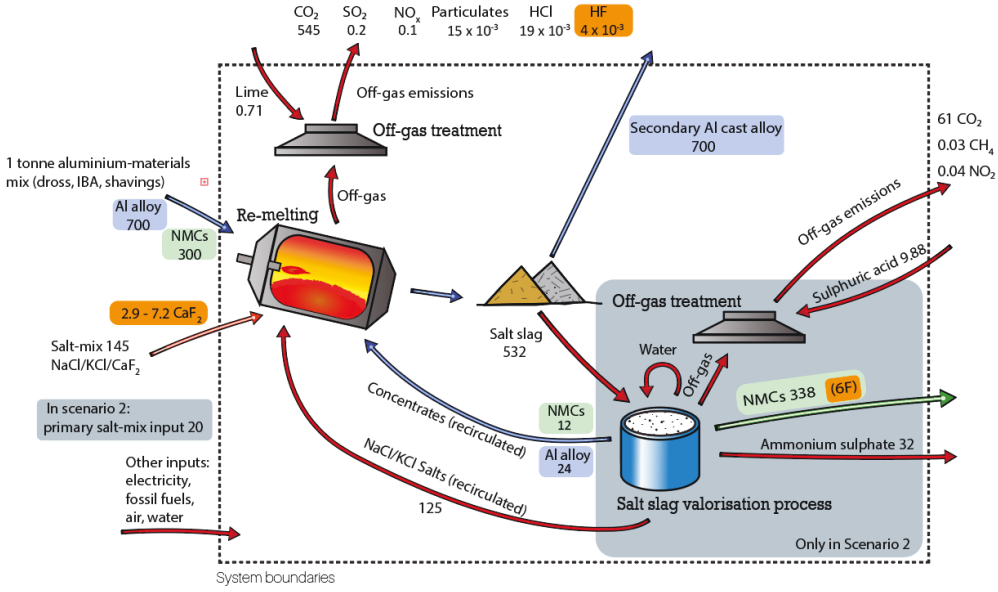

Figure 1. System considered for Scenario 2 with inputs and outputs for the two processes: recycling 1 tonne of aluminium-containing material mix in a rotary furnace and salt-slag residue valorisation treatment. The units are kg.

The scheme shows the raw materials, the products and wastes produced, and the gas emissions monitored during the re-melting processes. For better visualisation, it excludes the energy sources and process input gases (diesel, natural gas, electricity, N_2, O_2), detailed in the LCI tables provided in Appendix Tables A-1 and A-2. The mass balance of the aluminium alloys (metal), oxides and fluorides entering and exiting the system were calculated to discuss uncertainties linked to potential flows that may not have been considered, for example, due to process inefficiencies or non-monitored emissions. The flows of aluminium metal and NMCs were selected because they are the main contributors to environmental impacts.

The amount of aluminium metal and NMCs entering the furnace was calculated based on the metal yield values provided by the recycling plant. The guidelines to sample and analyse the metal content of scrap/side-streams are described in EN 13920-1 (CEN, 2003), and the Metal Yield is calculated according to Equation 1.

$$Metal\ Yield_{scrap}(\%) = \frac{Weight_{metal\ recovered}}{Weight_{scrap}} * 100 \qquad (Eq.1)$$

Assuming that the metal yield values (70 wt%) are equal to the material's metal content and that there are no re-melting metal losses, the output flow of secondary Al when charging 1 tonne of our material mix into the furnace would be 700 kg. However, the standards mention that the laboratory tests employed to calculate the metal yield usually render slightly higher values than those yields obtained during industrial production. Thus, it is likely that the process metal losses have been underestimated to some extent in this system. For instance, at least 24 kg of aluminium in concentrates (3.4 wt% with respect to the initial 700 kg of metal present assumed) are lost during re-melting by entrapment in the salt-slag, since such is the amount recovered from the salt-slag treatment. In addition, some metals may be transformed into NMCs due to oxidation or

reaction with other compounds such as C or N. This would agree with the mass imbalance of the NMCs displayed in Figure 1, where 300 kg of non-metallics enter the system, but 350 exit it (338 in the NMC fraction and 12 in the concentrates fraction). The input flow of NMCs was calculated by Equation 2, and the output flow was based on average production data, detailed in the following section (inventory analysis).

$$NMC_{scrap} = Weight_{scrap}\left(\frac{100 - Metal\ Yield\ (\%)_{scrap}}{100}\right) \qquad (Eq.2)$$

The mass flow of the fluorides is also interesting to discuss. It is common practice to add small amounts of fluorides (2-5 wt%) into the salt-flux to promote the coalescence of the metal and hence reduce the risk of small aluminium droplets being entrained by the salt-slag residues and lost (Capuzzi et al., 2018; Peterson, 1990; T. Utigard, 1998; Thoraval and Friedrich, 2015). Still, some aluminium recyclers avoid using fluorides, even at the expense of increasing the amount of aluminium lost, due to their higher environmental impact and costs (Delgado Sancho, 2017). For instance, fluorides could form perfluorinated compounds (PFCs, such as CF_4 and C_2F_6) which have large global warming potentials (Damgaard et al., 2009; McMillan and Keoleian, 2009) and controlling these emissions is a primary concern for the aluminium industry. Since the fluorides added into the fluxes cannot be recovered by the current salt-slag valorisation process (because CaF_2 is not soluble in water), as opposed to KCl/NaCl salts, the fluorine-containing compounds should largely end up in the NMCs in the system considered. In this study, the average composition of the NMCs (wt%), based on producer data, are: Al_2O_3 (60-72%), SiO_2 (7-12%), MgO (5-10%), CaO (2-3%), C (1-3%), F (0-4%) and moisture/volatiles (9-11%). Considering the above, a mass balance of the F-compounds entering and exiting the system was conducted to assess whether part of the fluorides could evaporate and/or escape the furnace as PFCs without being monitored during re-melting. According to the producer environmental report, only trace amounts of fluorine exit the rotary furnace through the off-gas treatment as HF (<4 g per cycle), and

the rest would end up in the NMCs fraction. The analysis of the smokestacks from the re-melting plant did not measure any CH_4, HFC, PFC, NF_3 or SF_6 emitted. Chemical analyses of three types of produced NMCs gave an average F concentration of 1.8 wt%. Considering that the amounts of CaF_2 charged into the furnace range between 2-5 wt% of the weight of the salts added, the theoretical F content on the NMCs, following the mass balance, should range between 0.42-1.05%. Since the theoretical concentration of F expected in the NMCs is lower than the measured one, it seems reasonable to accept that no hidden flows of F containing compounds are exiting the system.

2.2 Inventory analysis

The data was provided by European aluminium recycling and salt-slag treatment plants from their 2021 operations and environmental reports, where most data was expressed relative to the annual secondary aluminium produced or the salt-slag residue treated, e. g. tonne CO_2 emissions/tonne Al produced. The study considered the treatment of 1 tonne of material mix consisting of 1/3 incineration bottom ash (IBA), 1/3 dross, and 1/3 industrial shavings, which is a representative example from the industrial recycling processes, where it is common to mix different types of scrap together, depending on the scrap available and the alloy specifications for the secondary aluminium. Since the expected metal yield (Al alloy) of each of these material types individually was 74.6% for IBA, 64.7% for dross and 70.3% for shavings, the average metal yield of the scrap mix was 70%. However, for the scenario where the salt-slag residues are treated, and additional aluminium concentrates are recovered, the metal yield increases to 72.3%. This is because, based in the industrial data explained below, when 700 kg of Al is recovered, 532 kg of salt-slag is also generated, from which it is possible to recover ca. 36 kg of aluminium concentrates. Since the expected metal content of the aluminium concentrates is

67.3%, approximately 24 more kg of aluminium would be produced after recirculating them into a second re-melting cycle, as represented in Figure 1.
The inputs and outputs to the LCI inventory are collected in tables A-1 and A-2 in the Appendix for the scenarios with aluminium recycling with salt-flux landfill and salt-flux treatment. The following assumptions were made:

- A salt-mix composed of 70 wt% NaCl and 30 wt% KCl, and 2 wt% additions of CaF_2.
- The valorisation treatment of 1 tonne of salt-slag produces 236 kg of salts, 636 kg of NMCs, 67 kg of aluminium concentrates and 60 kg of ammonium sulphate.
- The NaCl and KCl recovered from salt-slag treatment are recirculated into the re-melting process. Consequently, 90% of the weight of salts needed is considered without burden, and only the remaining 10% of the required salt additions are included in the impact calculations. This is based on the following data for 1 cycle of the rotary furnace: 140 kg of salts are added per tonne of scrap treated and 760 kg of salt-slag are generated per tonne of secondary aluminium produced.
- The concentrates recovered from the salt-flux treatment are recirculated, which increases the effective material treated in Scenario 2 to 1.036 tonne instead of 1 tonne.

The systems evaluated consider European market conditions. The impact of some assumptions such as treating different types of scrap with varied metal yield is tested through sensitivity analysis, where hypothetical batches of the individual material streams are compared (UBCs, mixed packaging, dross of varied metal content).

2.3 Impact assessment and interpretation

The impact method used for this study is ReCiPe 2016 (Huijbregts et al., 2020). Calculations were developed in SimaPro v. 9.5.0.0 and background data was considered through ecoinvent 3.6 with allocation at the point of substitution (APOS).

3 Results and discussion

3.1 Net environmental impacts

Table 1 displays the environmental impacts, calculated by the ReCiPe (Huijbregts et al., 2020) method for 18 impact midpoint indicators, when treating 1 tonne of Al-materials through both scenarios. The results could also be expressed as end-point indicators, aggregated into three categories: human health, ecosystems, and resources. The conversion from the mid-point into end-point impact indicators is included in the Appendix Table A-4. The third column of Table 1 shows the relative improvement when implementing a salt-slag treatment with respect to landfilling the residue. The results when changing the F.U. to 1 tonne of secondary Al alloy produced are presented in Appendix Table A-3 to facilitate the comparison with the literature.

Table 1- LCA results for 18 midpoint indicators for recycling 1 tonne of aluminium-containing material mix in a rotary furnace for salt-slag residue landfill or valorisation treatment and relative improvement when salt-slag is treated.

Midpoint indicator	Salt-slag landfill	Salt-slag treatment	Improvement (%)	Unit
Global warming	-12,267	-13,221	7.8	kg CO2 eq
Stratospheric ozone depletion	0	0	9.8	kg CFC11 eq
Ionising radiation	-212	-229	8.0	kBq Co-60 eq
Ozone formation, Human health	-32	-34	7.2	kg NOx eq
Fine particulate matter formation	-26	-27	5.3	kg PM2.5 eq
Ozone formation, Terrestrial ecosystems	-32	-34	7.0	kg NOx eq
Terrestrial acidification	-56	-59	5.5	kg SO2 eq
Freshwater eutrophication	-5	-5	8.6	kg P eq
Marine eutrophication	0	0	6.1	kg N eq
Terrestrial ecotoxicity	-9,254	-11,078	19.7	kg 1.4-DCB
Freshwater ecotoxicity	-350	-411	17.5	kg 1.4-DCB
Marine ecotoxicity	-483	-567	17.6	kg 1.4-DCB
Human carcinogenic toxicity	-2,616	-3,141	20.1	kg 1.4-DCB
Human non-carcinogenic toxicity	-11,340	-13,058	15.2	kg 1.4-DCB
Land use	-1,001	-1,131	13.0	m2a crop eq
Mineral resource scarcity	-163	-203	24.6	kg Cu eq
Fossil resource scarcity	-2,596	-2,855	10.0	kg oil eq
Water consumption	-83	-89	6.8	m3

The results reveal that implementing a salt-slag recovery treatment improves the environmental performance of the recycling process; reducing the net impacts by between 5 and 25%. The most benefited indicators were mineral resource scarcity, human carcinogenic toxicity and terrestrial, marine, and freshwater ecotoxicity. However, these are just relative improvements may not be necessarily linked to the largest actual impacts on the environment.

The "Global warming potential" (GWP) is a well-established indicator usually discussed in metallurgical LCA studies (Santero and Hendry, 2016). In this study, treating 1 tonne of the considered Al-containing streams reduces the GPW by approximately 12 t CO_2 eq. when the salt-slag residue is disposed at the landfill, and by 13 tonnes of CO_2 eq. if the salt-slag residues are valorised. This falls within the ranges reported by Damgaard (Damgaard et al., 2009): GWP reductions between 5.0 to 19.3 tonne CO2 eq. per tonne of Al scrap processed. All the contributions per process input are provided for all midpoint impact indicators in the supplementary material, and the main contributions to the GWP are listed below.

When treating 1 tonne of Al-containing materials through this recycling process, the impacts to the GWP arising from process emissions were 170 kg CO_2 eq. for the salt-slag landfill route, and 234 kg CO_2 eq. for the salt-slag treatment route. Using natural gas to fire the furnaces led to 183 kg CO_2 eq. for salt-slag landfill and 250 kg CO_2 eq. for salt-slag treatment. The impacts of electricity consumption were also lower for salt-slag landfill than for salt-slag treatment; 27 kg CO_2 eq. vs. 48. This is logical since the salt-slag treatment includes the additional step of treating the salt-slag for recovery, which uses fuels and energy and generates emissions. However, the salt-slag treatment prevents significant impacts of the waste landfill (176 kg CO_2 eq.). In addition, recovering NMCs saves -394 kg CO_2 eq., ammonium sulphate -63 kg CO_2 eq., and recovering and recirculating NaCl/KCl salts into the rotary furnace reduces the emissions associated with salt production by 31 kg CO_2 eq. Finally, producing secondary

aluminium reduced the GWP by -13,355 for the salt-slag treatment and by -12,909 for the salt-slag landfill, being the difference of -445 kg CO_2 eq. due to the Al recovered from concentrates.

However, the rest of indicators may also represent significant environmental impacts and those factors affecting them must be identified. Therefore, for the contribution analysis presented in the next section, five midpoint indicators were selected based on 2 criteria: those that display a higher relevance for the endpoint categories (global warming, fine particulate matter and human carcinogenic toxicity, based on the analysis displayed in Table A-4 in the Appendix) and those that are more greatly affected by a change in scenario (mineral resource scarcity and terrestrial ecotoxicity, as seen in Table 1).

3.2 Contribution analysis

Figure 2 displays the normalised contributions of each input to the selected impact indicators for Scenario 1 (salt slag landfill) and 2 (salt-slag treatment).

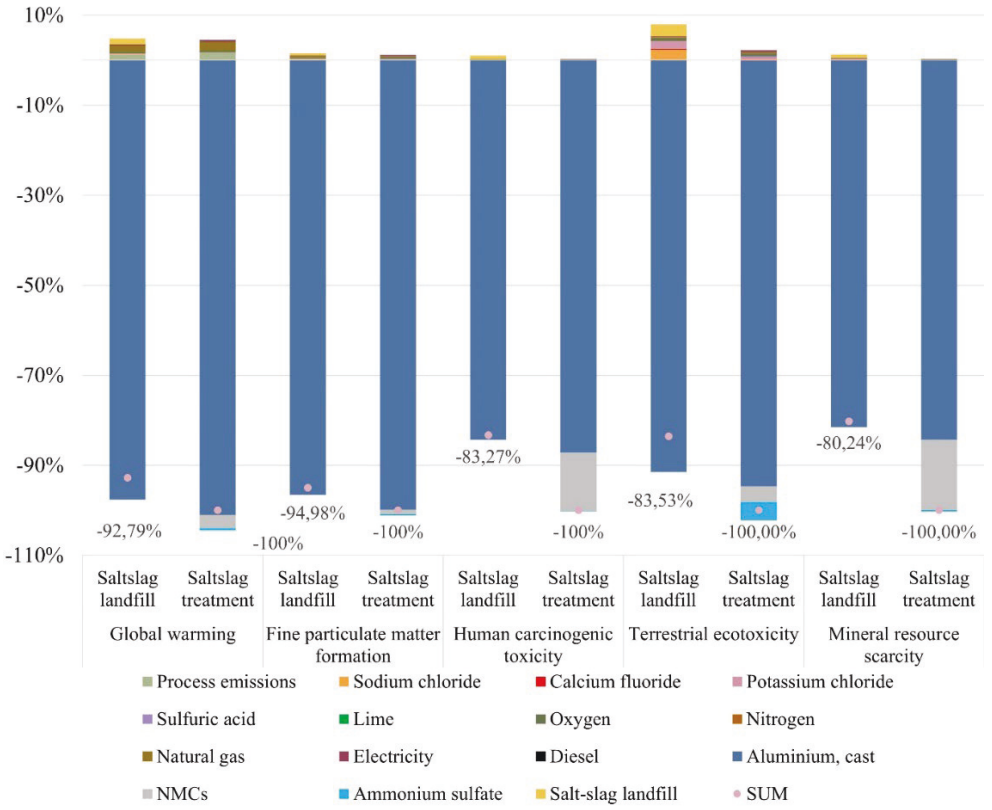

Figure 2. Contribution analysis to selected indicators during aluminium recycling in a rotary furnace for salt-slag landfill or salt-slag valorisation. Results normalised to 100% of the maximum relative impact per impact category.

The results show that the impacts of producing secondary aluminium dominate. The contribution of secondary aluminium is higher for the salt-slag treatment route because, as explained in the inventory analysis, this involves recovering additional aluminium from the concentrates in the salt-slag, which then can be recycled instead of landfilled. Recovering non-metallic compounds (NMCs) also show significant benefits for the human carcinogenic toxicity and mineral resource scarcity. To discuss the contributions of the rest of the inputs to the process, Figure 3 omits the recovered aluminium. The results are also normalised with respect to the salt treatment route.

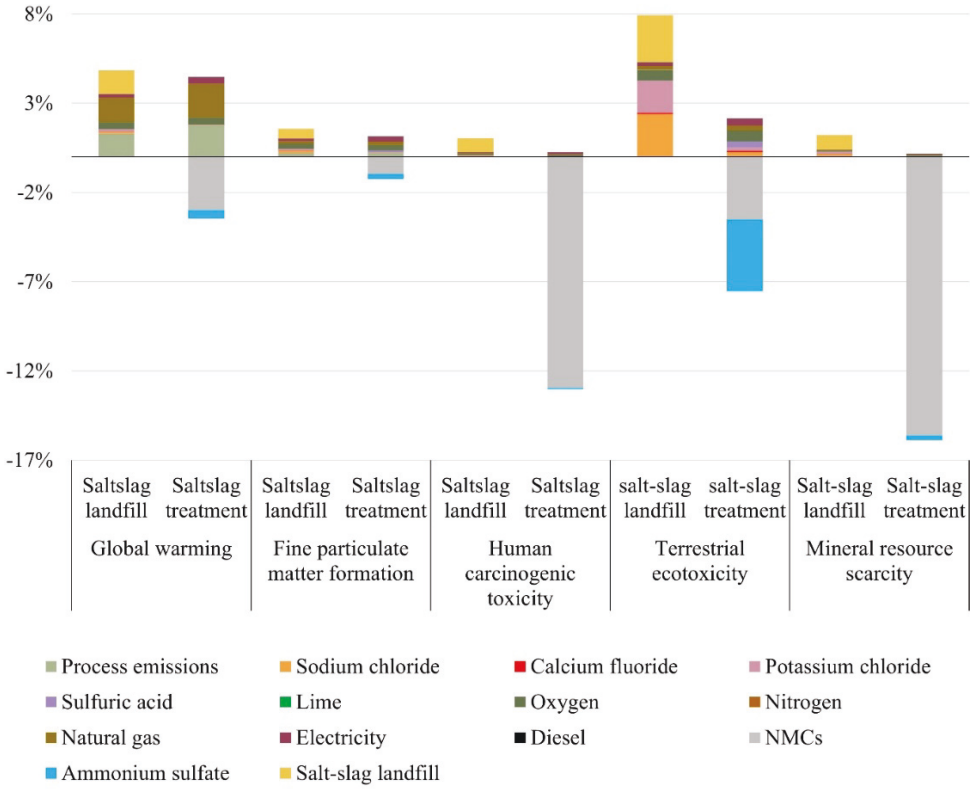

Figure 3. Contribution analysis after omitting the allocation of recovered aluminium selected midpoint indicators during aluminium recycling in a rotary furnace for salt-slag landfill or salt-slag treatment.

Figure 3 allows identifying the hotspots or most relevant potential areas for process improvement apart from minimising the aluminium metal losses. To reduce the process impacts into the GWP, efforts should focus into minimising process emissions and reducing the use of natural gas for thermal energy (e.g. substituting it by green hydrogen), since these appear as the two greatest negative contributors. Avoiding the landfill of the salt-slag and recovering the NMCs also provides substantial benefits. Recovering ammonium sulphate is another positive aspect of the salt-slag treatment, to a much lower extent but enough to compensate the impacts related to the use of oxygen and electricity, which are also visible. The rest of the contributions seem negligible in comparison, although their values can be found in the supplementary material.

For the midpoint indicator “fine particulate matter formation”, the relative contributions of the process emissions, the usage of oxygen, sodium chloride, electricity, natural gas, and the recovery of ammonium sulphate are of similar magnitudes. The impact of the salt-slag disposal is roughly three times as much as those mentioned, and the savings from recovering NMCs are the largest. The recovery of NMCs has the most substantial benefits for the indicators “human carcinogenic toxicity”, and “mineral resource scarcity”. The impact of preventing salt-slag landfill is visible for all indicators but especially beneficial for the “terrestrial ecotoxicity”. For this category, the reuse of NaCl and KCl are also significant benefits of the salt-slag treatment. Finally, the recovery of aluminium sulphate also saves substantial impacts on the “terrestrial ecotoxicity”, and the impacts related to using oxygen to fire the furnaces are also visible across all the selected indicators, although they are not affected by the choice of recycling route since the rotary furnace re-melting is present in both scenarios. The results in absolute values are plotted in Figure A-1 in the Appendix and included in the supplementary material.

3.3 Discussion

This LCA study describes a realistic scenario for a European recycler and allows comparing the salt-slag management routes and discussing potential areas where the efforts to improve the environmental performance of recycling via a rotary furnace should focus.

The largest contributor to all environmental impact savings was the recovered aluminium. Through the system expansion approach, by producing a secondary aluminium co-product, the market could avoid the production of primary aluminium, which has a high contribution to all impact categories, so discounting it from the total leads to great net environmental impact savings. Still, using GWP as an example, if the allocation of the recovered aluminium is omitted, the recycling process contributions would be 0.64 tonne CO_2 eq. for the

scenario where salt-slag is landfilled and 0.14 tonne CO_2 eq. for the route with salt-slag recovery. Damgaard attributed global warming impacts of the same magnitude (ranging between 360-1,260 kg CO_2 eq. t^{-1} aluminium scrap treated) to the recycling processes for aluminium post-consumer scrap in refiners (Damgaard et al., 2009). In (European-aluminium, 2018), there is some data from an environmental assessment for secondary cast alloy production in 2010 in Europe (refining model, using the software GaBi), where the GWP of the recycling processes was 510 kg CO_2 eq. tonne $^{-1}$ secondary aluminium, without considering the benefits from substitution. These numbers confirm that the GWP impacts of secondary aluminium production process are much lower than those from the primary production route, which was reported by (Liu and Müller, 2012) to generate between 5.92 to 41.10 tonnes of CO_2 eq., depending on the location, energy source and technologies used.

This study has shown that even small increases of 2.3 wt% in the metal yield bring forth significant environmental benefits. Thus, minimising the aluminium losses should be a priority to improve the environmental performance of the recycling and waste management processes. In addition, to improve the sustainability performance of re-melting scrap in a rotary furnace and its consequent salt-slag treatment processes, the results suggest focusing the efforts on maximising energy efficiency, cutting down process emissions and optimising the recovery and usage of NMCs.

The comparison between the salt-slag management scenarios showed that although adding the step of valorising the salt-slag also implies increasing the use of energy, water and raw materials of the process, the recovery of by-products from the salt-slag and its commercialisation or internal recirculation make this route overall more sustainable. The environmental benefits from valorising the salt-slag from aluminium recycling were also reported by Olivieri (Olivieri et al., 2006). Furthermore, salt-flux recycling makes it possible to recover aluminium from scrap which is complicated to recycle through other re-melting methods due to being partly oxidised and/or contaminated (e.g. dross,

IBA, post-consumer food packaging). However, if certain scrap types could be recycled efficiently without salts, e.g., by applying a thermal pre-treatment to clean the scrap from organics and then re-melting in a reverberatory furnace, a specific assessment should be conducted to determine the most sustainable and profitable route. This could apply to shavings and packaging waste, but not to partly oxidised scrap as dross or IBA where salt additions are needed to liberate the metal from the oxides it is surrounded by.

The addition of alloying elements or the need to refine the melt was not included in the study, as this will depend on the composition of the scrap and the requirements of the alloy under demand. The typical secondary cast alloys produced at the plant are $AlSi_9Cu_3$ / $AlSi_7Mg_{0.3}$, where Si is the main alloying element, with main applications in the transportation sector. In addition, it should be mentioned that the pre-treatments of scrap, such as shredding and sorting in material recycling facilities (MRF), were not considered. Damgaard (Damgaard et al., 2009) found that these contributions are negligible (6.8 kg CO_2-eq. $tonne^{-1}$ scrap treated) compared to the re-melting process. The emissions associated with the collection and transport of scrap, calculated in (Eisted et al., 2009), were also not considered, as they are not part of the scope of the study. Future work could expand this study by varying the energy/fuel sources or the applications of the recovered oxide by-products (NMCs) in different industries and locations.

4 Uncertainty and sensitivity evaluation

4.1 Sensitivity to the material type and recycling yield

The following sensitivity analysis assesses the influence of varying the metal yield on the GWP of recycling 1 tonne of materials/scrap via the salt-slag treatment route (Scenario 2). The metal yield of the material/scrap depends on one side on its intrinsic content of non-metallic contaminants (moisture,

organics, oxides), and on the other side on the metal losses during the high-temperatures processes, which are affected by factors such as its Mg content, specific surface area or the furnace operation (Rossel, 1990; Xiao and Reuter, 2002; Xiao Y, 2005). The average values for metal yields for different scrap categories are collected in Standard EN13920 (CEN, 2003). Some of those values were used for the sensitivity analysis, where the GWP of recycling different scrap types is compared to the materials considered in the present study in the hypothetical case where they would be re-melted in individual batches. The results are presented in the Appendix Table A-5 and Figure 4 below.

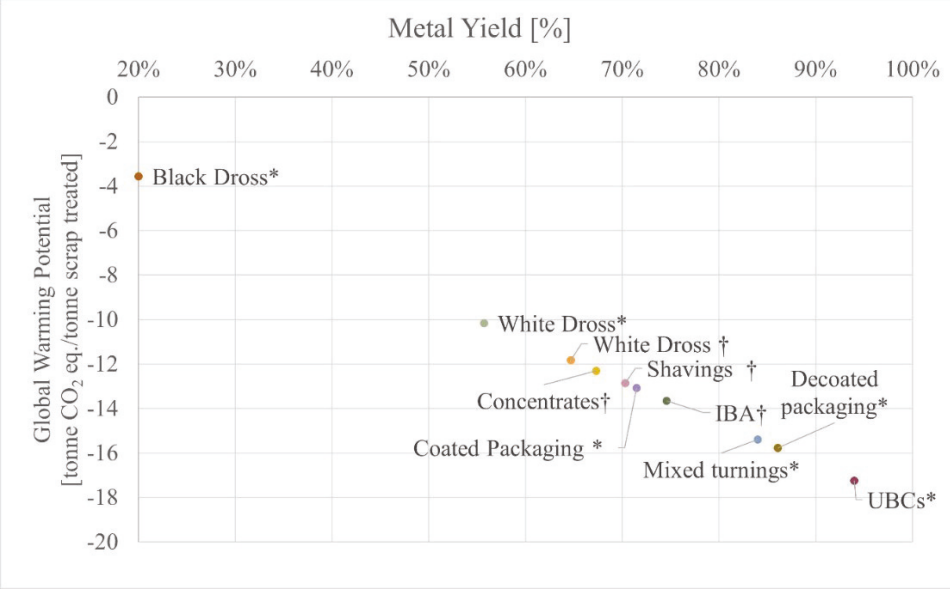

*Figure 4. Calculated global warming potentials for varying scrap types and metal yields. *Average metal yield values from Standard EN13920. †Metal yield values reported by recycling plant.*

The results show the importance of the metal yield assumptions; recycling 1 tonne of scrap with metal yields between ca. 20 and 95% varies between -3.5 and -17 tonnes CO_2 equivalent. Therefore, it is advisable that LCA studies which aim to compare recycling routes use fixed metal yield values or include a similar sensitivity analysis. It can be challenging to assess the environmental performance of recycling specific scraps because the metal yields can vary even within the same scrap type. Especially for dross, the metallic content varies

drastically depending on the production route. White dross, also known as wet dross, is generated during primary production and has typical metal contents between 15-80% (Peterson, 2011). However, black dross, also known as dry dross, which originates from secondary production routes, has typical metal contents as low as 10-20% (Tsakiridis et al., 2013). Still, even for black dross with metal contents as low as 20% of its weight, recycling saves 3.5 t CO_2 eq./tonne treated. The metal yield of incineration bottom ash (IBA) can also vary depending on its origin and size fraction. For example, in a laboratory study (Gökelma et al., 2020), recycling three different size fractions of IBA from the UK and USA gave average metal contents between 76-79% for the 2-6 mm size fraction, 83-85% for sizes between 6-12 mm and 88-89% for sizes between 12-30 mm. It is also interesting to observe that, according to this sensitivity analysis, recycling 1 tonne of de-coated packaging saves approximately 3 more tonnes of CO_2 eq. compared to recycling coated packaging. According to (Capuzzi et al., 2017; McAvoy B; McNeish, 1990), applying a de-coating treatment reduces the amount of metal lost during re-melting. However, the emissions associated with the additional thermal de-coating pre-treatment process should be controlled by similar off-gas systems as those utilised in the rotary furnace. The emissions from thermally de-coating aluminium products were studied in (Bateman et al., 1999). All considered, since the sensitivity analysis shows that slightly increasing the metal yield brings forth significant environmental benefits, the authors propose that successfully de-coating the scrap before re-melting it or preparing the scrap in other ways that decrease the re-melting losses, even just to a small extent, would improve the net environmental performance of the recycling process.

4.2 Pedigree, uncertainty, and one-at-a-time sensitivity analysis

A pedigree analysis (Ciroth et al., 2016), displayed in Table 2, was carried out for the evaluation of uncertainty.

Table 2. Pedigree analysis (based on Ciroth et al., 2016) of the flow categories used in the LCA study.

Flow	Reliability	Completeness	Temporal correlation	Geographical correlation	Further technological correlation	Squared (geometric) standard deviation (SD2)
Products (Al alloy, NMCs,	1	2	1	2	1	1.06
Salt-flux mix	2	2	1	2	1	1.08
Gas treatment (lime and sulfuric acid)	2	2	1	1	1	1.07
Water	2	2	1	1	1	1.07
Energy and fuels	2	2	1	1	1	1.07
Emissions	2	2	1	1	1	1.07
Solid waste (dust and sludge)	3	3	1	3	1	1.13

After the Pedigree evaluation, the squared standard deviation is incorporated into SimaPro to test how it affects the results of the assessment. A one-at-a-time (OAT) sensitivity analysis is carried out as shown in Figure 5.

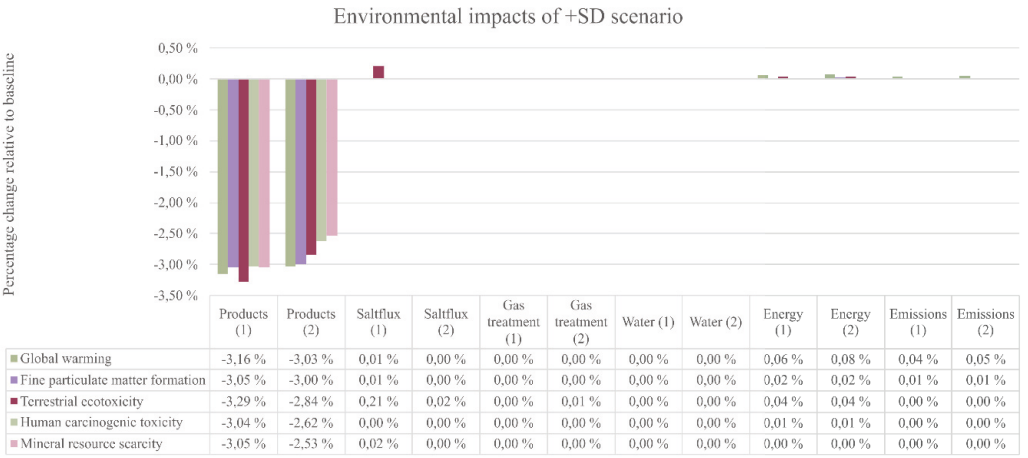

	Products (1)	Products (2)	Saltflux (1)	Saltflux (2)	Gas treatment (1)	Gas treatment (2)	Water (1)	Water (2)	Energy (1)	Energy (2)	Emissions (1)	Emissions (2)
Global warming	-3,16 %	-3,03 %	0,01 %	0,00 %	0,00 %	0,00 %	0,00 %	0,00 %	0,06 %	0,08 %	0,04 %	0,05 %
Fine particulate matter formation	-3,05 %	-3,00 %	0,01 %	0,00 %	0,00 %	0,00 %	0,00 %	0,00 %	0,02 %	0,02 %	0,01 %	0,01 %
Terrestrial ecotoxicity	-3,29 %	-2,84 %	0,21 %	0,02 %	0,00 %	0,01 %	0,00 %	0,00 %	0,04 %	0,04 %	0,00 %	0,00 %
Human carcinogenic toxicity	-3,04 %	-2,62 %	0,00 %	0,00 %	0,00 %	0,00 %	0,00 %	0,00 %	0,01 %	0,01 %	0,00 %	0,00 %
Mineral resource scarcity	-3,05 %	-2,53 %	0,02 %	0,00 %	0,00 %	0,00 %	0,00 %	0,00 %	0,00 %	0,00 %	0,00 %	0,00 %

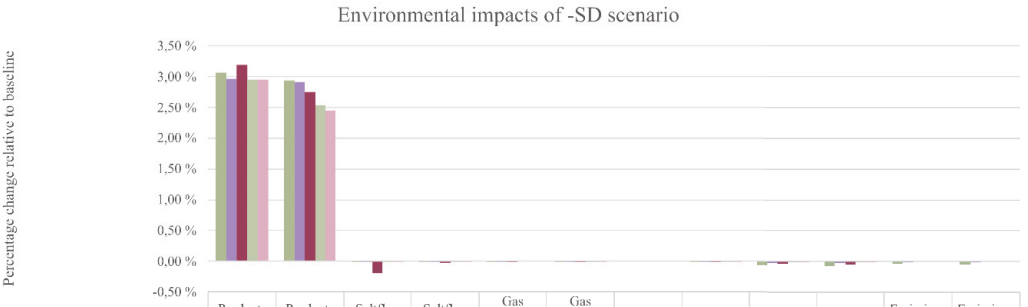

	Products (1)	Products (2)	Saltflux (1)	Saltflux (2)	Gas treatment (1)	Gas treatment (2)	Water (1)	Water (2)	Energy (1)	Energy (2)	Emissions (1)	Emissions (2)
Global warming	3,07 %	2,94 %	-0,01 %	0,00 %	0,00 %	0,00 %	0,00 %	0,00 %	-0,06 %	-0,08 %	-0,04 %	-0,05 %
Fine particulate matter formation	2,96 %	2,91 %	-0,01 %	0,00 %	0,00 %	0,00 %	0,00 %	0,00 %	-0,02 %	-0,03 %	-0,01 %	-0,01 %
Terrestrial ecotoxicity	3,19 %	2,76 %	-0,20 %	-0,02 %	0,00 %	-0,01 %	0,00 %	-0,01 %	-0,04 %	-0,05 %	0,00 %	0,00 %
Human carcinogenic toxicity	2,95 %	2,54 %	0,00 %	0,00 %	0,00 %	0,00 %	0,00 %	0,00 %	-0,01 %	-0,01 %	0,00 %	0,00 %
Mineral resource scarcity	2,96 %	2,45 %	-0,01 %	0,00 %	0,00 %	0,00 %	0,00 %	0,00 %	0,00 %	0,00 %	0,00 %	0,00 %

Figure 5. Percentage change compared to baseline by +SD (top) and -SD (bottom). The number in parenthesis represents the scenario considered. (1) = Salt slag landfill; (2) Salt slag treatment.

As it was expected and in accordance with the contribution analysis, products and co-products hold the greatest influence in the OAT and can account for more than 3% of variation. When the product ratio is increased, the environmental performance increases (is more negative) and vice versa. All other parameters effect stays below the 1% of variation. Regarding the different impact categories, they are similarly affected by the change in parameters, excluding the salt-flux that affects mostly terrestrial ecotoxicity. A significant variation is not found when comparing the different scenarios.

5 Conclusions

- Recycling 1 tonne of hard-to-recycle aluminium-containing streams (mix of dross, IBA and shavings with metal yield ~ 72 wt%) in a salt-based rotary furnace with subsequent salt-slag treatment, producing cast Al and byproducts, saves 13.2 t CO_2 eq. of GWP.
- The implementation of a salt-slag valorisation process reduces the GWP by 1 tonne of CO_2 eq. and brings forth significant environmental benefits (between 5-25%) for all other midpoint indicators considered when compared with slag landfilling.
- The midpoint indicators most benefitted by the salt-slag treatment were, in descending order: mineral resource scarcity and human carcinogenic toxicity (due to NMCs recovery), and terrestrial ecotoxicity (due to prevention of landfill, ammonium sulphate and salts recovery).
- The main contributors to reducing the global warming potential are the recovery of aluminium concentrates, NMCs, the avoidance of landfill, and to a lower extent the recovery of ammonium sulphate.
- Further efforts to improve the environmental performance the process should focus on minimising metal losses and optimising the recovery and usage of byproducts (NMCs).
- The metal yield assumptions have a substantial effect on the environmental performance of the recycling process, e.g., variations between 20 and 95 wt% lead to global warming potentials ranging from -3.5 to -17 t CO_2 eq.

Acknowledgements

The authors would like to gratefully acknowledge the European Research Council for funding the project SisAl (Grant Agreement nr. 869268) and the Norwegian Research Council for funding the project Alpakka—Circular Aluminium Packaging in Norway (NFR Project nr. 296276). The authors acknowledge Befesa Aluminium for facilitating the data and the valuable discussions.

6 References

Bateman, W., Guest, G., Evans, R., 1999. Decoating of aluminium products and the environment, in: Eckert, C. (Ed.), Light Metals 1999, p. 1099.

Capuzzi, S., Kvithyld, A., Timelli, G., Nordmark, A., Engh, T.A., 2017. Influence of Coating and De-Coating on the Coalescence of Aluminium Drops in Salt, in: Ratvik, A.P. (Ed.), Light Metals 2017. Springer International Publishing, Cham, pp. 1115-1121. https://doi.org/10.1007/978-3-319-51541-0_134.

Capuzzi, S., Kvithyld, A., Timelli, G., Nordmark, A., Gumbmann, E., Engh, T.A., 2018. Coalescence of Clean, Coated, and Decoated Aluminum for Various Salts, and Salt–Scrap Ratios. Journal of Sustainable Metallurgy 4, 343-358. https://doi.org/10.1007/s40831-018-0176-2.

CEN, 2003. EN 13920-1:2003 Aluminium and aluminium alloys scrap, Part 1: General requirements, sampling and test.

Ciroth, A., Muller, S., Weidema, B., Lesage, P., 2016. Empirically based uncertainty factors for the pedigree matrix in ecoinvent. The International Journal of Life Cycle Assessment 21, 1338-1348. https://doi.org/10.1007/s11367-013-0670-5.

Damgaard, A., Larsen, A.W., Christensen, T.H., 2009. Recycling of metals: accounting of greenhouse gases and global warming contributions. Waste Management & Research 27, 773-780. https://doi.org/10.1177/0734242X09346838.

Delgado Sancho, L.R., S ; Farrell, F ; Cusano, G ; Rodrigo Gonzalo, M, 2017. Best available techniques (BAT) reference document for the non-ferrous metals industries. Industrial Emissions Directive 2010/75/EU (integrated pollution prevention and control) Joint Research Centre (European Comission). https://eippcb.jrc.ec.europa.eu/sites/default/files/2020-01/JRC107041_NFM_bref2017.pdf

Eisted, R., Larsen, A.W., Christensen, T.H., 2009. Collection, transfer and transport of waste: accounting of greenhouse gases and global warming contribution. Waste Management & Research 27, 738-745. https://doi.org/10.1177/0734242X09347796.

EPA., U.S., 2015. Secondary Aluminium Processing Waste: Salt cake characterization and reactivity. International Decontamination Research and Development Conference. U.S. Environmental Protection Agency, Washington, DC, EPA/600/R-15/283, 2015.

European-aluminium, 2018. Environmental profile report, Life-Cycle inventory data for aluminium production and transformation processes in Europe. European Aluminium, Brussels.

European-Comission, 2015. Hazardous Wastes Catalogue - European Comission, in: Comission, E. (Ed.), 2000D0532 — EN — 01.06.2015 — 002.001. https://eur-lex.europa.eu/eli/dec/2000/532/2015-06-01.

Gökelma, M., Vallejo-Olivares, A., Tranell, G., 2021. Characteristic properties and recyclability of the aluminium fraction of MSWI bottom ash. Waste Management 130 (2021) p. 65–73. https://doi.org/10.1016/j.wasman.2021.05.012.

Huijbregts, M.A.J., Steinmann, Z.J.N., Elshout, P.M.F., Stam, G., Verones, F., Vieira, M., Zijp, M., Hollander, A., van Zelm, R., 2020. Correction to: ReCiPe2016: a harmonised life cycle impact assessment method at midpoint and endpoint level. The International Journal of Life Cycle Assessment 25, 1635-1635. https://doi.org/10.1007/s11367-016-1246-y.

ISO, 2006a. Environmental management life cycle assessment principles and framework, ISO 14040:2006.

ISO, 2006b. Environmental management life cycle assessment requirements and guidelines, ISO 14044:2006.

IAA, 2022. Primary aluminium smelting energy intensity, International Aluminium Association. https://international-aluminium.org/statistics/primary-aluminium-smelting-energy-intensity/
Joseph, P., Tretsiakova-McNally, S., 2010. Sustainable Non-Metallic Building Materials, Sustainability, pp. 400-427. https://doi.org/10.3390/su2020400.
Li, P., Zhang, M., Teng, L., Seetharaman, S., 2013. Recycling of Aluminum Salt Cake: Utilization of Evolved Ammonia. Metallurgical and Materials Transactions B 44, 16-19. https://doi.org/10.1007/s11663-012-9779-3.
Liu, G., Müller, D.B., 2012. Addressing sustainability in the aluminum industry: a critical review of life cycle assessments. Journal of Cleaner Production 35, 108-117. https://doi.org/10.1016/j.jclepro.2012.05.030.
López-Alonso, M., Martinez-Echevarria, M.J., Garach, L., Galán, A., Ordoñez, J., Agrela, F., 2019. Feasible use of recycled alumina combined with recycled aggregates in road construction. Construction and Building Materials 195, 249-257. https://doi.org/10.1016/j.conbuildmat.2018.11.084.
Lucheva, B.I., Petkov, R., 2005. Non-waste aluminium dross recycling. Journal of Chemical Technology and Metallurgy. https://api.semanticscholar.org/CorpusID:138746258.
Manfredi, S., Tonini, D., Christensen, T.H., 2011. Environmental assessment of different management options for individual waste fractions by means of life-cycle assessment modelling. Resources, Conservation and Recycling 55, 995-1004. https://doi.org/10.1016/j.resconrec.2011.05.009.
Mayes, W.M., Burke, I.T., Gomes, H.I., Anton, Á.D., Molnár, M., Feigl, V., Ujaczki, É., 2016. Advances in Understanding Environmental Risks of Red Mud After the Ajka Spill, Hungary. Journal of Sustainable Metallurgy 2, 332-343. https://doi.org/10.1007/s40831-016-0050-z.
McAvoy B., McNeish, J., Stevens, W., 1990. The alcan decoater process for UBC decoating. In: 2nd Int. Symp. Recycl. Met. Eng. Mater., van Linden, J.H.L., Stewart, D.L., and Sahai, Y., Eds., TMS–AIME, Warrendale, PA, 1990, p. 203.
McMillan, C.A., Keoleian, G.A., 2009. Not All Primary Aluminum Is Created Equal: Life Cycle Greenhouse Gas Emissions from 1990 to 2005. Environmental Science & Technology 43, 1571-1577. https://doi.org/10.1021/es800815w.
Milani, V., Timelli, G., 2023. Solid Salt Fluxes for Molten Aluminum Processing - A Review, Metals. https://doi.org/10.3390/met13050832.
Olivieri, G., Romani, A., Neri, P., 2006. Environmental and economic analysis of aluminium recycling through life cycle assessment. International Journal of Sustainable Development & World Ecology 13, 269-276. https://doi.org/10.1080/13504500609469678.
Padilla, I., Romero, M., López-Andrés, S., López-Delgado, A., 2022. Sustainable Management of Salt Slag, Sustainability. https://doi.org/10.3390/su14094887.
Peterson, R.D., 1990. Effect of salt flux additives on aluminium droplets coalescence. In: 2nd Int. Symp. Recycl. Met. Eng. Mater., van Linden, J.H.L., Stewart, D.L., and Sahai, Y., Eds., TMS–AIME, Warrendale, PA, 1990, p.69.
Peterson, R.D., 2011. A Historical Perspective on Dross Processing. Materials Science Forum 693, 13-23. https://doi.org/10.4028/www.scientific.net/MSF.693.13.
Rodrigues, M., Lund, R.J., ter Heijne, A., Sleutels, T., Buisman, C.J.N., Kuntke, P., 2022. Application of ammonium fertilizers recovered by an Electrochemical System. Resources, Conservation and Recycling 181, 106225. https://doi.org/10.1016/j.resconrec.2022.106225.

Rossel, H., 1990. Fundamental investigations about metal loss during remelting of extrusion and rolling fabrication scrap. In: Bickert, C.M. (Ed.), Light Metals 1990, p. 701.
Saevarsdottir, G., Padamata, S.K., Velasquez, B.N., Kvande, H., 2023. The Way Towards Zero Carbon Emissions in Aluminum Electrolysis, in: Broek, S. (Ed.), Light Metals 2023. Springer Nature Switzerland, Cham, pp. 637-645. https://doi.org/10.1007/978-3-031-22532-1_86.
Santero, N., Hendry, J., 2016. Harmonization of LCA methodologies for the metal and mining industry. The International Journal of Life Cycle Assessment 21, 1543-1553. https://doi.org/10.1007/s11367-015-1022-4.
Schlesinger, M.E., 2013. Aluminium recycling. CRC Press. https://doi.org/10.1201/b16192.
Sua-iam, G., Makul, N., 2013. Use of recycled alumina as fine aggregate replacement in self-compacting concrete. Construction and Building Materials 47, 701-710. https://doi.org/10.1016/j.conbuildmat.2013.05.065.
Sua-iam, G., Makul, N., 2017. Incorporation of high-volume fly ash waste and high-volume recycled alumina waste in the production of self-consolidating concrete. Journal of Cleaner Production 159, 194-206. https://doi.org/10.1016/j.jclepro.2017.05.075.
T. Utigard, K.F., R. Roy, J. Lim, A. Silny and C. Dupuis, 1998. The Properties and Uses of Fluxes in Molten Aluminium Processing. Journal of metallurgy. https://doi.org/10.1007/s11837-998-0285-7.
Thoraval, M., Friedrich, B., 2015. Metal Entrapment in Slag during the Aluminium Recycling Process in Tilting Rotary Furnace, European Metallurgy Conference.
Tsakiridis, P.E., Oustadakis, P., Agatzini-Leonardou, S., 2013. Aluminium recovery during black dross hydrothermal treatment. Journal of Environmental Chemical Engineering 1, 23-32. https://doi.org/10.1016/j.jece.2013.03.004.
Vadenbo, C., Hellweg, S., Astrup, T.F., 2017. Let's Be Clear(er) about Substitution: A Reporting Framework to Account for Product Displacement in Life Cycle Assessment. Journal of Industrial Ecology 21, 1078-1089. https://doi.org/10.1111/jiec.12519.
Xiao, Y., Reuter, M.A., 2002. Recycling of distributed aluminium turning scrap. Minerals Engineering 15, 963-970. https://doi.org/10.1016/S0892-6875(02)00137-1.
Xiao Y, Reuter, M.A., Boin U, 2005. Aluminium recycling and environmental issues of salt slag treatment. J Environ Sci Health A Tox Hazard Subst Environ Eng 40, 1061-1075. https://doi.org/10.1080/10934520500183824.

Appendix

Appendix Table A-1: Scenario 1 - LCI for recycling of 1 tonne Al scrap in a rotary furnace with salt slag landfill.

Input/Output – Industry data	Input/Output – Selected SimaPro flows	Amount
	Outputs to technosphere: products and co-products	
Incineration Bottom Ash Dross Shavings	1 t of aluminium waste flows treatment (selected as F.U., not linked to SimaPro flow)	1/3 tonne 1/3 tonne 1/3 tonne
	Outputs to technosphere: avoided products	
Aluminium cast alloys $AlSi_9Cu_3$ / $AlSi_7Mg_{0,3}$	Aluminium, cast alloy {GLO | aluminium ingot, primary, to market | APOS, U	698.66 kg
	Inputs from technosphere: materials/fuels	
NaCl (70-95% wt. salt-mix)	Sodium chloride, powder {RER} | production | APOS, U	98 kg
KCl (5-30% wt. salt-mix)	Potassium chloride, as K2O {RER} | potassium chloride production | APOS, U	42 kg
CaF_2 (2-5% wt. Salt-mix)	Fluorspar, 97% purity {GLO}| market for | APOS, U	2.8 kg
	Lime {RER} Market for lime | APOS, U	0.71 kg
O_2 gas	Oxygen, liquid {RER} Market for | APOS, U	83.84 kg
	Inputs from nature	
	Water, process, unspecified natural origin/m3, non-agri, ES	0.50304 m^3
	Inputs from technosphere: electricity/heat	
	Electricity, high voltage {Europe without Switzerland}| market group for | APOS, U	670.72 kWh
Natural gas	Heat, district or industrial, natural gas {Europe without Switzerland} | heat production, natural gas, at industrial furnace low-NOx >100kW | APOS, U	63.88 kWh
	Diesel {Europe without Switzerland} | market for | APOS, U	1.04 kg
	Emissions to air	
	Carbon dioxide, fossil	169.70 kg
	Sulfur dioxide, ES	0.21 kg
	Nitrogen oxides, ES	0.10 kg*
	Particulates	15.37 g*
	Hydrochloric acid	18.86 g*
	Hydrogen fluoride	4.19 g
	Heavy metals, unspecified	0.6 g
	Outputs to technosphere: waste and emissions to treatment	
	Dust, unspecified	19.56 kg
Salt-slag	Sludge, NaCl electrolysis | treatment of sludge, NaCl electrolysis, residual material landfill	530.99 kg

[1] Higher limit, since emissions were reported as < to the reported value.

Appendix Table A-2: Scenario 2 – LCI for recycling 1 tonne Al scrap in rotary furnace with salt slag treatment.

Input/Output – Industry data	Input/Output – Selected Simapro flows	Amount
	Outputs to technosphere: products and co-products	
Incineration Bottom Ash (IBA)	1 t of aluminium waste flows treatment (selected as F.U., not linked to SimaPro flow)	1/3 tonne
Dross		1/3 tonne
Shavings		1/3 tonne
	Outputs to technosphere: avoided products	
Aluminium cast alloys $AlSi_9Cu_3$ / $AlSi_7Mg_{0,3}$	Aluminium, cast alloy {GLO} | aluminium ingot, primary, to market | APOS, U	722.75 kg
Non Metallic Compounds (NMCs)	Aluminium oxide, non-metallurgical {IAI Area, EU27&EFTA} | aluminium oxide production | APOS, U	349.45 kg
	Ammonium sulfate, as N {RER} | ammonium sulfate production | APOS, U	32.90 kg
	Inputs from nature	
	Water, process, unspecified natural origin/m3, non-agri, ES	0.54929+0.52038 m^3
	Inputs from technosphere: materials/fuels	
NaCl (70-95% wt. salt-mix)	Sodium chloride, powder {RER} | production | APOS, U	10.65 kg
KCl (5-30% wt. salt-mix)	Potassium chloride, as K2O {RER} | potassium chloride production | APOS, U	4.56 kg
CaF_2 (2-5% wt. salt-mix)	Fluorspar, 97% purity {GLO}| market for | APOS, U	2.9 kg
	Sulfuric acid {RER} | market for sulfuric acid | APOS, U	10.22 kg
	Lime {RER} | market for lime | APOS, U	0.74 kg
O_2 gas	Oxygen, liquid {RER}| market for | APOS, U	86.73
	Nitrogen {RER} | market for | APOS, U	0.389 kg
	Inputs from the technosphere: electricity/heat	
	Electricity, high voltage {Europe without Switzerland}| market group for | APOS, U	116 kWh
Natural gas	Heat, district or industrial, natural gas {Europe without Switzerland} | heat production, natural gas, at industrial furnace low-NOx >100kW | APOS, U	917 kWh
	Diesel {Europe without Switzerland} | market for | APOS, U	1.41 kg
	Emissions to air	
	Carbon dioxide, fossil	233 kg
	Sulfur dioxide, ES	0.21 kg
	Nitrogen oxides, ES	0.14 kg*
	Particulates	15.90 g*
	Hydrochloric acid	19.51 g*
	Hydrogen fluoride	4.33 g
	Heavy metals, unspecified	6.50 g
	Methane	28.01 g
	Outputs to technosphere: waste and emissions to treatment	
	Dust, unspecified	20.23 kg

[1] Higher limit since emissions were reported as < to the reported value.

Appendix Table A-3- LCA results for 18 midpoint indicators for producing 1 tonne of secondary aluminium in a rotary furnace for salt-slag residue landfill (1.431 tonne of material processed) or salt-slag residue treatment (1.384 tonne of material processed) and relative improvement when salt-slag is treated.

Midpoint indicator	Salt-slag landfill	Salt-slag treatment	Improvement (%)	Unit
Global warming	-17,555	-18,292	4.2	kg CO_2 eq/tonne Al
Stratospheric ozone depletion	0	0	6.1	kg CFC11 eq/tonne Al
Ionising radiation	-303	-316	4.4	kBq Co-60 eq/tonne Al
Ozone formation, Human health	-45	-47	3.6	kg NO_x eq/tonne Al
Fine particulate matter formation	-37	-37	1.8	kg PM2.5 eq/tonne Al
Ozone formation, Terrestrial ecosystems	-45	-47	3.4	kg NO_x eq/tonne Al
Terrestrial acidification	-81	-82	2.0	kg SO_2 eq/tonne Al
Freshwater eutrophication	-6	-7	5.0	kg P eq/tonne Al
Marine eutrophication	0	0	2.6	kg N eq/tonne Al
Terrestrial ecotoxicity	-13,242	-15,328	15.8	kg 1.4-DCB/tonne Al
Freshwater ecotoxicity	-501	-569	13.6	kg 1.4-DCB/tonne Al
Marine ecotoxicity	-691	-785	13.7	kg 1.4-DCB/tonne Al
Human carcinogenic toxicity	-3,743	-4,346	16.1	kg 1.4-DCB/tonne Al
Human non-carcinogenic toxicity	-16,227	-18,066	11.3	kg 1.4-DCB/tonne Al
Land use	-1,432	-1,565	9.2	m_2a crop eq/tonne Al
Mineral resource scarcity	-233	-280	20.5	kg Cu eq/tonne Al
Fossil resource scarcity	-3,715	-3,950	6.3	kg oil eq/tonne Al
Water consumption	-119	-123	3.3	m^3

Appendix Table A-4- Salt-slag treatment scenario (2). Impact Assessment of midpoint effect into End Points using the software SimaPro and the method ReCiPe 2016 Endpoint (H) V1.08 / World (2010) H/A. The three most impactful midpoints are highlighted.

Impact category	Unit	Total	Total
Functional Unit		**1 tonne material processed** (0.722 tonne secondary Al produced)	**1 tonne secondary Al alloy produced** (1.384 tonne of material processed)
Total	Pt	-735.96	-1,018.26
Global warming, Human health	**Pt**	**-204.65**	**-283.14**
Global warming, Terrestrial ecosystems	Pt	-10.01	-13.85
Global warming, Freshwater ecosystems	Pt	0.00	-0.00
Stratospheric ozone depletion	Pt	-0.03	-0.04
Ionizing radiation	Pt	-0.03	-0.05
Ozone formation, Human health	Pt	-0.52	-0.72
Fine particulate matter formation	**Pt**	**-283.47**	**-392.21**
Ozone formation, Terrestrial ecosystems	Pt	-1.18	-1.64
Terrestrial acidification	Pt	-3.42	-4.73
Freshwater eutrophication	Pt	-0.89	-1.23
Marine eutrophication	Pt	0.00	-0.00
Terrestrial ecotoxicity	Pt	-0.03	-0.05
Freshwater ecotoxicity	Pt	-0.08	-0.11
Marine ecotoxicity	Pt	-0.02	-0.02
Human carcinogenic toxicity	**Pt**	**-173.92**	**-240.64**
Human non-carcinogenic toxicity	Pt	-49.63	-68.66
Land use	Pt	-2.71	-3.76
Mineral resource scarcity	Pt	-0.33	-0.46
Fossil resource scarcity	Pt	-3.72	-5.15
Water consumption, Human health	Pt	-1.20	-1.66
Water consumption, Terrestrial ecosystem	Pt	-0.11	-0.15
Water consumption, Aquatic ecosystems	Pt	0.00	-3.39E-05

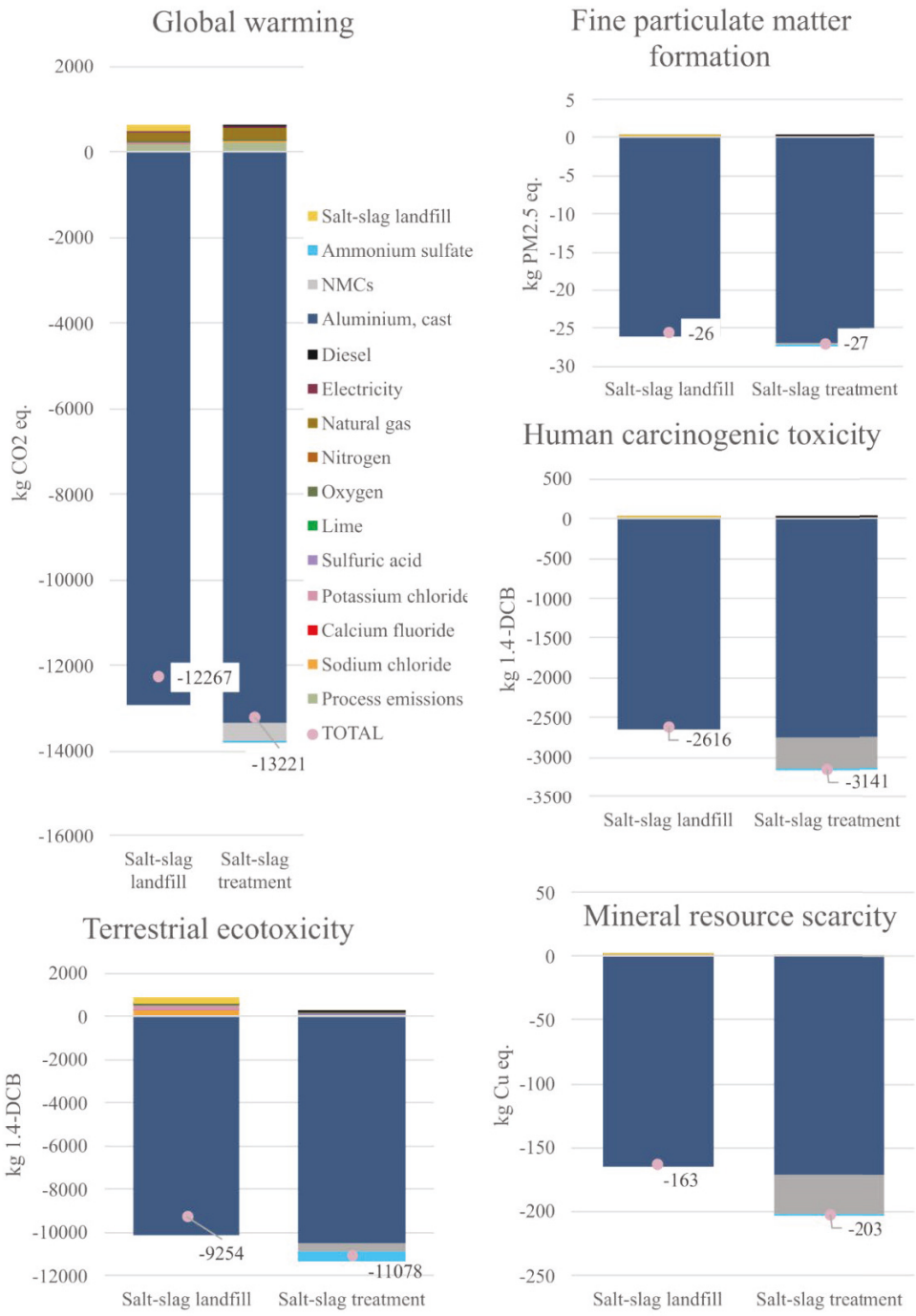

Appendix Figure A-1. Contribution analysis in absolute values to global warming, fine particulate matter formation and human carcinogenic toxicity during aluminium recycling in a rotary furnace for options of salt-slag landfill or salt-slag treatment for recovery. The total net results are marked by the pink dot and the label, and the net process contributions for the rest of the midpoint indicators were given in Table 1.

*Appendix Table A-5. Calculated global warming potentials for varying scrap types and metal yields. *Average metal yield values from Standard EN13920. †Metal yield values from industrial data.*

Scrap type	Metal Yield	Global warming potential
Black Dross*	20%	-3,559 kg CO_2 eq
White Dross*	55.7 %	-10,156 kg CO_2 eq
White Dross †	64.7 %	-11,818 kg CO_2 eq
Concentrates †	67.3 %	-12,299 kg CO_2 eq
Shavings †	70.3 %	-12,855 kg CO_2 eq
Coated packaging*	71.5 %	-13,075 kg CO_2 eq
IBA †	74.6 %	-13,648 kg CO_2 eq
Mixed turnings*	84.0 %	-15,385 kg CO_2 eq
Decoated packaging*	86.1 %	-15,773 kg CO_2 eq
UBCs*	94.0 %	-17,233 kg CO_2 eq

ISBN 978-82-326-7800-6 (printed ver.)
ISBN 978-82-326-7799-3 (electronic ver.)
ISSN 1503-8181 (printed ver.)
ISSN 2703-8084 (online ver.)

NTNU

Norwegian University of
Science and Technology